SCIENCE & TECHNOLOGY

ARS JOURNAL

A PUBLICATION OF THE AMERICAN ROCKET SOCIETY

VOLUME 30 NUMBER 2 FEBRUARY 1960

LOS ANGELES PUBLIC LIBRARY

FEB 2 4 1960

BIND

SURVEY ARTICLE

Recent Advances in Condensed Media Detonations . . . . . S. J. Jacobs 151

CONTRIBUTED ARTICLES

Theory of Liquid Propellant Rocket Combustion Instability and Its Experimental Verification . . . . . Luigi Crocco, Jerry Grey and David T. Harrje 159

Rapid Approximate Method for Analyzing Nuclear Rocket Performance . . . . . Alan H. Stenning 169

Experimental Investigation of Propellant Erosion . . . . . Tage Marklund and Arne Lake 173

Estimate of Chemical Space Heating Rates in Gas-Phase Combustion With Application to Rocket Propellants . David A. Bittker and Richard S. Brokaw 179

TECHNICAL NOTES

Mixture Ratio Distribution in the Drops of Spray Produced by Impinging Liquid Streams . . . . . Desso Somogyi and Charles E. Feller 185

Chemical Nonequilibrium Effects on Hydrogen Rocket Impulse at Low Pressures . . . . . J. Gordon Hall, A. Q. Eschenroeder and J. J. Klein 188

Pure Shock Environmental Testing of Condensed-Phase, Unstable Materials . . T. A. Erikson 190

Calibration of Turbine Flowmeters for Cryogenic Operation . . . . . Jerry Grey 192

Expansion of Liquid-Oxygen RP-1 Combustion Products in a Rocket Nozzle . . . . . Frederick S. Simmons 193

Some Weight Considerations for Manned Lunar Missions . . . . . Hans B. Schechter 196

Some Exact Solutions of the Equations of Motion of a Solar Sail With Constant Sail Setting . . . . . Howard S. London 198

Hypervelocity Glider at Large Angles of Inclination . . . . . W. H. T. Loh 201

Gravitational Torque on a Satellite of Arbitrary Shape . . . . . Russell A. Nidey 203

Perturbation Approach to the Effect of the Geomagnetic Field on a Charged Satellite . . . . . H. R. Westerman 204

Approximate Method for Determining Laminar Heat Transfer Rates . . . . . Harold S. Pergament and Melvin Epstein 206

Maximum Turbulent Boundary Layer Heating Rates on a Hemispherical Nose . . . . . Paul D. Arthur and James C. Williams III 207

DEPARTMENTS

Book Reviews 208

New Patents 214

Technical Literature Digest 216

KEY
TO
MISSILE
OPERATION

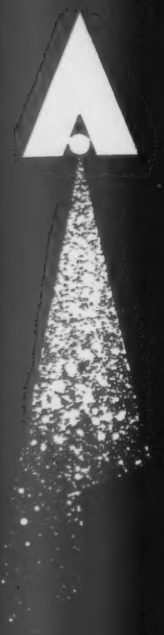

ELECTRICAL
ELECTRONIC
MECHANICAL

DESIGN
INSTALLATIONS
TEST

MARTIN
ACTIVATION

New horizons in infra-red... by Bulova

Bulova designer-engineers can help you from concept to production

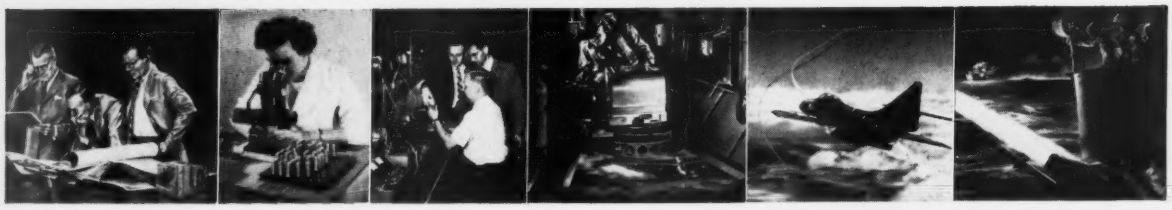

Bulova infra-red, camera, TV and radar techniques are being combined with Bulova analysis and display systems for defense and industry.

Bulova infra-red R & D extends to fire control systems, filters, reticles and thermistor bolometers, as well as advanced work in mosaic and photoconductor cells. Here is a proven capability ready to assist you in any area of IR development from black body emanations through detection to final display.

Experience in precision design and precision manufacture is the Bulova tradition, the Bulova capability. It has been for over 80 years. For more information write—

Industrial & Defense Sales, Bulova, 62-10 Woodside Ave., Woodside 77, N.Y.

BULOVA

VISIT OUR BOOTH NUMBERS #1719–#1721 — I.R.E. SHOW, N.Y.C.

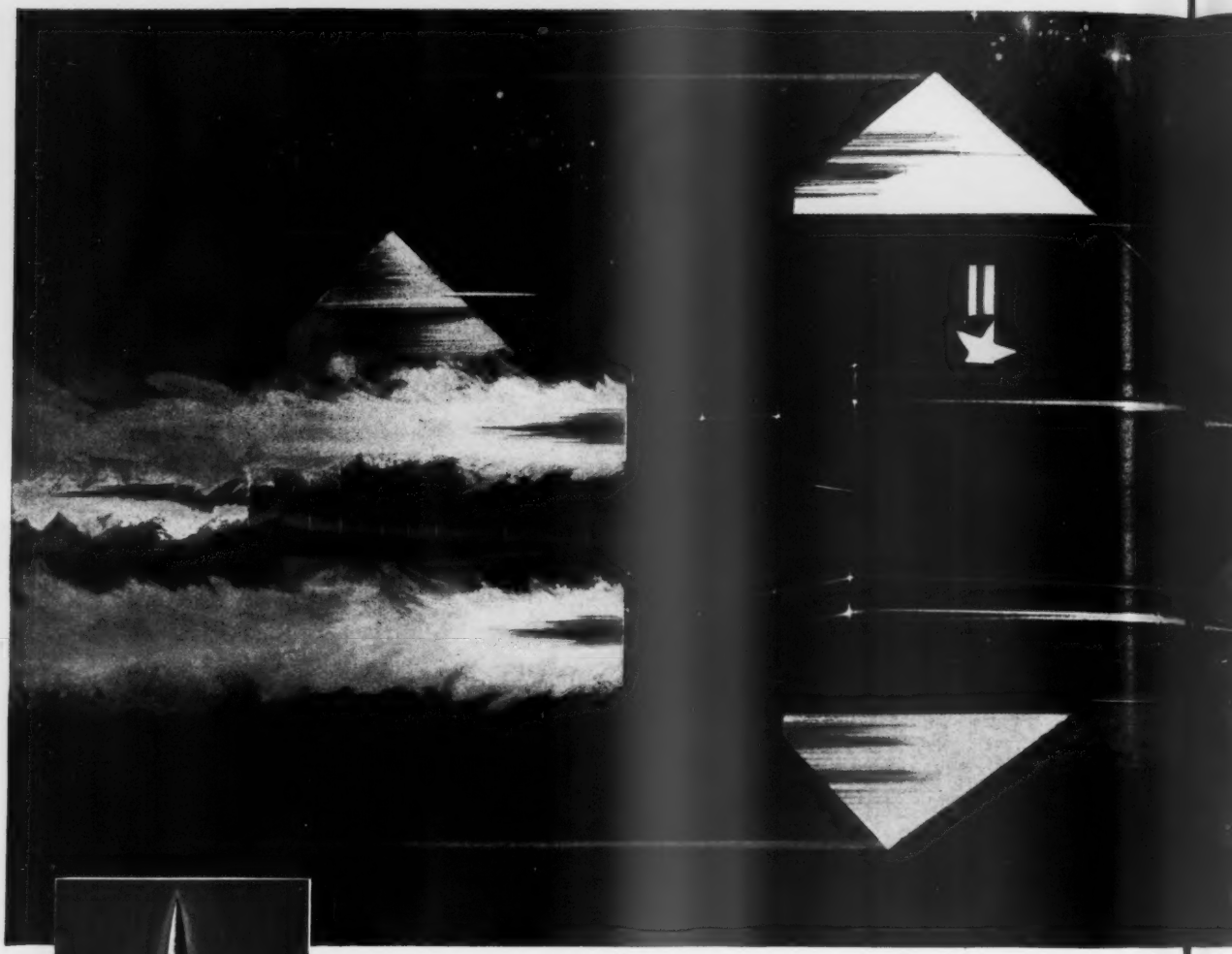

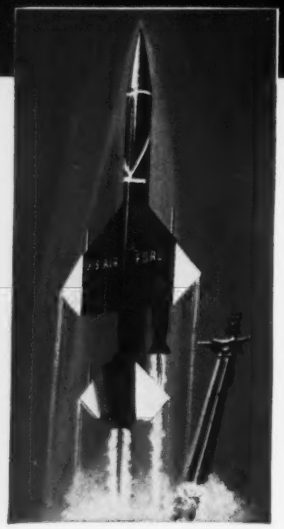

Keeping pace with the nation's missile
BOMARC "B" by BOEING. To be launched
motor — this new weapons system when
OFF THE GROUND FASTER FOR MORE

To strengthen our defenses, the armed forces and industry — as a team — ceaselessly strive to improve America's weapons systems. The U. S. A. F.'s BOMARC "B" highlights this unified effort.

An advanced weapon, now in the testing phase, BOMARC "B" features solid propellant rocket boosters built by THIOKOL. Instant firing action over extended periods of time and quick reach of high

Thiokol® CHEMICAL CORPORATION BRISTOL, PENNA.

®Registered trademark of the Thiokol Chemical Corporation for its rocket propellants, liquid polymers, plasticizers, and other chemical products.

U.S.A.F. BOMARC

needs, the U.S.A.F. has under development
with a THIOKOL solid propellant
it becomes operational will move . . . .
DISTANT INTERCEPT than earlier models

altitudes to meet attacking aircraft are the promises of these specially designed powerplants.

Continued cooperative action by the military and thousands of contractors like THIOKOL Chemical Corporation and BOEING, whose contributions to the air age, jet age and space age are immeasurable, is vital to America's defense.

BOEING AIRPLANE COMPANY
PILOTLESS AIRCRAFT DIVISION SEATTLE, WASHINGTON

ARS JOURNAL

A PUBLICATION OF THE AMERICAN ROCKET SOCIETY

EDITOR — Martin Summerfield

ASSOCIATE TECHNICAL EDITOR — Irvin Glassman

MANAGING EDITOR — Barbara Nowak

ART EDITOR — John Culin

CONTRIBUTOR — George F. McLaughlin

ASSOCIATE EDITORS

J. George Adashko, *Russian Supplement;* **Ali Bulent Cambel,** *Northwestern University, Book Reviews;* **Charles J. Mundo Jr.,** *American Bosch Arma Corporation, Guidance;* **Bernard H. Paiewonsky,** *Aeronautical Research Associates of Princeton, Flight Mechanics;* **M. H. Smith,** *Princeton University, Technical Literature Digest*

ASSISTANT EDITORS

Julie Hight, Estelle Metz, Carol Rubenstein

ADVERTISING AND PROMOTION MANAGER

William Chenoweth

ADVERTISING PRODUCTION MANAGER

Walter Brunke

ADVERTISING REPRESENTATIVES

New York
D. C. Emery and Associates
400 Madison Ave., New York, N. Y.
Telephone: Plaza 9-7460

Los Angeles
James C. Galloway and Co.
6535 Wilshire Blvd., Los Angeles, Calif.
Telephone: Olive 3-3223

Chicago
Jim Summers and Associates
35 E. Wacker Dr., Chicago, Ill.
Telephone: Andover 3-1154

Detroit
R. F. Pickrell and Vincent Purcell
318 Stephenson Bldg., Detroit, Mich.
Telephone: Trinity 1-0790

Boston
Robert G. Melendy
17 Maugus Ave., Wellesley Hills, Mass.
Telephone: Cedar 5-6503

Pittsburgh
John W. Foster
239 4th Ave., Pittsburgh, Pa.
Telephone: Atlantic 1-2977

American Rocket Society

500 Fifth Avenue, New York 36, N. Y.

Founded 1930

OFFICERS

President	Howard S. Seifert
Vice-President	Harold W. Ritchey
Executive Secretary	James J. Harford
Treasurer	Robert M. Lawrence
Secretary and Asst. Treasurer	A. C. Slade
General Counsel	Andrew G. Haley
Director of Publications	Irwin Hersey

BOARD OF DIRECTORS

Terms expiring on dates indicated

Ali B. Cambel	1962	William H. Pickering	1961
Richard B. Canright	1962	Simon Ramo	1960
James R. Dempsey	1961	William L. Rogers	1960
Herbert Friedman	1962	David G. Simons	1961
Robert A. Gross	1962	John L. Sloop	1961
Samuel K. Hoffman	1960	Martin Summerfield	1962
A. K. Oppenheim	1961	Wernher von Braun	1960
	Maurice J. Zucrow 1960		

TECHNICAL COMMITTEE CHAIRMEN

Lawrence S. Brown, Guidance and Navigation

Milton U. Clauser, Magnetohydrodynamics

William H. Dorrance, Hypersonics

Herbert Friedman, Instrumentation

George Gerard, Structures and Materials

Milton Greenberg, Physics of the Atmosphere and Space

Stanley V. Gunn, Nuclear Propulsion

Andrew G. Haley, Space Law and Sociology

Samuel Herrick, Astrodynamics

Maxwell W. Hunter, Missiles and Space Vehicles

Herbert L. Karsch, Logistics and Operations

David B. Langmuir, Ion and Plasma Propulsion

Y. C. Lee, Liquid Rockets

Max Lowy, Communications

Paul E. Sandorff, Education

Richard A. Schmidt, Test Facilities and Support Equipment

William B. Shippen, Ramjets

John L. Sloop, Propellants and Combustion

Ivan E. Tuhy, Solid Rockets

Stanley C. White, Human Factors and Bio-Astronautics

George F. Wislicenus, Underwater Propulsion

Abe M. Zarem, Power Systems

Scope of ARS JOURNAL

This Journal is devoted to the advancement of astronautics through the dissemination of original papers disclosing new scientific knowledge and basic applications of such knowledge. The sciences of astronautics are understood here to embrace selected aspects of jet and rocket propulsion, spaceflight mechanics, high speed aerodynamics, flight guidance, space communications, atmospheric and outer space physics, materials and structures, human engineering, overall system analysis, and possibly certain other scientific areas. The selection of papers to be printed will be governed by the pertinence of the topic to the field of astronautics, by the current or probable future significance of the research, and by the importance of distributing the information to the members of the Society and to the profession at large.

Information for Authors

Manuscripts must be as brief as the proper presentation of the ideas will allow. Exclusion of dispensable material and conciseness of expression will influence the Editors' acceptance of a manuscript. In terms of standard-size double-spaced typed pages, a typical maximum length is 22 pages of text (including equations), 1 page of references, 1 page of abstract and 12 illustrations. Fewer illustrations permit more text, and vice versa. Greater length will be acceptable only in exceptional cases.

Short manuscripts, not more than one quarter of the maximum length stated for full articles, may qualify for publication as Technical Notes or Technical Comments. They may be devoted to new developments requiring prompt disclosure or to comments on previously published papers. Such manuscripts are published within a few months of the date of receipt.

Sponsored manuscripts are published occasionally as an ARS service to the industry. A manuscript that does not qualify for publication, according to the above-stated requirements as to subject, scope or length, but which nevertheless deserves widespread distribution among jet propulsion engineers, may be printed as an extra part of the Journal or as a special supplement, if the author or his sponsor will reimburse the Society for actual publication costs. Estimates are available on request. Acknowledgment of such financial sponsorship appears as a footnote on the first page of the article. Publication is prompt since such papers are not in the ordinary backlog.

Manuscripts must be double spaced on one side of paper only with wide margins to allow for instructions to printer. Include a 100 to 200 word abstract. State the authors' positions and affiliations in a footnote on the first page. Equations and symbols may be handwritten or typewritten; clarity for the printer is essential. Greek letters and unusual symbols should be identified in the margin. If handwritten, distinguish between capital and lower case letters, and indicate subscripts and superscripts. References are to be grouped at the end of the manuscript and are to be given as follows. For journal articles: Authors first, then title, journal, volume, year, page numbers; for books: Authors first, then title, publisher, city, edition and page or chapter numbers. Line drawings must be clear and sharp to make clear engravings. Use black ink on white paper or tracing cloth. Lettering should be large enough to be legible after reduction. Photographs should be glossy prints, not matte or semi-matte. Each illustration must have a legend; legends should be listed in order on a separate sheet.

Manuscripts must be accompanied by written assurance as to security clearance in the event the subject matter lies in a classified area or if the paper originates under government sponsorship. Full responsibility rests with the author.

Preprints of papers presented at ARS meetings are automatically considered for publication.

Submit manuscripts in duplicate (original plus first carbon, with two sets of illustrations) to the Managing Editor, ARS JOURNAL, 500 Fifth Avenue, New York 36, N.Y.

ARS JOURNAL is published monthly by the American Rocket Society, Inc. and the American Interplanetary Society at 20th & Northampton Sts., Easton, Pa., U. S. A. Editorial offices: 500 Fifth Ave., New York 36, N. Y. Price: $12.50 per year, $2.00 per single copy. Second-class mail privileges authorized at Easton, Pa. This publication is authorized to be mailed at the special rates of postage prescribed by Section 132.122. Notice of change of address should be sent to the Secretary, ARS, at least 30 days prior to publication. Opinions expressed herein are the authors' and do not necessarily reflect the views of the Editors or of the Society.

© Copyright 1960 by the American Rocket Society, Inc.

AN ANNOUNCEMENT OF BROAD SIGNIFICANCE TO

CHEMISTS, ENGINEERS & PHYSICISTS

WITH SPECIAL KNOWLEDGE OF SOLID FUEL & COMPONENT R&D

AMCEL
PROPULSION INC.
A New Subsidiary of
Celanese Corporation of America

NOW FORMING RESEARCH & DEVELOPMENT GROUPS TO INVESTIGATE PROPELLANTS & PROPULSION DEVICES

AMCEL is uniquely qualified to advance high energy fuel technology. It can draw upon Celanese's 35 years of research experience in organic chemicals, polymers and plastics. Years of experience in nitration techniques, organic chemicals and polymers provide a solid basis for growth in this field.

Initial research and development effort at AMCEL will be on solid fuel, fuel components and design of improved thrust chambers. Later, complete propulsion systems, auxiliary power units and related projects will be added to the roster.

The 1300-acre site includes a missile and rocket test-firing range, fully equipped manufacturing and assembly facilities and laboratory. The location (2300 feet above sea level), on the outskirts of the famous Asheville, North Carolina resort, offers professional people an opportunity to live in an exhilarating climate amid glorious scenery (half way between the Great Smokies and the Blue Ridge Mountains) where educational, cultural and recreational facilities are available far beyond the usual "small city" calibre.

Opportunities are now available to qualified engineers and scientists to become "founder members" and to initiate programs in the propellant field. Your inquiries are invited. Please address Mr. E. O. Whitman.

AMCEL PROPULSION INC.

P.O. BOX #3049 ASHEVILLE, NORTH CAROLINA

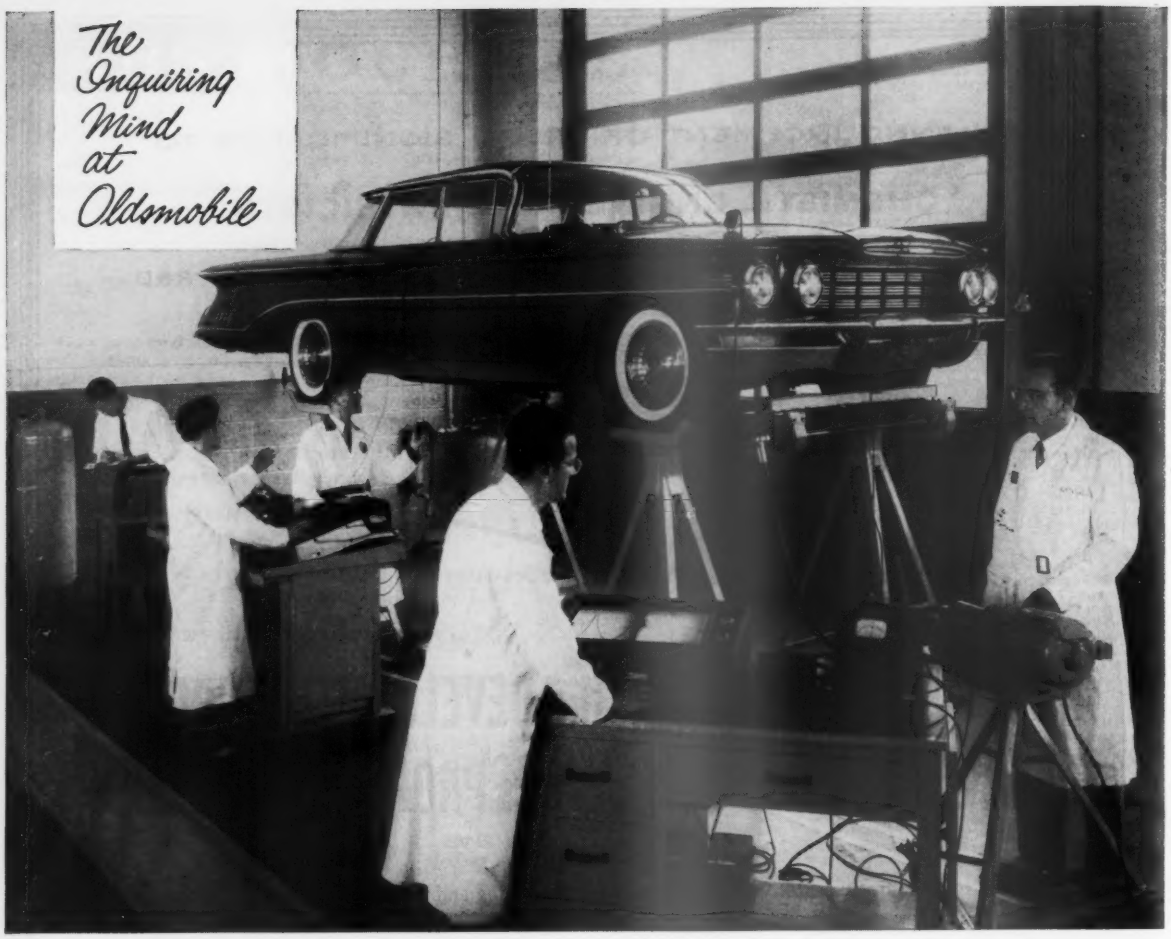

no. 10 OF A SERIES

IT'S THE QUIETEST RIDE YOU'VE EVER TRIED!

New Vibra-Tuned Body Mountings—electronically located at the nodal points of the frame by Oldsmobile engineers—produce an exceptionally quiet and satisfying ride.

Quietness in a fine automobile is a mark of superior quality. To make the 1960 Oldsmobile the quietest, most comfortable car on the road, Oldsmobile engineers have developed many advanced testing techniques to insulate against all types of road noise.

One of the unique ways in which noise and vibration are isolated by Oldsmobile engineers is through Vibra-Tuned body mountings. These mountings—direct attaching points between the body and frame—are critical to comfort and to the life of the car. If they are not properly placed, severe road vibrations can literally shake the car apart in a few thousand miles. But, by using the most advanced electronic measuring techniques, a softer and quieter ride is achieved by placing the body mounts at the nodal points of the frame. In this way, inherent road vibrations and shocks are practically isolated from the passenger compartment.

In the "tuning" of the chassis and body, the car is subjected to severe shaking, at a frequency of 7½ to 15 cycles per second, by a mechanical oscillator to produce torsional and bending moments. By using numerous electronic pick-ups, movement of the frame and body at a given point can be determined quickly and translated into an accurate magnitude vs. frequency curve through an X-Y plotter. By a complete and thorough examination of the entire car in such a manner, it can be determined where the "dead" or nodal points are on the frame, and the body mounts can then be scientifically placed. Then, after being located, the hysteresis characteristics of the body mounts are determined to give the most satisfying ride.

These methods, and many more up-to-the-minute techniques, have enabled Oldsmobile engineers to build consistently fine quality automobiles year after year. Visit your local authorized Quality Dealer and drive a 1960 Oldsmobile. See why it's the most satisfying car you've ever known . . . *the finest the medium-price class has to offer!*

OLDSMOBILE DIVISION • GENERAL MOTORS CORPORATION

OLDSMOBILE **Where Proven Quality Is Standard!**

Recent Advances in Condensed Media Detonations

S. J. JACOBS

U. S. Naval Ordnance Laboratory
Silver Spring, Md.

Dr. Jacobs is now a Senior Scientist in the Explosions Research Department, Naval Ordnance Laboratory, White Oak, Maryland. He received his B.Ch.E. from the University of Minnesota (1933) and the M.S. in Chemistry (1952). In 1942, he joined the staff of the Explosives Research Laboratory (CIT), Pittsburgh, to work on deflagration and detonation in condensed media. He joined the Naval Ordnance Laboratory in 1945 to establish a group to study detonation and related explosives problems. In 1950, he was sent by the Naval Ordnance Laboratory to the van der Waals Laboratory, University of Amsterdam for a year of study in Molecular Physics. His work there on "Rapid Expansion of Dense Gases" earned him the Ph.D. in Physics (1953). Since accepting his present position, Dr. Jacobs has directed his efforts to consulting and research in the fields of detonation hydrodynamics and propellant sensitivity.

"CONDENSED DETONATION" is used as a contraction of "Detonation of Liquids and Solids." The condensed substances which are detonable are more commonly referred to as explosives. It should be recognized that omission of the word "explosive" in referring to a compound or mixture does not imply inability to detonate. In this respect many, if not all, solid and liquid monofuels are detonable under given initial conditions when subjected to the necessary stimulus. As in gases a steady-state detonation in condensed media may be described as a supersonic wave of compression in which the release of chemical energy is triggered so rapidly that a wave corresponding to a state of complete or nearly complete reaction moves with it at the same speed. A distinction may be made between detonation and explosion by invoking the condition that detonations require the supersonic compression wave. The initiation of detonation may be defined as the process of establishing a compression wave which is of sufficient amplitude to induce a rapid reaction which will indirectly support a detonation.

The study of condensed detonations is not a field apart from that of detonation in gases. In this respect the survey by Gross and Oppenheim (1)[1] and the references therein can be taken as an introduction to the present subject. The most apparent difference between condensed and gaseous detonations is the result of the great difference in density of the media. Because of the higher density the products of the reactions can no longer be considered ideal gases. This leads to the requirement for knowledge of the equation of state for very dense states. The detonation pressures are a factor of 10^3 to 10^4 higher than for gases ($\sim 10^5$ atm). This leads to the usefulness of high explosives. But because the pressure is so high the experimental approach is markedly affected. In the study of condensed detonations it has become necessary to determine physical quantities largely by the wave and particle motions produced. The study of condensed detonations has therefore required a much wider use of hydrodynamic theory. It is not sufficient in this field to limit hydrodynamics usage to that of the conditions across the wave in steady-state one-dimensional (1-D) flows. The field of condensed detonations came of age when investigators came to the realization that detonation and the flow behind the wave was a compressible flow phenomena and that the broad picture required the use of all the knowledge of hydrodynamics. It was soon recognized that the solution of the hydrodynamic problems required fairly precise knowledge of the equations of state of not only the explosive media at very high pressure but also many other materials, gaseous, liquid and solid. The development of this knowledge through theoretical and experimental approaches and the coupling of this knowledge to hydrodynamic theory has given the researcher and theoretician some of the tools whereby they could more rigorously solve many problems concerning the detonation itself. The result of the advances already made has produced an awareness of new problems of greater complexity which remain for the future.

Received Nov. 25, 1959.

[1] Numbers in parentheses indicate References at end of paper.

Theory

The theory for 1-D steady detonations dates back over a half a century. The equations have been deduced in great detail so many times (2 to 6) that only the results will be given here for future reference. The equations will be written in the simplest form in which compositional changes in reaction products is neglected. If we use the definitions

D = shock velocity
u = particle velocity
c = sound speed

p = pressure
ρ = density in gm/cm³
e = energy per gm (pv energy)
q = energy released in reaction
$v = 1/\rho$ = specific volume
T = temperature
S = entropy
t = time
x = distance
0 = subscript for initial state
1 = subscript for final state
j = subscript for Chapman-Jouguet product states

then the equation of mass conservation becomes

$$(D - u_1)\,\rho_1 = (D - u_0)\,\rho_0 \qquad [1]$$

The equation for momentum is

$$p_1 - p_0 = (D - u_0)\,(u_1 - u_0)\,\rho_0 \qquad [2]$$

and the energy conservation law becomes

$$e_1 - e_0 - q = (p_1 + p_0)\,(v_0 - v_1)/2 \qquad [3]$$

Equation [3] is known as the Hugoniot relation. A dynamic p-v adiabat satisfying [3] is called a Hugoniot. When $q = 0$ the equations reduce to those for a pure shock. The shock discontinuity for $q = 0$ is assumed as a step jump but in actuality p, ρ and e are functions of position containing finite gradients resulting from the effect of viscosity and heat conduction. It has been demonstrated by Courant and Friedrichs (C-F) (2), that the results are the same if states 0 and 1 precede and follow the transition region. It is useful to examine Equations [1 to 3] in terms of a shock tube or piston model in which $u_0 = 0$ and state 1 corresponds to the uniform region between a piston driven at velocity u_1 and the wave of velocity D. In this model Equation [2] can be written as[2]

$$p_1 - p_0 = D\,u_1\,\rho_0 \qquad [2a]$$

and a new energy relation which reduced to Equation [3] can be written as

$$p_1 u_1 = (e_1 - e_0 - q + u_1^2/2)\,D\rho_0 \qquad [4]$$

Equation [2a] indicates that the piston must supply a force p_1 per unit area to retain the constancy of u_1 between the piston and a point at which reaction is complete. It is just Newton's second law of motion. The piston must therefore work at the rate $p_1 \cdot u_1$ to retain the steady flow behind the wave. In addition to the foregoing equations there will be equations of state, $p = p\,(\rho, T)$, and energy or caloric equations of state $e = e\,(p,\rho)$ for any state. The sound speed for any state is given by $c^2 = (dp/d\rho)_s$. For the case $u_0 = 0$, Equations [1 and 2] give

$$D^2 = v_0^2\,(p_1 - p_0)/(v_0 - v_1) \qquad [5]$$

In a p-v diagram Equation [5] is a straight line passing through v_0, p_0 for any value of D. This is often called the Rayleigh line.[3] If the caloric equation of state is substituted into Equation [3] a number of Hugoniots will result dependent on the value of q. Of greatest interest are the Hugoniots, $H(0)$ for $q = 0$ and $H(1)$ for $q = q_1$. The intersection of the Rayleigh line with these curves defines the states that can be steady for zero reaction and complete reaction for any value of D. For normal Hugoniots (the only type experimentally found) the intersection of the Rayleigh line with the $H(0)$ curve always is of higher pressure and lower specific volume than that for the $H(1)$ curve. There is always a minimum value of D for intersecting the $H(1)$ curve, a point of tangency. In the Chapman-Jouguet (C-J) theory this minimum is postulated as the solution for the steady detonation. There is a nice hydrodynamic argument for this postulate given by Brinkley and Richardson (10,11). The tangency to $H(1)$ is equivalent to

$$u_1 + c_1 = D \qquad [6]$$

In the presence of rarefactions which move at speeds c relative to the medium only detonations satisfying Equation [6] will remain unaffected by the rarefactions which follow. All higher values of D require additional force and work from a supporting piston to maintain constancy. Until von Neumann (7), Zeldovich (8) and Doering (9) there was considerable vagueness about the states through the reaction. These authors showed that a detonation could be treated as a shock followed by a hydrodynamic deflagration in which pressure was decreased along the Rayleigh line to satisfy the steady-state condition [see (2) for discussion]. This argument assumes that the shock transition is complete before reaction becomes appreciable. The assumption concerning decoupling of shocks from reactions in gases was investigated by Hirschfelder. The result, reviewed in (1), shows the possibility that decoupling is not complete. Despite the coupling argument the von Neumann theory remains of great significance as it continues to supply a logical hydrodynamic link between shocks in reactive media and detonations. The Hirschfelder argument adds the effect of viscosity and heat conduction to make the theory more complete.

The first major problem of condensed detonations has been the theoretical and experimental solution of Equations [1 to 6], thus determining the system of seven unknowns. Thus three of the seven unknowns must be determined through additional information. This can be attained theoretically once the caloric equations of state and q are known. Experimentally the measurement of 2 parameters of the set D, u_1, c_1, ρ_1 and p_1 determine the others and $e = e_1 - e_0 - q$ which often is sufficient. We will first consider the theoretical approach to this problem in which experimental observations of detonation velocity vs. initial density are used to substantiate the results.

Properties of Detonation Products

Prior to 1940 the field of explosive detonation was largely empirical. Even the difference between high explosives and solid propellants and the relative impulse of explosives was described by an empirical measure called "brissance," defined by the dent which a given charge could punch into a massive steel block. The first important physical measurement was the detonation velocity [see Taylor (4) for history]. Solid explosives like TNT were found to propagate high pressure waves at velocities in the range 4000 to 8000 m per sec. For a given explosive in large diameter cylinders the rate of detonation is very nearly a linear function of the initial bulk, or loading density, ρ_0

$$D = D_{1.0} + M(\rho_0 - 1) \qquad [7]$$

Work since the early forties confirmed this result for many explosives (19). Demonstration that the $D(\rho_0)$ relation was the result of departure from ideal gas behavior made Equation [7] the chief experimental fact for determining pressure, density and particle flow for many years.

Work since the early forties was pursued with great mathematical detail. The objectives were: 1—To determine physical and chemical properties behind the wave as a function of explosive composition and density; 2—to obtain necessary isentropic expansion data for the solution of flow problems with given initial boundary conditions. Literature in the fields of thermodynamics, statistical mechanics and quantum mechanics and in particular the reports on the equation of state of dense gases, liquids and solids were put to use.

[2] For condensed media at 1 atm, $p_0 \ll p_1$ and can be neglected.
[3] Historically Rankine should be credited with this result (12).

Table 1 f and g for Equation [8]

f		g
$(1 - b\rho)^{-1}$	van derWaals	$-a\rho^2$
$(1 - b\rho)^{-1}$	Abel (Schmidt, Langweiler)	0
$[1-\rho\alpha(v, T)]^{-1}$	Abel or $\alpha(v)$ (Cook)	0
$1 + x \exp(\beta x)$	Halford-Kistiakowsky-Wilson[a]	0
$1 + x \exp(x)$	Becker[b]	$-a\rho^2+h\rho^7$
C/ρ	Jones (dense states)	$aA \exp(-a/\rho)-B$
1.0	Jones (moderate density)	$\rho(bp+cp^2+dp^3)$
$1+x+0.625x^2+0.287x^3+0.193x^4$	Modified Boltzmann (Patterson)[b]	0
4.0	Landau (Zeldovich)	$a\rho^3$

[a] $x = \rho k T^{-\alpha}$; $\beta = 0.3$; $\alpha = 0.25$.
$x = \rho k(T + \theta)^{-\alpha}$; $\beta = 0.09$; $\alpha = 0.5$; $\theta = 400$ K.
[b] $x = b\rho$.

When the problem of the state of detonation products is attacked in a general way a large number of auxiliary equations arise for determining the composition, temperature and energy. The exact form of these expressions and the results of computations depend on the equation of state selected. This accounts for the emphasis on equation of state and the variety of results in the detonation literature on product properties. Equations of state are usually found to fit the general form

$$p = nRT\rho f(\rho, T) + g(\rho, T) \qquad [8]$$

In very dense states $RT\rho f$ represents the effect of the vibrational energy of the molecules (or atoms) on pressure while g relates to the contribution of positional forces between these particles. When the state is less dense f represents the deviation from ideal gas behavior due to the finite volume of the molecule. It describes the increase in collision frequency due to the reduction of the mean free path. A comparison of some of the equations used in detonation studies is shown in Table 1.

Schmidt (13) and Langweiler (14) used the Abel equation with assumed constant co-volume b. When they solved for b using available detonation data it was found to be a function of loading density and therefore of the final density and possibly temperature. The result should have led to a reappraisal of the solution since a variable b changes the answer. This was left for later workers. Patterson (15,4) used a theoretical equation of state equivalent to a variable co-volume. It was derived originally by Boltzmann for a gas consisting of rigid spherical molecules. The equation had been verified by Majumdar (16) in the virial form shown and modified by Hirschfelder and Roseveare (17) to fit an equation considered applicable to liquid density. Co-volume parameters b were derived from high temperature values for each molecular species and treated as constants, see (4). In the use of this equation all necessary data were determined without reference to detonation experiments. Therefore a priori calculations of detonation velocity could be made for any condensed explosive. Calculated detonation velocities are in rather good agreement with experiment. Cook (18,19) used the variable co-volume $\alpha(v,T)$ in an Abel equation to obtain the correct formal solution for the detonation state. Using arguments concerning the internal energy (which determines the dependence of α on T) he concluded that the co-volume would not depend greatly on T. This permitted his determining α as a function of v from the density effect on detonation velocity only. From this value of α other properties may be determined. The co-volumes for many compositions when plotted against volume were shown to fall very nearly on one curve. For explosives containing C, H, N and O only, the imperfection term f of Equation [8] from the experimental data is quite close to that of the Boltzmann equation with an appropriate value of b. The analysis has included several high density explosives containing lead and mercury. Although these appear to extend the universal $\alpha(v)$ curve they introduce anomalous results when considered in terms of $f(\rho)$. The latter is found to have a maximum from Cook's data in the range $v=0.4$ to 0.25 gm/cm^3. This would indicate the general $\alpha(v)$ curve is inapplicable to the description of the states of an organic explosive at high density ($\rho > 2.5$).

Jones (20,6) solved the state problem for TNT by a different approach. He first assumed a solid state model to determine constants for equations as shown in Table 1 using Bridgman's data for nitrogen. His prediction of the detonation velocity by this direct approach was about 15 per cent high. Jones and Miller (21) later used their second equation (Table 1) with slightly different constants to determine the isentrope connected to the computed detonation pressure and density. Brown (22) discussed the equation of state for detonation products and arrived at a form in which f of Equation [8] is given by the result of Hirschfelder and Roseveare while g relates to a result of Leonard-Jones and Devonshire (23). The approach looks promising but no results are given to compare with other work. An extensive computation of the detonation state on the basis of $D(\rho_0)$ data for many condensed explosives was instigated by Kistiakowsky and Wilson (24) with the assistance of Halford. The work was continued by Brinkley and Wilson (25). The equation of state appears in Table 1. The constants of the equation were fit to experimental D vs. density data to get best agreement between experimental and calculated velocities for a large number of materials. Since the original work this equation has had many revisions as new data became available. The last is due to Cowan and Fickett (26) who had the benefit of a few experimental pressure measurements for their effort. Their result for isentropic expansion and shock reflection from the C-J state has been successfully employed in hydrodynamic problems. Because of the variable co-volume parameter the H-K-W equation gives an internal energy term as does Jones. The temperatures are lower than those obtained by Patterson and Cook because of this internal energy term. Snay and Christian in an unpublished report (27) have re-evaluated k's for gas molecules and systematized the calculation procedure. Isentropes computed with the revised co-volumes result in good agreement between underwater shock predictions and experimental results.

An ingenious approach to the detonation pressure was advanced by Jones (28). He started with the Hugoniot equation, the equation for the Rayleigh line and the condition $D=D(\rho_0)$. The Hugoniot and Rayleigh lines were generalized as surfaces in a three-dimensional space of coordinates p, $v=1/\rho$, $z=1/\rho_0$). The Chapman-Jouguet condition requires that the surfaces be tangent along some line in this space. The condition of tangency gives in addition to previous results a new equation which can be expressed as

$$\frac{D}{u} = (2 + \alpha)\left(1 + \frac{d \ln D}{d \ln \rho_0}\right) \qquad [9]$$

The last term is just $(\rho_0/D)M$ if we assume $D(\rho_0)$ given by

Equation [7]. The term α contains essentially all the thermodynamics of the problem. It is defined by Jones and shown to be greater than 0 and much less than 2. The value of Equation [9] lies in this fact. Jones shows that one can estimate the detonation pressure quite accurately from Equations [9 and 2a] by assuming α as a constant having a value of about 0.25. Computations of pressure based on this result are generally quite close to measured values.

A number of papers on equations of state using solid or liquid state models for the dense state have appeared since 1950. Of particular interest is the solid state approach of Parlin and Giddings (29). They have discussed the problem of using a lattice model with atoms at lattice sites, and show how it can be reconciled with an assumption of the existence of molecular species. They also show the resemblance between the oscillator frequencies of a lattice model and the collision frequencies of a gas at low density. Other interesting approaches are the hydrogen molecule-ion analog of Cottrell and Patterson (30), the virial form based on a Leonard-Jones ninth power repulsion term by Kihara and Kikita (31), and the study of the use of various interatomic potentials by Fickett, Wood and Salsburg (32). Recently Fickett and Wood (33) have analyzed the new isentrope of Deal (34) in terms of a variable gamma equation for the expansion. Implications of the experiment concerning internal energy of the gas is discussed. In a recent paper Zeldovich et al. (35) have mentioned an equation credited to Landau and Staniukovich (36) for describing the state behind a condensed detonation. It is shown in Table 1 and quite clearly is based on solid state concepts. Another recent study of the equation of state is given by Smith and Alder (37).

By way of summary one finds: 1—That irrespective of the method of approach most calculations of detonation pressure fall into a range of about ±10 per cent. 2—For organic solids of crystal density, ρ_0 about 1.6–1.7 gm/cm^3, the ratio D/u is very nearly 4. 3—The isentropes given by Jones and by the H-K-W equation can be expressed by a gamma law equation

$$\frac{p}{p_j} = \left(\frac{\rho}{\rho_j}\right)^{\gamma} \qquad j = \text{C-J value} \qquad [10]$$

with gamma in the vicinity of 3.0. Equation [10] is acceptable for hydrodynamic usage down to about 1 per cent of detonation pressure. Better results require the initial equations normalized to experimental data. 4—In regard to temperature and composition, agreement is unsatisfactory. The objective to determine chemical properties has not been reached to everyone's satisfaction. 5—Use of solid state models, in which transition to gaseous states is taken into account in the theory, offer promise in gaining a better understanding of the real conditions behind detonation waves in condensed media.

Theoretical Hydrodynamics

The first attempt to solve a hydrodynamic problem for a condensed detonation was published in 1938 by Langweiler (14). It was an approximate solution of the rarefaction following a detonation in a closed tube (the piston problem of the section on theory, with piston at rest). He noted (see Eq. [4]) that the piston had to do work to maintain a uniform state, 1. Since detonations in solids are more akin to a piston at rest he argued that the work must come from expansion of the product gases. To solve the problem he assumed a rarefaction discontinuity which moved slower than the detonation. This led to the assumption of a detonation head of constant pressure which increased linearly with time. The solution is in error because rarefactions spread and the initial pressure decay must move at $u_1 + c_1$ which is the detonation velocity for a C-J detonation. The real beginning of complete hydrodynamics solutions of detonation problems occurred when Taylor (38) gave the correct solution to this problem for both polytropic gases and for TNT using Jones' isentrope.[4] Pfriem (39) obtained the same solution for polytropic gases at almost the same time. Taylor has also solved the case for a spherically expanding detonation. The latter solution was used by Penney and Dasgupta (40) to compute by the method of characteristics the shock transmitted into water. This is the first direct solution of a boundary value problem for an explosive. These problems are discussed by Cole (6) together with several others, by Bethe and Kirkwood, and Kirkwood and Brinkley on shocks generated in water by condensed explosives. Hill and Pack (41) solved the first two-dimensional steady-state problem for condensed media. This is the problem of the Prandtl-Meyer flow behind a detonation in a finite slab of explosive. The problem was solved to show the pressure distribution and the lateral air shock developed by the wave using Jones' isentrope for TNT. The solution for an ideal gas is given by Doering and Burkhardt (42). The results agree in the general contour of the pressure decay along the plane of symmetry. Both results show rarefaction to begin, as expected, on the detonation front since on this plane the Mach number for the flow is 1.

An important contribution to the study of condensed detonations was made when Courant and Friedrichs (2) published their analysis and literature survey on "Supersonic Flow and Shock Waves." This work awakened explosives investigators to the realization that many detonation problems find their counterpart in the examples of compressible flow phenomena in gases. This work introduces the areas of compressible flow which are pertinent to the exact solution of detonation problems. The extensive use of fluid dynamics in recent papers on condensed detonation attests to its importance.[5] Since the work of C-F a number of other books useful to the study of condensed detonations have appeared. One is "The Dynamics and Thermodynamics of Compressible Fluid Flow" (43). It is of interest for its treatment of the method of characteristics for 1-D transient and 2-D steady flows. The series "High Speed Aerodynamics and Jet Propulsion" (44) adds many useful concepts on the solution of hydrodynamic problems.

The solution of hydrodynamic problems in condensed detonation has been greatly facilitated in recent years by the developments in high speed computers. For this reason the work of von Neumann and Richtmeyer (45) on numerical solutions of shock problems and the book by Richtmeyer (46) must be considered part of the literature of this field. An example of the use of the von Neumann-Richtmeyer scheme is the solution of the air shock effects generated by a spherical charge detonated at its center [Brode (47)]. This problem was first solved by Wecken [see Schardin (48)] by the characteristic method. Both Wecken and Brode have shown the generation of a second shock in the air. This had been observed experimentally before but its source was not previously understood. New approaches to the numerical solutions of flows with shocks are given by Lax (49) and Ludford, Polachek and Seeger (50). A discussion of the solution of unsteady 2-D hydrodynamic problems is given by Kolsky (51). Recently the use of hydrodynamics with re-

[4] In this and most hydrodynamic solutions the reaction is assumed to occur instantaneously in the detonation wave. Since the zone of reaction is usually small the error is not great.

[5] It is pertinent here to note that about 1945 investigators began to realize that the isentrope for expansion of gases from solid explosives at or near crystal density could be quite well approximated by the polytropic gas equation in which "gamma" is about 3. Thus all of the polytropic gas results of C-F and others can be applied with reasonable accuracy to describe flows behind detonation waves. In addition it has been found that a "polytropic form" $p + A = A(\rho/\rho_0)^{\gamma}$ known as the Tait equation can be used to describe the compression of solids and liquids. For many problems the results of the Tait equation are the same as for the polytropic gas. The major difference is that density and sound speed do not go to zero at zero pressure. One can also use the gamma law as an energy equation, $e = pv/(\gamma - 1)$ to solve problems of reflected shocks in detonation products.

action kinetics has begun to explain some of the problems of shock initiation. This will be discussed in the section on "Initiation of Reaction in Detonations."

Experimental Hydrodynamics

About 1942 Schall employed a new submicrosecond flash radiograph technique to determine the density increase behind a detonation in a small charge of TNT. For an initial bulk density of 1.50 he found an increase of 22 per cent. This indicates u_1/D to be 0.18 for D taken as 6500 m/sec. The pressure then becomes 115 kilobars.[6] The result is about 20 per cent low but was very good for that early date. The error is probably due to neglect of rarefaction behind the wave. More recent work of Schall on flash x-ray techniques, detonations and shocks is found in (52–55).

About 1945 Goranson (56) [see (57,58)] proposed a method to determine the particle velocity in a detonation through the use of the measured shock and initial free surface velocity induced in a metal target impacted by a normally incident plane detonation wave. He showed that for most metals at the pressure levels involved the initial free surface velocity of the metal would be very nearly twice the prior particle velocity in the metal. Thus it was possible through these observable velocities to determine the density change and pressure in the shocked metal. By a solution of the boundary conditions for a detonation (treated as a shock followed by a rarefaction) impacting the metal he obtained an approximate value for the detonation pressure. The approximation made could have led to an error of about 2–4 per cent. An improvement of the boundary solution reduces this error to less than the error in measuring the velocities. The shock and initial free surface velocities were determined by transit time measurements using electrical contacts and oscillograph recording. Goranson and his co-workers measured these quantities as a function of target thickness (care being taken to avoid the inclusion of second wave effects on the free surface velocity) and found the free surface velocity vs. thickness curve to have an inflection at some value x_0. Between the minimum measurable x and $x = x_0$ the slope was quite steep. For $x > x_0$ a lower slope was found. The inflection, which is unmistakable in a series of experiments, can be related to the change in pressure at the explosive interface. Such inflection in the detonation wave had already been predicted by von Neumann. Thus Goranson's experiment establishes through hydrodynamic reasoning the ability to determine four important details of condensed detonations: 1—Pressure and density in shock compressed metals over a wide range of pressure hitherto unreachable, 2—the pressure, density and other parameters in the detonation state, 3—the existence and approximate magnitude of the over-pressure in the reaction zone predicted by the von Neumann theory, and 4—an approximate measure of the reaction time between a detonation shock and the C-J plane. The contribution of Goranson and those who followed him are of great significance in furthering our understanding of condensed detonations.

The first published data on the equation of state of metals at high pressure was that of Pack, Evans and James (65). Shortly thereafter Walsh and Christian (59) published their first results on aluminum, zinc and copper to 500 kilobars. They used the approach first employed by Goranson but simplified the technique by using a smear camera to measure shock and free surface velocity of the metals. The relation between free surface velocity and particle velocity in the target is discussed. It is shown that in this pressure range $u_{fs} = 2\,u_p \pm 2$ per cent. A correction can be made for this difference. Hugoniots were obtained by use of the conservation equations for shocks. Twenty-degree isotherms were also determined. Goranson and co-workers (58) have discussed the shock compression of metals and have supplied data on aluminum, cadmium and steel. The latter exhibits an elastic wave velocity at force per unit area below 15 kilobars. The measurements were made by two methods: 1—Pin-oscillograph for shock and free surface measurement, and 2—direct pressure measurement by use of a z-cut tourmaline crystal. The results of the two methods are in agreement to about 4 per cent. In later papers Walsh et al. (60) gave data for shock compression of 27 metals to about 600 kilobars and discussed the results in terms of the Mie-Gruneisen equation of state for metals. This work is summarized in (61). Other work on the compressibility of metals below one megabar is to be found in (62–67). Two recent papers by Al'tshuler and co-workers (68,69) have appeared in *Soviet Physics-JETP*. They discuss the dynamic compression of metals to about 5 megabars, using both the free surface velocity method and an impact or reflected wave method. In the latter the assumption of doubling of particle velocity at the free surface is unnecessary when a driver is of the same material as the target. These authors show that for most solids the free surface assumption $u_{fs} = 2\,u_p$ is valid to a density ratio of about 1.4 in the shock. They show experimental agreement between the two methods for steel well over 1 megabar.

Of particular interest to the study of the shock initiation of explosives is the work by Walsh and Rice (70) on the dynamic compressibility of liquids. In this work aluminum was used as a driver of known pressure, shock and particle velocity. The shock velocity induced by the driver permits determination of the pressure and particle velocity in the unknown. The equation of state for water to 250 kilobars is discussed in detail (71). The transmitted shock method has been used by Garn (72) to determine points on the unreacted Hugoniot for liquid TNT in the range 44 to 110 kilobars. Between 110 and 165 kilobars detonation developed in the sample whose thickness was 3.8 mm. Majowicz and Jacobs (73) studied the unreacted Hugoniot for several solid explosives in the range 80 to 120 kilobars by the transmitted shock method. They used a wedge of the unknown so that the observation of shock velocity could be extrapolated to the driver interface, thus permitting observation of effects due to onset of reaction as well. Flash radiographic techniques have been used by Vodar et al. (101,102) to measure the shock compression of a number of substances. Among the materials studied were liquid argon and oxygen, water and Plexiglas.

A technique for the precise measurement of detonation velocity is discussed in a paper by Campbell et al. (99). Results of the effect of particle size and density on detonation velocity by this method are described in (100). The detonation pressure of cast Composition B at $\rho_0 = 1.67$ has been determined by Duff and Houston (57) to be 271 kilobars using the target method of Goranson. Their results show clear evidence of the overpressure predicted by von Neumann. Reaction distance was estimated to be 0.13 mm in the wave. The pressure profile in the reaction zone is not determined with any great certainty due to the difficulty of obtaining measurements for thin targets. Detonation pressure for cast Composition B,[7] TNT and RDX are given by Deal (74). His method was somewhat less accurate than Duff's for determining reaction zone effects but of comparable accuracy for detonation pressures. In a recent paper Deal (34) has given the isentropic expansion and shock compression curve for products of Composition B over a range of about 0.5 to 600 kilobars. He states the results to be in agreement with a polytropic gas equation with a gamma of 2.77. Reported C-J pressure for $\rho_0 = 1.714$ gm/cm^3 is 290 kilobars, probably the most reliable result at this time. His previous result was 293 kilobars. When corrected for density effect the result is found to be about 3 per cent higher than that

[6] 1 kilobar = 10^9 dynes/cm^2 = 987 atm.

[7] Composition B is a mixture of RDX (cyclotrimethylene trinitramine), TNT (trinitrotoluol) and Wax in the approximate weight ratio, 60/39/1.

of Duff. The Jones relation (Eq. [9]) gives Deal's result to within 1 per cent.

The pressure and density at the C-J point do not give information on the relation between thermal and internal energy in detonation products. This could be estimated if the temperature could be measured. Gibson (75) has attempted this measurement by observation of the radiation through a transparent rod embedded in the detonating charge. The results are not completely satisfying since the effect on the observed radiation of the boundary between explosive and the rod is not established. Confirmation of the results by methods which avoid this potential source of error is needed.

Initiation of Reaction in Detonations

The initiation of explosive-like materials can be divided into two areas of study. Reaction can be started by relatively weak energy stimuli such as thermal sources, friction, mild impact, sparks and radiation. These stimuli usually cause only deflagrations. Studies of this type of initiation are to be found in the work of Bowden and his co-workers (79) and in a number of works presented at a symposium sponsored by the Royal Society under the leadership of Bowden (80). The development of true detonation is found to require shocks in the kilobar range. Once deflagration has developed it may generate sufficient compression in the remaining material to cause detonations to form. General discussions of this transition from burning, deflagration, to detonation (DDT) can be found in a paper by Kistiakowsky (76) and in one by Ubbelohde (77). The formation of shocks from deflagrations in nonporous media and the transition to detonation was recently discussed by Maček (78).

It has been found convenient to study the shock to detonation transition as a separate problem from shock buildup from deflagration. It is then treated as the final stage of a DDT process. This has been done because it is easier to control experiments involving only a shock source. In addition the phenomena involved can be analyzed without consideration of the shock source provided the shock amplitude and duration can be described. Muraour first suggested an experiment in which the initiation of detonation could be related to shock amplitude (81). Through the work of Hertzberg and Walker (93,5) and many others (82–85) the use of explosive generated shocks has been employed to develop a number of "gap sensitivity" experiments. In its most recent form a gap test employs a cylinder of explosive "donor" which is detonated to send a shock through an inert "barrier" made of paper, water, air or a solid. The shock is transmitted to a cylindrical test charge "acceptor." In a series of trials the barrier thickness "gap" is varied. A critical gap is found at which no detonation is observed in the acceptor. This critical gap is defined as the "gap sensitivity." Hertzberg found a sharp cutoff in the gap between detonation and failure. He also noted that smear camera records showed the detonation seemed to appear in the acceptor at an appreciable distance from the barrier. This distance increased with the gap. Later workers (80,85–90) have investigated this phenomenon in great detail using smear cameras, high speed framing cameras and electrical probes. The effect is seen very nicely in the framing camera photos of Cook et al. (86,19). The most accepted explanation of the effect involves hydrodynamics and chemical reaction rates. In this hypothesis the shock entering the acceptor initiates a chemical reaction at the barrier interface. The rate of this reaction is dependent on the shock amplitude. When reaction has developed sufficiently to release a substantial amount of energy the pressure at the interface will rise. This causes waves of compression to be sent into the acceptor behind the initial shock. In this wave reaction speeds up with distance and eventually the compression wave overtakes the shock. The shock accelerates as the result of reaction and compression and soon thereafter the shock strength becomes that of a detonation with reaction time correspondingly short behind this strengthened wave. If a greater gap is used the initial shock transmitted is weaker. As a consequence reaction is slower and the time and distance for development of the detonation increases. The usual geometry for the experiment employs rather small diameter charges. For weak shocks the diameter of the acceptor is small compared to the distance at which final detonation appears. Lateral expansion of the acceptor behind the primary shock can then cause pressure decay which competes with the compression wave and the transition process is slowed down. The use of larger donors and gap material make it possible to simplify the hydrodynamic problem. This was done by Cotter(91)[8] for nitromethane. Holland, Campbell and Malin(94) used a wedge made from a single crystal of PETN (pentaerythritol tetranitrate) as the acceptor and struck it with a plane shock. They found initially for their experimental conditions a shock (they called it low order detonation) transmitted at 5560 m/sec. After a few tenths of a microsecond the wave front accelerated to 10,450 m/sec and then decayed to the normal rate of 8280 m/sec. The entire phenomenon took about 1 to 2 μsec. Similar results have been obtained by Majowicz and Jacobs (73) for a number of cast and pressed explosives. In some cases the overshoot seen by Holland is observed, in others the velocity grows continuously from that of a shock to that of a normal detonation. The initial wave cannot very likely be other than a shock because its velocity depends on the pressure transmitted in the barrier. To cite two examples; in the case of cast composition B an initial velocity of 5060 m/sec (about 120 kilobars shock) increased to 6000 m/sec in 2 mm and 7990 m/sec, the detonation velocity, in 2.8 mm and remained at that value. For an initial shock velocity of 4410 m/sec (about 85 kilobars) it rose to 6000 in 5 mm and to 8000 in 6.0 mm where it remained. A pressed charge of composition B at 91 per cent of crystal density started with a shock velocity of 4600 m/sec, developed an overshoot of about 13,000 m/sec in 1.6 mm and then decayed to the normal velocity of 7900 m/sec at 2.1 mm. These results can be explained quite well by the use of hydrodynamic theory supplemented by reaction kinetics. Hubbard and Johnson (95) have set up a model for computing the transition from shock to detonation and have solved the 1-D hydrodynamic problem on a high speed computer with several reaction rate equations. They and Boyer, who is continuing the work, have found that by varying the assumed kinetics both experimental results, gradual buildup or overshoot, can be derived by computation. At present their equations of state are not the best available so the results do not fit the experiments other than in general appearance. An equation of state which correctly describes the temperature in the unreacted shock must still be established. An alternate hypothesis for the transition to detonation has been given by Cook et al. (86,97). That explanation agrees with the former in regard to beginning of reaction at the acceptor-barrier interface. For subsequent effects it postulates the formation of a metallic state of high thermal conduction behind the primary shock. After onset of reaction a heat pulse is said to flash across the interval between barrier and shock front where it causes rapid decomposition. The flash across, one of the mainstays of the hypothesis, has not been observed outside of the laboratories involved in this work. Other workers including the writer are inclined to believe the observed flash across reported on a liquid explosive to be evidence of a second shock in the liquid due to reaction. This shock would arrive at the free surface with a phase velocity much greater than the real value to produce the observed effect. The metallic state is not impossible but it would require many more mobile electrons than observed

[8] Chaiken (92) investigated nitromethane initiation and postulated a detonation in the shocked liquid to explain his results.

to have even a minor influence on thermal conduction. Moderately high electron density is more likely to affect reaction rates. The electrical phenomena observed by Cook deserve more experimental study to determine the role they play in condensed detonations.

Detonations in cylinders are known to have reduced propagation velocities at small diameters and to fail at some critical value of the diameter. These effects can be related to the dependence of the reaction time on shock strength as in the gap experiments. Lateral expansion can explain the reduction of initial shock strength at the axis as indicated in the approximate theories (96,5,19). A complete theory requires the solution of a transonic flow problem in which heat is added to the flow. Wood and Kirkwood (98) have discussed some aspects of this problem but have not treated it entirely. A comparison of two of the earlier theories with experiment is given in (100).

The gap experiment has been a convenient tool for determining the susceptibility of solids and liquids to detonation by shock. When these experiments are conducted in diameters of donor and acceptor of about 2 in. it is found that many materials will not detonate at even zero gap. In these instances it is clear that the diameter must be less than the failure diameter of the acceptor. Consequently experiments must be scaled to larger diameter to obtain a measure of the sensitivity. In these cases the failure diameter becomes an alternate measure of shock sensitivity. In recent years there have been attempts to correlate the results of gap and diameter effects to the potential detonability of a solid propellant in a rocket motor. For some materials the failure diameter has been found to be so large that it becomes unlikely that explosions of motors filled with these materials can be directly related to this extreme shock insensitivity. This indicates that other properties particularly rheological properties under moderate dynamic load may be dominant in determining the inherent safety of these fuels. In the study of propellant detonability the properties which lead to explosion short of detonation cannot be overlooked. The generation of strong shocks from deflagrations has not had the emphasis in the literature which it deserves.

Summary

The subject of condensed detonation can be seen to be very broad. In its recent evolution it has required the use of many disciplines. In its fluid dynamical aspects it seems to be following the course taken in aerodynamics. That field passed the stage of elementary problems over a decade ago and then turned to problems of boundary layers, transonic flow and other more difficult subjects such as magnetohydrodynamics. The hydrodynamics of detonation is also emerging from the realm of elementary problems. One may anticipate that problems in transonic flow and boundary flow will be attacked in particular for the understanding of the initiation of reaction. A considerable effort will have to be made to fully understand the properties of materials under high pressure. In this realm electrical effects have been observed (conduction and charge generation in dielectrics and explosives under shock loading) which will have to be understood. At the present time solids (including metals) are being considered with few exceptions as fluids when the compressions are large. This simplification has enabled the solution of many problems related to condensed detonation. There are many examples however in which this assumption does not lead to useful answers. Likewise the effect of prior compression on solid fuels and its relation to the transition to detonation problem is an area of considerable interest. The study of condensed detonation has solved many theoretical and applied problems. Many more are yet to be born. The bibliography given here is far from complete. The author believes it will serve as a guide to the extensive literature on the subject.

References

1 Gross, R. A. and Oppenheim, A. K., "Recent Advances in Gaseous Detonations," ARS JOURNAL, vol. 29, no. 3, March 1959, pp. 173–179.

2 Courant, R. and Friedrichs, K. O., "Supersonic Flow and Shock Waves," Interscience Publishers, Inc., N. Y., 1948.

3 Lewis, B. and von Elbe, G., "Combustion, Flames and Explosions of Gases," Academic Press, Inc., N. Y., 1951.

4 Taylor, J., "Detonation in Condensed Explosives," Clarendon Press, Oxford, Eng., 1952.

5 Eyring, H., Powell, R., Duffy, H. and Parlin, R. B., "The Stability of Detonation," *Chem. Revs.*, vol. 49, no. 1, 1949, pp. 61–181.

6 Cole, R. H., "Underwater Explosions," Princeton Univ. Press, Princeton, 1948.

7 von Neumann, J., "Theory of Detonation Waves," OSRD Rep. no. 549, 1942.

8 Zeldovich, Y. B., "Theory of Propagation of Detonations in Gaseous Systems," *J. Expil. Theoret. Phys. (USSR)*, vol. 10, 1940, p. 542.

9 Doering, W., "Uber der Detonations-vorgang im Gasen," *Ann. Physik*, vol. 43, 1943, p. 421.

10 Brinkley, S. R. and Richardson, J. G., "On the Structure of Plane Detonation Waves with Finite Reaction Velocity," in "Fourth Symposium on Combustion," Williams and Wilkins Co., Baltimore, 1953, pp. 450–457.

11 Brinkley, S. R. and Richardson, J. G., "On the Condition of Stability of the Plane Detonation Wave," in "Third Symposium on Combustion Flames and Explosions," Williams and Wilkins Co., Baltimore, 1949, pp. 586–590.

12 Lamb, H., "Hydrodynamics," Cambridge Univ. Press, 1932; Dover Publications, Inc., N. Y., 1945.

13 Schmidt, A., "Uber die Detonation von Sprengstoffen und die Beziehung Zwischen Dichte und Detonationsgeschwindigkeit," *Z. für das Gesampte Schiess und Sprengstoffwessen*, vol. 30, 1935, p. 364; vol. 31, 1936, p. 8.

14 Langweiler, H., "Beitrag zur Hydrodynamischen Detonations Theorie," *Z. für Technische Physik*, vol. 19, 1938, pp. 271–283.

15 Patterson, S., "Hydrodynamic Theory of Detonation, Part II, On Absolute Calculation for Condensed Explosives," *Research*, vol. 1, 1948, p. 221.

16 Majumdar, R., "On the Equation of State," *Bull. Calcutta Math. Soc.*, vol. 21, 1929, p. 107.

17 Hirschfelder, J. O. and Roseveare, W. E., "Intermolecular Forces and the Properties of Gases," *J. Phys. Chem.*, vol. 43, 1939, p. 15.

18 Cook, M. A., "An Equation of State for Gases at Extremely High Pressure and Temperature from the Hydrodynamic Theory of Detonation," *J. Chem. Phys.*, vol. 15, no. 7, 1947, p. 518.

19 Cook, M. A., "The Science of High Explosives," Reinhold Publishing Corp., N. Y., 1958.

20 Jones, H., British Reps. RC-166, RC-212, 1941 (not available). See (4, 6 and 21) for results.

21 Jones, H. and Miller, A. R., "The Detonation of Solid Explosives," Proc. Roy. Soc. London, vol. A-194, 1948, p. 480.

22 Brown, F. W., "Theoretical Calculations for Explosives, II, Explosion Pressures," U. S. Bureau of Mines, Tech. Rep. no. 643, 1942; "I," Tech Rep. no. 632, 1941.

23 Leonard-Jones, J. E. and Devonshire, A. F., "Critical Phenomena in Gases—I," Proc. Roy. Soc. London, vol. A-163, 1937, p. 53.

24 Kistiakowsky, G. B. and Wilson, E. B., "The Hydrodynamic Theory of Detonation and Shock Waves," OSRD no. 114, 1941.

25 Brinkley, S. R. and Wilson, E. B., "Revised Method of Predicting the Detonation Velocities in Solid Explosives," OSRD no. 905, 1942.

26 Cowan, R. O. and Fickett, W., "Calculation of the Detonation Properties of Solid Explosives with the Kistiakowsky-Wilson Equation of State," *J. Chem. Phys.*, vol. 24, no. 5, 1956, pp. 932–939.

27 Christian, E. A. and Snay, H. G., "Analysis of Experimental Data on Detonation Velocities," Naval Ordnance Rep. no. 1508, 1951 (classified, not available).

28 Jones, H., "Properties of Gases at High Pressures—Deduced from Explosion Experiments," in "Third Symposium on Combustion Flame and Explosions," Williams and Wilkins Co., Baltimore, 1949, p. 590.

29 Parlin, R. B. and Giddings, J. C., "A Solid State Model for Detonation," 2nd ONR Symposium on Detonation, Washington, D. C., Feb. 1955.

30 Cottrell, T. L. and Patterson, S., "Equation of State Applicable to Gases at Densities Near that of Solid and Temperatures Far Above Critical," Proc. Roy. Soc. London, vol. A-213, 1952, p. 214.

31 Kihara, T. and Kikita, T., "Equation of State for Hot Dense Gases and Molecular Theory of Detonation," in "Fourth Symposium on Combustion," Williams and Wilkins Co., Baltimore, 1953, p. 458.

32 Fickett, W., Wood, W. W. and Salsburg, Z. W., "Investigation of the Detonation Properties of Condensed Explosives with Equations of State Based on Intermolecular Potentials. I. RDX with Fixed Produce Composition," *J. Chem. Phys.*, vol. 27, no. 6, 1957, p. 1324.

33 Fickett, W. and Wood, W. W., "A Detonation Product Equation of State Obtained from Hydrodynamic Data," *Phys. Fluids*, vol. 1, no. 6, 1958, pp. 528–534.

34 Deal, W. E., "Measurement of the Reflected Shock Hugoniot and Isentrope for Explosive Reaction Products," *Phys. Fluids*, vol. 1, no. 6, 1958, pp. 523–527.

35 Zeldovich, Ia. B., Kormer, S. B., Sinitsyn, M. V. and Kuriapin, A. I., "Temperature and Specific Heat of Plexiglas under Shock Wave Compression," *Soviet Phys. Doklady*, vol. 3, no. 5, 1958, pp. 938, 939.

36 Landau, L. D. and Staniukovich, K. P., *Doklady Acad. Nauk SSSR*, vol. 46, no. 9, 1945, p. 362.

37 Smith, E. B. and Alder, B. J., "Perturbation Calculations in Equilibrium Statistical Mechanics. I. Hard Sphere Basis Potential," *J. Chem. Phys.*, vol. 30, no. 5, 1959, pp. 1190–1199.

38 Taylor, G. I., "The Dynamics of the Combustion Products Behind Plane and Spherical Detonation Fronts in Explosives," Proc. Roy. Soc. London, vol. A-200, 1950, p. 235; from British Rep. no. RC-178, 1941 (not available).

39 Pfriem, H., "The Stationary Detonation Wave in Gases," *Forschung auf dem Gebiet des Ing. Wissenschaften*, vol. 12, 1941, p. 143.

40 Penney, W. G. and Dasgupta, H. K., British Rep. no. RC-333, 1942. See (6) for results.

41 Hill, R. and Pack, D. C., "An Investigation by the Method of Characteristics of the Lateral Expansion of the Gases Behind a Detonating Slab of Explosive," Proc. Roy. Soc. London, vol. A-191, 1947, p. 524.

42 Doering, W. and Burkhardt, G., "Contributions to the Theory of Detonation," Wright-Patterson AFB Tech. Rep. F-TS-1227 (GDAM 9-T-46). Translation released May 1949.

43 Shapiro, A., "The Dynamics and Thermodynamics of Compressible Fluid Flow" (2 vols.), Ronald Press Co., N. Y., 1953–1954.

44 "High Speed Aerodynamics and Jet Propulsion," 12 vols., Princeton Univ. Press, Princeton, 1950–1958.

45 von Neumann, J. and Richtmeyer, R. D., "A Method for the Numerical Calculation of Hydrodynamic Shocks," *J. Appl. Phys.*, vol. 21, 1950, p. 232.

46 Richtmeyer, R. D., "Difference Methods for Initial Value Problems," Interscience Publishers, Inc., N. Y., 1957.

47 Brode, H. L., "Blast Wave from a Spherical Charge," *Phys. Fluids*, vol. 2, no. 2, 1959, p. 217.

48 Schardin, H., "Measurement of Spherical Shock Waves," *Communs. Pure and Appl. Math.*, vol. 7, 1954, pp. 223–243.

49 Lax, P. D., "Hyperbolic Systems of Conservation Laws II," *Communs. Pure and Appl. Math.*, vol. 10, no. 1, 1957, p. 537.

50 Ludford, G., Polachek, H. and Seeger, R. J., "On Unsteady Flow of Compressible Viscous Fluids," *J. Appl. Phys.*, vol. 24, no. 4, 1953, p. 490.

51 Kolsky, H. G., Unclassified Los Alamos Rep. no. LA-1867, 1955.

52 Schall, R., "Rontgenblitzrohre in Betrieb und Anwendung," *Arch. Tech. Messen*, no. 74-13, May 1953, pp. 117–120.

53 Schall, R., "Flash X-ray Experiments on Non-ideal Detonation Waves," *Z. Angew. Physik*, vol. 4, no. 8, 1952, pp. 291–293.

54 Schall, R., "Equation of State of Water at High Pressures by Flash Radiography of Strong Shocks," *Z. Angew. Physik*, vol. 2, no. 6, 1950, pp. 252–254.

55 Schall, R., *Z. Electrochem.*, vol. 61, 1957, p. 629.

56 Goranson, R. W., Los Alamos Classified Rep. LA 487, 1945 (not generally available).

57 Duff, R. E. and Houston, E., "Measurement of the C-J Pressure and Reaction Zone Length in a Detonating High Explosive," 2nd ONR Symposium on Detonation, Washington, D. C., Feb. 9–11, 1955; *J. Chem. Phys.*, vol. 23, 1955, pp. 1268–1273.

58 Goranson, R. W., Bancroft, D., Burton, B. L., Blechar, T., Houston, E., Gittings, E. and Landeen, S. A., "Dynamic Determination of the Compressibility of Metals," *J. Appl. Phys.*, vol. 26, 1955, pp. 1472–1479.

59 Walsh, J. M. and Christian, R. H., "Equation of State of Metals from Shock Wave Measurements," *Phys. Rev.*, vol. 97, no. 6, 1955, pp. 1544–1556.

60 Walsh, J. M., Rice, M. H., McQueen, R. G. and Yarger, F. L., "Shock-Wave Compressions of Twenty-seven Metals. Equation of State of Metals," *Phys. Rev.*, vol. 108, no. 2, 1957, pp. 196–216.

61 Rice, M. H., McQueen, R. G. and Walsh, J. M., "Compression of Solids by Strong Shock Waves," Solid State Physics, edited by F. Seitz and D. Turnbull, vol. 6, Academic Press, Inc., N. Y., 1958, pp. 1–63.

62 Katz, S., Doran, D. G. and Curran, D. R., "Hugoniot Equation of State of Aluminum and Steel from Oblique Shock Measurements," *J. Appl. Phys.*, vol. 30, no. 4, 1959, p. 568.

63 Doran, D. G., Fowler, G. R. and Peterson, G. A., "Shock-Wave Compression of Aluminum," *Phys. Rev. Letters*, vol. 1, no. 11, Dec. 1958, p. 402.

64 Mallory, H. D., "Propagation of Shock Waves in Aluminum," *J. Appl. Phys.*, vol. 26, 1955, p. 555.

65 Pack, D. C., Evans, W. M. and James, H. J., "The Propagation of Shock Waves in Steel and Lead," Proc. Phys. Soc. London, vol. 60, 1948, pp. 1–8.

66 Minshall, S., "Properties of Elastic and Plastic Waves Determined by Pin Contractors and Crystals," *J. Appl. Phys.*, vol. 26, 1955, p. 463.

67 Bancroft, D., Peterson, E. L. and Minshall, S., "Polymorphism of Iron at High Pressures," *J. Appl. Phys.*, vol. 27, 1956, p. 291.

68 Al'tshuler, L. V., Krupnikov, K. K., Ledenov, B. N., Zhuchikhin, V. I. and Brazhnik, M. I., "Dynamic Compressibility and Equation of State of Iron Under High Pressure," *Soviet Phys.-JETP*, vol. 34 (7), no. 4, 1958, pp. 606–614; *Zhur. Eksp. i Teoret. Fiz.*, vol. 34, 1958, pp. 874–885.

69 Al'tshuler, L. V., Krupnikov, K. and Brazhnik, M. I., "Dynamic Compressibility of Metals under Pressure from 400,000 to 4,000,000 Atmospheres," *Soviet Physics-JETP*, vol. 34 (7), no. 4, 1958, pp. 614–619; *Zhur. Eksp. i Teoret. Fiz.*, vol. 34, 1958, pp. 886–893.

70 Walsh, J. M. and Rice, M. H., "Dynamic Compressibility of Liquids from Measurements on Strong Shock Waves," *J. Chem. Phys.*, vol. 26, no. 4, 1957, pp. 815–823.

71 Rice, M. H. and Walsh, J. M., "Equation of State of Water to 250 Kilobars," *J. Chem. Phys.*, vol. 26, no. 4, 1957, pp. 824–830.

72 Garn, W. B., "Determination of the Unreacted Hugoniot for Liquid TNT," *J. Chem. Phys.*, vol. 30, no. 3, 1959, pp. 819–823.

73 Majowicz, J. M. and Jacobs, S. J., "Initiation to Detonation of High Explosives by Shocks," presented at Lehigh Meeting of Fluid Dynamics Division, American Physical Society, Nov. 1957 (based on classified Naval Ordnance Rep. no. 5710, March 1958, not available). *See also* Jacobs, S. J., "Examples of High Speed Photographic Techniques at the Naval Ordnance Laboratory," in "Proceedings of Fourth International Congress on High Speed Photography," Cologne, Germany, 1958.

74 Deal, W. E., "The Measurement of C-J Pressure for Explosives," 2nd ONR Symposium on Detonation, Washington, D. C., 1955; *J. Chem. Phys.*, vol. 27, 1957, p. 796.

75 Gibson, F. C., Bowser, M. L., Summers, C. R., Scott, F. H. and Mason, C. M., "Use of an Electro-Optical Method to Determine Detonation Temperatures in High Explosives," *J. Appl. Phys.*, vol. 29, no. 4, 1958, pp. 628–632.

76 Kistiakowsky, G. B., "Initiation of Detonation of Explosives," in "Third Symposium on Combustion, Flames, and Explosions," Williams and Wilkins Co., Baltimore, 1949, p. 560; "Initiation of Detonation in Gases," *Ind. Engng. Chem.*, vol. 43, 1951, p. 2794.

77 Ubbelohde, A. R., "Transition from Deflagration to Detonation. The Physico-Chemical Aspects of Stable Detonation," in "Third Symposium on Combustion, Flames, and Explosions," Williams and Wilkins Co., Baltimore, 1949, p. 566.

78 Maček, A., "Transition from Deflagration to Detonation in Cast Explosives," *J. Chem. Phys.*, vol. 31, no. 1, 1959, pp. 162–167.

79 Bowden, F. P. and Yoffe, A. D., "Initiation and Growth of Explosion in Liquids and Solids," Cambridge Univ. Press, Cambridge, 1952.

80 Bowden, F. P. (leader), "A Discussion on Initiation and Growth of Explosion in Solids," Proc. Roy. Soc. London, vol. A-246, 1958, pp. 145–297.

81 Muraour, H., "Note on the Determination of the Sensitivity of Explosives to Shock," Mem. Artill Francaisse, vol. 12, 1933, pp. 559–572.

82 Eyster, E. H., Smith, L. C. and Walton, S. R., "The Sensitivity of High Explosives to Pure Shock," classified Naval Ordnance Laboratory Memo., 1949 (not available).

83 Edwards, G. D. and Rice, T. K., "Liquid Monopropellants; Detonation Sensitivity," classified Naval Ordnance Rep., 1953 (not available).

84 Shamgar, A. and Bordman, I., "Determination of the Sensitivity of Explosives to Initiation," 27th International Congress of Ind. Chem. (Powders and Explosives), Brussels, Sept. 1954, pp. 100–102.

85 Cachia, G. P. and Whitbread, E. G., "The Initiation of Explosives by Shock," Proc. Roy. Soc. London, vol. A-246, 1958, p. 268.

86 Cook, M. A., Pack, D. H., Cosner, L. N. and Gey, W. A., "Instrumented Card Gap or SPHF-Plate Test," *J. Appl. Phys.*, vol. 30, no. 10, 1959, pp. 1579–1594.

87 Winning, C. H. and Sterling, E., "Étude Photographiques de l'Amorcage de la Pentolite a Travers l'Eau," 27th International Congress of Ind. Chem. (Powders and Explosives), Brussels, Sept. 1954.

88 Berger, J., Favier, J. and Fauquignon, C., "Mecaniques des Explosifs," *Compt. rend.*, vol. 247, 1958, pp. 1305–1307.

89 Favier, J. and Fauquignon, C., "Mecaniques des Explosifs," *Compt. rend.*, vol. 248, 1959, pp. 1291–1294.

90 Adams, G. K., Holden, J. and Whitbread, E. G., "The Explosive Initiation of a Single Crystal of Cyclotrimethylene Trinitromine (RDX)," 31st International Congress Ind. Chem. (Powders and Explosives), Liege Sept. 1958, pp. 3–8.

91 Cotter, T. P., "The Structure of Detonation in Some Liquid Explosives," Doctor's Thesis, Cornell Univ., Sept. 1953.

92 Chaiken, R. F., "Kinetic Theory of Detonation of High Explosives," Master's Thesis, Brooklyn Polytechnic Inst., June 1958.

93 Hertzberg, G. and Walker, R., "Initiation of High Explosives," *Nature* (London), vol. 161, April 24, 1948, pp. 647, 648.

94 Holland, T. E., Campbell, A. W. and Malin, M. E., "Phenomena Associated with Detonation in Large Single Crystals," *J. Appl. Phys.*, vol. 28, no. 10, 1957, p. 1217.

95 Hubbard, H. W. and Johnson, M. H., "Initiation of Detonation," *J. Appl. Phys.*, vol. 30, no. 5, 1959, pp. 765–769.

96 Jones, H., "A Theory of the Dependence of the Rate of Detonation of Solid Explosives on the Diameter of the Charge," Proc. Roy. Soc. London, vol. A-189, 1947, p. 415.

97 Cook, M. A., Pack, D. H. and Gey, W. A., "Deflagration to Detonation Transition," in "Seventh Symposium on Combustion," Butterworths Scientific Publications, Ltd., London, 1958.

98 Wood, W. W. and Kirkwood, J. G., "Diameter Effect in Condensed Explosives. The Relation Between the Velocity and Radius of Curvature of the Detonation Wave," *J. Chem. Phys.*, vol. 22, no. 11, 1954, pp. 1920–1924.

99 Campbell, A. W., Malin, M. E., Boyd, T. J. and Hull, J. A., "Precision Measurement of Detonation Velocities in Liquid and Solid Explosives," *Rev. Sci. Instr.*, vol. 27, no. 8, 1956, pp. 567–574.

100 Malin, M. E., Campbell, A. W. and Mautz, C. W., "Particle Size Effects in Explosives at Finite and Infinite Diameters," *J. Appl. Phys.*, vol. 28, no. 1, 1957, pp. 63–69.

101 Dapoigny, J., Kieffer, J. and Vodar, B., a—"Étude de la Compression des Milieux Denses Partir de la Radiographie d'une Onde de Choc Unique," *Compt. rend.*, vol. 245, 1957, pp. 1502–1505; b—"Quelques Resultats sur la Compression de l'Eau dans une Ondes de Choc," *Compt. rend.*, vol. 238, 1954, pp. 215–217; c—"Ondes de Choc Engendrées dans l'Argon Liquide et Leurs Étude par Radiographie Ultrarapide Compression de l'Argon aux Trés Hautes Pressions," *J. Phys. Radium*, vol. 16, 1955, pp. 733–734; d—"Compression de l'Oxygene aux Trés Haute Pressions par Ondes de Choc Engendrées dans le Liquide," *J. Phys. Radium*, vol. 17, 1956, p. 606; e—"Les Ondes de Choc en Milieu Dense II," *J. des Recherches du C.N.R.S.*, vol. 31, 1955, pp. 260–270.

102 Burgeon, R., Kieffer, J. and Vodar, B., "Equation d'Etat de l'Argon aux Trés Hautes Pressions et sa Compressibilité dans l'Ondes de Choc," *J. Phys. Radium*, vol. 16, 1955, pp. 813–814.

Theory of Liquid Propellant Rocket Combustion Instability and Its Experimental Verification

LUIGI CROCCO,[2] JERRY GREY[3] and DAVID T. HARRJE[4]

Princeton University
Princeton, N. J.

A straightforward theoretical formulation of the longitudinal high frequency rocket stability criteria is presented. Based on Crocco's sensitive combustion time lag theory, the derivation is considerably simpler, although somewhat less rigorous, than previously published detailed treatments. A series of rocket motor experiments is described, demonstrating that there exists an upper limit to the chamber length at which each mode of longitudinal high frequency pressure oscillations will occur, and that this limit is accurately predicted by the theory over a wide range of mixture ratios on two different injectors. The method used to compare experimental results with the theoretical stability limit predictions (including a simple experimental technique for determination of the sensitive time lag) is described.

Phenomenon of Rocket Combustion Instability

EXCEPT for starting and cutoff transients, rocket motors are designed for steady operation. Two kinds of unsteadiness have nevertheless been observed to be present. First, the combustion in a rocket is always more or less "rough"; that is, *random* pressure fluctuations of larger or smaller amplitude cannot be avoided. Second, under proper conditions *organized* pressure oscillations at well-defined frequencies and distributions may appear. The latter form of unsteady operation is given the general title of "combustion instability."

There are three recognized types of combustion instability. The first, the "low frequency instability" (1–3,6,7)[5] is due to interaction between the processes taking place in the combustion chamber and the propellant feed system; it is now sufficiently understood and comparitively easy to avoid or cure.

The second, the "intermediate frequency instability" (4,5), results from a so-called "entropy wave" produced cyclically in the chamber and interacting with the exhaust nozzle. Of the three, it is the least frequent.

The third, the "high frequency instability," consists of the excitation of acoustic vibrational modes of the combustion chamber. This is by far the most destructive kind of instability and the hardest to control. The present paper deals with certain theoretical and experimental results concerning this third type of instability.

Nonsteady Flow Equations With Gas Generation

A possible cause for high frequency instability was first advanced in 1950 (6). It was speculated that if pressure waves are produced in the chamber, they must produce an effect on the rates of the various physico-chemical processes leading to combustion. These modified rates, in turn, by causing periodic intensification or weakening of the local gas evolution or heat release, could sustain the pressure waves under the appropriate conditions. A somewhat oversimplified model, introduced to express quantitatively the sensitivity of the combustion rates to the pressure oscillations, was able to demonstrate that high frequency instability could indeed be produced (6). This simple model was refined over the years in order to treat the problem in a more realistic manner. The results of these theoretical treatments, presented in a number of publications, were finally collected in a single volume (7) to which the reader is referred for the complete story. This reference includes a complete theoretical treatment of the longitudinal mode of high frequency oscillations. Transverse modes have been treated separately and will be discussed in a later publication. For convenience to the interested reader, we shall derive the significant equations in a simpler but less rigorous manner. Those not interested in the details of these theoretical derivations may skip directly to the section on "Experimental Apparatus for Measurement of Longitudinal Stability Limits."

We call x the abscissa along the cylindrical chamber of length L, and choose $x = 0$ at the injector end, so that $x = L$ at the nozzle entrance. We call

$$\rho(t, x) \qquad P(t, x) \qquad T(t, x) \qquad u(t, x)$$

$$h(t, x) = C_p T + \text{constant} = \left[\frac{\gamma}{\gamma - 1}\right]\frac{P}{\rho} + \text{constant}$$

the density, pressure, temperature, axial velocity and enthalpy of the combustion gases respectively at a given instant of time t and at a given axial section x. C_p is the specific heat at constant pressure, and γ the specific heat ratio. We assume, for simplicity, that the combustion of each element of propellant is instantaneous, but that different elements of propellant burn at different distances from the injector. With this assumption the flow at each section is made up exclusively of unburned propellants and gases of complete combustion. If we indicate by $w(t, x)$ the instantaneous rate of production of combustion gases between stations 0 and x,

Presented at ARS Semi-Annual Meeting, June 8–12, 1959, San Diego, Calif.

[1] Sponsored by Powerplant Division, Bureau of Aeronautics, U. S. Navy, under Contract NOas 53-817-c.

[2] Robert H. Goddard Professor of Jet Propulsion. Fellow Member ARS.

[3] Assistant Professor of Aeronautical Engineering. Member ARS.

[4] Staff Research Engineer. Member ARS.

[5] Numbers in parentheses indicate References at end of paper.

we can derive the mass balance of combustion gases (continuity equation) in the form

$$\frac{\partial \rho}{\partial t} + \frac{\partial}{\partial x}(\rho u) = \frac{\partial w}{\partial x} \qquad [1]$$

The momentum balance can be written in a simple form if the assumption is made that the unburned propellant contributes very little to the variations of momentum and occupies a negligible portion of the cross section (for example, if the unburned propellant is in the form of liquid droplets, this assumption is correct when the drag of the droplets is small, so that their momentum is practically unaffected by velocity variations). Then the momentum equation can be written in the usual form

$$\frac{\partial}{\partial t}(\rho u) + \frac{\partial}{\partial x}(\rho u^2) = -\frac{\partial P}{\partial x} \qquad [2]$$

Finally we should write an equation for the conservation of energy and one relating the gas generation rate $w(t, x)$ to the conditions in the chamber. Both will be introduced later.

Linearization of the Equations for Small Perturbations

Expressions for small perturbations of the conditions in the chamber can be derived from Equations [1 and 2] by defining

$$\rho = \bar{\rho} + \rho' \quad P = \bar{P} + P' \quad T = \bar{T} + T' \quad u = \bar{u} + u' \qquad [3]$$

where the primed quantities represent the instantaneous perturbations (depending on t and x) and the steady (barred) quantities are functions only of x. Introducing Equations [3] into Equations [1 and 2], and neglecting terms which are nonlinear in the perturbations, we obtain the steady-state relations

$$\frac{d}{dx}(\bar{\rho}\bar{u}) = \frac{d\bar{w}}{dx} \qquad \frac{d}{dx}(\bar{\rho}\bar{u}^2) = -\frac{d\bar{P}}{dx} \qquad [4]$$

and the time dependent perturbation equations

$$\frac{\partial \rho'}{\partial t} + \frac{\partial}{\partial x}(\bar{\rho}u' + \bar{u}\rho') = \frac{\partial w'}{\partial x} \qquad [5]$$

$$\frac{\partial}{\partial t}(\bar{\rho}u' + \bar{u}\rho') + \frac{\partial}{\partial x}(2\bar{\rho}\bar{u}u' + \bar{u}^2\rho') = -\frac{\partial P'}{\partial x} \qquad [6]$$

The steady-state part of the energy equation may also be written

$$\bar{h}^0 = \bar{h} + (\bar{u}^2/2) = h_p{}^0 = \text{const} = \bar{h}_0 \qquad [7]$$

which expresses the fact that the stagnation enthalpy $\bar{h}^0$ must be the same as the stagnation enthalpy of the unburned propellants $h_p{}^0$ (i.e., their enthalpy including their heat of formation and kinetic energy), and also the same as the enthalpy $\bar{h}_0$ at the injector face, where $u = 0$. For simplicity, the stagnation enthalpy of the propellants has been taken to be constant (an assumption justified by the fact that both the variations of kinetic energy due to droplet drag and the heating from the hot gases can be neglected with respect to the large value of the heat of formation).

Integrating Equations [4] we obtain the relations

$$\bar{\rho}\bar{u} = \bar{w} \qquad \bar{\rho}\bar{u}^2 = \bar{P}_0 - P \qquad [8]$$

Equation [7] and the second part of Equation [8] can be written in the forms

$$\frac{\bar{T}_0}{\bar{T}} = 1 + \frac{\gamma - 1}{2} M^2 \qquad \frac{\bar{P}_0}{\bar{P}} = 1 + \gamma M^2$$

where the Mach number $M = \bar{u}/\bar{c}$ has been introduced, with $\bar{c}^2 = (\gamma \bar{P}/\bar{\rho}) = \gamma R \bar{T}$ and R is the combustion gas constant. The maximum value of this quantity is achieved at the end of the combustion process, supposedly completed before the nozzle entrance. Thus if M_e, the Mach number at the nozzle entrance, is assumed to be such that $M_e{}^2 \ll 1$, then

$$\bar{P} \approx \bar{P}_0 \qquad \bar{T} \approx \bar{T}_0 \qquad \bar{\rho} = \bar{\rho}_0 \qquad \bar{c} = \bar{c}_0 \qquad [9]$$

the last two relations being consequences of the other two. We also conclude that

$$\frac{1}{\bar{P}_0}\frac{d\bar{P}}{dx} \quad \frac{1}{\bar{T}_0}\frac{d\bar{T}}{dx} \quad \frac{1}{\bar{\rho}_0}\frac{d\bar{\rho}}{dx} \quad \frac{1}{\bar{c}_0}\frac{d\bar{c}}{dx} \qquad \text{are } O(M_e{}^2) \qquad [10]$$

Equation [4] or the first part of Equation [8] also provide that

$$\frac{d\bar{w}}{dx} \approx \bar{\rho}_0 \bar{c}_0 \frac{dM}{dx} \qquad [11]$$

Within the same approximation we may write the equation for the entropy s

$$\rho \frac{ds}{dt} = \rho\left(\frac{\partial s}{\partial t} + u\frac{\partial s}{\partial x}\right) \approx \frac{h_p{}^0 - h}{T}\frac{\partial w}{\partial x} \qquad [12]$$

expressing the fact that the substantial rate of increase of the entropy of an elementary volume is equal to the rate of burning within the same volume times the enthalpy deficiency with respect to the surroundings, divided by the temperature (Eq. [12] can be derived rigorously from the energy equation after neglecting terms of order $M_e{}^2$). When applied to the steady-state condition, Equation [12] simply tells that the variations of $\bar{s}$ are of $O(M_e{}^2)$, so that if quantities of this order are negligible $\bar{s} \approx \bar{s}_0$, a result immediately obtained from Equation [9]. Taking into account this result and that $h_p{}^0$ is a constant, and replacing $\bar{s} = \bar{s} + s'$ in Equation [12], we obtain

$$\bar{\rho}\left(\frac{\partial s'}{\partial t} + \bar{u}\frac{\partial s'}{\partial x}\right) = -\frac{h'}{\bar{T}}\frac{d\bar{w}}{dx} = -C_p\frac{T'}{\bar{T}}\bar{\rho}_0\bar{c}_0\frac{dM}{dx} \qquad [13]$$

where use has been made of Equation [11].

Assuming now that all quantities oscillate harmonically, and using the complex representation of such oscillating quantities, we can define the nondimensional amplitudes of oscillation σ, φ, ν, and q (functions of x only) from the following relations[6]

$$\frac{\rho'}{\bar{\rho}_0\sigma(x)} = \frac{P'}{\bar{P}_0\varphi(x)} = \frac{u'}{\bar{c}_0\nu(x)} = \frac{w'}{\bar{\rho}_0\bar{c}_0 q(x)} = e^{i\omega t} \qquad [14]$$

When these values of ρ', P', u', w' are introduced in Equations [5 and 6], and terms of the order of $M_e{}^2$ are neglected, we obtain the following linear ordinary differential equations for the amplitudes

$$i\omega\bar{\rho}_0\sigma + \bar{\rho}_0\bar{c}_0\frac{d}{dx}(\nu + M\sigma) = \bar{\rho}_0\bar{c}_0\frac{dq}{dx} \qquad [15]$$

$$i\omega\bar{\rho}\bar{c}_0(\nu + M\sigma) + 2\bar{\rho}_0\bar{c}_0{}^2\frac{d}{dx}(M\nu) = -\bar{P}_0\frac{d\varphi}{dx} \qquad [16]$$

In deriving these equations we have taken into account the relations [9, 10], and the fact that $\bar{u}(x) \approx \bar{c}_0 M(x)$. The exponential time dependent factor has been suppressed from all terms. Further, in view of the relations

$$s' = c_v\frac{P'}{\bar{P}} - C_p\frac{\rho'}{\rho} \approx C_p\left[\frac{\varphi(x)}{\gamma} - \sigma(x)\right]e^{i\omega t}$$

$$\frac{T'}{\bar{T}} = \frac{P'}{\bar{P}} - \frac{\rho'}{\bar{\rho}} = [\varphi(x) - \sigma(x)]e^{i\omega t}$$

[6] Observe that these amplitudes are generally complex numbers as a result of the phase differences between the various quantities.

an additional equation between σ and φ may be obtained from Equation [13]

$$i\omega\bar{\rho}_0\left(\frac{1}{\gamma}\varphi-\sigma\right)+\bar{\rho}_0\bar{c}_0M\frac{d}{dx}\left(\frac{\varphi}{\gamma}-\sigma\right)=-\bar{\rho}_0\bar{c}_0(\varphi-\sigma)\frac{dM}{dx} \quad [17]$$

Taking into account that $\gamma\bar{P}_0=\bar{\rho}_0\bar{c}_0^2$, Equations [15 to 17] become

$$\frac{i\omega\sigma}{\bar{c}_0}+\frac{d}{dx}(M\sigma)=\frac{dq}{dx}-\frac{d\nu}{dx} \quad [18]$$

$$\frac{i\omega}{\bar{c}_0}(\nu+M\sigma)+2\frac{d}{dx}(M\nu)=-\frac{1}{\gamma}\frac{d\varphi}{dx} \quad [19]$$

$$\frac{i\omega\sigma}{\bar{c}_0}+\frac{d}{dx}(M\sigma)=i\frac{\omega}{\bar{c}_0}\frac{\varphi}{\gamma}+\frac{d}{dx}(M\varphi)-\frac{\gamma-1}{\gamma}M\frac{d\varphi}{dx} \quad [20a]$$

Introducing into the last term of Equation [20a] the value of $d\varphi/dx$ derived from Equation [19], neglecting terms of $O(M_e^2)$, and equating the second members of Equations [18 and 20a] we obtain

$$\gamma\frac{d\nu}{dx}+\frac{i\omega\varphi}{\bar{c}_0}=\gamma\frac{dq}{dx}-\gamma\frac{d}{dx}(M\varphi)-\frac{i\omega}{\bar{c}_0}\gamma(\gamma-1)M\nu \quad [20b]$$

Observing from Equation [17 or 20a] that the quantity $[(\varphi/\gamma)-\sigma]$ (which represents the amplitude of ς'/C_p), is found to be of $O(M_e)$, and that the only term in Equation [19] where σ appears is of $O(M_e)$, Equation [19], within the present approximation, can be rewritten as

$$\frac{d\varphi}{dx}+\frac{i\omega\gamma\nu}{\bar{c}_0}=-\frac{i\omega M\varphi}{\bar{c}_0}-2\gamma\frac{d}{dx}(M\nu) \quad [21]$$

If the gas generation rate q can be expressed in terms of the pressure and velocity variables φ and ν, the system of Equations [20b and 21] contains only these two variables, and can be used for the solution of our problem.

Rate of Gas Generation

The problem of determining the rate at which gases are being generated and the perturbation of this rate under nonsteady conditions is beyond our present capabilities. We assume, therefore, that for the given chamber the steady-state gas generation rate is known and results in a given $\bar{M}(x)$ (see Eq. [11]). Observe that, within the gas generation scheme used here, the combustion chamber is filled with products of complete combustion in an approximately uniform state through which each element of propellant travels until it reaches the conversion point. During this journey the processes which finally lead to the conversion of the element (such as atomization, heat transfer, evaporation, mixing and chemical processes) take place at certain rates that are more or less affected by the local physical conditions of the gases.

In nonsteady operation these physical conditions are functions not only of the location, but also of the time, and so, therefore, are the process rates. As a consequence the conversion point of the elements may change, and local intensification or rarefaction of gas generation may result. The following assumptions will be made (7):

1 Among the physical conditions which determine the variations of the process rates, it is necessary to consider only the state of the gases, the effect of the velocity perturbations being of secondary importance.

2 The rates of the processes taking place soon after injection are less affected by the state of the gases than those taking place just before the conversion point. Schematically, the whole time lag τ_t between injection and conversion (different for each element) can be broken into an "insensitive time lag" during which the rates are unaffected by the variations of the state of the gases, and a "sensitive time lag," of duration τ, during which the rates are "uniformly" affected.

By virtue of assumption 1, and as a consequence of the already established fact that oscillations of the gases are almost isentropic so that the state of the gas can be represented by a single state variable (e.g., the pressure), the variations of the rates during the sensitive time lag can be assumed to depend only on the pressure perturbation. The simplest functional relationship between the sensitive time lag and P' is, in agreement with assumption 2

$$\tau'=\tau-\bar{\tau}=-n\int_{t-\tau}^{t}\frac{P'(x,\theta)}{\bar{P}}d\theta \quad [22]$$

where

τ = instantaneous value of the *sensitive* time lag
$\bar{\tau}$ = mean value of the *sensitive* time lag

Equation [22] expresses the fact that, for an element burning at time t, the rate at each previous instant θ within the sensitive time lag τ is increased proportionally to the fractional pressure perturbation. The nondimensional factor n, called the "interaction index," has been taken uniform for all θ consistently with assumption 2, and is a measure of the relative sensitivity of the rates to variations of gas state.

As a result of the variation of τ, the conversion point of the element in question oscillates around its steady-state location, but this spatial effect on the combustion distribution is small and can be neglected, as shown in (7). Observe that τ may be different for different elements. Here it shall be assumed for simplicity to be identical for all elements.

Differentiating Equation [22], and writing $\bar{\tau}$ instead of τ in the lower limit of the integral (a substitution which produces only terms of order higher than linear in the perturbations), we obtain

$$\frac{d\tau}{dt}=-\frac{n}{\bar{P}_0}[P'(t)-P'(t-\bar{\tau})] \quad [23]$$

where use has been made of Equation [9].

Now consider the gas generation in a length dx and during an interval dt at a location x and time t, i.e., $(\partial w/\partial x)dxdt$. This amount of gas corresponds to a certain fraction of the propellant injected at a previous time $(t-\tau_t)$ during an interval $d(t-\tau_t)$ (here τ_t is the *total* time lag). The other fractions injected during the same interval burn at other stations. Calling $\delta[m_i(t-\tau_t)]$ the fraction of the injection flow rate at time $(t-\tau_t)$ that burns at station x in an interval dx, we must have

$$\frac{\partial w}{\partial x}dxdt=\delta[m_i(t-\tau_t)]d(t-\tau_t)$$

Under steady conditions τ_t is a constant for the element considered, and we have, assuming that the injection rate is not affected by the nonsteadiness

$$\frac{d\bar{w}}{dx}dxdt=\delta[m_i(t-\tau_t)]dt$$

Here the elementary length dx has been taken the same in both cases since, as already explained, the effect of the displacement of the conversion point in nonsteady operation can be neglected. Eliminating δm_i from the two equations in the foregoing, and remembering that the only variable part of τ_t is the *sensitive* time lag τ, we obtain

$$\frac{\partial w}{\partial x}=\frac{d\bar{w}}{dx}\left(1-\frac{d\tau}{dt}\right)$$

Introducing here Equation [23] and substituting from Equa-

tions [14 and 8], we have finally

$$\frac{dq}{dx} = \frac{\Xi}{\gamma}\varphi\frac{dM}{dx} \qquad [24]$$

where Ξ is defined by

$$\Xi \equiv \gamma n[1 - e^{-i\omega\tau}] \qquad [25]$$

This is the expression to be introduced in Equation [20b].

We can observe now that a certain number of drastic assumptions were necessary to the derivation of Equation [24]. We see clearly that these assumptions are not dictated by actual knowledge of the details of the combustion process, but rather by very rough intuitive reasoning and, especially, by the need for covering our ignorance of these processes. One feels a priori that this formulation may have a qualitative value, but that its chances for quantitative description of the actual phenomena are slim. Therefore, when the results of the analytical developments based on Equation [24] are applied to the experimental data described in the following it is truly amazing to see how surprisingly closely the experimental results correlate with the theory. It is this experimental verification which provides confidence in the quantitative application of the combustion Equation [24].

Solution of the Equations

After substituting Equation [24] into Equation [20b], Equations [20b and 21] become

$$\frac{d}{dx}(\gamma v) + \frac{i\omega\varphi}{\bar{c}_0} = \Xi\varphi\frac{dM}{dx} - \gamma\frac{d}{dx}(M\varphi) - \frac{i\omega}{\bar{c}_0}\gamma(\gamma-1)Mv$$

$$\frac{d\varphi}{dx} + \frac{i\omega\gamma v}{\bar{c}_0} = -\frac{i\omega M\varphi}{\bar{c}_0} - 2\frac{d}{dx}(\gamma M v) \qquad [26]$$

The boundary conditions are as follows: At $x = 0$ (the injector wall), the velocity perturbation $v = 0$ and the pressure variation φ can be assigned an arbitrary magnitude φ_0. At $x = L$ (the nozzle entrance), v and φ must be related by the nozzle characteristics for oscillating flow. These have been expressed in terms of a "specific admittance ratio" α, calculated (7,8) and verified experimentally (9,10) elsewhere. This ratio α is defined by

$$\frac{\gamma v_e}{\varphi_e} = M_e\alpha = M_e(\alpha_r + i\alpha_i) \qquad [27]$$

The quantity α is complex: It depends on the nozzle geometry and on the reduced frequency $\omega l_{sub}/\bar{c}_t$, with l_{sub} representing the length of the convergent portion of the deLaval nozzle, and $\bar{c}_t = \bar{c}_0\sqrt{2/(\gamma+1)}$ indicating the velocity at the throat. The subscript e refers to the entrance section of the nozzle, and therefore to the conditions at the chamber exit, $x = L$.

Equations [26] have been written in a form in which the expressions at the left are of the order of the perturbations, while those at the right are of order M_e times the perturbations, and hence, within the forementioned assumption that M_e is small, are substantially smaller than those on the left-hand side. This fact can be used for an iterative solution scheme. Neglecting first the quantities on the right-hand side, as if M vanished, Equations [26] become

$$\frac{d}{dx}[\gamma v^{(0)}] + \frac{i\omega}{\bar{c}_0}\varphi^{(0)} = 0$$

$$\frac{d\varphi^{(0)}}{dx} + \frac{i\omega\gamma}{\bar{c}_0}v^{(0)} = 0$$

The solution, with the conditions $v^{(0)}(0) = 0$, $\varphi^{(0)}(0) = \varphi_0$ is

$$\frac{\varphi^{(0)}}{\varphi_0} = \cos\left(\frac{\omega x}{\bar{c}_0}\right) \qquad \frac{\gamma v^{(0)}}{\varphi_0} = -i\sin\left(\frac{\omega x}{\bar{c}_0}\right) \qquad [28]$$

This may be considered the "zeroth iteration."

We could apply now the condition of Equation [27], in which, for consistency, M_e must take vanishing values, so that it becomes simply $v_e^{(0)} = 0$. Thus we find

$$\frac{\gamma v^{(0)}(L)}{\varphi_0} = 0 = -i\sin\left(\frac{\omega L}{\bar{c}_0}\right)$$

or

$$\frac{\omega L}{\bar{c}_0} = k\pi \qquad [29]$$

with k an integer. The value of ω so determined is an "eigenvalue" of the equations for the case $M = 0$. Observe that this result coincides with the known behavior of the organ pipe with two closed ends. For $k = 1$ we have the so-called fundamental mode, for which L contains half of a wave length; $k = 2, 3, \ldots$ corresponds to the second, third, ... harmonics, with 3, 5, ... halves of a wave length contained in L.

Disregarding for the moment the condition of Equation [27], and postponing determination of the eigenvalues ω, we will proceed to a first iteration by introducing the zeroth iteration [28] into the right-hand side of Equations [26], obtaining the following

$$\frac{d}{dx}\left[\frac{\gamma v^{(1)}}{\varphi_0}\right] + \frac{i\omega}{\bar{c}_0}\frac{\varphi^{(1)}}{\varphi_0} = \Xi\frac{dM}{dx}\cos\left(\frac{\omega x}{\bar{c}_0}\right) - \gamma\frac{d}{dx}\left[M\cos\left(\frac{\omega x}{\bar{c}_0}\right)\right] - (\gamma-1)\frac{\omega}{\bar{c}_0}M\sin\left(\frac{\omega x}{\bar{c}_0}\right)$$

$$\frac{d}{dx}\left[\frac{\varphi^{(1)}}{\varphi_0}\right] + \frac{i\omega}{\bar{c}_0}\frac{\gamma v^{(1)}}{\varphi_0} = -i\frac{\omega}{\bar{c}_0}M\cos\left(\frac{\omega x}{\bar{c}_0}\right) + 2i\frac{d}{dx}\left[M\sin\left(\frac{\omega x}{\bar{c}_0}\right)\right]$$

This system of nonhomogeneous linear equations can be solved by conventional methods. After some manipulation, the solution satisfying the prescribed boundary conditions at $x = 0$ may be written

$$\frac{\varphi^{(1)}}{\varphi_0} = \cos\left(\frac{\omega x}{\bar{c}_0}\right) + i\left[2M\sin\left(\frac{\omega x}{\bar{c}_0}\right) - \frac{\omega}{\bar{c}_0}(\Xi + 2 - \gamma)A(x,\omega) + \frac{\omega}{\bar{c}_0}\cos\left(\frac{\omega x}{\bar{c}_0}\right)C(x)\right]$$

$$\frac{\gamma v^{(1)}}{\varphi_0} = -i\sin\left(\frac{\omega x}{\bar{c}_0}\right) - \gamma M\cos\left(\frac{\omega x}{\bar{c}_0}\right) + \Xi M\cos\left(\frac{\omega x}{\bar{c}_0}\right) - \frac{\omega}{\bar{c}_0}(\Xi + 2 - \gamma)B(x,\omega) + \frac{\omega}{\bar{c}_0}\sin\left(\frac{\omega x}{\bar{c}_0}\right)C(x) \qquad [30]$$

with

$$A(x,\omega) = \int_0^x M(x')\cos\left[\frac{\omega(x-2x')}{\bar{c}_0}\right]dx'$$

$$B(x,\omega) = \int_0^x M(x')\sin\left[\frac{\omega(x-2x')}{\bar{c}_0}\right]dx'$$

$$c(x) = \int_0^x M(x')dx' \qquad [31]$$

The solution expressed by Equation [30] differs from Equation [28] in the presence of additional terms of order M_e which depend on the Mach number distribution. It also differs in the first terms of order unity because the value of ω may be, and in fact is, different from the value given by Equation [29]. The solution [30] could be used in principle to find a second iteration in which terms of order M_e^2 would also be included; however, this is inconsistent, because quantities of order M_e^2 have already been neglected in deriving Equations [26], and unnecessary, because Equation [30] is already sufficiently accurate for our purpose.

The values of $\varphi_e^{(1)}$ and $\nu_e^{(1)}$ can be calculated from Equations [30] by setting $x = L$. Introducing these values into Equation [27], the resulting equation can be solved for Ξ. The result is given in the form (recalling the definition [25])

$$\Xi = \gamma n(1 - e^{-i\omega\tau}) = \frac{I_r + iI_i}{J_r + iJ_i} \qquad [32]$$

with

$$I_r = (\alpha_r + \gamma)M_e \cos\left(\frac{\omega L}{\bar{c}_0}\right) - 2M_e^2\alpha_i \sin\left(\frac{\omega L}{\bar{c}_0}\right) +$$

$$(2 - \gamma)\frac{\omega}{\bar{c}_0}[B(L, \omega) + M_e\alpha_i A(L, \omega)] -$$

$$\frac{\omega}{\bar{c}_0}\left[\sin\frac{\omega L}{\bar{c}_0} + M_e\alpha_i \cos\left(\frac{\omega L}{\bar{c}_0}\right)\right] C(L)$$

$$I_i = M_e\alpha_i \cos\left(\frac{\omega L}{\bar{c}_0}\right) + (1 + 2M_e^2\alpha_r) \sin\left(\frac{\omega L}{\bar{c}_0}\right) -$$

$$(2 - \gamma)\frac{\omega}{\bar{c}_0} M_e\alpha_r A(L, \omega) + \frac{\omega}{\bar{c}_0} M_e\alpha_r \cos\left(\frac{\omega L}{\bar{c}_0}\right) C(L)$$

$$J_r = M_e \cos\left(\frac{\omega L}{\bar{c}_0}\right) - \frac{\omega}{\bar{c}_0} B(L, \omega) - M_e\alpha_i \frac{\omega}{\bar{c}_0} A(L, \omega)$$

$$J_i = M_e\alpha_r \frac{\omega}{\bar{c}_0} A(L, \omega)$$

..... [33]

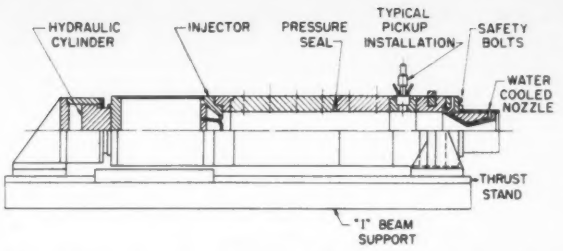

Fig. 1 Diagram of experimental liquid bipropellant rocket motor

Here A, B and C are given by Equations [31] with $x = L$. Also, $M_e\alpha_r$ and $M_e\alpha_i$ depend on the nozzle geometry and, as already mentioned, on the reduced frequency

$$\frac{\omega l_{sub}}{\bar{c}_t} = \sqrt{\frac{\gamma + 1}{2}}\,\frac{\omega L}{\bar{c}_0}\,\frac{l_{sub}}{L} \qquad [34]$$

We observe that certain terms retained in the definitions [33] seem to be of order M_e^2. The point is that, as Fig. 8 shows, $M_e\alpha_i$ can be of order unity rather than M_e, so that terms in $M_e^2\alpha_i$ are of order M_e. On the contrary, the quantity $M_e\alpha_r$ remains of order M_e, and the terms in $M_e^2\alpha_r$ could be neglected in the expressions [33].

Examining the definitions [33 and 31], we can see that the four quantities defined by Equations [33] would be functions of $(\omega L/\bar{c}_0)$ alone if M were assigned as a function of x/L rather than x, and if l_{sub}/L could be given a constant value. If, however, as in the following application, $M(x)$ and l_{sub} are assigned independently of L, and L is varied, then the four quantities defined by Equations [33] are functions of both $(\omega L/\bar{c}_0)$ and L.

We point out here that Equation [32] has been derived under the two explicit limitations that M_e is small compared to unity and that the derivative dM/dx is of the same order as M_e/L. The more rigorous derivation of (7), however, shows that an additional limitation requiring $(\omega L/\bar{c}_0)$ to be of order unity must also be satisfied (for large values of this quantity, an equation somewhat more complicated than Eq. [32] has

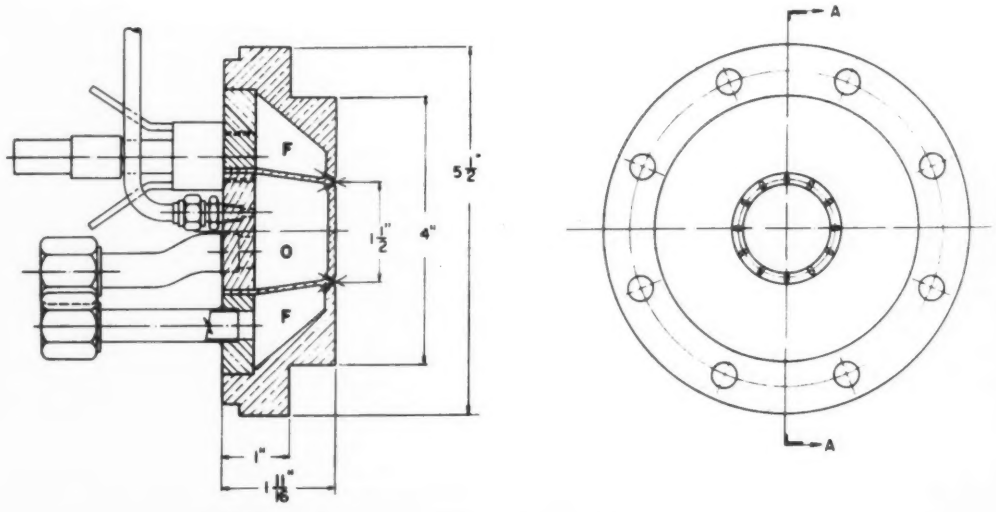

Fig. 2 Typical rocket injector configuration

been derived in (7)). The reference further demonstrates that the limitation on the order of magnitude of dM/dx can be waived. This is also illustrated by the fact that the final Equations [30 and 31] do not contain dM/dx but only M.

Before discussing the meaning of Equation [32] and its application to a particular type of experiment, we shall first describe the test apparatus and the experimental program.

Experimental Apparatus for Measurement of Longitudinal Stability Limits

The basic experimental equipment consisted of a small uncooled copper rocket motor (Fig. 1) having a 3-in. inner diameter and length variable in 1-in. increments from approximately $2\frac{1}{2}$ to approximately $36\frac{1}{2}$ in. Length changes were made by adding or removing cylindrical sections, and the motor was held together by a hydraulic cylinder arrangement to facilitate these changes. The injectors (Fig. 2) were of a simple one-on-one impinging pair design with 12 pairs of holes and zero impingement distance. The propellants were liquid oxygen and 95 per cent ethyl alcohol (Solox), with injector hold dimensions designed for oxidant/fuel weight mixture ratios of 1.4 (first injector) and 2.0 (second injector) for a given injector pressure drop. Mixture ratio could, however, be varied from these design figures simply by changing the injection pressure level of each propellant. The exhaust nozzle was a simple 30-deg half-angle conical convergent cone 2 in. long blending into a circular-arc throat and followed by a 15-deg half-angle divergent cone. The nominal nozzle throat diameter was 0.875 in., providing a contraction ratio of 11.3.

The pressurized feed system (Fig. 3) included cavitating venturis for flow regulation and control throttling valves in addition to the usual propellant shutoff valves. The throttling valves were operated by a servo control system (11) which maintained simultaneous preset constant values of mixture ratio and chamber pressure. This provided the necessary duplication of chamber operating conditions from run to run. Duration of each test run varied from 5 to about 15 sec.

Standard instrumentation included the usual steady-state equipment (thrust, propellant flow rates, chamber and injector pressures, etc.) and a high response strain-gage pressure transducer (12) flush mounted in the chamber approximately 3 in. upstream of the nozzle entrance. The signal from this transducer was split into steady-state and transient components, the steady-state portion appearing on a recording potentiometer and the transient portion on an FM magnetic tape recorder. Amplitudes and frequencies of the recorded transient pressure oscillations were then measured electronically from the tape recording. Typical recordings appear in Fig. 9, to be discussed later.

Other novel instrumentation features were those devised to measure the internal axial Mach number distribution $M(x)$ required for the theoretical prediction of stability limits (see Eq. [31]). Because of the high nozzle contraction ratio, the momentum pressure drop was very low (about 0.5 psi), and hence this measurement entailed some difficulty. The three methods used were: 1—Axial static pressure drop, using high pressure differential manometers (13), 2—streak-camera photography through a full length

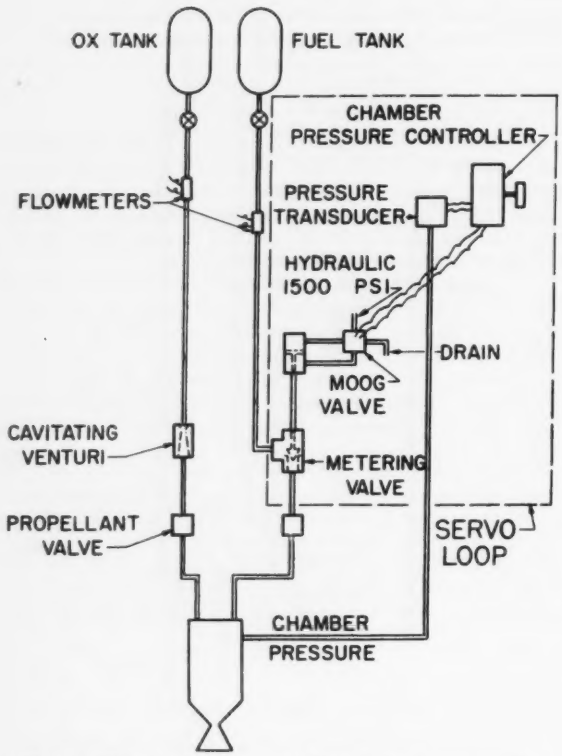

Fig. 3 Diagram showing main feed system components

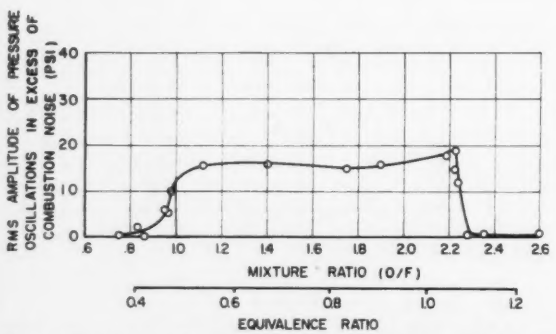

Fig. 4 Typical experimental constant-length mixture ratio survey (L = 8.56 in.), illustrating degree of definition of the longitudinal mode stability boundaries. The nominal chamber pressure is 300 psia

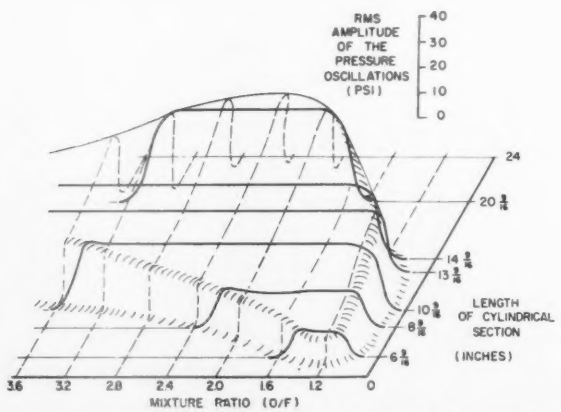

Fig. 5 Experimental determination of longitudinal stability boundaries for the first injector (design O/F = 1.4) in terms of chamber length and mixture ratio, illustrating again the degree of definition. The nominal chamber pressure is 300 psia, and only the fundamental longitudinal mode is shown for clarity

Lucite window (14), and 3—determination of the falloff in characteristic velocity with decreasing chamber length. Actually, none of these methods was fully satisfactory due to the high degree of recirculation and the high contraction ratio mentioned previously; however, the rather low sensitivity of the theory to errors in this velocity distribution permitted the use of rather coarse measurements. In fact, replacing the observed velocity distribution by the extreme idealization of a step function (zero to exit velocity) located at the point of maximum observed velocity gradient had little effect on the theoretically predicted stability limits. Despite this low sensitivity to error, however, further effort is now being devoted to the determination of more suitable axial velocity distribution data.

The test procedure was to make a series of test runs at different mixture ratios for each chamber length, using the same injector and chamber pressure level for each series of chamber lengths. The observed pressure oscillation amplitudes are shown in Fig. 4 for one of these constant length surveys. The region in which longitudinal pressure oscillations appear is clearly observed. Putting together a composite picture of surveys similar to that of Fig. 4 but at different chamber lengths, we obtain for the first injector the three-dimensional plot of Fig. 5 (in which the second and third harmonic regions have been omitted for clarity). Selecting the stability boundaries from plots of this type, the data may finally be plotted as shown in Fig. 6, where longitudinal oscillations in the indicated modes appeared only within the shaded regions. A similar plot was obtained for the second injector (see Fig. 14). Fig. 6 represents a stability map for the particular injector-nozzle configuration at one chamber pressure level, and provides an *experimental* determination of the boundaries predicted theoretically by Equation [32].

In addition to the stability boundary data of the type shown in Fig. 6, some additional information was needed for calculations of the theoretical boundaries from Equation [32]. The primary requirements, in addition to the velocity distribution discussed previously, are the frequency ω, the speed of sound $\bar{c}_0$ in the chamber, and the complex nozzle admittance ratio α.

The frequencies were measured directly from tape records at or near the stability boundaries. The speed of sound $\bar{c}_0$ was obtained by assuming, as before, that the chamber was filled with gas at a mean temperature $\approx T_0$. Experimental values of the characteristics velocity c^* may then be directly related to this chamber temperature T_0

$$c^* \equiv \frac{P_0 A_t}{\dot{m}} = \frac{P_0 A_t}{f(\gamma) P_0 A_t} \sqrt{RT_0} = f_1(\gamma) \sqrt{RT_0} = f_2(\gamma) \bar{c}_0$$

where

A_t = throat area
$\dot{m}$ = mass flow rate

The necessary values of γ, the specific heat ratio, were obtained from conventional theoretical propellant performance calculations as functions of the mixture ratio. Experimental values of the characteristic velocity c^* needed to establish $\bar{c}_0$ are shown in Fig. 7.

The nozzle admittance ratio was calculated on a digital computer for the conical nozzle by the method of Appendix C of (7). These values are shown in Fig. 8 for the frequency range of interest.

Before returning to the comparison of theory with the experimental results, it is of some interest to observe the nature of the instabilities observed on these tests. Photographs were taken of the actual wave shapes observed in the regions marked by circled numbers in Fig. 6. These photos appear in Fig. 9, and clearly demonstrate the nature of the various instabilities, e.g., near the stability boundaries the wave shapes are less steep, as would be expected. The higher

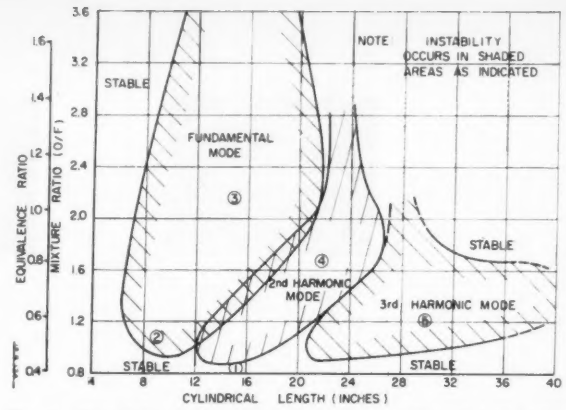

Fig. 6 Complete experimental stability boundary data for the first injector (design $O/F = 1.4$), showing the three observed modes of longitudinal oscillations. Numbers in circles indicate locations of the wave shape photographs shown in Fig. 9

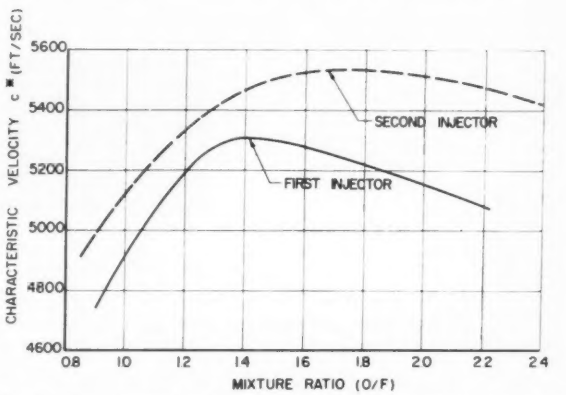

Fig. 7 Experimental values of characteristic velocity c^* used to determine the chamber sound speed $\bar{c}_0$. Dependence on chamber length was small, but is included in the data reduction as indicated in the text

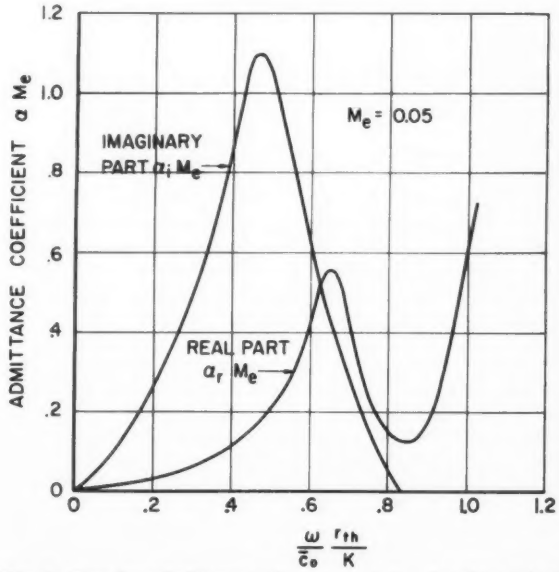

Fig. 8 Complex admittance ratio $\alpha = \alpha_r + i\,\alpha_i$ for the conical nozzle used on these tests. M_e is the gas Mach number at the nozzle entrance, r_{th} is the nozzle throat radius (0.438 in.), K is a geometrical factor, ω is the frequency, and $\bar{c}_0$ the chamber sound speed

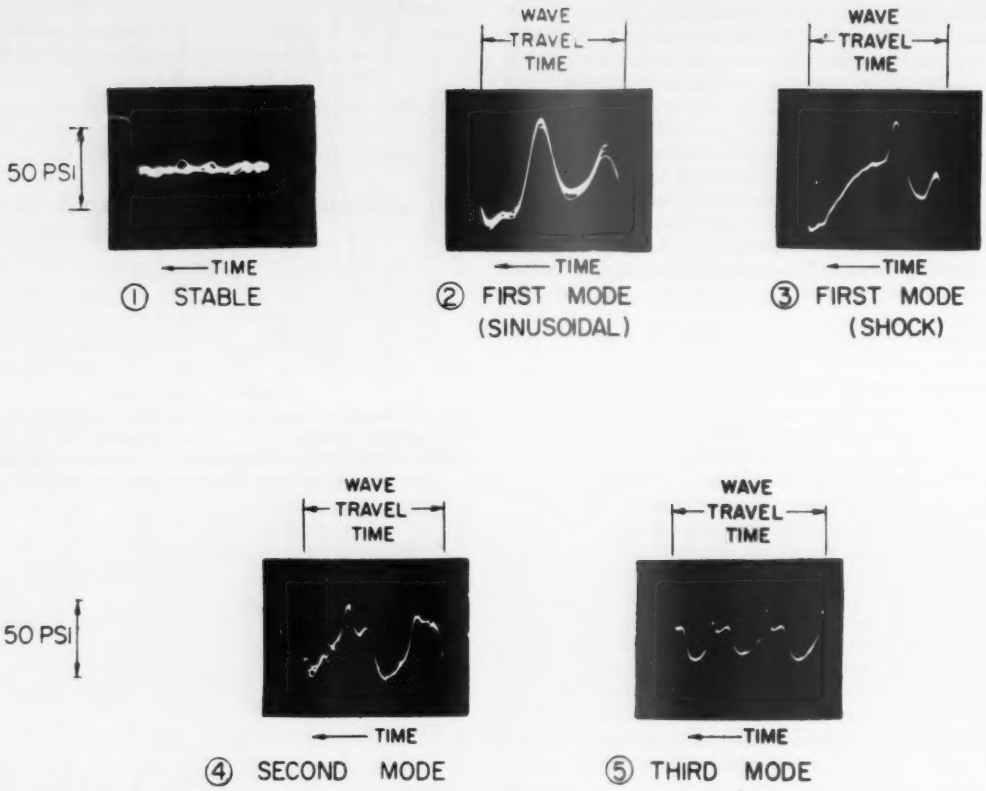

Fig. 9 Experimentally observed wave shapes of the oscillations. The two peaks which appear on each cycle correspond to upstream and downstream traveling waves. Circled numbers one through five indicate regions of the stability boundary map shown in Fig. 6

modes are clearly distinguishable, but at these very high frequencies it should be noted that the natural frequency of the pressure transducer (~25,000 cps) will cause some rounding of the steep wave shapes expected.

Interpretation of Equation [32] and Comparison With the Experimental Results

First we notice that since in the theoretical treatment all perturbations have been taken to vary harmonically with time, not only must the perturbations be very small, but also their amplitudes must not change with time. Obviously this condition is not verified for stable operation where, by definition, the perturbations die out with time, or for unstable operation, where the perturbations are amplified until they eventually reach a regime amplitude which may not be small (this regime is reached as a result of nonlinear damping factors not considered in the analysis). Therefore, for consistency, the analytical results only apply to the condition of operation between stable and unstable; i.e., to the *limits* of stability where, again by definition, the perturbation amplitudes are neither damped nor amplified.

During the experiments described above, in which the chamber length is varied, the combustion distribution and hence $M(x)$ was not affected. Also the nozzle convergent section length l_{sub} was constant, since the nozzle was always the same. Hence, as pointed out at the end of the section on "Solution of the Equations," the expressions [33] are functions of L and $(\omega L/\bar{c}_0)$.

Equation [32], being complex, can be split into two real equations the solution of which with respect to the parameters n and $\omega\tau$ gives

$$n = \frac{1}{2\gamma}\frac{I_r^2 + I_i^2}{I_r J_r + I_i J_i}$$

$$\omega\tau = \pi + 2\tan^{-1}\frac{J_i}{J_r} - 2\tan^{-1}\frac{I_i}{I_r} \qquad \text{.....[35]}$$

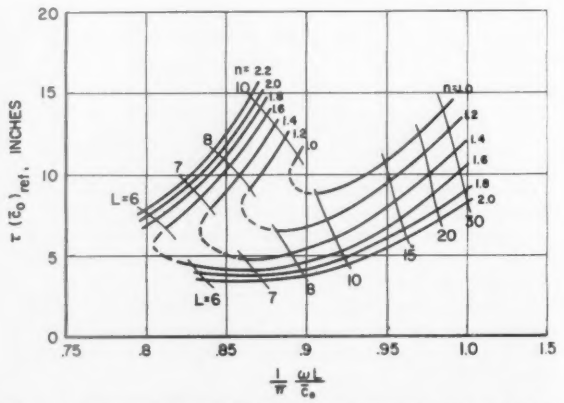

Fig. 10 Theoretical results for the fundamental mode solution of Equation [32]. τ is the sensitive time lag, n the interaction index, L the chamber length, ω the frequency, $\bar{c}_0$ the true chamber sound speed, $(\bar{c}_0)_{ref}$ the value of $\bar{c}_0$ at the proper mixture ratio, but at a reference length (6.56 in.). For a given mixture ratio, $(\bar{c}_0)_{ref}$, τ and n are constant, so the two intersections of the proper horizontal line with the appropriate n curve represent the two (lower and upper) stability boundaries

The value of $\omega\tau$ given here is the smallest solution of the corresponding trigonometric equation, and the one of highest physical interest. In view of the previously mentioned dependence of the I's and the J's on L and $(\omega L/\bar{c}_0)$, the foregoing equations give the interaction index and the sensitive time lag in the form

$$n = f_1\left(L, \frac{\omega L}{\bar{c}_0}\right) \qquad \frac{\bar{c}_0\tau}{L} = f_2\left(L, \frac{\omega L}{\bar{c}_0}\right) \qquad [36]$$

These relations can be inverted (although not analytically) to give the equations

$$L = f_3(n, \bar{c}_0\tau) \qquad \frac{\omega L}{\bar{c}_0} = f_4(n, \bar{c}_0\tau) \qquad [37]$$

which can be interpreted as follows: For the given injector at a given mixture ratio r (oxidant/fuel), n and $\bar{c}_0\tau$ have fixed values. For these values Equations [37] give the eigenvalues L and $(\omega L/\bar{c}_0)$; that is, the length and the frequency corresponding to the stability limit. For lengths above or below the calculated L the operation will be either stable or unstable, switching from one to the other when the length is L. Comparing this with the simple case of the cylinder closed at two ends, we see that the second Equation [37] corresponds to Equation [29] and, actually, would also present a multiplicity of solutions of which, however, only the lowest has been represented by f_4; this solution corresponds to $k = 1$ in Equation [29], i.e., to the fundamental mode. The first Equation [37] has no correspondence to the closed cylinder in which oscillations are always neutral.

Both Equations [37] can be represented graphically, as is done, for instance, in Fig. 10. Curves of constant n and L are drawn here in a plane whose abscissa is $(1/\pi)(\omega L/\bar{c}_0)$ and whose ordinate is $(\bar{c}_0)_{\text{ref}}\tau$, where $(\bar{c}_0)_{\text{ref}}$ is the value of $\bar{c}_0$ corresponding to a fixed chamber length $L = 6.56$ in. and to each mixture ratio r. This has been done in order to take into account the (small) dependence of $\bar{c}_0$ on the length of the chamber, assuming that $\bar{c}_0/(\bar{c}_0)_{\text{ref}}$ is a function only of L and not of r. Fig. 10 holds for the fundamental mode at all values of r. For higher modes, $(\omega L/\bar{c}_0)$ becomes too large to allow the use of Equation [32], and the more complicated equations derived in (7) should be used. The corresponding figures are not presented here.

If we knew the magnitude of n and τ for the given injector and the actual operating pressure and mixture ratio, Fig. 10 would provide the values of L and $(\omega L/\bar{c}_0)$ corresponding to the stability limits of the fundamental mode. Since this knowledge of n and τ is not available, figures like that of Fig. 10 can be used, when a stability limit is determined, to derive the values of n and τ. We see clearly (in both Fig. 10 and the experimental Figs. 4, 5 and 6) that for the same n and τ, that is, for the same pressure and mixture ratio, there must exist *another* limit of stability, for which the values of L and $(\omega L/\bar{c}_0)$ can be obtained from curves of the type shown in Fig. 10.

This procedure has been used in the present investigation. Starting from the lower limit of stability for each mixture ratio r, the values of n and τ have been determined, and are presented in Figs. 11 and 12 for the two injectors used in the tests. The upper stability limit is then determined from the theoretical curves (Fig. 10). These theoretically determined limits may then be compared with the experimental upper limits (e.g., as in Fig. 6) obtained from the previously described tests on both injectors. The comparison, shown for the two injectors in Figs. 13 and 14, demonstrates the remarkably close correlation between theory and experiment.

This close correlation between theory and experiment is not limited to the alcohol-oxygen propellant combination alone. Fig. 15 illustrates this same close agreement for the case of iso-octane and oxygen where the alternate comparison has been made; i.e., the lower limit has been determined theoretically and compared with experimental values.

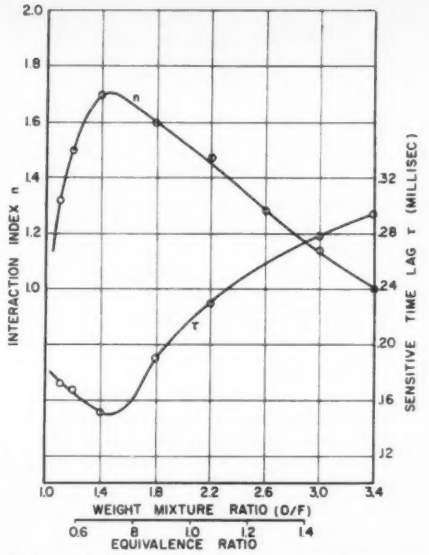

Fig. 11 Values of the sensitive time lag τ and interaction index n determined from the experimental *lower* stability boundary (Fig. 6) for the fundamental longitudinal mode. This figure shows results for the first injector (design $O/F = 1.4$) at a nominal chamber pressure of 300 psia

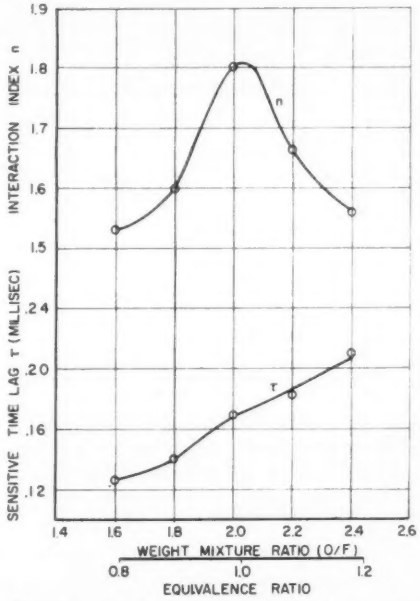

Fig. 12 Experimental values of n and τ for the second injector (design $O/F = 2.0$)

It appears from these results that the combustion model discussed in the section on rate of gas generation represents very closely the actual combustion behavior of the configurations used in the tests despite the number of simplifications, approximations and assumptions involved. This does not mean that the parameters n and τ can be given a clearcut interpretation relating them to the rates of a well-defined process such as evaporation or gas-phase chemical kinetics. Rather, n and τ must be interpreted as a kind of average among all processes which respond to the variations of the chamber conditions. Nevertheless, it is interesting to observe that, qualitatively, the behavior and magnitude of n and τ correspond quite well to those that might be ex-

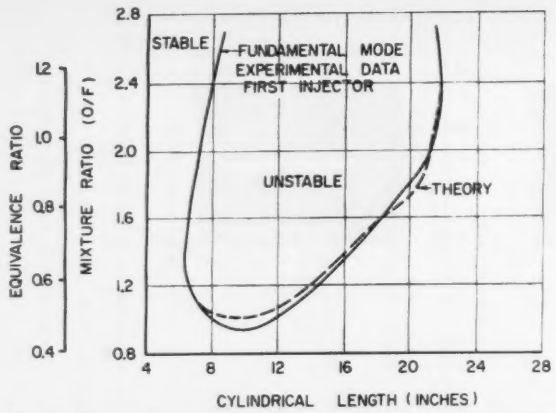

Fig. 13 Comparison of the *upper* experimental stability boundary for the fundamental longitudinal mode (Fig. 6) with theoretical predictions of this boundary (Fig. 10), based on n and τ data determined from experimental measurements at the lower boundary (Fig. 11). These results are for the first injector (design $O/F = 1.4$) at a nominal chamber pressure of 300 psia

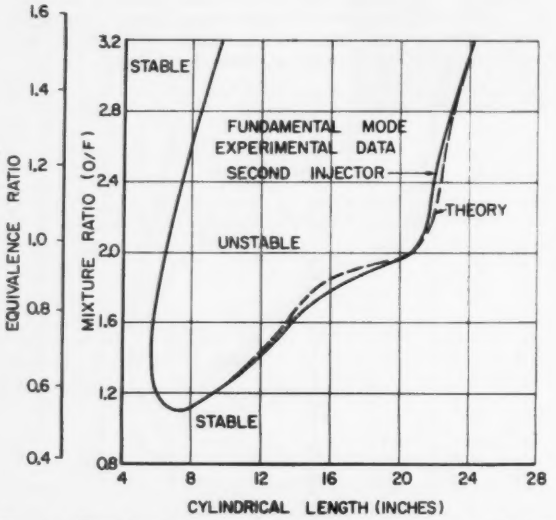

Fig. 14 Experimental theoretical correlation similar to that of Fig. 13, but for the second injector (design $O/F = 2.0$)

pected from considerations of chemical kinetics. In fact the time lag is in the right range, and exhibits, as expected, a minimum not far from stoichiometric conditions. The value of n also, from the chemical kineticist's viewpoint (disregarding the effects of the temperature variations), would be around 2 for the second-order reactions near stoichiometric and would tend to drop to 1 for the first-order reactions at very lean or very rich mixtures. This agreement is, however, only of a qualitative nature, and the fact that chemical kinetics is not the only process determining the values of n and τ is clearly established by the difference between the values obtained for the two injectors. In the case of premixed gases such as studied by Zucrow and Osborn (15) it is very likely that n and τ would fall closer to the chemical kinetic values.

Finally it must be observed that the ability of the theoretical combustion model to describe the actual behavior for injectors and propellants other than those considered here has still to be established by further testing, which is now in process at Princeton.

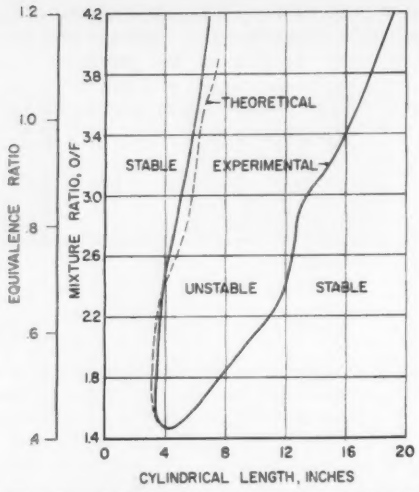

Fig. 15 Experimental-theoretical correlation similar to that of Figs. 13 and 14 but for iso-octane and oxygen where the *lower* stability limits are compared. The injector was designed for an optimum c^* mixture ratio of 2.4

Acknowledgments

The authors wish to thank Dr. Eva Kronenberg, who was instrumental in the data reduction and interpretation, and Mr. Frederick H. Reardon, who supervised much of the experimental testing. Financial support by the Powerplant Division of the United States Navy's Bureau of Aeronautics under Contract NOas 53-817-c made this study possible.

References

1 Gunder, D. F. and Friant, D. R., "Stability of Flow in a Rocket Motor," *J. Appl. Mech.*, vol. 17, 1950, p. 327.

2 Yachter, M., "Discussion of the Paper of Reference 1," *J. Appl. Mech.*, vol. 18, 1951, p. 114.

3 Summerfield, M., "A Theory of Unstable Combustion in Liquid Propellant Rocket Systems," Journal of the American Rocket Society, vol. 21, no. 5, 1951, p. 108.

4 Scala, S. M., "Transverse Wave and Entropy Wave Combustion Instability in Liquid Propellant Rockets," Princeton University (Ph.D. Thesis), Aero. Engng. Rep. no. 380, April 1, 1957.

5 Crocco, L. and Grey, J., "Combustion Instability in Liquid Propellant Rocket Motors," Proc. Gas Dynamics Symposium—Aerothermochemistry, Northwestern Univ., Evanston, Ill., 1956, p. 55.

6 Crocco, L., "Aspects of Combustion Instability in Liquid Propellant Rockets," Journal of the American Rocket Society; Part I: vol. 21, No. 6, Nov.–Dec., 1951, p. 163; Part 2: vol. 22, no. 1, Jan.–Feb., 1952, p. 7.

7 Crocco, L. and Cheng, S. I., "Theory of Combustion Instability in Liquid Propellant Rocket Motors," AGARD Monograph no. 8, Butterworths Scientific Pub., Ltd., London, 1956.

8 Crocco, L., "Supercritical Gaseous Discharge with High-Frequency Oscillations," *L'Aerotecnica*, vol. 33, 1953, p. 46.

9 Lambiris, S., "Experimental Verification of Nozzle Admittance Theory in a Similated Rocket Chamber," Project Squid Tech. Rep. PR 75-R, Sept. 15, 1957; *also* Princeton University Aeron. Engng. Rep. no. 401, Sept. 15, 1947.

10 Crocco, L., Monti, R. and Grey, J., "Substantiation of Nozzle Admittance Theory by Direct Measurement of the Admittance Parameter," Tech. Note (in preparation).

11 Reardon, F. H., "An Automatic Chamber Pressure and Mixture Ratio Control System for Liquid-Propellant Rocket Motors," ARS Preprint no. 571–57, 1957.

12 Li, Y. T., "Dynamic Pressure Measuring System for Jet Propulsion Research," Journal of the American Rocket Society, vol. 23, no. 3, May–June, 1953, p. 124.

13 Grey, J., "Experimental Determination of the Longitudinal Limits of Stability in a Liquid Bipropellant Rocket Motor," Appendix D to Fourteenth Quarterly Installment of Princeton University Aeron. Engng. Rep. no. 216-n, Dec. 1, 1955.

14 Berman, K. and Cheney, S. H., "Combustion Studies in Rocket Motors," Journal of the American Rocket Society, vol. 23, no. 2, March–April, 1953, p. 89.

15 Zucrow, M. J. and Osborn, J. R., "An Experimental Study of High-Frequency Combustion Pressure Oscillations," Jet Propulsion, vol. 28, no. 10, Oct. 1958, p. 654.

Rapid Approximate Method for Analyzing Nuclear Rocket Performance

ALAN H. STENNING[1]

Massachusetts Institute of Technology
Cambridge, Mass.

The effects of core geometry and surface temperature limitations on nuclear rocket performance are studied using the heat transfer friction analogy and one-dimensional gasdynamics. Approximate relationships between thrust coefficient, specific impulse, core geometry and maximum surface temperature are obtained. High thrust coefficient and high specific impulse are not compatible, and a compromise must be made between these two requirements. Off-design operation is also considered.

Optimizing the Core Design

IN A NUCLEAR rocket, the propellant is pressurized by a turbopump, heated in the reactor core, and then accelerated in the nozzle (Fig. 1). The temperature of the propellant leaving the core (and therefore the specific impulse) is limited by the heat transfer characteristics of the core and by the maximum temperature that the core structure will tolerate. The mass flow in the core is limited by the inlet pressure available and by the combined heat transfer and friction characteristics of the core. Within the limitations imposed by the allowable core temperature and the inlet pressure of the propellant, it is desired to maximize the thrust per unit flow area and the specific impulse of the propellant.

To simplify the analysis, we shall consider that the maximum surface temperature of the core is limited to some value T_s. The inlet temperature of the propellant is T_{01} and the outlet temperature is T_{02}. The ratio T_s/T_{01} is much greater than unity because cryogenic fluids will be employed as propellants.

If the axial power density within the core is constant (linear temperature rise), then the maximum surface temperature occurs at the outlet, where T_0 equals T_{02}. Equating the enthalpy increase of the fluid to the heat transferred

$$mc_{p2}\frac{dT}{dx}\,dx = h_2\Delta T_2\,\frac{dS_h}{dx}\,dx \qquad [1]$$

where

$$\frac{dT}{dx} = \frac{T_{02} - T_{01}}{L}$$

$$\frac{dS_h}{dx} = \frac{S_h}{L}$$

Hence

$$\frac{\Delta T_2}{T_{02} - T_{01}} = \frac{mc_{p2}}{h_2 S_h} = \frac{m/A_1 c_{p2}}{h_2}\,\frac{A_1}{S_h} \qquad [2]$$

where

ΔT	=	the temperature difference between surface and propellant
S_h	=	the heat transfer area
A_1	=	the flow cross section area
L	=	the channel length
$h/(m/A)c_p$	=	Stanton number N_{st}
A_1/S_h	=	$D/4L$
D	=	hydraulic diameter of the channels
L	=	length of the core

From the heat transfer friction analogy, N_{st} equals $f/2$ (1)[2] where f is the friction factor. This relationship is valid if the Prandtl number of the fluid is close to unity, which is true for hydrogen and some of the other potential propellants. Thus

$$\frac{\Delta T_2}{T_{02} - T_{01}} = \frac{2}{f_2}\cdot\frac{D}{4L} \qquad [3]$$

$$T_s - T_{01} = T_{02} + \Delta T_2 - T_{01} \qquad [4]$$

$$\frac{T_s/T_{01} - 1}{T_{02}/T_{01} - 1} = 1 + \frac{2}{(4f_2L/D)} \qquad [5]$$

This relationship is plotted in Fig. 2. For purposes of comparison, the value of $(T_s/T_{01} - 1)/(T_{02}/T_{01} - 1)$ for a cosine axial power density distribution is also shown. For the cosine power distribution, the relationship is given by the following equation (2)

$$\frac{T_s/T_{01} - 1}{T_{02}/T_{01} - 1} = \frac{1}{2} + \sqrt{\left(\frac{\pi}{4f_2L/D}\right)^2 + \frac{1}{4}} \qquad [6]$$

The difference between Equations [5 and 6] is small. In the region of interest the assumption of constant power density

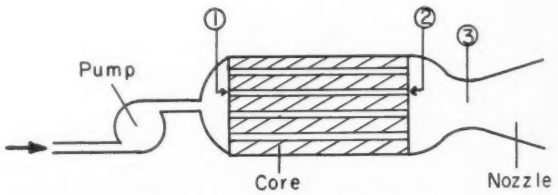

Fig. 1 Schematic of nuclear rocket

Received May 5, 1959.

[1] Assistant Professor of Nuclear Engineering. Member ARS.

[2] Numbers in parentheses indicate References at end of paper.

is the more conservative, and will therefore be used throughout the remainder of the paper. From Equation [5], allowable values of T_{02}/T_{01} may be obtained in terms of T_s/T_{01}, $(4f_2L/D)$. It is assumed that the channels are arranged within the core to give the same temperature rise for each channel.

The mass flow and stagnation pressure change in the core are governed by the friction and acceleration effects in the heat transfer channels. The exact differential equations for combined heat addition and friction are complicated and cannot in general be integrated analytically (3). However, it is possible to avoid these difficulties by making the reasonable assumption that the wall shear stress in the channels increases linearly from inlet to outlet. Since

$$\tau_w = f\frac{\rho V^2}{2g_0} = f\frac{(m/A_1)V}{2g_0}$$

this assumption is correct if the velocity increases linearly from inlet to outlet. If the stagnation temperature is linear with distance along the channel, then the velocity gradient is almost constant and the approximation is a good one, giving errors in mass flow of only a few per cent when the overall temperature ratio is large and the quantity $(f_2L/D)M_2^2$ is less than 0.7.

With this approximation, the momentum equation for the whole channel is

$$(p_1 - p_2)A_1 = \frac{A_1\rho_2V_2^2}{g_0} - \frac{A_1\rho_1V_1^2}{g_0} + \frac{1}{2}S_h\left(\frac{f_1\rho_1V_1^2}{2g_0} + \frac{f_2\rho_2V_2^2}{2g_0}\right) \quad [7]$$

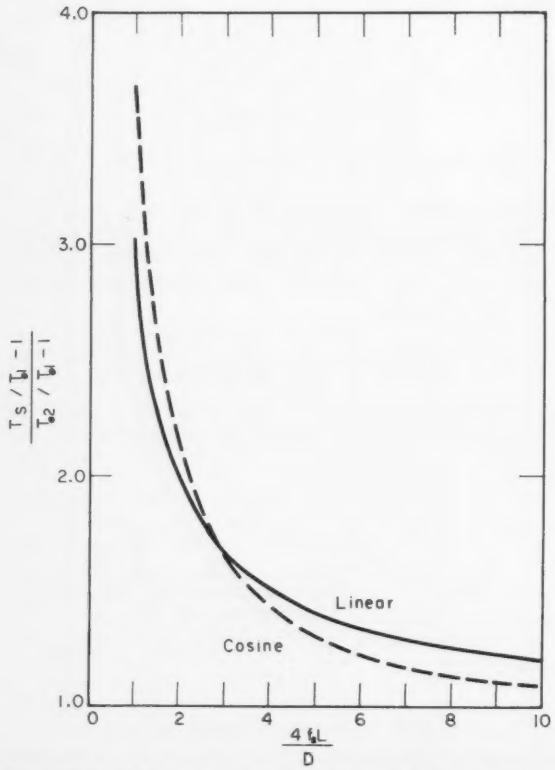

Fig. 2 Effect of core geometry on maximum surface temperature

For a perfect gas, $(\rho V^2/g_0)$ equals γpM^2, and Equation [7] becomes

$$p_1\left[1 + \gamma_1M_1^2\left(1 - \frac{f_1L}{D}\right)\right] = p_2\left[1 + \gamma_2M_2^2\left(1 + \frac{f_2L}{D}\right)\right] \quad [8]$$

where γ_1, γ_2 are the ratios of specific heats at 1 and 2, respectively. Also

$$\frac{p_0}{p} = \left(1 + \frac{\gamma - 1}{2}M^2\right)^{\gamma/(\gamma-1)} \quad [9]$$

Substituting Equation [9] into [8]

$$\frac{p_{01}}{p_{02}} = \frac{\{1 + [(\gamma_1 - 1)/2]M_1^2\}^{\gamma_1/(\gamma_1-1)}\{1 + \gamma_2M_2^2[1 + (f_2L/D)]\}}{\{1 + [(\gamma_2 - 1)/2]M_2^2\}^{\gamma_2/(\gamma_2-1)}\{1 + \gamma_1M_1^2[1 - (f_1L/D)]\}} \quad [10]$$

When M_1 is much smaller than unity, Equation [10] reduces to

$$\frac{p_{01}}{p_{02}} = \frac{\{1 + \gamma_2M_2^2[1 + (f_2L/D)]\}}{\{1 + [(\gamma_2 - 1)/2]M_2^2\}^{\gamma_2/(\gamma_2-1)}} \quad [11]$$

$$p = \rho RT = \frac{(m/A)RT}{V} \quad [12]$$

Substituting Equation [12] in [8] and using the relation $V = M\sqrt{\gamma g_0RT}$

$$\frac{\sqrt{T_1}}{M_1\sqrt{\gamma_1}}\left[1 + \gamma_1M_1^2\left(1 - \frac{f_1L}{L}\right)\right] = \frac{\sqrt{T_2}}{M_2\sqrt{\gamma_2}}\left[1 + \gamma_2M_2^2\left(1 + \frac{f_2L}{D}\right)\right] \quad [13]$$

Also

$$T_0/T = 1 + [(\gamma - 1)/2]M^2 \quad [14]$$

whence

$$\frac{T_{02}}{T_{01}} = \frac{\gamma_2M_2^2}{\gamma_1M_1^2} \times \frac{\{1 + [(\gamma_2 - 1)/2]M_2^2\}\{1 + \gamma_1M_1^2[1 - (f_1L/D)]\}^2}{\{1 + [(\gamma_1 - 1)/2]M_1^2\}\{1 + \gamma_2M_2^2[1 + (f_2L/D)]\}^2} \quad [15]$$

When T_{02}/T_{01} is much larger than 1, $M_1 \ll 1$ and the equation reduces to the form

$$M_1^2 = M_2^2\left(\frac{\gamma_2T_{01}}{\gamma_1T_{02}}\right)\frac{\{1 + [(\gamma_2 - 1)/2]M_2^2\}}{\{1 + \gamma_2M_2^2[1 + (f_2L/D)]\}^2} \quad [16]$$

When T_{02}/T_{01} is greater than 20, Equation [16] yields values for M_1 within 1 per cent of those given by Equation [15]. A convenient mass flow parameter is

$$\frac{m\sqrt{T_0}}{Ap_0\sqrt{(\gamma g_0/R)}}$$

In (3), it is shown that

$$\frac{m\sqrt{T_0}}{Ap_0\sqrt{(\gamma g_0/R)}} = \frac{M}{\{1 + [(\gamma - 1)/2]M^2\}^{(\gamma+1)/2(\gamma-1)}} \quad [17]$$

When M is much smaller than 1

$$\frac{m\sqrt{T_0}}{Ap_0\sqrt{(\gamma g_0/R)}} = M$$

and this is an excellent approximation at the entrance to the

core. Thus, the inlet mass flow parameter is given by

$$\frac{m\sqrt{T_{01}}}{A_1 p_{01}\sqrt{(\gamma_1 g_0)/R}} = M_2\sqrt{\frac{\gamma_2 T_{01}}{\gamma_1 T_{02}}}\frac{\{1+[(\gamma_2-1)/2]M_2^2\}^{1/2}}{\{1+\gamma_2 M_2^2[1+(f_2L/D)]\}} \quad [18]$$

The specific impulse I is equal to (v_j/g_0), where

$$v_j = \sqrt{2g_0\frac{\gamma_2}{\gamma_2-1}RT_{02}\left[1-\left(\frac{p_a}{p_{02}}\right)^{(\gamma_2-1)/\gamma_2}\right]} \quad [19]$$

assuming no additional stagnation pressure losses between the reactor and the nozzle exit. We define

$$I_{max} = (v_j)_{max}/g_0$$

where

$$(v_j)_{max} = \sqrt{2g_0\frac{\gamma_2}{\gamma_2-1}RT_s\left[1-\left(\frac{p_a}{p_{01}}\right)^{(\gamma_2-1)/\gamma_2}\right]}$$

I_{max} is the maximum specific impulse attainable if the propellant could be heated to the maximum surface temperature with no stagnation pressure loss. I/I_{max} is thus a figure of merit for the design

$$\frac{I}{I_{max}} = \sqrt{\frac{T_{02}}{T_s}}\frac{\sqrt{1-(p_a/p_{02})^{(\gamma_2-1)/\gamma_2}}}{\sqrt{1-(p_a/p_{01})^{(\gamma_2-1)/\gamma_2}}} \quad [20]$$

The thrust coefficient is

$$\frac{F}{A_1 p_{01}} = \frac{mI}{A_1 p_{01}} \quad [21]$$

Substituting Equation [19] in [21]

$$\frac{F}{A_1 p_{01}} = \frac{m\sqrt{T_{01}}}{A_1 p_{01}\sqrt{(\gamma_1 g_0/R)}}\sqrt{\frac{T_{02}}{T_{01}}}\times \sqrt{1-\left(\frac{p_a}{p_{02}}\right)^{(\gamma_2-1)/\gamma_2}}\sqrt{\frac{2\gamma_1\gamma_2}{\gamma_2-1}} \quad [22]$$

The results of the analysis do not depend on the state equation of the fluid entering the core, since γ_1 cancels out of Equation [22]. Equations [20 and 22] are therefore valid for any substance which obeys the gas laws at high temperatures.

In designing a core with given T_s/T_{01}, p_{01}/p_a, we wish to determine the effect of the core geometry parameter $(4f_2L/D)$ and the exit Mach number M_2 on the attainable performance. Using Equations [5,11,18,20 and 22], the specific impulse parameter I/I_{max} and the thrust coefficient may be computed for different values of $(4f_2L/D)$, keeping M_2 constant. The results of such a calculation are shown in Fig. 3 for $T_s/T_1 = 50$, $p_{01}/p_a = 100$, $\gamma_2 = 1.4$, $M_2 = 1.0$. I/I_{max} increases as $(4f_2L/D)$ is increased, but flattens out for $(4f_2L/D)$ greater than 5. With increase in friction parameter, the mass flow parameter (Eq. [18]) decreases with consequent reduction in thrust coefficient (Eq. [22]). Similar curves are obtained when different values of M_2 are selected, but the effect of exit Mach number on performance is not a simple one. As M_2 is increased from zero with fixed values of $(4f_2L/D)$ and (T_{02}/T_{01}), the stagnation pressure loss increases and the specific impulse decreases slightly. The inlet mass flow parameter predicted by Equation [18] reaches a maximum and then decreases. In consequence, the thrust coefficient predicted by the present analysis also passes through a maximum and then decreases slightly as M_2 is increased to unity. The predicted decrease in mass flow and thrust coefficient at high Mach numbers is spurious, and is a consequence of the overestimation of wall shear resulting from the assumption of linear shear stress change between inlet and outlet. Numerical solutions show that the mass flow parameter increases rapidly as predicted by the present analysis for M_2 up to 0.5–0.6 and then flattens out but does not drop. In Fig. 4, I/I_{max} and (F/A_1p_{01}) are plotted against M_2 for $T_s/T_{01} = 50$, $(p_{01}/p_a) = 100$, $(4f_2L/D) = 4$ and $\gamma_2 = 1.4$. Disregarding the erroneous drop in thrust coefficient predicted at high values of M_2, it is still obvious that little improvement in thrust is to be gained by increasing the exit Mach number above 0.6, while the specific impulse drops as M_2 is increased. In addition, the losses in the mixing region after the core (ignored in this analysis) also increase as M_2 is raised. It would therefore appear to be desirable to design for $M_2 < 0.7$.

For higher values of $(4f_2L/D)$, the thrust coefficient flattens out at lower values of M_2, and the value of M_2 at the "peak" (which may be taken as indicative of the highest M_2 which is

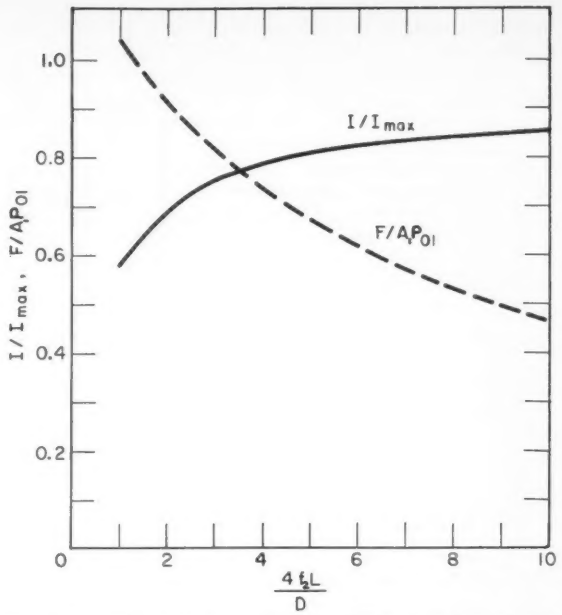

Fig. 3 Specific impulse and thrust coefficient as functions of $(4f_2\,L/D)$

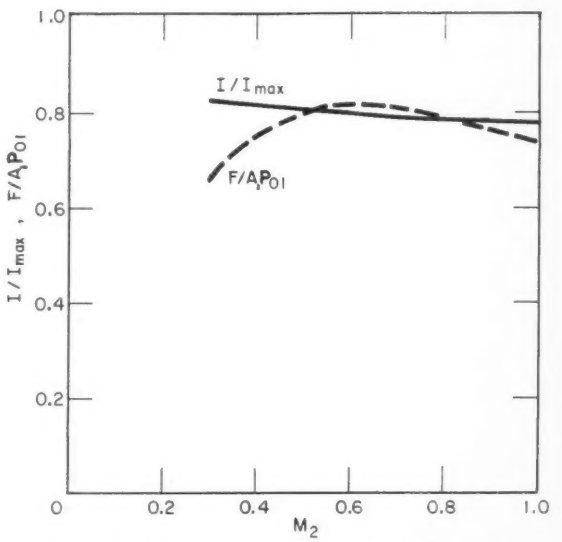

Fig. 4 Effect of variation of M_2 on rocket performance

profitable to use) is in fact equal to $[1/\sqrt{1 + \gamma_2(f_2L/D)}]$. We denote this value by M_2^*. In Fig. 5, I/I_{max} and F/A_1p_{01} are shown as functions of $(4f_2L/D)$ for the same example as Fig. 3, but here the exit Mach number has been made equal to M_2^* for each geometry. The effect is to improve the predicted performance at higher values of $(4f_2L/D)$, but the general trend is unchanged. Fig. 5 is practically a universal plot for all nuclear rockets, since variations in T_a/T_{01} and p_{01}/p_a have very little effect on the values of I/I_{max} and F/A_1p_{01}. We therefore conclude that the compromise choice of $(4f_2L/D)$ for reasonably good specific impulse and thrust coefficient will probably lie between 4 and 8 and will be governed by the requirements of the vehicle. In cases where the minimum channel diameter is limited by fabrication methods and the maximum core length has been set, an upper limit on $(4f_2L/D)$ will exist regardless of the preceding considerations. For example, if the maximum core length is 6 ft, the minimum D is $\frac{1}{4}$ in., and f_2 is 0.005, then $(4f_2L/D)$ cannot exceed 5.8 for a single pass design.

If the mean shear stress is taken as $0.4\ (\tau_1 + \tau_2)$ instead of $0.5\ (\tau_1 + \tau_2)$ improved accuracy is obtained for $M_2 > 0.5$, at the cost of a small decrease in accuracy for $M_2 < 0.5$.

Off-Design Operation

In considering off-design operation, we are concerned with the behavior of a core with fixed L/D, followed by a jet nozzle, when the thermal power of the reactor and the inlet pressure depart from the design values. Since f is inversely proportional to the fifth root of the Reynolds number for a smooth channel and varies very little, it is convenient to neglect changes in f and consider $(4f_2L/D)$ to be constant for a given core.

The core is followed by a nozzle which is choked under all operating conditions after the starting transient. $(m\sqrt{T_{03}})/(A_3p_{03})$ is therefore constant and $(m\sqrt{T_{02}})/(A_2p_{02})$ must also be constant, since T_{02} equals T_{03}, A_2/A_3 is fixed and the stagnation pressures are equal. M_2 is then fixed for all operating conditions. p_{01}/p_{02} is also constant, from Equation [11].

Thrust changes can be made only by changing the core inlet pressure p_{01}. The thrust is independent of the reactor thermal output. This result follows from combining Equations [18 and 22] to give

$$\frac{F}{A_1p_{01}} = \frac{M_2\{1 + [(\gamma_2 - 1)/2]M_2^2\}^{1/2}}{\{1 + \gamma_2M_2^2[1 + (f_2L/D)]\}} \times \sqrt{1 - \left(\frac{p_a}{p_{02}}\right)^{\gamma_2/(\gamma_2-1)}} \sqrt{\frac{2\gamma_2^2}{\gamma_2 - 1}} \quad [23]$$

Control over specific impulse is obtained by varying the reactor power level and hence T_{02}.

For fast thrust control the inlet pressure p_{01} can be changed without moving the control rods. A sudden increase in p_{01} raises the mass flow rate and lowers the outlet and surface temperatures. The reactor negative temperature coefficient will tend to restore the outlet temperature to its original value if given time to do so. Slow thrust changes should be made with reactor power proportional to p_{01}, so that the outlet temperature, surface temperature and specific impulse do not change.

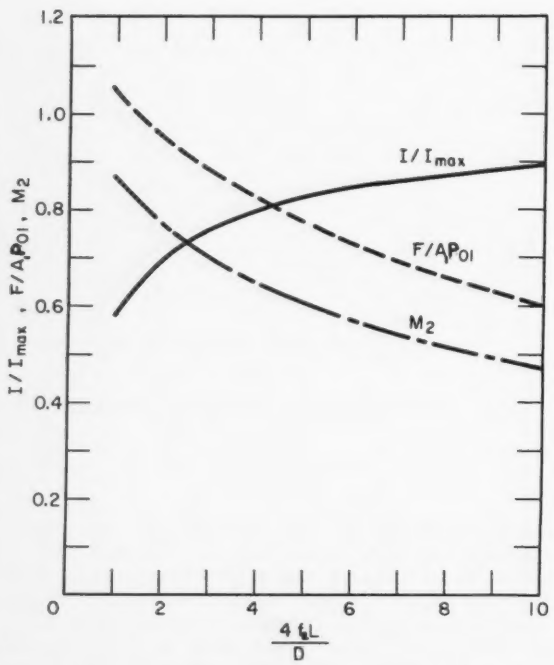

Fig. 5 Optimized thrust coefficient and specific impulse as functions of $(4f_2L/D)$

Nomenclature

- A = cross section flow area
- c_p = specific heat at constant pressure
- D = channel hydraulic diameter
- f = friction factor
- F = thrust
- g_0 = proportionality constant in Newton's law: Force = mass × acceleration/g_0
- h = heat transfer coefficient
- I = specific impulse
- L = channel length
- m = mass flow rate
- M = Mach number
- p = stream pressure
- p_0 = stagnation pressure
- R = gas constant
- S_h = heat transfer area
- T = stream temperature
- T_0 = stagnation temperature
- T_s = maximum surface temperature
- V = velocity
- v_j = jet velocity
- γ = ratio of specific heats
- ρ = density
- τ = wall shear stress

Subscripts

- 1 = entering channel
- 2 = leaving channel
- 3 = at nozzle throat
- a = atmospheric

References

1 Eckert, E. R. G., "Introduction to the Transfer of Heat and Mass," McGraw-Hill Book Co., Inc., N. Y., 1950, first ed., p. 124.

2 Diamond, J., "Heat Removal from Nuclear Power Reactors," Inst. of Mech. Engrs. (Great Britain) Symposium on Nuclear Energy, 1956, published by the Institution, London.

3 Shapiro, A. H., "The Dynamics and Thermodynamics of Compressible Fluid Flow," Ronald Press Co., N. Y., 1954, first ed., chaps. 4, 8.

Experimental Investigation of Propellant Erosion

TAGE MARKLUND[1] and ARNE LAKE[2]

Research Institute of National Defense
Stockholm, Sweden

Erosion test methods, characterized by separate gas producing charges and separate specimens in the gas stream, are described. The specimens have been tablets, strips and nozzle inserts of composite propellants. Changing the temperature of the gas stream over a propellant specimen from 1690 to 2550 K did not seem to influence the erosion at constant gas velocity and pressure. Erosion on tablets of ϕ 1.4 cm was about 40 per cent higher than on strips, at a distance of 7.0 cm from the front edge for a certain propellant. Erosion at near sound velocity in a propellant nozzle was found to be of the same order of magnitude as on strips at lower gas velocity but the same mass velocity. Results are discussed particularly in view of the Lenoir and Robillard theory of propellant erosion. The strip method especially seems to be a useful tool for studies of the temperature resistance of materials for thermal insulation of rocket motors, nozzle inserts, etc.

PROPELLANT erosion studies started some years ago at FOA (Research Institute of National Defense, Sweden). An x-ray flash was used to produce pictures of the burning propellant tubes in the motor chamber. This investigation had reference to a certain rocket project. Our intention, however, was to develop a small-scale method for comparison of the erosion of different propellants. It then seemed to be more convenient to separate the gas producing part from the specimen. Work was carried on from that point of view.

In all these studies, the eroding gas was produced in a separate motor chamber. The specimen was placed in a steel tube connected to the motor. The motor pressure and the flow rate of gas were varied by changing the nozzle throat area and the main charge.

The specimens have been short tubes (burning internally), tablets, strips and nozzle inserts of composite propellants. Propellant data are given in Table 1.

X-Ray Flash Method

Our first studies of burning propellant changes with an x-ray flash were followed by an investigation using the equipment illustrated in Fig. 1. We intended to study erosion in channels and used as specimens propellant tubes with their outer surfaces thermally insulated and fitting properly in the steel tube.

The main charge is initiated and produces a gas flow through the specimen tube whose burning is supposed to start in a negligible time delay. After a time interval, which can be chosen arbitrarily, the flash goes and a picture of the tube is received at this moment of burning. From the increase of the hole diameter during the actual time interval, the average burning rate r cm sec^{-1} is calculated. Knowing the mean pressure p bars during the interval, and the burning rate r_0 cm sec^{-1} of the propellant at zero gas velocity and at this pressure (strand burning rate), the erosive burning rate r_e is calculated as $r_e = r - r_0$.

Only propellant A was studied using this method. The results were rather scattered according to the averaging problem and the unfavorable geometric configuration of the specimen. However the influence on the erosive rate of gas velocities from 50 to 300 m sec^{-1} and pressures from 15 to 150 bars was determined. About 30 per cent lower values of r_e were received than later results from the tablet method (see the following).

Tablet Method

Separate gas producing charge and propellant tablets as specimens characterized a method developed at Bofors (2).[3]

Received May 1, 1959.

[1] Head of Solid Propellant Rocket Section.

[2] Research Engineer, Solid Propellant Rocket Section.

[3] Numbers in parentheses indicate References at end of paper

Table 1 Propellant data

Propellant type	Components	Oxidizer: Weight, per cent	Oxidizer: Av. particle size, μ	Binder weight, per cent	Propellant density, gm cm^{-3}	Propellant gas: Flame temp., K	Propellant gas: Av. mol. weight	Propellant gas: Exptl. discharge coeff., 10^{-4} sec m^{-1}	Sound veloc., m sec^{-1}
A	NH_4ClO_4 + polyester	65	24–30	35	1.62	1690	21	8.60	930
B	NH_4ClO_4 + polysulfide-epoxy	65	24–30	35	1.63	1750	22	8.50	940
C	NH_4ClO_4 + polysulfide-epoxy	75	24–30	25	1.70	2550	25	7.5	1020
D	$NH_4ClO_4/KClO_4$ (3/1) + polysulfide-epoxy	70	24–30 ($KClO_4$ 20 μ)	30	1.74	2220	26	8.2	940

The tablets are cemented on quartz window plugs and placed in the gas stream with their surfaces parallel to the flow direction. Light from the propellant gas through the quartz windows indicates via photomultipliers the burnout times of the tablets. Using tablets of different thicknesses allows determination of the burning rate as the difference in thickness through the difference in burnout times.

This method does not involve the same averaging problem as the x-ray flash method described. However it is difficult to apply to transparent propellants, i.e., many composite propellants.

At FOA, pressure gages are used for the indication (Fig. 2). The tablet is cemented over a small hole in the pressure pickup plug and a rapid increase of the pressure in the plug is registered when the tablet is consumed. This method is of course appropriate to transparent propellants too and has been used for investigations of the composite propellants listed in Table 1.

The total burning rate r of propellants A and C has been measured at very different gas velocities and pressures. The burning rate r_0 at about zero gas velocity has been carefully determined in an ordinary strand burning bomb and with a rather high degree of accuracy. Results—single values—are shown in Figs. 3 and 4. We observe that the erosive effect of propellant C is negligible at low pressures and gas velocities. It is remarkable that the total burning rate of these two propellants are of the same order of magnitude at higher pressures, although their energy contents and strand burning rates are so different. This is still more obvious in Fig. 5 where average values corrected to pressures of 20, 50 and 100 bars are used. Some results for propellant B are included.

In Fig. 6 these results are presented in another way together with values for propellant D. The erosive burning rate r_e is plotted over the mass velocity G gm cm^{-2} sec^{-1}. Average values are used. It seems that high strand burning rate r_0 for these propellants means: Low erosive burning rate, a pronounced threshold mass velocity, and strong influence of G on r_e.

The influence of different temperatures in the gas flow over the propellant surface has been studied in a special investigation of about 50 rounds. The burning rate of propellant tablets was compared using alternatively propellant A and propellant C as the main charge. At every series of comparison the port area over the tablet and the nozzle area, i.e., the Mach numbers, were the same for the two main charges. The pressure was adjusted to the same level by changing the burning surfaces of the main charges. Results reduced to the same gas velocities and pressures are given in Table 2.

The two main charges give the same burning rates—and erosive burning rates—at fixed velocities and pressures.

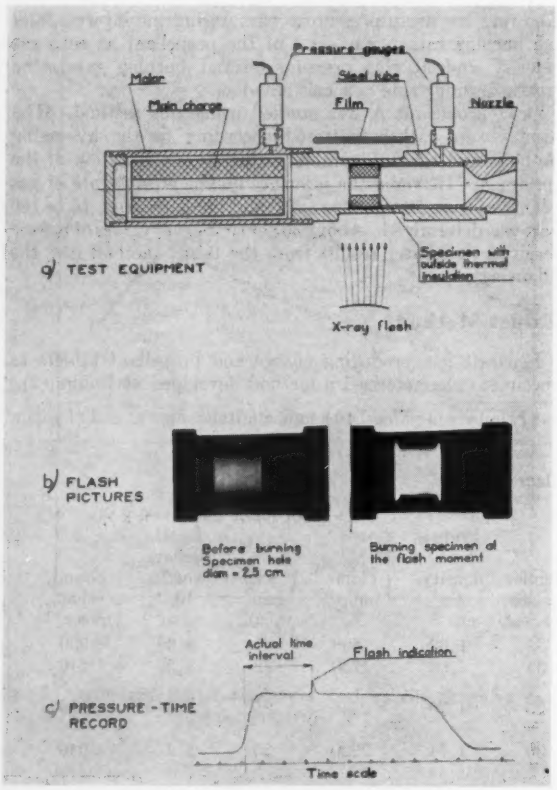

Fig. 1 The x-ray flash method

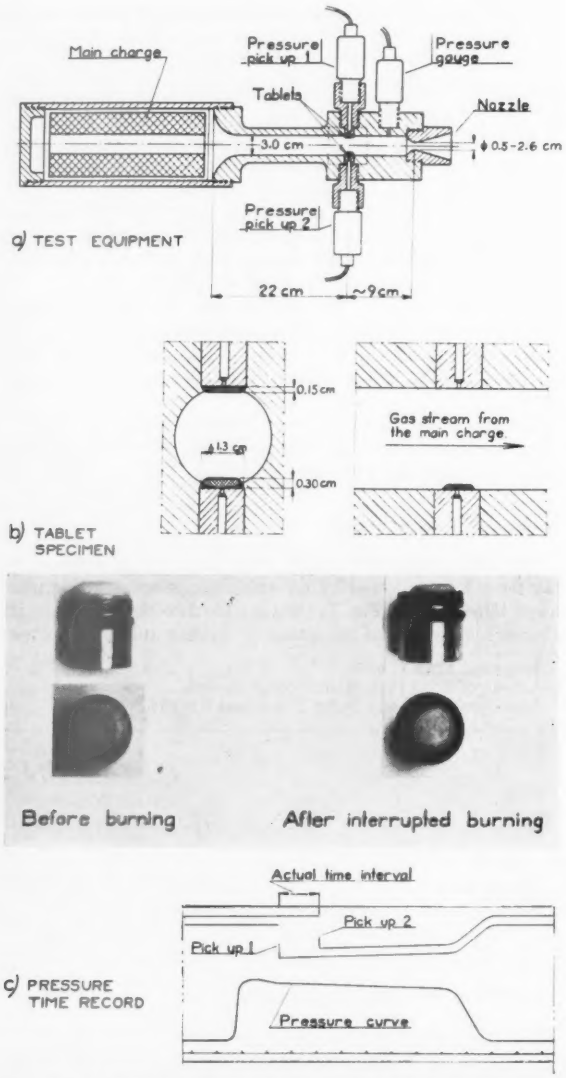

Fig. 2 Tablet method with pressure pickup indication

Table 2 Total burning rate of tablets at different gas temperatures T_f

Tablet of propellant	Flow conditions: Gas veloc. u, m sec^{-1}	Flow conditions: Motor pressure p, bars	Total burning rate r cm sec^{-1}: Main charge of propellant A, T_f = 1690 K	Total burning rate r cm sec^{-1}: Main charge of propellant C, T_f = 2550 K	Strand burning rate r_0, cm sec^{-1}
A	50	20	0.29 ± 0.01	0.30 ± 0.01	0.26
	50	100	0.75 ± 0.05	0.72 ± 0.01	0.47
	100	20	0.38 ± 0.02	0.39 ± 0.02	0.26
	100	100	1.03 ± 0.06	1.02 ± 0.04	0.47
C	50	100	0.90 ± 0.04	0.95 ± 0.01	0.85
	100	100	1.20 ± 0.02	1.19 ± 0.03	0.85
	225	20	0.60 ± 0.02	0.63 ± 0.02	0.51

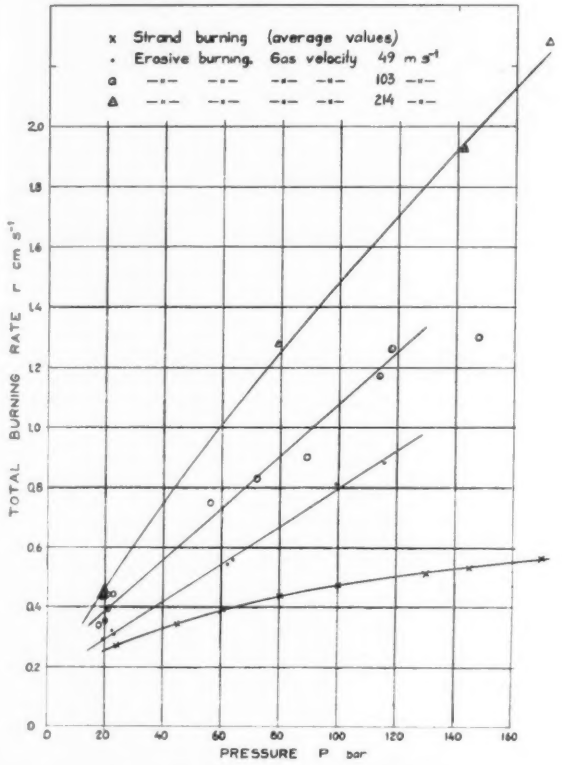

Fig. 3 Erosive burning of propellant A

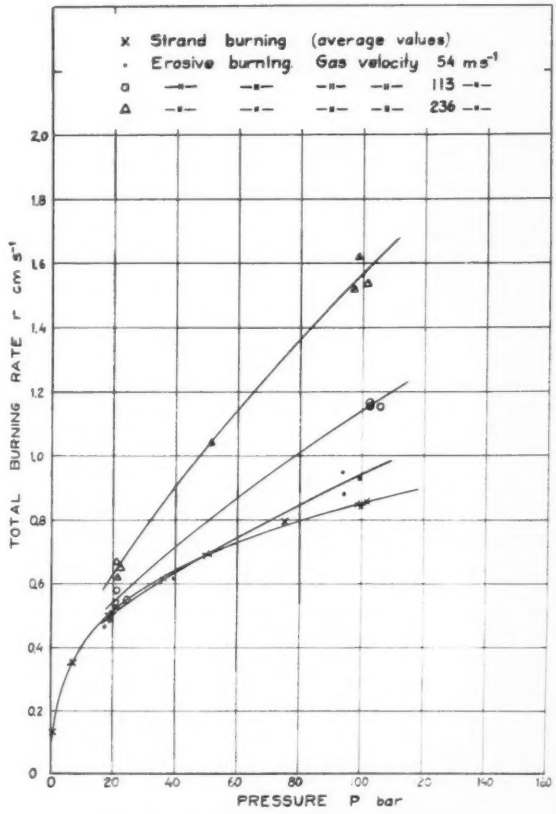

Fig. 4 Erosive burning of propellant C

Strip Method

The effect of changing the specimen dimensions was studied, using strips instead of tablets. The arrangement is shown in Fig. 7. Strips with sharp front edges of propellants A and C and of some plastics were exposed to gas flow at p = 50 bars and u = 100 to 200 m sec^{-1} from main charges of short burning times. The surfaces of the partly consumed specimens were studied and measured. The regression of the surface of the propellants, i.e., the total burning rate r, was found to be slightly decreasing downstream. By subtraction of the strand burning rate r_0 corresponding to the actual average pressure, the erosive rate r_e was obtained. It was 20 to 30 per cent higher at a distance x = 0.7 cm from the front edge than at x = 7.0 cm. A similar decrease of r_e was observed for the strips of Plexiglas, polysulfide and polysulfide-epoxy.

After this preliminary investigation, table and strip erosion were compared for propellant A. The strips were given a form according to Fig. 7b. The erosive burning rate was determined by pressure indication at x = 0.7 cm as before for the tablets and x = 7.0 cm for the strips. About 40 per cent higher erosive rates were obtained for the tablets. The results are discussed later; see Fig. 9.

Nozzle Method

Propellant erosion at sound velocities is of interest for development of high performance rockets. We have made some preliminary studies using nozzle inserts of the propellants A and C (Fig. 8). The regression rate was measured as before by pressure indication using two holes drilled in the nozzle. An auxiliary nozzle was used to reduce pressure drop

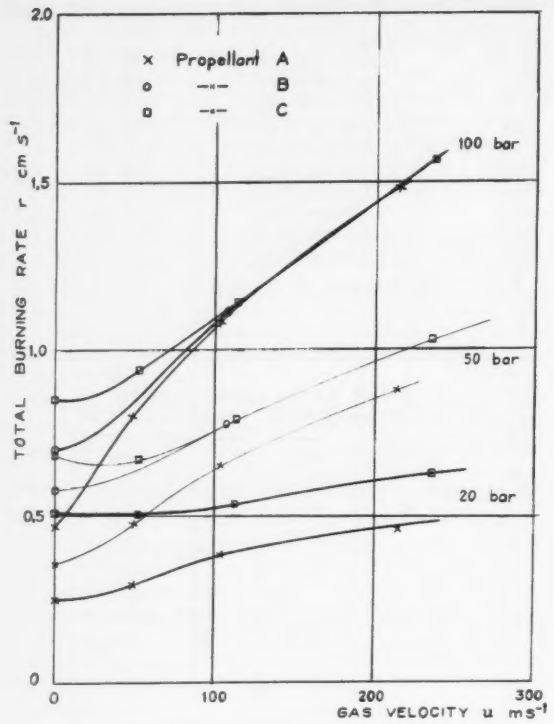

Fig. 5 Erosive burning of propellants A, B and C

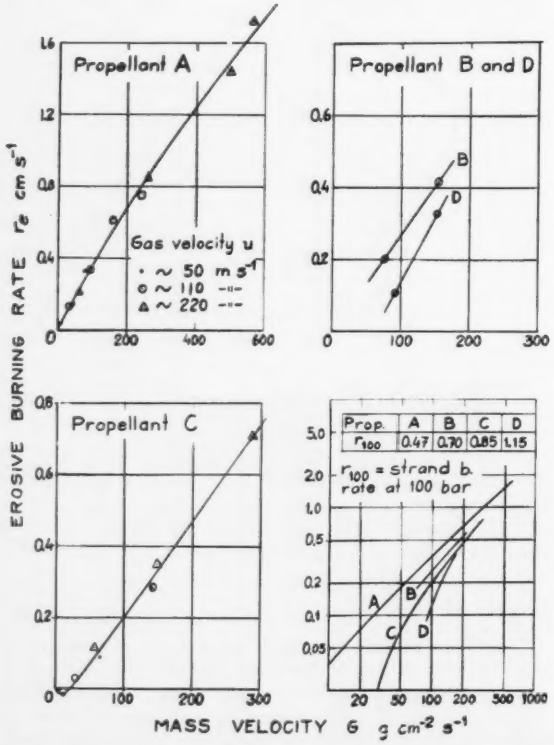
Propellant A
Propellant B and D
Propellant C
Gas velocity u
~ 50 m s⁻¹
~ 110 -"-
~ 220 -"-
Prop. A B C D
r100 0.47 0.70 0.85 1.15
r100 = strand b. rate at 100 bar
EROSIVE BURNING RATE re cm s⁻¹
MASS VELOCITY G g cm⁻² s⁻¹

Fig. 6 Erosive burning rate as a function of mass velocity

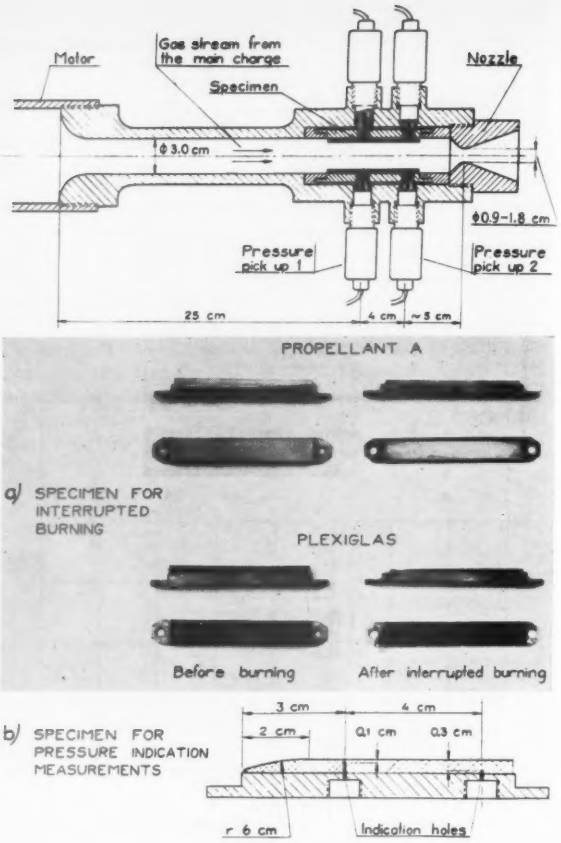

Fig. 7 Strip method

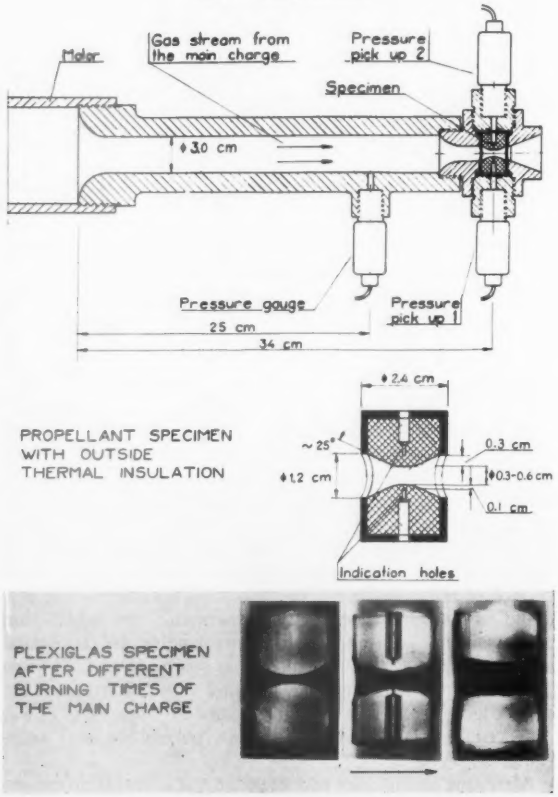

Fig. 8 Nozzle method

in the motor as the diameter of the propellant nozzle increased (from about ϕ 0.8 to about ϕ 1.1 cm between two indications). Motor pressures were about 25 to 60 bars. The pressure in the nozzle throat was measured by the indication gages to enable estimation of the corresponding value of r_0. The mass velocity was calculated as the product of motor pressure and nozzle discharge coefficient. See Table 3.

The erosion in these nozzles is obviously of the same order of magnitude as on strips. However flow conditions are rather different, and the gas temperature is due to expansion lower than in the motor. Other experiments have also shown some influence on the results from the throat area and from the pressure. On some of the pressure records "resonance burning" was observed, perhaps because of the auxiliary nozzle.

Discussion

Lenoir and Robillard (1,3) have proposed a theory which states that the erosive rate will be equal to the additional heat transferred divided by the heat required to raise the propellant to the surface temperature. Assuming empirical relationships for turbulent pipe flow and transpiration cooling, they arrive at the following expression

$$r_e = \alpha \cdot G^{0.8} \cdot x^{-0.2} \cdot e^{-\beta \rho_s r / G} \qquad [1]$$

where

$$\alpha = 0.0288\, c_g \mu_g^{0.2} P r_g^{-0.67} \frac{T_f - T_s}{\rho_s c_s (T_s - T_i)} \qquad [2]$$

The experimental conditions described in this paper are quite different from those assumed by Lenoir and Robillard, and it would not be expected that the same heat transfer coefficient would hold especially with regard to the length term $x^{-0.2}$. As the other terms, however, should be approximately the same, let us interpret our results according to the theory.

From Fig. 6 it is obvious that our results cannot be explained by the ordinary turbulent heat transfer theory without transpiration and with $r_e \sim G^{0.8}$. Following Lenoir and Robillard we estimate the empirical constant β according to Equation [1] and use results from Figs. 4 and 5. We find that for the ammonium perchlorate propellants A, B and C, β is equal to approximately 20, 45 and 70. From a few results for propellant D containing potassium perchlorate no definite β value could be estimated. The correlation between r_e and $G^{0.8} \cdot e^{-\beta \rho_s r / G}$ for propellants A and C is given in Fig. 9. Results from the comparison of tablets and strips of propellant A are plotted in this diagram too. The agreement seems to be fairly good and supports the Lenoir and Robillard theory. However some remarks should be made.

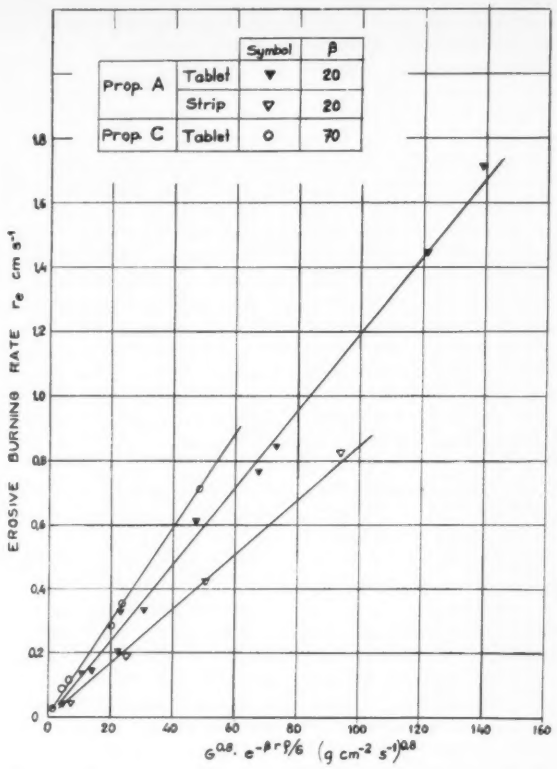

Fig. 9 Erosive burning rate as a function of $G^{0.8} \cdot e^{-\beta r \rho / G}$

Table 3 Propellant erosion in nozzles

Propellant	Round no.	Mean motor pressure between pickup indications p, bars	Mass velocity G, gm·cm^{-2}·sec^{-1}	Total burning rate r, cm·sec^{-1}	Strand burning rate (at nozzle pressure) r_0, cm·sec^{-1}	Nozzle erosion r_0, cm·sec^{-1}	Strip erosion r_e, cm·sec^{-1}
	1	26	222	0.69	0.18	0.51	...
	2	36	310	0.78	0.20	0.58	...
A	3	46	396	1.33	0.23	1.10	...
	4	27	236	0.66	0.18	0.48	...
	Mean values after interpolation to motor pressure p = 38 bars		326	0.99	0.21	0.78	0.80
	1	50	395	1.61	0.61	1.00	...
	2	54	486	1.86	0.63	1.23	...
C[a]	3	57.5	454	1.77	0.63	1.14	...
	4	45.5	360	1.49	0.59	0.90	...
	Mean values after interpolation to motor pressure p = 50 bars		395	1.66	0.61	1.05	0.78

[a] According to lack of propellant C an ammonium perchlorate propellant with T_f = 2200 K was used as the main charge. Propellant C was used for the nozzle (strip).

According to theory α should be rather strongly dependent on the flame temperature. Assuming a surface temperature of, say, 800 K gives for propellants A and C $\alpha_C/\alpha_A \simeq 1.8$ if the thermodynamic terms in Equation [2] are the same. Empirically determined α values for the two propellants do not differ so much. They were estimated by multiplying the slope of the curves of Fig. 9 by $x^{0.2}$ where $x = 0.7$ cm was assumed for the tablets and $x = 7.0$ cm for the strips. Tablets of propellant A gave $\alpha = 0.011$ and strips 0.012. Tablets of propellants B and C gave 0.011 and 0.014, respectively. From these results we get $\alpha_C/\alpha_A \simeq 1.3$ compared to 1.8 previously obtained. For $T_s > 800$K the difference is still more marked.

At constant gas velocity and pressure the erosive burning rate seems to be independent of the gas temperature which is shown in Table 2. This result is not quite in accordance with the theory although, for example, high α values for hot core gases are compensated to some extent by low mass flow and (due to this) a more effective transpiration cooling. See Equation [1].

A question is the validity of the basic assumption $r = r_0 + r_e$ where r_0 represents the strand burning rate at different flow conditions. We notice the tendency of $r < r_0$ at low flow rates for propellant C in Fig. 4.

Vandenkerckhove (4) suggests that erosion of double base propellants is attributable to increasing turbulence in the thin fizz zone close to the surface. The extension of this interesting theory to composites might be based on the assumptions that the heat flow to the perchlorate crystals form the premixed perchlorate preflame zone is rate determining and that the diffusion flame temperature or (at erosive burning) the main gas flame temperature has only minor influence. Although the temperature of the heat delivering zone would be only about 1200 K this is enough to sustain a deflagration rate of ammonium perchlorate of the actual order of magnitude (5–7).

Summary

In conclusion, we will briefly summarize our experience of the different measuring methods as follows.

The advantages of the x-ray flash method are that the burning process is not influenced by the method, and that flow conditions are representative for the flow in propellant tube channels. Its shortcomings are the averaging problem and difficulties in measuring distances on the negatives.

The tablet method is characterized by handier equipment expecially using pressure indication. Advantages are the possibility of using small amounts of propellant and the less difficult averaging problem. However, flow conditions are somewhat undefined. The method seems to be useful for comparison of different propellants, but for estimation of the absolute erosive rate the method has to be studied in more detail, especially from the hydrodynamic point of view.

The strip method should be better in that respect; however, we have so far made only a preliminary study. We hope the strip method will provide less dispersion than the tablet method, and believe that it will also be a useful tool for investigation of materials for thermal isolation, etc., as the nozzle method.

Large dispersion was observed, especially using the x-ray flash method. However, all these methods are characterized by different measurements. Some sources of error for the tablet method are, for example:

1 Uncontrollable variations of tablet composition—degree of polymerization of the binder and particle size of the oxidizer.

2 Variations of the measured distance according to separate initiation and different burning rates of the tablets and different thickness of the thin web over the hole in the plug when the tablet is nearly consumed.

3 Variations of the gas flow over the tablets. The strand burning rate as the reference for calculating r_e is determined in a great number of tests. However even these values are scattered according to errors in the uncontrollable variations of the tablet composition and particle size of the oxidizer.

Nomenclature

A = cross-sectional area of flow channel, cm^2
A_t = area of nozzle throat, cm^2
c_D = experimental nozzle discharge coefficient, sec cm^{-1}
c_g = heat capacity of propellant gas, cal gm^{-1}K^{-1}
c_s = heat capacity of propellant, cal gm^{-1}K^{-1}
G = cross-sectional average mass velocity of combustion gas, $G = c_D \cdot p \cdot A_t/A$, gm cm^{-2} sec^{-1}
p = pressure in the gas producing rocket motor, bars
Pr_g = Prandtl number of propellant gas
r = (total) burning rate of propellant under given conditions of pressure, propellant temperature (about 20 C) and gas velocity, cm sec^{-1}
r_0 = burning rate of propellant under same conditions of pressure and propellant temperature, measured in strand burning tests with no tangential gas velocity (strand burning rate), cm sec^{-1}
r_e = erosive burning rate, $r_e = r - r_0$, cm sec^{-1}
T_f = isobaric flame temperature of propellant (stagnation temperature of gas flow), deg K
T_i = ambient propellant temperature, deg K
T_s = propellant surface temperature, deg K
u = cross-sectional average linear gas velocity, m sec^{-1}
x = characteristic length, cm
α = erosive constant, cm$^{2.8}$ gm$^{-0.8}$ sec$^{-0.2}$
β = dimensionless exponential constant
ρ_s = mass density of propellant, gm cm^{-3}
μ_g = dynamic viscosity of propellant gas, gm cm^{-1} sec^{-1}

References

1 Lenoir, J. M. and Robillard, G., "Sixth Symposium on Combustion," Reinhold Publishing Corp., N. Y., 1957, pp. 663–667.

2 Lenngren, C. E., Person, L. and Petersson, S. "A Method of Investigation of the Erosion of Rocket Propellants," Tech. Rep. NZP 7-55, Bofors, 1955 (in Swedish).

3 Lenoir, J. M., "Hot Wire Apparatus for Measurement of Transpiration Effects on Heat-transfer Coefficients," JPL Progress Rep. no. 20-300, 1956.

4 Vandenkerckhove, J., "Combustion and Propulsion," Third Agard Colloquium, London, Pergamon Press, Inc., N. Y., 1958, pp. 423–425.

5 Schultz, R. and Green, L., Jr., "Combustion and Propulsion," Third Agard Colloquium, London, Pergamon Press, Inc., N. Y., 1958, p. 394.

6 Sutherland, G. S., "The Mechanism of Combustion of an Ammonium Perchlorate-Polyester Resin Composite Solid Propellant," Thesis, Princeton University, May 1956.

7 Friedman, R., Nugent, R. G., Rumbel, K. E. and Scurlock, A. C., "Deflagration of Ammonium Perchlorate," Sixth Symposium on Combustion, Reinhold Publishing Corp., N. Y., 1957 pp. 612–618.

Estimate of Chemical Space Heating Rates in Gas-Phase Combustion With Application to Rocket Propellants

DAVID A. BITTKER[1] and RICHARD S. BROKAW[2]

NASA, Lewis Research Center
Cleveland, Ohio

This paper presents a simple, approximate method for calculating maximum chemical space heating rates in combustion processes. Calculations are made by employing the fundamental physical and chemical properties of the combustion mixture. The results represent the theoretical maximum possible heat release rate to be expected from a unit volume of a reacting fuel-oxidant mixture. An important purpose of this work is the application of the method to several rocket propellant combinations. Comparison of the results with estimated heat release rates for the same propellants in experimental rocket engines shows that the latter are several orders of magnitude less than the calculated maximum chemical rate for a given propellant.

AN IMPORTANT problem in the development of high output practical combustion systems is that of obtaining a very high heat release rate per unit volume of the combustion zone. It has usually been considered that processes such as liquid drop evaporation and gaseous mixing are rate controlling upon the heat release at high pressure. However, the question of whether the rate of gaseous chemical reaction could ever become the limiting factor has received increased attention recently (1,2).[3] In addition, Longwell and his co-workers (3,4) have reported studies with a highly stirred spherical combustor which approaches experimentally the concept of chemical rate controlled combustion. Data are still quite sparse, however, regarding the rates of high temperature chemical reactions.

Calculations of approximate chemical reaction and space heat release rates for gas-phase combustion have been reported by Avery (1) and by Potter and Berlad (5). Simplified one-step kinetics expressions have been applied to a highly stirred reactor and to a laminar flame, respectively, in (1 and 5). The present work reports another approximate treatment of the stirred reactor model which uses the same assumption, namely that the dependence of chemical reaction rate on temperature is the same for the stirred reactor and the laminar flame. The use of this idea permits the chemical reaction rate to be calculated directly from readily available fundamental burning velocity data and eliminates working with the kinetics expression directly. Only the reaction order and activation energy have to be known. A simple relationship is obtained which gives, approximately, the theoretical maximum heat release rate to be expected from unit volume of a reacting fuel-oxidant mixture. Many simplifying assumptions are made and only order-of-magnitude accuracy can be claimed for the results. The method does, however, give an insight into the dependence of the heat release rate upon the kinetics parameters. Moreover, these order-of-magnitude values can give useful information when the method is applied to rocket engine combustion, and this application is an important purpose of the present work. Space heat release rates for several gaseous rocket propellant combinations have been calculated and compared with values for actual experimental rocket engines.

Heat release rates have also been calculated for several fuel-air combinations and compared with experimental measurements reported in the literature for laminar flames and the highly stirred spherical reactor. These comparisons help to verify the order-of-magnitude accuracy of the method and the primary assumption. The fuel-air combinations used are propane-air, isooctane-air, hydrogen-air, propylene oxide-air and isopropyl chloride-air. The rocket propellant combinations are isooctane-oxygen, ammonia-oxygen, hydrogen-oxygen and hydrogen-fluorine.

Theoretical Considerations

The calculation of maximum chemical heat release rates requires a method of determining the chemical reaction rate. To do this one can use the equation of Semenov (6) which gives the relation between fundamental laminar burning velocity for a combustible mixture and the chemical reaction rate as follows

$$U_f = \frac{1}{\rho_0 L}\sqrt{2\lambda_f Q' \int_0^{T_f} \omega dT} \qquad [1]$$

This equation can be put in another form by defining ΔH_v as the heat of combustion of the initial mixture per unit volume. Then, under the assumption that the mixture has a constant average heat capacity from temperature T_0 to T_f, it is true that

$$\Delta H_v = \rho_0 L = c_p(T_f - T_0) = (C_p p/RT_0)(T_f - T_0)F \qquad [2]$$

where

c_p = average heat capacity per unit volume of the mixture
C_p = average molar heat capacity
F = conversion factor from calories to cm³-atm

Next we define the average chemical reaction rate in the combustion zone as

$$\bar{\omega} = \frac{1}{T_f - T_0}\int_0^{T_f} \omega dT \qquad [3]$$

Then the average space heating rate $\bar{q}$ in the reaction zone is

$$\bar{q} = \bar{\omega}Q' = \frac{1}{T_f - T_0}\int_0^{T_f} Q'\omega dT \qquad [4]$$

Presented at ARS Semi-Annual Meeting, June 8–12, 1959, San Diego, Calif.

[1] Rocket Combustion Section. Member ARS.
[2] Chief, Physical Chemistry Branch. Member ARS.
[3] Numbers in parentheses indicate References at end of paper.

Equation [1] can now be rewritten by using Equations [2 and 4] as

$$U_f = \sqrt{\frac{2\lambda_f}{C_p}\frac{RT_0}{p\Delta H_v}\bar{q}\left(\frac{1}{F}\right)} \qquad [5]$$

The maximum space heating rate q_{max} can now be introduced by the following equation

$$q_{max} = \left(\frac{\omega_{max}}{\bar{\omega}}\right)\bar{q} \qquad [6]$$

The combination of Equations [5 and 6] gives

$$q_{max} = FU_f^2\left(\frac{C_p}{2\lambda_f}\right)\left(\frac{p\Delta H_v}{RT_0}\right)\left(\frac{\omega_{max}}{\bar{\omega}}\right) \qquad [7]$$

The ratio $\omega_{max}/\bar{\omega}$ can be evaluated (5) by assuming a particular form for the chemical reaction rate of the overall process occurring in the combustion zone. A simple Arrhenius-type expression is used

$$\omega = Aa^l b^{n-l} e^{-E/RT}$$

where

a, b = molar concentrations of fuel and oxidant at the temperature T

A = temperature independent part of the rate constant

The extent of reaction is defined by the following expression

$$\epsilon = (T - T_0)/(T_f - T_0) \qquad [8]$$

We now restrict consideration to a stoichiometric initial mixture for which one can write

$$a = a_0(1 - \epsilon)(T_0/T)$$

$$b = b_0(1 - \epsilon)(T_0/T)$$

So for a stoichiometric initial mixture the reaction rate can be written in terms of a_0 and b_0 as

$$\omega = Aa_0^l b_0^{n-l}\left[\left(\frac{T_0}{T}\right)\frac{T_f - T}{T_f - T_0}\right]^n e^{-E/RT} \qquad [9]$$

Differentiation of Equation [9] gives immediately T_m, the temperature at which $\omega = \omega_{max}$

$$T_m = \frac{T_f}{1 + (nRT_f/E)} \qquad [10]$$

By employing Equations [9 and 10] with an approximate evaluation of the integral $\int_0^{T_f}\omega dT$ suggested by Semenov, the following approximate expression is obtained

$$\frac{\omega_{max}}{\bar{\omega}} \cong \left(\frac{E}{RT_f}\right)\left(\frac{T_f - T_0}{T_f}\right)\left(\frac{n}{e}\right)^n \qquad [11]$$

A more detailed treatment, given in Appendix A, along with a somewhat better approximation to the rate integral leads to a more exact expression for $\omega_{max}/\bar{\omega}$, namely

$$\frac{\omega_{max}}{\bar{\omega}} = \frac{1}{K[\Gamma(n+1)]}\left(\frac{E}{RT_f}\right)\left(\frac{T_f - T_0}{T_f}\right)\left(\frac{n}{e}\right)^n \qquad [12]$$

In this expression $\Gamma(n + 1)$ is the gamma function and K is a correction factor which depends on n and also on the quantity $z = E/RT_f$. A full explanation of K will be found in Appendix A. Now Equations [7 and 12] can be combined to obtain the following simple equation for calculating the maximum space heating rate in a combustion zone

$$q_{max} = \frac{F}{K[\Gamma(n+1)]}\left(\frac{E}{RT_f}\right)\left(\frac{T_f - T_0}{T_f}\right)\left(\frac{n}{e}\right)^n \times \left(\frac{C_p}{2\lambda_f}\right)\left(\frac{p}{RT_0}\right)U_f^2\Delta H_v \qquad [13]$$

where $F = 2.4213 \times 10^{-2}$ cal/cm³ atm.

Method of Calculation

The method of estimating the various reaction mixture properties deserves some detailed explanation. Each variable will be discussed separately.

Flame temperatures were usually calculated using the method and data of Huff, Gordon and Morrell (7). In the case of propane-air, however, experimental values were used for consistency in the comparison with experimental heat release rates.

Activation energies and overall reaction orders. Hydrocarbon values were taken from (2), ammonia data from (8), hydrogen data from (9 and 10) and the hydrogen-fluorine activation energy estimate from (11). The order for the hydrogen-fluorine reaction was arbitrarily taken as 2.0, since no information was found. Reaction order for propylene oxide and isopropyl chloride was taken the same as the hydrocarbon order. Activation energies for these fuels were taken from (25) after multiplication by 1.538 to adjust for the fact that this reference reports a lower hydrocarbon activation energy than (2).

Heat capacities were calculated at the temperature T_m using the tables of (7) and the simple mixture rule

$$C_p = \sum_{i=1}^{n} x_i(C_p)_i \qquad [14]$$

The reaction mixture was assumed to consist of only the major products, except that account was taken of the amount of reactants remaining in the case of H_2-O_2 and H_2-F_2. This correction is quite small in these cases.

Thermal conductivities were calculated at the temperature T_m using a mixing rule given in (12)

$$\lambda_{mix} = \frac{1}{2}\left[\sum_{i=1}^{n} x_i\lambda_i + \left(\sum_{i=1}^{n}\frac{x_i}{\lambda_i}\right)^{-1}\right] \qquad [15]$$

Individual component conductivities were calculated with the aid of the equations of (13 and 14). The simple combustion products were assumed. Again allowance was made for the amount of unchanged reactants present in the combinations using hydrogen. The correction is quite significant here, since hydrogen has a much higher conductivity than the other species present.

Burning velocities are taken from the literature for 1 atm pressure. The rough estimate of Grosse (15) was used as the value for hydrogen-fluorine. The following values of the pressure dependence exponent of burning velocity were used

Table 1 Comparison of calculated and experimental heat release and chemical reaction rates for laminar propane-air flames

Author	Equivalence ratio, φ	$\omega_{max}/\bar{\omega}$, exptl.	$\omega_{max}/\bar{\omega}$, Eq. [12] Method 1	$\omega_{max}/\bar{\omega}$, Eq. [12] Method 2	q_{max}, exptl., cal/cm³ sec	q_{max}, cal/cm³ sec, Eq. [13] Method 1	q_{max}, cal/cm³ sec, Eq. [13] Method 2
Fristrom (19,20)	1.0	1.86	3.67	2.91	36	322	255
Friedman and Burke (21)	0.54	4.44	4.15	3.64	1.18	2.0	1.7

to convert the burning velocities from 1 to 15 atm pressure:

Hydrocarbon-air, −0.2 (16).
Hydrocarbon-oxygen, +0.2 (17).
Ammonia-oxygen, 0.0 (16).
Hydrogen-oxygen, +0.45 (18).
Hydrogen-fluorine, +0.45.

Since no information was available for hydrogen-fluorine, the value for hydrogen-oxygen was arbitrarily used for it as well.

The heat of combustion per unit volume was obtained from the heat of combustion of one mole of fuel, calculated for the simple stoichiometric reaction forming gaseous products. The thermodynamic data of (7) were used.

Results and Discussion

Comparison With Experimental Results

Two pieces of work reporting the space heat release rates of laminar propane-air flames are available for a direct comparison with values calculated from Equations [12 and 13]. Fristrom (19,20) has reported heat release rate measurements for a conical stoichiometric propane-air flame at 0.25 atm pressure and Friedman and Burke (21) have reported similar data for a lean, flat propane-air flame at 0.0594 atm. Plots of their heat release rate profiles, calculated from experimental temperature profiles, are shown in Figs. 1 and 2. Table 1 shows a comparison of calculated and experimental values of $\omega_{max}/\bar{\omega}$ and q_{max} for these two flames. Although Equations [12 and 13] are derived for a stoichiometric initial mixture only, they have been used for the lean flame, with appropriate stoichiometry adjustments for the composition of the reaction mixture. Exact calculations of T_m and $\bar{\omega}$ for this one lean flame indicated that the errors to be incurred would be small compared to the expected accuracy of the results for a stoichiometric flame. Two methods of calculation were used for these flames. Method 1 employed the experimental T_f and an assumed activation energy of 40,000 cal per mole. T_m was then calculated by Equation [10] and was found to differ slightly from the experimental value. Method 2 used the experimental values of T_f and T_m to calculate the quantity E/RT_f from Equation [10]. This method amounts to using a considerably lower activation energy than 40,000 cal. A reaction order $n = 1.8$ was used for all calculations.

The data in Table 1 show that Equation [12] is fairly good (within a factor of 2) for predicting $\omega_{max}/\bar{\omega}$, considering the number of approximations used in its derivation. It is, in fact, better for the lean flame than for the stoichiometric one. Similar comments can be made about Equation [13] for q_{max}, although the maximum deviation is by a factor of 9. The largest part of the error in q_{max} is due to the failure of the Semenov relation, Equation [5], to predict the experimental burning velocity when the experimental value of $\bar{q}$ is used. Any error in U_f is doubled when the heat release rate is calculated, since U_f enters as the square in Equation [13]. So perhaps for other flames, the accuracy of any maximum space heat release rate calculation can be judged by the agreement between experimental and calculated burning velocities, employing the Semenov equation in any one of its forms.

Experimental heat release rates calculated for the highly stirred spherical reactor developed by Longwell (3,4) can be compared to values calculated by Equation [13]. Table 2 shows comparisons for several different fuel-air mixtures at 1 atm pressure. The isooctane comparison is quite straightforward. Good burning velocity data are available for use in Equation [13], and the experimental value of q_{max} reported was given in (3). The situation is different for hydrogen, propylene oxide and isopropyl chloride. Reference (4) reports only the blowoff loading factor ($N/Vp^{1.8}$) as a function of initial mixture equivalence ratio φ for each fuel. Moreover, no actual data are given for $\varphi = 1.0$, so that extrapolation is necessary for these mixtures. A full discussion of this

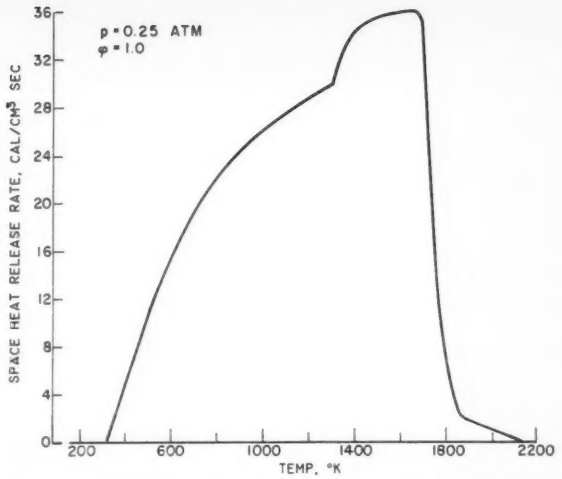

Fig. 1 Heat release rate vs. temperature for a stoichiometric propane-air flame. See Fristrom (19 and 20)

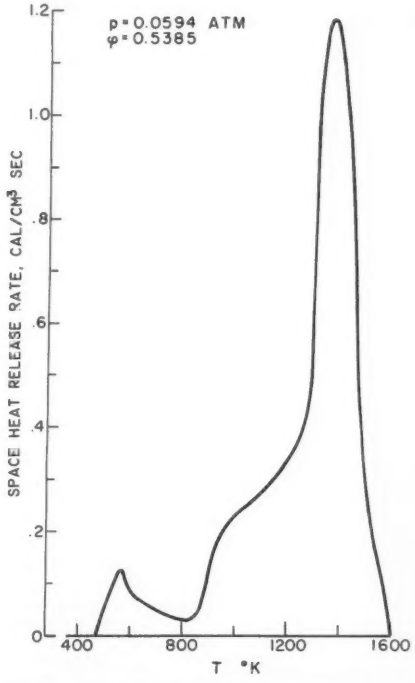

Fig. 2 Heat release rate vs. temperature for a lean propane-air flame. See Friedman and Burke (21)

extrapolation and of the conversion from loading factors to actual space heat release rates is found in Appendix B. Also included is a discussion of some of the data used in applying Equation [13] to all the fuels listed in Table 2.

In spite of the extrapolations involved in making some of the calculations of Table 2 it is felt that the results can still give an idea of the validity of Equation [13]. The maximum difference in Table 2 between a calculated and an experimentally estimated heat release rate is a factor of 7 for propylene oxide. In all other cases agreement is within a factor of 4. In Tables 1 and 2 the results calculated from Equation [13] are usually larger than the corresponding experimentally

Table 2 Heat release rates for the well-stirred spherical reactor at T_0 = 400 K and pressure = 1 atm

Mixture	Equivalence ratio, φ	n[a]	U_f,[a] cm/sec	E,[a] cal/mole	q_{max}, calc. by Eq. [13] cal/cm³ sec	q_{max}, calc. by Eq. [13] Btu/ft³ hr	q_{max}, calc. from exptl. loading factor cal/cm³ sec	q_{max}, calc. from exptl. loading factor Btu/ft³ hr
isooctane-air	1.0	1.8	54	40,000	3140	1.3×10^9	740	3.0×10^8
H_2-air	0.4	2.2	33	18,000	400	1.6×10^8	700	2.8×10^8
H_2-air	1.0	2.2	304	18,000	0.43×10^5	1.7×10^{10}	1.4×10^5	5.5×10^{10}
H_2-air	4	2.2	295	18,000	12,900	5.2×10^9	6100	2.5×10^9
propylene oxide-air	1.0	1.8	100	38,500	12,200	4.9×10^9	1660	6.7×10^8
isopropyl chloride-air	1.0	1.8	43	46,000	2130	8.6×10^8	560	2.3×10^8

[a] Value used in Equation [13].

estimated values. Only the lean and stoichiometric hydrogen-air mixtures fail to follow this trend. In summary, Tables 1 and 2 show that the expected agreement between the results of Equation [13] and an experimentally estimated heat release rate should be, at best, within a factor of 2, and at worst, within an order of magnitude.

These comparisons, as well as comparisons with the calculated space heating rates in (2 and 5), support the order-of-magnitude accuracy claim made for the method and also the basic kinetics assumption involved.

Calculation of Maximum Space Heat Release Rates for Rocket Propellant Combinations

Equation [13] can be used to predict the maximum space heat release rate to be expected from the highly stirred gas-phase combustion of various rocket propellant combinations. These values may be viewed only as idealized upper limit heating rates. Calculated results for the combinations isooctane-oxygen, ammonia-oxygen, hydrogen-oxygen and hydrogen-fluorine are summarized in Table 3. All calculations were done for a stoichiometric initial mixture at two pressures, 1 and 15 atm. Calculations are included for isooctane-air at the same initial temperature for comparison purposes. The poorest of the combinations is ammonia-oxygen with a heat release rate hardly more than an order of magnitude greater than that for isooctane-air at either pressure. Hydrogen-fluorine has the highest calculated heat release rate; however, the values listed are the most approximate ones in the table, since very rough burning velocity estimates had to be made for calculations with this combination. Other factors could be reasonably well estimated except the activation energy of the reaction. From the work of Penner (11), a good idea of the maximum and minimum possible activation energies can be obtained. Calculations were performed for these limiting values of 10 and 50 kcal, and Table 3 shows that this wide variation in E causes a negligible change in the space heat release rate. The isooctane-oxygen and hydrogen-oxygen values are practically the same at both pressures, within the accuracy limits of Equation [13]. The increase for these combinations over isooctane-air is a little greater than 2 orders of magnitude at 1 atm pressure and 3 to 4 orders of magnitude at 15 atm.

Role of Chemical Kinetics in Rocket Combustion

For an estimate of how important the rate of chemical heat release alone is among all the processes occurring in a rocket thrust chamber, the values of space heating rate just calculated can be compared with calculated values of overall space heat release rate in actual test engines. Table 4 shows approximate overall space heat release rates for several propellant combinations employed in experimental engines at NASA (22). The calculations were made under the assumption that all the heat was released in the volume up to the throat. The values reported are calculated from the flow rate of the propellant in deficient supply, along with the experimental combustion efficiency. These average rates are not significantly lower than the maximum local rates for these relatively low efficiency engines. The chemical heating rates

Table 3 Space heat release rates for rocket propellant combinations (For all mixtures equivalence ratio = 1.0, T_0 = 300 K)

Combination	Adiabatic flame temperature T_f, K	Activation energy E, cal/mole	Reaction order, n	Combustion pressure, atm	Burning velocity U_f, cm/sec	Average heat capacity C_p, cal/mole	Average thermal conductivity λ_f, cal/cm sec, K	Maximum space heat release rate q_{max}, Btu/ft³ hr
$C_8H_{18} + O_2$	3056	40,000	1.8	1	400	13.55	4.59×10^{-4}	4.5×10^{11}
	3422	40,000	1.8	15	688	13.60	4.97×10^{-4}	2.7×10^{14}
$NH_3 + O_2$	2782	49,500	1.7	1	110	11.43	5.12×10^{-4}	1.5×10^{10}
	3041	49,500	1.7	15	110	11.62	5.50×10^{-4}	3.0×10^{12}
$H_2 + O_2$	3018	18,000	2.2	1	1010	9.70	6.74×10^{-4}	4.6×10^{11}
	3384	18,000	2.2	15	3417	9.76	7.28×10^{-4}	1.1×10^{15}
$H_2 + F_2$	3962	50,000	2.0	1	10,000[a]	8.75	8.28×10^{-4}	7.2×10^{13}
	4546	50,000	2.0	15	33,800[a]	8.87	9.00×10^{-4}	1.6×10^{17}
	3962	10,000	2.0	1	10,000[a]	8.11	5.31×10^{-4}	7.7×10^{13}
	4546	10,000	2.0	15	33,800[a]	8.18	5.54×10^{-4}	2.0×10^{17}
C_8H_{18} + air	2251	40,000	1.8	1	34	9.74	2.82×10^{-4}	9.9×10^8
	2316	40,000	1.8	15	20	9.77	2.87×10^{-4}	7.3×10^{10}

[a] These values are very rough estimates.

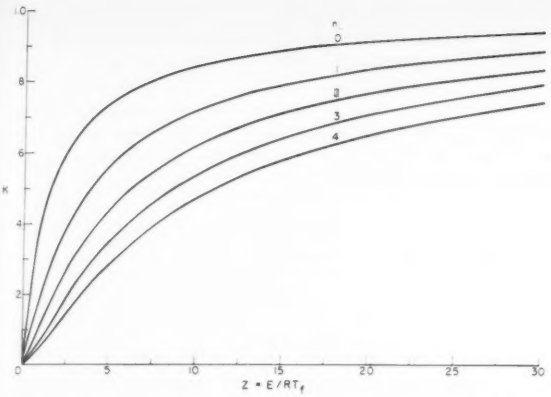

Fig. 3 Correction factor K vs. z for several reaction orders

in the last column were estimated by fitting the results in Table 3 to an assumed pressure dependence $q_{max} = Bp^m$, where B and m are constants for a given propellant. Although only two points are available for each system, this approximate method was considered accurate enough to obtain values for comparison with the experimental data at the experimental chamber pressure. The several orders-of-magnitude difference between the chemical rates and the experimental engine values indicates that purely chemical heat release is not the controlling factor in rocket combustion under normal conditions of stable operation. However, under unusual circumstances, for example in high frequency oscillatory combustion, heat release rates can increase many times over their normal values. Estimates of the possible upper limit of these increased rates based on drop shattering behind a shock wave give values which are several orders of magnitude greater than the observed steady-state space heating rates. In this situation the rate of chemical reaction certainly cannot be neglected in considering the mechanism and rate of the combustion process.

The chemical heat release rates reported here are the local upper limit values which would not necessarily be desirable in an actual combustion chamber, because of the accompanying loss in efficiency. These approximate calculations have indicated that only a small part of the possible space heat release is realized in current rocket engines. Although practical considerations may make it now undesirable to increase these rates, this may not always be the case. It is, therefore, important to realize that space heat release rates in rocket combustion may be considerably increased over their present values.

Appendix A: Evaluation of the Ratio $\omega_{max}/\tilde{\omega}$

The only problem in evaluating the ratio $\omega_{max}/\tilde{\omega}$ is the evaluation of the integral

$$I = \int_0^{T_f} \omega dT = (T_f - T_0)\tilde{\omega}$$

Equation [11] was obtained with the use of the Semenov approximate evaluation of I suggested by Dugger and Simon (23), namely

$$I^* = Aa_0^i b_0^{n-i} \left(\frac{T_0}{T_f}\frac{RT_f^2/E}{T_f - T_0}\right)^n \frac{RT_f^2}{E} e^{-E/RT_f} \qquad [16]$$

A more detailed approximate evaluation of I gives the expression

$$I \cong I^*\Gamma(n+1) \qquad [17]$$

where $\Gamma(n+1)$ is the gamma function of $n+1$, which is equal to $n!$ when n is an integer. If this better approximation is called I_1, then

$$I_1 = I^*\Gamma(n+1) \qquad [18]$$

If a correction factor K is now defined as the ratio of the true value of the integral to the I_1 approximate value (I/I_1), the following relation can be written

$$\frac{I}{I^*} = \frac{I}{I_1} \times \frac{I_1}{I^*} = K\Gamma(n+1) \qquad [19]$$

A comparison of Equation [19] with Equation [11], obtained using the I^* approximation, shows that a more exact expression for $\omega_{max}/\tilde{\omega}$ is

$$\frac{\omega_{max}}{\tilde{\omega}} = \frac{1}{K\Gamma(n+1)}\left(\frac{E}{RT_f}\right)\left(\frac{T_f - T_0}{T_f}\right)\left(\frac{n}{e}\right)^n$$

which is Equation [12].

The factor K can be evaluated by first using Equations [9, 16 and 19] to obtain

$$K = \frac{(-1)^n}{\Gamma(n+1)} z^2 e^z \int_{-\infty}^{-z} (z+s)^n \frac{e^s}{s^2}\, ds \qquad [20]$$

in which $z = E/RT_f$. The use of the binomial theorem permits the evaluation of K exactly for any integral reaction order n. Results are written in terms of the exponential integral designated $Ei(-z)$

$$Ei(-z) = \int_{-\infty}^{-z} \frac{e^s}{s}\, ds$$

where z is a positive quantity and equal to E/RT_f in our case. This function is tabulated in (24). The expressions for K valid for integral n from 0 to 3 are as follows

$n = 0$ $\quad K = z^2[(1/z) + e^z Ei(-z)]$ [21]

$n = 1$ $\quad K = -z^2[e^z Ei(-z)(z+1) + 1]$ [22]

$n = 2$ $\quad K = (z^2/2)[e^z Ei(-z)(z^2 + 2z) + z + 1]$ [23]

$n = 3$ $\quad K = -(z^2/6)[e^z Ei(-z)(z^3 + 3z^2) + z^2 + 2z - 1]$ [24]

Values of K for nonintegral n are obtained from crossplots of K against integral n for any desired value of z. For the range of z values encountered with the fuel-oxidant combinations used here, the correction factor $K\Gamma(n+1)$ did not have a great effect on the calculated heat release rates, when one considers the order-of-magnitude nature of the whole calculation. Shown in Fig. 3 are plots of K against z for several integral reaction orders.

Reference (24) tabulates $Ei(-z)$ up to $z = 15$. For the present work three additional values for $z = 20$, 25 and 30

Table 4 Comparison of rocket engine space heating rates with calculated chemical rates

Propellant combination	Chamber pressure, atm	Engine space heating rate, Btu/ft³ hr	Maximum calculated space heating rate, Btu/ft³ hr
n-heptane-liq O_2	18.4	7.1×10^8	4×10^{14}[a]
liq NH_3-liq O_2	10.9	3.9×10^8	2×10^{12}
gas H_2-liq O_2	20.4	8.4×10^8	2×10^{15}
gas H_2-liq F_2	25.2	8.5×10^8	7×10^{17}

[a] Value for isooctane fuel.

Table 5 Values of the quantity $e^z Ei(-z)$

z	$e^z Ei(-z)$
20	$-4.771854550 \times 10^{-2}$
25	$-3.851469884 \times 10^{-2}$
30	$-3.228973876 \times 10^{-2}$

were computed using the series expansion

$$Ei(-z) = \gamma + \ln z + \sum_{i=1}^{\infty} \frac{(-1)^n z^n}{n \cdot n!}$$

where $\gamma = 0.5772156649$ and is called Euler's constant. Table 5 presents values of the quantity $e^z Ei(-z)$ for these additional z values.

Appendix B: Heat Release Calculations for Hydrogen, Propylene Oxide and Isopropyl Chloride in the Well-Stirred Reactor

Experimental Values

There are two problems involved in estimating heat release rates from experimental data for these fuels. First of all, there is the matter of extrapolating the experimental plots of blowout loading factor against mixture equivalence ratio to $\varphi = 1.0$. This is easily done for propylene oxide and isopropyl chloride, since the experimental data come close to the stoichiometric condition. For hydrogen, no data could be obtained near $\varphi = 1.0$. For the very lean and very rich data presented, however, the ratio between hydrogen-air and isooctane-air loading factors at a given equivalence ratio is approximately constant. So the stoichiometric blowout loading factor for hydrogen was taken as approximately 200 times the corresponding value for isooctane.

With loading factors determined, there still remains the problem of estimating the extent of reaction ϵ of the reactor to convert the oxidant flow rate N to the actual burning rate of oxidant and fuel. To obtain ϵ Equations [10 and 8] were used to calculate, respectively, T_m and thence ϵ at the blowout point. The value $n = 1.8$ was used with all three fuels for consistency with (4). Activation energies used were those listed in Table 3. This procedure gave good agreement with the value of ϵ for isooctane given in (3), so it was assumed to be satisfactory for the other fuels.

Calculated Values

Inasmuch as these calculations were performed for an elevated initial temperature (400 K) a few points should be mentioned about the burning velocity values given in Table 2. Those listed for the isooctane and the rich and stoichiometric hydrogen mixtures are the experimental values reported by Heimel (26,27). Good burning velocity data are not available for very lean hydrogen-air mixtures. Lewis and von Elbe (28) report the data of Jahn extrapolated to lean equivalence ratios. Although this extrapolation is questionable, his value was used here as the only one available for $\varphi = 0.4$. The room temperature burning velocity thus obtained was adjusted to 400 K initial temperature by use of the $T_0^{1.732}$ temperature dependence obtained by Heimel for the stoichiometric mixture. Experimental room temperature burning velocities for propylene oxide and isopropyl chloride are reported by Fenn and Calcote (25). These values were adjusted to $T_0 = 400$ K in an approximate manner with the help of the Semenov burning velocity equation as written by these authors.

For all the fuels except hydrogen the reaction order n used with the experimental loading factors is the same as the value used in Equation [13]. With hydrogen the recent (10) experimentally determined value of $n = 2.2$ was used in Equation [13] rather than $n = 1.8$, the value assumed in (4). This difference in reaction order has no effect on the comparison of experimental and calculated heat release rates, inasmuch as small changes in n have negligible effects on a calculation using Equation [13].

Nomenclature

a,b	= concentrations of fuel and oxidant, respectively, in the reaction zone at temperature T, moles/cm³
a_0,b_0	= concentrations of fuel and oxidant, respectively, in the initial mixture at temperature T_0
c_p	= average heat capacity of the reaction mixture per unit volume, cal/cm³ K
C_p	= average molar heat capacity of reaction mixture over the temperature range T_0 to T_f, cal/mole K
E	= activation energy of the chemical reaction, cal/mole of fuel
e	= base of the natural logarithms
F	= conversion factor = 2.4213×10^{-2} cal/cm³ atm
ΔH_v	= heat of combustion per unit volume of initial reaction mixture, cal/cm³
l	= order of the chemical reaction with respect to fuel
L	= heat of combustion per unit mass of the initial mixture, cal/gm
n	= overall order of the entire chemical reaction
N/V	= flow rate of oxidant per unit volume of reaction zone, moles/cm³ sec
N/Vp^n	= loading factor for the highly stirred reactor, moles/cm³ sec atm^n
p	= pressure, atm
Q'	= heat of combustion of the fuel, cal/mole
$\bar{q}$	= average space heating rate over the temperature range T_0 to T_f, cal/cm³ sec
q_{max}	= maximum space heating rate for the chemical reaction
R	= universal gas constant (1.987 cal/mole K)
T_0,T	= temperatures of the initial mixture and of the reaction zone, respectively, K
T_f	= adiabatic flame temperature
T_m	= reaction temperature for maximum chemical reaction rate
U_f	= laminar burning velocity, cm/sec
x_i	= mole fraction of species i of a mixture
z	= E/RT_f
ϵ	= extent of reaction, defined by the ratio $(T - T_0)/(T_f - T_0)$
λ_f	= average thermal conductivity of the reaction mixture, cal/cm sec K
ρ_0	= density of initial mixture, gm/cm³
$\bar{\omega}$	= average chemical reaction rate over the temperature range T_0 to T_f, moles of fuel/cm³ sec
ω_{max}	= maximum chemical reaction rate, moles of fuel/cm³ sec
φ	= equivalence ratio = (fuel/oxidant ratio)/(fuel/oxidant ratio at stoichiometric)

References

1 Avery, W. H., "Space Heating Rates and High Temperature Kinetics," in "Fifth Symposium (International) on Combustion," Reinhold Publishing Corp., N. Y., 1955, pp. 86–91.

2 Avery, W. H. and Hart, R. W., "Combustor Performance with Instantaneous Mixing," *Ind. Engng. Chem.*, vol. 45, 1953, pp. 1634–1637.

3 Longwell, J. P. and Weiss, M. A., "High Temperature Reaction Rates in Hydrocarbon Combustion," *Ind. Engng. Chem.*, vol. 47, 1955, pp. 1634–1643.

4 Weiss, M. A., Lang, R. J. and Longwell, J. P., "Combustion Rates in Spherical Reactors—Effect of Inlet Temperature and Fuel Type," *Ind. Engng. Chem.*, vol. 50, 1958, p. 257.

5 Potter, A. E., Jr. and Berlad, A. L., "A Relation Between Burning Velocity and Quenching Distance," NACA Tech. Note 3882, 1956, pp. 8–18.

6 Semenov, N. N., "Thermal Theory of Combustion and Explosion. III—Theory of Normal Flame Propagation," NACA Tech. Memo. 1026, 1942, pp. 30, 34.

7 Huff, V. N., Gordon, S. and Morrell, V. E., "General Method and Thermodynamic Tables for Computation of Equilibrium Composition and Temperature of Chemical Reactions," NACA Rep. 1037, 1951.

8 Verwimp, J. and Van Tigglen, A., "Experimental Study of Slow Oxidations. II—Reaction of Mixtures of Ammonia and Oxygen," *Bull. Soc. Chem. Belges*, vol. 63, 1953, p. 205.
9 Wonterghem, J. and Van Tigglen, A., "The Activation Energy in Flame Propagation," *Bull. Soc. Chem. Belges*, vol. 64, 1955, p. 99.
10 Fine, B., "Stability Limits and Burning Velocities of Laminar Hydrogen-Air Flames at Reduced Pressure," NACA Tech. Note 3833, 1956.
11 Penner, S. S., "Application of Near Equilibrium Criteria During Adiabatic Flow to Representative Propellant Systems," *J. Franklin Inst.*, vol. 249, 1950, p. 441.
12 Brokaw, R. S., "Estimating Thermal Conductivities for Nonpolar Gas Mixtures—Simple Empirical Method," *Ind. Engng. Chem.*, vol. 47, 1955, pp. 2398–2400.
13 Hirschfelder, J. O., Curtiss, C. F. and Bird, R. B., "Molecular Theory of Gases and Liquids," John Wiley & Sons, Inc., N. Y., 1954, p. 534.
14 Hirschfelder, J. O., "Heat Conductivity in Polyatomic or Electronically Excited Gases, II," *J. Chem. Phys.*, vol. 26, 1957, pp. 282–285.
15 Grosse, A. V. and Kirschenbaum, A. D., "The Premixed Hydrogen-Fluorine Flame and Its Burning Velocity," *J. Amer. Chem. Soc.*, vol. 77, 1955, p. 5012.
16 Gilbert, M., "The Influence of Pressure on Flame Speed," in "Sixth Symposium (International) on Combustion," Reinhold Publishing Corp., N. Y., 1957, pp. 74–83.
17 Manton, J. and Milliken, B. B., "Study of Pressure Dependence of Burning Velocity by the Spherical Vessel Method," Proc. Gas Dynamics Symposium (Aerothermochem.), Northwestern Univ., 1956, pp. 151–157.
18 Strauss, W. A. and Edse, R., "Investigation of Flames Burning at Pressures up to 100 Atmospheres," WADC Tech. Rep. 56–49, 1956, p. 46.
19 Fristrom, R., "The Structure of Laminar Flames," in "Sixth Symposium (International) on Combustion," Reinhold Publishing Corp., N. Y., 1957, pp. 96–110.
20 Fristrom, R. and Westenberg, A. A., "Flame Zone Studies. IV. Microstructure and Material Transport in a Laminar Propane-air Flame Front," *Combustion and Flame*, vol. 1, 1957, p. 217.
21 Friedman, R. and Burke, E., "The Measurement of Temperature Distribution in a Low-Pressure Flat Flame," *J. Chem. Phys.*, vol. 22, 1954, pp. 824–830.
22 Clark, B. J., Hersch, M. and Priem, R. J., "Propellant Vaporization as a Criterion for Rocket-Engine Design; Experimental Performance, Vaporization, and Heat-Transfer Rates with Various Propellant Combinations," NASA Memo 12–29–58E, 1958.
23 Dugger, G. and Simon, D. M., "Prediction of Flame Velocities of Hydrocarbon Flames," in "Fourth Symposium (International) on Combustion," The Williams and Wilkins Co., Baltimore, 1953, pp. 336–345.
24 "Tables of Sine, Cosine and Exponential Integrals," vol. II, prepared by Federal Works Agency, WPA, N. Y., 1940.
25 Fenn, J. B. and Calcote, H. F., "Activation Energies in High Temperature Combustion," in "Fourth Symposium (International) on Combustion," The Williams and Wilkins Co., Baltimore, 1953, pp. 231–239.
26 Heimel, S. and Weast, R. C., "Effect of Initial Mixture Temperature on the Burning Velocity of Benzene-Air, n-Heptane-Air, and Isooctane-Air Mixtures," in "Sixth Symposium (International) on Combustion," Reinhold Publishing Corp., N. Y., 1957, pp. 296–302.
27 Heimel, S., "Effect of Initial-Mixture Temperature on Burning Velocity of Hydrogen-Air Mixtures with Preheating and Simulated Preburning," NACA Tech. Note 4156, 1957.
28 Lewis, B. and von Elbe, G., "Combustion, Flames and Explosions of Gases," Academic Press, Inc., N. Y., 1951, p. 460.

Technical Notes

Mixture Ratio Distribution in the Drops of Spray Produced by Impinging Liquid Streams

DEZSO SOMOGYI[1] and CHARLES E. FEILER[2]

Lewis Research Center, NASA, Cleveland, Ohio

A colorimetric method was employed to determine the mixture ratio of the individual drops in the spray of three types of injector. The distributions, mixture ratio against number of drops, and mixture ratio against spatial location were determined for each injector. The three injectors, in order of decreasing mixing efficiency, were the triplet, the impinging jet and the swirl cup. Mixture ratio varied appreciably for a given injector as well as among different injectors.

PROPELLANT mixing is one of the fundamental parameters in rocket combustion that has received little attention. For combustion to occur the propellants must be mixed at some stage in the combustion process. Many times the performance of a combustor can be explained by the amount of mixing achieved by the injector(1).[3] The extent of mixing may contribute to other phenomena in rocket engines such as combustion instability (2) and local burnout as well as the overall performance. In the case of hypergolic liquid propellants, mixing becomes especially important if one desires to take advantage of liquid phase reactions that may occur with these systems.

Rupe(3) evaluated the time average-spatial distribution of mixture ratio for an impinging-jet type injector over a wide range of geometry and flow variables. In another study, mixing efficiency was determined by measuring the temperature rise of an acid base reaction where mixing efficiency was given by the per cent of theoretical temperature rise (4). Since all injectors ultimately produce droplets of propellants, it seems desirable to determine the degree of mixing in individual drops. As mentioned previously, this determination would be more important when one is dealing with liquid phase reaction. For a miscible liquid propellant system, mixing may be defined as the distribution of propellants among the drops produced by the injector. Perfect mixing would be achieved if the input mixture ratio occurred in each drop.

A preliminary study was therefore undertaken to evaluate a colorimetric method for determining the mixture ratio in individual drops. The mixing efficiency of the injector was obtained from a random sampling of the collected drops. Three injectors, a triplet, an impinging jet and a swirl cup were evaluated at one flow condition using miscible fluids. The data are compared in three ways: Spatial distribution of mixture ratio, distribution of mixture ratio among drops, and finally the mixing efficiency of the injectors was obtained.

Experiments

Technique and instrumentation

Propellants were simulated in this study by aqueous dye solutions. A discussion of the principles of colorimetric analysis may be found in (5). Essentially the solutions should follow Beer's law and each solution should absorb light at the

Received July 20, 1959.
[1] Aeronautical Research Scientist.
[2] Engineer, Rocket Chemical Branch. Member ARS.
[3] Numbers in parentheses indicate References at end of paper.

EDITOR'S NOTE: The Technical Notes and Technical Comments sections of ARS JOURNAL are open to short manuscripts describing new developments or offering comments on papers previously published. Such manuscripts are usually published without editorial review within a few months of the date of receipt. Requirements as to style are the same as for regular contributions (see masthead page).

wave length of maximum transmission of the other. Filters are then selected to give the wave lengths corresponding to maxima of transmission of the two solutions. If the transmission at each wave length is measured for a series of mixtures of known ratio, a calibration curve such as that in Fig. 1 may be obtained. It is seen that measurement of transmission at each wave length uniquely determines the mixture ratio of an unknown mixture.

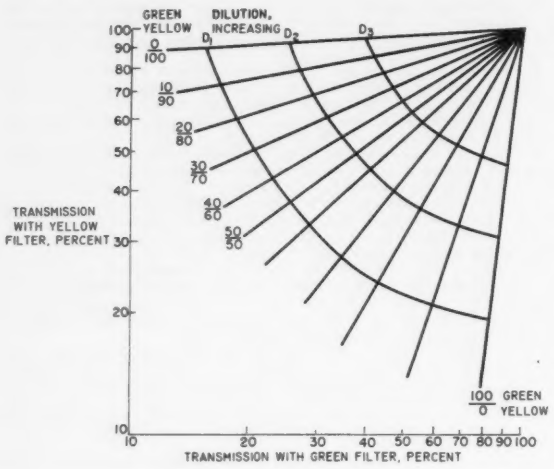

Fig. 1 Typical calibration curve

A block diagram of the colorimeter is shown in Fig. 2. The instrument was a Leeds & Northrup microdensitometer with provisions for adding filters. The sample holder consisted of two sheets of Lucite spaced 0.025 in. apart that also served to flatten the drop surfaces normal to the light beam. The optics of this system introduce a lower limit of drop diameter that can be measured; however, this limitation can be overcome by dilution of the drop with water to the minimum size. Dilution has no effect on the mixture ratio. It does, however, decrease sensitivity since the curves converge with increasing dilution, as shown by Fig. 1. The two dyes used were a green dye (brilliant green) and a yellow dye (proflavine sulfate). The filters were a Wratten no. 16 (yellow) and a liquid filter using the green dye solution.

A sample of the drops in the spray of each injector was obtained by means of the shutter mechanism also shown in Fig. 2. The drops were collected on a 20-in.-square greased plate so that their individual identity was maintained. A series of perpendicular grid lines 1 in. apart was scribed on the plate to obtain spatial location of the drops. An average of about 25 per cent of the drops in each square was selected at random for analysis. The sampling distance was 12 in. in each case.

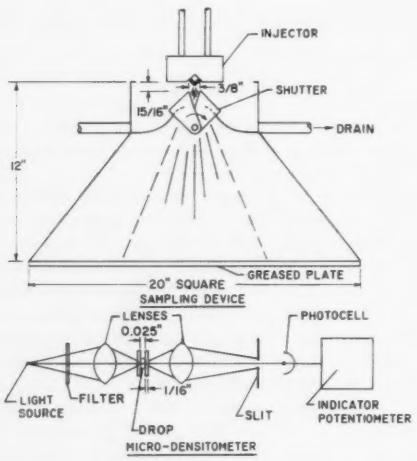

Fig 2 Apparatus

Injectors

The three injectors studied were a triplet, an impinging jet and a swirl cup. Their dimensions are shown in Fig. 3. These designs are typical of those used in many rocket combustion studies. Each injector was operated at a pressure drop of 45 psi, giving input flow ratios, green to yellow, of 1 except for the swirl cup, which had an input ratio of 2. These flow ratios are based on calibrations of the flow rates. The patterns formed by the spray on the collection plate are also indicated.

Results and Discussion

Spatial distribution

Each spray was found to have an axis of symmetry with respect to mixture ratio indicated as the x axis in Fig. 3. Thus along lines of constant x distance there was only a random variation in mixture ratio. Along lines of constant y distance, however, a continuous variation in mixture ratio was found that was readily explained from the injector geometry. This variation is shown in Fig. 4 where the average mixture ratio (per cent green) is plotted as a function of distance from the y axis. Each point represents the average value of mixture ratio of the drops in an area bounded by the total y distance and a 1-in. increment of x distance. The standard deviation of the data was computed for each x station, and since these

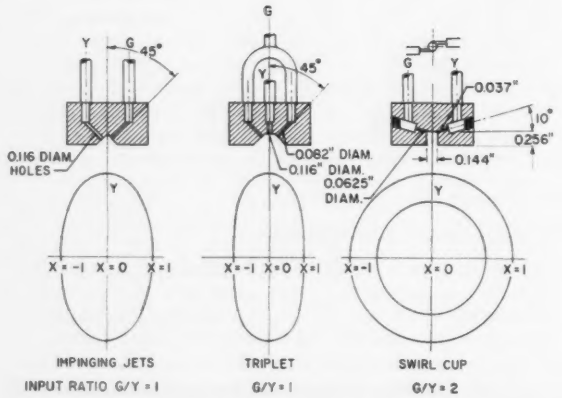

Fig. 3 Injectors

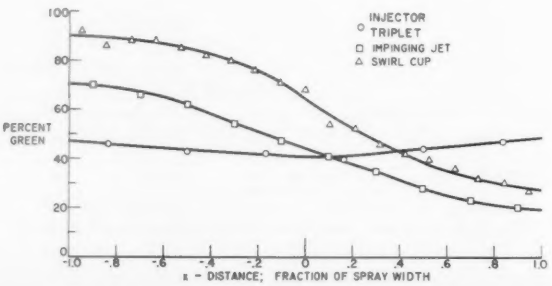

Fig. 4 Spatial distribution of mixture ratio

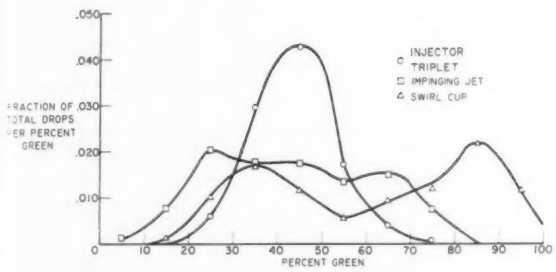

Fig. 5 Mixture ratio distribution among drops

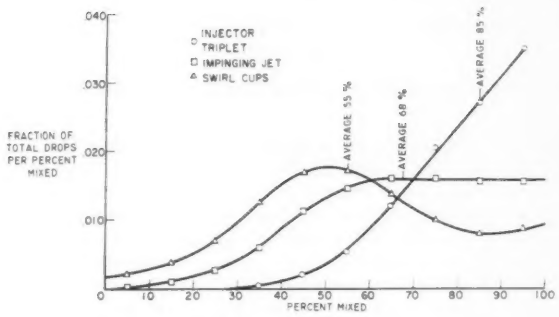

Fig. 6 Mixing efficiency distribution among drops

values did not differ greatly, they were averaged. Thus, the standard deviations were 8.3, 5.7 and 6.9 per cent green for the triplet, impinging jet and swirl cup injectors, respectively. The triplet produces a symmetric spatial distribution with the largest amount of yellow component appearing at the center, corresponding to its plane of injection. For the other injectors, there is a continuous decrease in mixture ratio as the spray is traversed with the nominal input ratio occurring near the center. The integrated average mixture ratios obtained from experimental data agreed reasonably well with the nominal input ratios obtained from flow calibration. Nominal ratios (per cent green/per cent yellow) were 50/50 for the triplet and impinging jet and 67/33 for the swirl cup, whereas the experimental averages were 44/56 and 62/38, respectively. For the impinging jet injector, interpenetration of the two streams occurred, so that higher concentrations of the components appeared in the spray on the side opposite to that of injection.

The configuration of the swirl cup injector presumably imparts an angular motion to the liquids, so that the axes of the spray pattern would depend on sampling distance. The orientation of injector and spray pattern shown previously in Fig. 3 was observed at 12 in. A hollow cone spray is typical of this injector type. The mixture ratio about the annular section varied sinusoidally. Starting at $x = -1$ and proceeding clockwise, the per cent green was a maximum at 0 deg and a minimum at 180 deg, while the input ratio occurred at 90 and 270 deg.

Mixture ratio distribution among drops

The distribution of drops with respect to mixture ratio is shown in Fig. 5 for each injector. According to the stated definition, if mixing were ideal all drops would have the input mixture ratio. From Fig. 5, the triplet injector approaches ideality most closely. The swirl cup produced drops in two ranges, each rich in one of the components, while the impinging jet was intermediate, giving a relatively flat distribution.

Mixing efficiency

If it is assumed that the direction of deviation of mixture ratio (i.e., richer or leaner) from the input ratio has no significance, it is possible to arrive at a mixing efficiency for each injector by considering what fraction of the material in a drop is in the input ratio. The following equations, also given in (3), give the per cent mixed in individual drops

$$\text{per cent mixed} = 100\left[1 - \left(\frac{R - r}{R}\right)\right] \qquad r < R$$

$$\text{per cent mixed} = 100\left[1 - \left(\frac{R - r}{R - 1}\right)\right] \qquad r > R$$

where

R = nominal input mixture ratio expressed as fraction of green

r = mixture ratio in the given drop expressed in the same way

Fig. 6 shows the fraction of total drops as a function of their per cent mixed for each injector. Ideally, all drops should be at 100 per cent. The average values of per cent mixed (mixing efficiency) also indicated in the figure, show the triplet to give the highest mixing efficiency (85 per cent) followed in order by the impinging jet (68 per cent) and swirl cup (55 per cent). The 68 per cent value for the impinging jet is of the same order as that found in (3). A previous evaluation of the mixing efficiency using the temperature-rise method gave a value of about 70 per cent for the swirl cup (4). These data were obtained at pressure drops of about 200 psi compared with 45 psi in the present study. It is likely that this additional energy would improve mixing.

Concluding Remarks

The liquid phase mixing of three injectors was studied by determining the mixture ratio occurring in individual drops of the sprays. The colorimetric technique used to measure mixture ratios seems to be satisfactory. The results show that appreciable differences may be found in the way the various injector types mix and distribute the injected fluids. The injectors in decreasing order of mixing efficiency were a triplet, an impinging jet and a swirl cup or premix type. Knowledge of these distributions should materially aid in the interpretation of rocket combustion phenomena when applied to a specific propellant combination or a specific combustor. For example, with hypergolic propellants, ignition may proceed more smoothly at a mixture ratio considerably different from that of optimum performance for which injectors are generally designed. The obtaining of satisfactory ignition under such conditions may be due in part to the wide range of mixture ratios found to exist in the drops of spray produced by the injector.

References

1 Heidmann, M. F. and Auble, C. M., "Injection Principles from Combustion Studies in a 200-Pound-Thrust Rocket Engine Using Liquid Oxygen and Heptane," NACA RM E55C22, 1955.

2 Feiler, C. E., "Effect of Fuel Drop Size and Injector Configuration on Screaming in a 200-Pound-Thrust Rocket Engine Using Liquid Oxygen and Heptane," NACA RM E58A20a, 1958.

3 Rupe, J. H., "The Liquid-Phase Mixing of a Pair of Impinging Streams," Prog. Rep. no. 20-195, Jet Prop. Lab., California Institute of Technology, Aug. 6, 1953.

4 Feiler, C. E. and Baker, R. M. L., Jr., "A Study of Fuel-Nitric Acid Reactivity," NACA RM E56A19, 1956.

5 Willard, H. H., Merritt, L. L., Jr. and Dean, J. A., "Instrumental Methods of Analysis," D. Van Nostrand Co., Inc., Princeton, N. J., 1948.

Chemical Nonequilibrium Effects on Hydrogen Rocket Impulse at Low Pressures[1]

J. GORDON HALL,[2] A. Q. ESCHENROEDER[3] and J. J. KLEIN[4]

Cornell Aeronautical Laboratory, Inc., Buffalo, N. Y.

POTENTIALLY large gains in specific impulse with highly dissociated hydrogen as the propellant are indicated in the results of Sänger-Bredt (1).[5] A high degree of hydrogen dissociation is possible at practical chamber temperatures by use of sufficiently low chamber pressures. During flow expansion through the nozzle, atom recombination will release dissociation energy and thus will increase specific impulse beyond that for no dissociation at the same chamber temperature. In such a flow process, the impulse gain from dissociation depends very much on the degree to which local chemical equilibrium is maintained. To the authors' knowledge, previously published calculations of nonequilibrium flow for hydrogen-like propellants have been limited to essentially one chamber temperature, and to relatively high pressures and small expansions where nonequilibrium effects are relatively small (2,3,4). The purpose of the present note is to report calculations of nonequilibrium hydrogen flows for a lower range of pressures as well as a wider range of temperatures and nozzle geometry than previously considered.

The present calculations were made using a convenient, approximate method of analysis for such flows given in (5). This method involves a local relaxation length criterion for determination of the freezing of gas composition, the criterion being evaluated on the basis of corresponding equilibrium flow solutions. Comparisons with exact numerical solutions (5) show the criterion to give an accurate prediction of the frozen dissociation level.

For simplicity and generality, the hyperbolic axisymmetric nozzle geometry of Fig. 1, top, was assumed. The nozzle is symmetric about the throat, and is characterized in size and shape by throat diameter D and (asymptotic) cone semi-angle $\theta = \tan^{-1} a$. Although the geometry of the nozzle upstream of the throat does not closely resemble that for conventional rockets, the upstream geometry does not greatly influence freezing. Changes in the upstream convergence angle by factors of 2 or 3, for example, have relatively small effect on the frozen dissociation level and specific impulse.

At the reservoir or chamber ($x = -\infty$) the gas was taken to be at rest and in complete thermochemical equilibrium. Subsequent flow through the nozzle was assumed to be pseudo one-dimensional without transport or wall effects. Dissociation and recombination were assumed to occur at finite rates by two- and three-body collisions, respectively. Vibrational excitation was taken as that for a harmonic oscillator in thermodynamic equilibrium with translational and rotational degrees of freedom. The latter degrees were assigned full equipartition energies. Hydrogen atoms and molecules were supposed equally effective as second- or third-body colliders, and specific recombination rate coefficient k_R was considered independent of temperature.

With given reservoir (chamber) conditions, the foregoing model can be solved exactly by numerical forward integration of the basic equations governing finite reaction rate flow. Exact solutions have recently been obtained in this way for nozzle flows of dissociated oxygen over a wide range of reservoir pressures (5,6). These exact calculations show a characteristic freezing of dissociation level at finite nozzle areas due to effective vanishing of atom recombination rate at sufficiently low densities. The final, frozen value of α(α = local mass fraction dissociated) has a very strong dependence on chamber pressure (density), since the rate of atom recombination varies as the density cubed. A power dependence of k_R on temperature was found to have slight influence on freezing. A similar behavior in these respects may be expected for hydrogen.

Rather than obtain exact numerical solutions, it was sufficient in the present study to demonstrate nonequilibrium effects on nozzle performance in terms of specific impulse I using the approximate method of analysis of (5). The approximate method is particularly convenient for determining the limiting specific impulse I_∞ attained by expansion to infinite area and zero pressure. Since the specific total enthalpy h_0 is constant, I_∞ is given in terms of h_0 and the final, frozen degree of dissociation α_f by

$$I_\infty = \frac{u_\infty}{g} = \frac{1}{g}\sqrt{2\left(h_0 - \frac{E_D\alpha_f}{M}\right)}$$

where

u_∞ = velocity at infinite area
g = standard gravitational acceleration
E_D = molar dissociation energy of diatomic species
M = diatomic molecular weight

Thus, determination of I_∞ for given chamber conditions required only the determination of α_f. The limiting values of α_f are zero for flow in local thermochemical equilibrium throughout ($k_R \to \infty$), and α_0 the chamber value, for flow which is completely frozen ($k_R \to 0$).

Values of α_f for finite reaction rates were obtained from corresponding equilibrium flow solutions by application of the local relaxation length criterion for freezing (5). Briefly, the freezing criterion is derived from the exact rate equation expressed in a form developed by Heims (7), namely, $d\alpha/dx = (\alpha - \alpha_e)/r$, where α_e is the local equilibrium value of α for the actual temperature and density and r is a local relaxation length depending on k_R as well as on local values of α, α_e, temperature T, density ρ, velocity u. It can be shown (5) that substantial freezing of gas composition may be expected to occur when the equality $d\alpha/dx = -\alpha_e/r$ is satisfied locally. In application, this criterion may be evaluated along the equilibrium α vs. x curve by employing the average values $d\alpha/dx = (1/2)\, d\alpha_{e,\infty}/dx$ and $\alpha_e = \alpha_{e,\infty}/2$ which apply through the freezing region, where $\alpha_{e,\infty}$ denotes the value of α for infinite rate equilibrium. The point at which the equality is satisfied defines a value of α approximating the frozen dissociation level α_f, and an area at which substantial freezing has occurred. For the oxygen flow studies of (5), this approximate method of determing α_f was found to give values in excellent agreement with the exact numerical solutions obtained over a wide range of reservoir pressures. Fairly close agreement was also found with results from an approximate method previously given by Bray (6).

Equilibrium solutions for given chamber pressure p_0 and chamber temperature T_0 were obtained on an IBM-704 digital computer. Solutions were run for p_0 down to 0.1 atm and T_0 up to 4500 K. The relaxation length was then applied to each equilibrium case to determine α_f for a range of values of the rate-geometry parameter $\Omega = k_R D/a$. Regarding the magnitude of k_R, to the authors' knowledge there are no experimental rate data for hydrogen in the temperature range of present interest. Wilde (4) has recently suggested a value for k_R of 10^{14} cm^6 per mole^2 sec for temperatures around 3000 K, on the basis of shock tube studies of iodine and bromine dissociation rates. This value is less than the value 10^{16} previously used in calculation studies for hydrogen (3).

Received Dec. 3, 1959.

[1] This work was carried out under Cornell Aeronautical Laboratory Internal Research and employed calculation methods developed under Air Force Office of Scientific Research, Mechanics Division, Contract no. AF 18(603)-141.

[2] Principal Aerodynamicist.

[3] Associate Aeronautical Engineer. Member ARS.

[4] Assistant Physicist.

[5] Numbers in parentheses indicate References at end of paper.

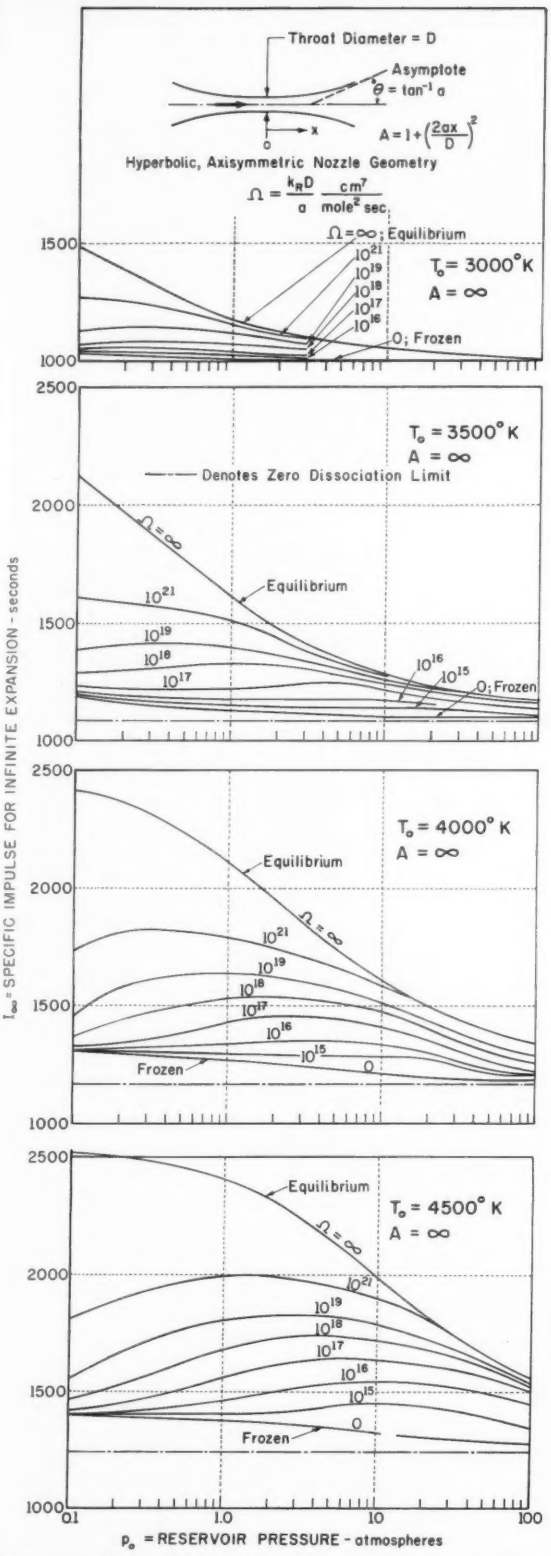

Fig. 1 Specific impulse (I_∞) for infinite expansion ratio (A = exit area/throat area = ∞) vs. reservoir pressure (p_0) at various reservoir temperatures (T_0) and values of rate-geometry parameter (Ω)

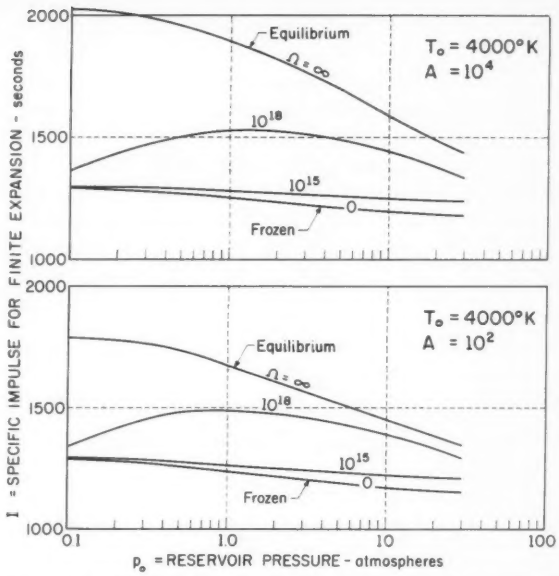

Fig. 2 Specific impulse (I) at finite expansion ratios $A = 10^2$ and 10^4 vs. reservoir pressure (p_0) for various values of Ω at $T_0 = 4000$ K

For $k_R = 10^{14}$, Ω becomes about 4×10^{14} cm^7 per mole^2 sec for a 1-cm nozzle throat diam and a total cone angle of 30 deg.

In addition to determination of I_∞ for a range of values of T_0, calculations were also made to determine I for finite values of exit to throat area ratios A of 10^2 and 10^4 at $T_0 = 4000$ K and Ω values of ∞, 10^{18}, 10^{15} and zero. Specific impulse at finite area is determined by the corresponding exit velocity and pressure (neglecting ambient pressure). Values of exit velocity and pressure were determined by employing a frozen flow solution (appropriate to α_f) downstream of the nozzle area at which freezing was indicated by the relaxation criterion. The pressure contribution to I was only a few per cent at $A = 10^2$, and negligible at $A = 10^4$.

The results obtained for infinite expansion ratio are summarized in Fig. 1 in terms of I_∞ vs. p_0 at various chamber temperatures with Ω as a parameter. The significant aspect of the results is the drastic reduction of I_∞ from the equilibrium limit as Ω decreases through finite values. Although I_∞ for equilibrium flow is greatly increased at the lowest pressures over that for no dissociation ($p_0 \to \infty$), relatively little of this possible gain can be realized assuming reasonable nozzle geometry and currently accepted values of k_R. For example, even with the values $k_R = 10^{15}$ cm^6 per mole^2 sec, $D = 50$ cm and $\theta = 7.5$ deg, Ω is only 4×10^{17} cm^7 per mole^2 sec, giving a gain in I_∞, over that for no dissociation, of only some 10 to 15 per cent at $T_0 = 3500$ K. An important feature of the results is the fact that for constant Ω, I_∞ passes through a maximum value with decreasing pressure. The maximum results from the fact that at high pressure levels h_0 increases faster than α_f as the chamber pressure decreases, but at sufficiently low pressure levels this behavior is reversed. It will be noted that the maxima shift toward higher values of p_0 with decreasing Ω and increasing T_0.

Similar features are evident in the results for finite expansion ratios shown in Fig. 2 for $T_0 = 4000$ K. Here it will be

noted that although I is significantly less than I_∞ for $\Omega = \infty$, the effects of finite area are small for finite values of Ω. In particular, for $\Omega = 10^{16}$, which might be considered a practical upper bound, the maximum value of I at $A = 10^2$ is only about 3 per cent less than the maximum value for infinite expansion. With increasing expansion ratios, the maxima in I shift slightly to higher chamber pressures.

The nozzle expansion ratio at which freezing is essentially complete decreases with decreasing p_0, T_0 and Ω. In the present examples, freezing was delayed longest at 4500 K, and in this case was substantially complete at an expansion area ratio of 10 for all chamber pressures and values of Ω less than about 10^{17} cm^7 per mole^2 sec.

References

1 Sänger-Bredt, I., "Thermodynamics of Working Gases in Atomic Rockets," *J. Brit. Interplanet. Soc.*, vol. 15, no. 5, Sept.-Oct. 1956, pp. 233–247.

2 Penner, S. S., "Chemical Reactions in Flow Systems," Butterworths Sci. Pub., London, 1955.

3 Krieger, F. J., "Chemical Kinetics and Rocket Nozzle Design," JOURNAL OF THE AMERICAN ROCKET SOCIETY, vol. 21, no. 6, Nov. 1951, pp. 179–185.

4 Wilde, K. A., "Effect of Radical Recombination Kinetics on Specific Impulse of High Temperature Systems," JET PROPULSION, vol. 28, no. 2, Feb. 1958, pp. 119–120.

5 Hall, J. G. and Russo, A. L., "Studies of Chemical Nonequilibrium in Hypersonic Nozzle Flows," presented at Combustion Institute Meeting, Western States Section, Los Angeles, Nov. 2–5, 1959; *also*, Cornell Aeronautical Laboratory Rep. no. AD-1118-A-6, AFOSR TN 59-1090, Nov. 1959.

6 Bray, K. N. C., "Atomic Recombination in a Hypersonic Wind-Tunnel Nozzle," *J. Fluid Mech.*, vol. 6, pt. 1, July 1959, pp. 1–32.

7 Heims, S. P., "Effect of Oxygen Recombination on One-Dimensional Flow at High Mach Numbers," NACA TN 4144, Jan. 1958.

Pure Shock Environmental Testing of Condensed-Phase, Unstable Materials

T. A. ERIKSON[1]

Armour Research Foundation of Illinois Institute of Technology, Chicago, Ill.

THERE are numerous procedures described in the classified and unclassified literature for use in the evaluation of explosive sensitivity. Each test (impact, card gap, adiabatic compression, spark, etc.) has been developed to evaluate specific questions regarding the safety requirements of unstable materials such as propellants and explosives. There is little information (1, 2)[2] that describes the general features of a pure shock environment test.

The principles and applications of shock waves and shock tubes have been described in detail by many investigators (3, 4, 5). Qualitatively the reflected shock region in a shock tube provides an energy source which can be well-controlled and made sufficiently intense to cause the response (go) of many types of unstable, condensed-phase systems.

A schematic diagram of the equipment is shown in Fig. 1. Basically, the apparatus consists of a steel tube, 1 in. in diameter, which is divided into a 1-ft driver and a 2-ft driven section. The driven (test) section has a streamlined reduction to a $\frac{1}{2}$-in. diameter for the last 6 in. The tube is mounted vertically, and the driver and driven sections are separated by a rupture disk which is selected to produce the desired burst pressure. An inert driver gas (usually helium) is used, whereas the driven gas is ordinarily oxygen or nitrogen. About 1 to 5 gm of the material to be tested is placed in the bottom of a glass tube which is aligned and attached to the shock tube by a standard steel-to-glass 28/12 ball joint. The driven gas pressure (above the material being tested) is adjusted to produce a preselected shock wave, and the driver gas pressure is slowly increased until the rupture disk breaks. An appropriate pressure gage with a lazy hand is used to register the driver gas pressure at time of rupture. A mercury barometer, an Alphatron gage, or a suitable pressure gage is used to measure the driven gas pressure. Positive response (go) of the unstable material is detected by light emission, sound intensity and fragmentation of the glass tube containing the sample. With negative response (no go), the glass tube and sample are usually unaffected.

The "go-no go" result can be evaluated in terms of the driver to driven gas pressure ratio (P_4/P_1) and the driven gas pressure (P_1). One practical aspect of a safety requirement is described by the P_4/P_1 ratio, which has also been shown to define the incipient temperature to which the test sample is exposed (4). The absolute value of P_1 is also important, probably because P_1 defines the incipient pressure (in conjunction with P_4/P_1) that the condensed phase experiences. The time of contact between the "hot" shocked gas and the surface of the condensed-phase material is less than $\frac{1}{2}$ millisec. As shown in Fig. 1, the sample environment can be controlled completely. That is, the initial temperature (T) can be maintained by an appropriate thermal reservoir, and the initial pressure (P_1) can be adjusted with the driven gas manifold.

Some representative results obtained with various unstable materials are shown in Table 1 where the system, its initial state and the values of P_1 and P_4/P_1 for 50 per cent response are indicated. With P_4/P_1 used as a measure of energy, the data can be analyzed statistically in a manner similar to that described for impact testing (6).

One result of general interest was found during the testing of the ozone-oxygen mixtures. At −196 C, a two-phase separation occurs in a mixture containing greater than 90.8 per cent by weight of ozone in oxygen (7). This separation results in a light phase (9.0 per cent ozone) resting on a heavy phase (90.8 per cent ozone). These phases can be clearly

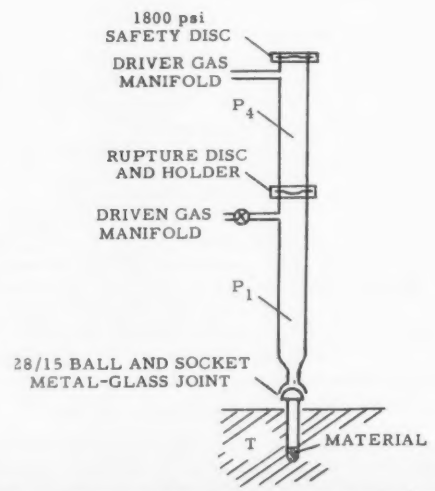

Fig. 1 Schematic diagram of shock tube apparatus

Received July 23, 1959.

[1] Research Chemical Engineer, Propellant Research Section, Chemistry and Chemical Engineering Research Division. Member ARS.

[2] Numbers in parentheses indicate References at end of paper.

Table 1 Typical values of P_4/P_1 and P_1 for 50 per cent explosive response of various systems

System			Gas			
Material	State	Temperature, C	Driver	Driven	P_1, mm Hg	P_4/P_1[a]
100 per cent ozone	liquid	−183	nitrogen	oxygen	50–700	47.5 ± 3.5
100 per cent ozone	liquid	−183	helium	oxygen	50–700	18 ± 4.0
100 per cent ozone	liquid	−196	helium	oxygen	50–200	22.4 ± 4.0
92 per cent ozone in oxygen	liquid[b]	−196	helium	oxygen	~200	>70
90 per cent ozone in oxygen	liquid	−196	helium	oxygen	200–700	27.5 ± 2.5
TNETB	liquid	100	helium	oxygen	1–20	930 ± 80
ammonium nitrate	solid	25	helium	oxygen	700	26
TNT	solid	25	helium	oxygen	700	20
nitroglycerine	liquid	25	helium	oxygen	1–100	>3000
nitroglycerine	liquid	25	helium	oxygen	300–400	24.5 ± 2.5
lead styphnate	solid	−183	helium	oxygen	1–100	17.6 ± 2.0
lead styphnate	solid	25	helium	oxygen	1–100	9.4 ± 1.0
hydrazine nitrate	liquid	80	helium	oxygen	300–400	17.0 ± 4
n-propyl nitrate	liquid	20	helium	nitrogen	760	>30
n-propyl nitrate	liquid	20	helium	oxygen	1–100	>300
n-propyl nitrate	liquid	20	helium	oxygen	600–1000	7.5 ± 1.0

[a] For 50 per cent explosive response ± (100% − 0%)/2.
[b] Two-phase.

identified by the distinct difference in their color intensities. This phenomenon can be used as a convenient method of analysis. As oxygen is slowly added or pumped out of the mixture, the concentration can be adjusted to about 90 per cent ozone (barely two-phase) or about 92 per cent (single-phase). The former mixture is not susceptible to weak shock; that is P_4/P_1 ratios of greater than 70 do not cause any response, whereas the latter mixture having no light phase on the surface responds readily at P_4/P_1 ratios of 27. This result indicates that only surface events are involved in explosion initiation by this technique. The effect of compression waves transmitted through the bulk of the sample can be neglected.

The results reported for lead styphnate at 20 and −183 C demonstrate the effect of the initial temperature of the sample. Another aspect of this type of testing is demonstrated by the results obtained with n-propyl nitrate. When the driven gas is changed from a relatively inert (nitrogen) to a chemically reactive (oxygen) type, very "sensitive" states result. Thus the reactivity of the environment gas can be evaluated by this technique.

It should be emphasized that the data in Table 1 were chosen to demonstrate the character of the results. That is, the P_4/P_1 results are particularly dependent on the P_1 pressure over wide ranges. The relations of P_4/P_1 and P_1 are obviously a result of the energy level and the energy density requirements for the initiation of an unstable, condensed-phase system.

The general technique and the representative data presented in Table 1 lead to several conclusions concerning the application of the "pure" shock environmental test to the establishment of a relative sensitivity scale, and the merits of the test as a research tool for studying the initiation problem in general:

1 This test can define a "go-no go" region for the explosive response of condensed-phase materials. The P_4/P_1 ratio and the P_1 level serve as relative indexes of sensitivity which are at least as good as the Wh (gm-cm) in impact, E (joules) in spark, N (number of cards) in card gap, etc.

2 The test is reproducible in that the data can be tested in a statistical fashion to define a fairly narrow range of 0, 50 and 100 per cent points for explosive response.

3 The range of the test is wide, in that explosive response has been established for materials as "insensitive" as ammonium nitrate and as "sensitive" as lead styphnate.

4 The versatility is good, in that tests have been performed on liquids and solids, at temperatures ranging from −196 to 130 C, and at initial pressures from 0.02 to 100 psia.

The possible implications of the data are more important. For example, the fact that specific levels of P_4/P_1 *and* P_1 are required for explosive response indicates that the incipient temperature and the incipient pressure of the reflected shock region may be considered as pertinent intensive variables of the "hot" gas environment in contact with the surface of the condensed phase. The results with ozone indicate that only surface events are involved. The principles of the kinetic theory and/or heat transfer can be utilized to evaluate the actual energy requirements for initiation under the high flux, short time conditions of the reflected shock. Recently a newly designed shock tube has been instrumented to measure pressure, temperature and time delay variables, and it is expected that the results obtained with a specific explosive system will be ready for publication in the near future.

References

1 Gey, W. and Bennett, A., "Sensitivity of Explosives to Pure Shocks," *J. Chem. Phys.*, vol. 23, 1955, p. 1979.

2 Summerfield, M. and McAlevy, R., "Shock Tube as a Tool for Solid Propellant Research," JET PROPULSION, vol. 28, 1958, p. 478.

3 Bleakney, W., Weimer, D. K. and Fletcher, C. H., "The Shock Tube: A Facility for Investigations in Fluid Dynamics," *Rev. Sci. Instr.*, vol. 20, 1949, p. 807.

4 Resler, E. L., Lin, S. and Kantrowitz, A., "The Production of High Temperature Gases in Shock Tubes," *J. Appl. Phys.*, vol. 23, 1952, p. 1390.

5 Penner, S., Harshbarger, F. and Valis, V., "Combustion Researches and Reviews, 1957," Butterworths Scientific Publ., London, 1957, pp. 134–172.

6 Bowden, F. and Yoffe, A., "Initiation and Growth of Explosion in Liquids and Solids," University Press, Cambridge, England, 1952.

7 Brown, C., Berger, A., and Hersh, C., "Phase Diagram of Liquid Oxygen-Ozone System," *J. Chem. Phys.*, vol. 23, 1955, p. 1340.

Calibration of Turbine Flowmeters for Cryogenic Operation

JERRY GREY[1]

Princeton University, Princeton, N. J.

The errors introduced by water calibrations of cryogenic fluid flowmeters are estimated. In addition to the thermal contraction, it is shown that the effect of very low fluid viscosities is quite important for accurate measurements in the smaller pipeline sizes. Some rather limited experimental data appear to corroborate the predicted calibration error.

Thermal Contraction

THE SPEED of a turbine flowmeter may be written

$$\omega = \frac{V \tan \alpha}{R} = \frac{Q}{A_h - A_r} \frac{\tan \alpha}{R}$$

where

ω = rotor angular velocity
V = average flow velocity at the blades
α = blade angle with pipe axis
R = average radius of blade center of pressure
Q = volumetric flow rate
A_h = internal cross-sectional area of housing
A_r = maximum cross-sectional area of rotor

Small changes $\Delta\omega$ in rotor speed at constant volumetric flow rate therefore become

$$\frac{\Delta\omega}{\omega} \approx -\frac{\Delta(A_h - A_r)}{A_h - A_r} + \frac{\Delta(\tan \alpha)}{\tan \alpha} - \frac{\Delta R}{R}$$

If we now consider a temperature change ΔT in the flowmeter material, the resulting change in rotor speed is

$$\Delta\omega/\omega \approx [-2\beta_t + (\beta_t - \beta_a) - \beta_t]\Delta T$$

where

β_t = transverse coefficient of expansion of rotor and housing
β_a = axial coefficient of expansion

For isotropic rotor material, $\beta_t = \beta_a \equiv \beta$, and the fractional error thus becomes

$$\Delta\omega/\omega \approx -3\beta\Delta T \qquad [1]$$

where

$\Delta T = T - T_0$
T = cryogenic operating temperature
T_0 = calibration temperature

The approximate volumetric error (for isotropic rotor materials) resulting from application of 60 F calibration data to test runs at typical cryogenic fluid operating temperatures is shown in Fig. 1 for the various meter materials. Note that the error is independent of the meter dimensions, as indicated by the foregoing analysis.

Viscosity

The effect of viscosity on turbine meter output is shown diagrammatically in Fig. 2. It is clear from this sketch that thicker boundary layers, i.e., larger viscosities, will cause a turbine meter to read high.

Although the marked difference between laminar and turbulent profiles has been well cataloged (see Cases A and B of Fig. 2), the much smaller effect on two turbulent profiles

Received Aug. 4, 1959.

[1] Assistant Professor of Aeronautical Engineering; also Consultant, Potter Aeronautical Corp. Member ARS.

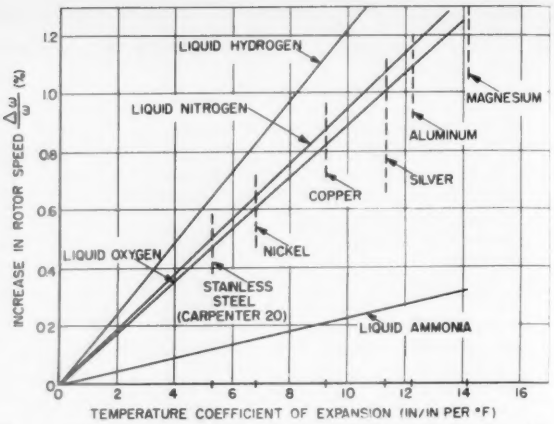

Fig. 1 Effect of thermal contraction: Theoretical volumetric error resulting from use of water calibration at 60 deg for some cryogenic liquids (atmospheric pressure)

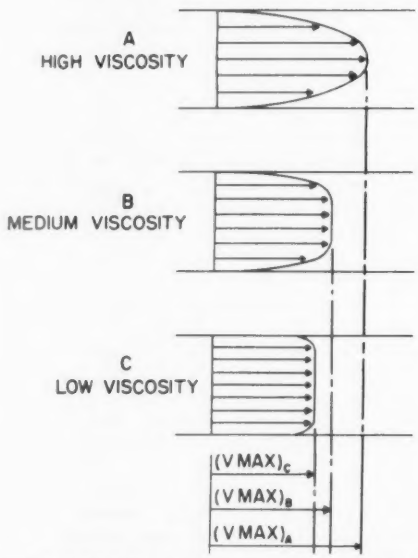

Fig. 2 Effect of viscosity on uncompensated turbine flowmeter: Volumetric flow rate = $\int VdA$, same for all three cases, but fluid C (low viscosity) reads lowest

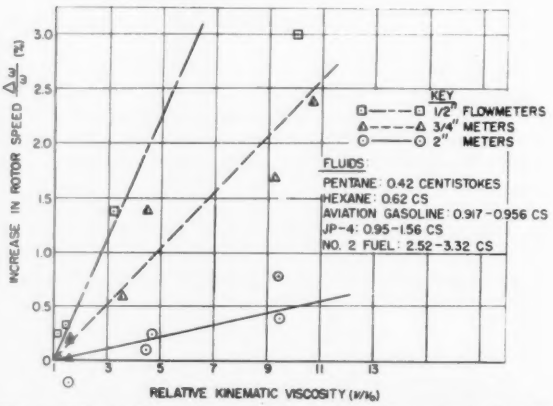

Fig. 3 Effect of viscosity on observed mean pipe velocity (cycles per gal) for low viscosities. ν_0 corresponds to lowest viscosity tested

having different Reynolds numbers also exists (e.g., Cases B and C of Fig. 2). This small effect can be of major importance when considering high accuracy measurements in fluids of low but widely different viscosities, such as water and the various cryogenic liquids.

A comparison of Cases B and C of Fig. 2 may be used to provide an estimate of the viscosity error involved in calibrating a cryogenic fluid on water. To maintain constant volumetric flow of an incompressible fluid

$$\pi D\delta^* V_i \approx (\pi D^2/4)(V_a - V_i)$$

where

δ^* = boundary layer displacement thickness
D = pipe diameter
V_a = actual free stream fluid velocity
V_i = velocity of a frictionless fluid which would be necessary to produce an equal volumetric flow rate

and the approximation $\delta^*/D << 1$ has been made for the low viscosity turbulent flows under consideration.

Thus, since the turbine meter reads V_a when it should read V_i, the *absolute* viscosity error becomes, in terms of rotor speed change $\Delta\omega$

$$\frac{\Delta\omega}{\omega} = \frac{V_a - V_i}{V_i} = 4\,\frac{\delta^*}{D}$$

In order to provide the best possible correlation with actual turbine meter operation, the displacement thickness δ^* is represented only functionally in terms of flow parameters, i.e.

$$\delta^* \sim 1/Re^n$$

where

Re = flow Reynolds number
n = constant to be determined experimentally under actual operating conditions

The error thus becomes

$$\frac{\Delta\omega}{\omega} \sim \frac{1}{D\,Re^n} \sim \frac{\nu^n}{D^{n+1}} \qquad [2]$$

where ν is the kinematic viscosity and the velocity change has been taken as zero for the constant volumetric flow rate assumed.

Rough values for the exponent n were established by volumetric experiments on fluids having different viscosities, but operating at the same temperature (to eliminate any effect of dimensional change). These data are summarized in Fig. 3, in which the observed relative increase in meter constant (output frequency per unit volume delivered) as a function of relative kinematic viscosity is given for several pipeline sizes. The reference fluid is arbitrarily taken as that with the lowest viscosity in each case.

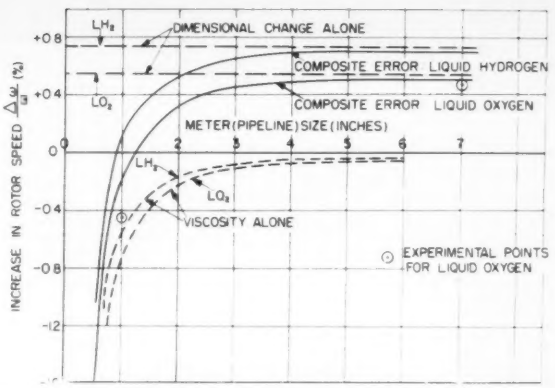

Fig. 4 Rough predicted error for cryogenic tests based on water calibrations at 60 F

The error due to viscosity differences between calibrating and operating fluids may thus be obtained from Equation [2] and the data of Fig. 3 for any pipe size D. Sample results for liquid oxygen and liquid hydrogen are shown in Fig. 4, where representative ratios ν/ν_0 for water/oxygen and water/hydrogen were taken at 5.5 and 4.4, respectively. In addition to the viscosity error of Equation [2], Fig. 4 also includes the dimensional error for stainless steel meters as given by Equation [1] and the resulting composite error predicted by including both effects.

Comparison With Experimental Data

The only data available at the present time against which to check the theoretical prediction of Fig. 4 have been recorded for liquid oxygen on a 1-in. meter at Princeton and on a 7-in. meter at ABMA. (The 7-in. meters were aluminum, so the results were normalized to the stainless steel case of Fig. 4 by the use of Fig. 1.) These results, although admittedly rather meager, appear to correlate at least qualitatively the predicted calibration error.

Note that this method of estimating calibration errors is also applicable to hot fluids of reasonably low viscosity (e.g., aviation or jet fuels at high temperatures). Thus by proper application of Equations [1 and 2] and the experimental data of Fig. 3, curves similar to those of Fig. 4 may be drawn for each fluid at one operating temperature, or, conversely, the error may be plotted as a function of temperature for the given fluid at any one meter size.

Expansion of Liquid-Oxygen RP-1 Combustion Products in a Rocket Nozzle

FREDERICK S. SIMMONS[1]

Rocketdyne, a Division of North American Aviation, Inc., Canoga Park, Calif.

Gas temperature measurements at the nozzle exit of a rocket motor utilizing liquid oxygen and RP-1 have been made over a wide range in propellant mixture ratio. The assumption of a nozzle flow process consisting of a frozen composition expansion with some additional burning is shown to be in reasonable accord with the observed motor performance.

CALCULATIONS of the theoretical performance of rocket engines are currently based on the usual simplifying assumptions: Completely reacted products at the nozzle inlet, and a one-dimensional, isentropic expansion with the chemical composition remaining "frozen" at the chamber equilibrium value, or with the composition changing as required for equilibrium at the local values of temperature and pressure. The two choices for the expansion correspond, of course, to assumptions of zero and infinite rates of reaction

Received Aug. 7, 1959.

[1] Engineering Specialist, Research Sub-Division. Member ARS.

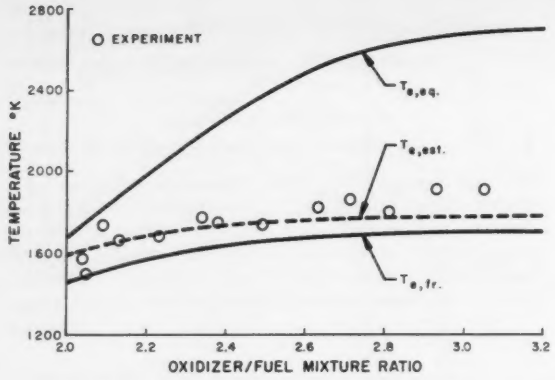

Fig. 1 Gas temperature at the nozzle exit

in the recombination of dissociated species. Since little quantitative information is available on the reaction rates of current interest in rocketry, e.g., those encountered in the expansion of liquid oxygen and hydrocarbon fuel products, the nature of the expansion can only be inferred from experimental measurements of rocket performance.

A parameter particularly sensitive to the type of process in the nozzle is the temperature of the expanded gas at the exit. For the direct measurement of this temperature, a two-path technique based on photographic pyrometry has recently been employed at Rocketdyne (1).[2] By this means, temperatures at the nozzle exit planes of a number of rocket motors utilizing liquid oxygen and RP-1 had been determined, but the data had been somewhat difficult to interpret in view of the limited range of mixture ratio encountered in the usual test operations. Recently, however, a series of tests with a research motor (nominally 5000-lb thrust at 600-psi chamber pressure, with a 8:1 conical nozzle) has provided such measurements over a much wider range of operation. The resultant data are presented in Fig. 1 in comparison with the temperatures predicted from theory (2,3). The exit temperatures appear intermediate between the two theoretical values at the very low mixture ratios, but distinctly approach those corresponding to a "frozen" expansion for leaner combustion.

In order to estimate the possible effects of burning during the expansion, values of an "effective" nozzle inlet temperature can be calculated using the theoretical and the measured values of the characteristic exhaust velocity C^* and the theoretical chamber temperature in the relation

$$T_{c,\,\mathrm{eff}} = T_{c,\,\mathrm{theor}} (C^*/C^*_{\mathrm{theor}})^2$$

Were the molecular weight and specific heat ratio invariant with the degree of completeness of combustion, this relation would presumably provide a reliable estimate of the actual chamber temperature. Since, however, changes in these properties are not known nor easily estimated for incomplete combustion, the relation is useful only as a rough approximation. The experimental values of C^* are shown in Fig. 2; the values of "effective" chamber temperature determined therefrom are presented in Fig. 3. The effect of burning in the nozzle can then be handled in the following manner: Letting the nozzle inlet temperature be represented by the dashed curve in Fig. 3, an upper limit for the nozzle exit temperature can be determined by assuming the expansion to be isentropic to the exit plane, where the additional combustion takes place instantaneously and completely. For this case, the nozzle exit temperatures can be estimated by a simple heat balance

$$T_{e,\,\mathrm{est}} = \left(\frac{T_e}{T_c}\right)_{\mathrm{isen}} T_{c,\,\mathrm{eff}} + \left(\frac{C_{p,c}}{C_{p,e}}\right)(T_{c,\,\mathrm{theor}} - T_{c,\,\mathrm{eff}})$$

[2] Numbers in parentheses indicate References at end of paper.

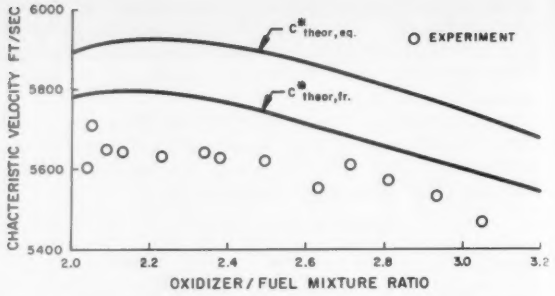

Fig. 2 Theoretical and experimental values of characteristic velocity

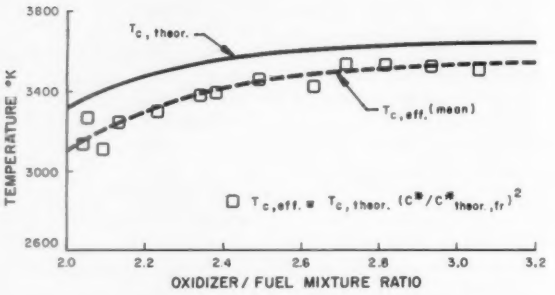

Fig. 3 Gas temperature at the nozzle inlet

The estimates of nozzle exit temperature represented by the dashed curve in Fig. 1 result from the use of values of the isentropic temperature ratio and the specific heats at the nozzle inlet and exit reported in (3).

The preceding calculations, based on such moot premises, are intended only to indicate that a description of the actual nozzle process as one corresponding to a theoretically "frozen" expansion with some additional burning is reasonably consistent with the observed motor performance. A more conclusive indication of the true nature of the expansion could be obtained from an experiment which includes direct measurement of the nozzle inlet as well as the exit temperature; such studies are currently being undertaken. It would not be unreasonable to infer from the present results, however, that for the liquid oxygen and RP-1 propellant combination, an assumption of a "frozen" or constant composition expansion is clearly more justified than one in which chemical equilibrium is presumed to be maintained.

Nomenclature

C^* = characteristic velocity
C_p = specific heat at constant pressure
T = temperature

Subscripts

c = chamber
e = nozzle exit
eff = effective
est = estimated
fr = corresponding to a "frozen" expansion
eq = corresponding to an "equilibrium" expansion
isen = isentropic
theor = theoretical

References

1 Simmons, F. S. and DeBell, A. G., "Photographic Pyrometry of Rocket Exhaust Jets," *Aircraft Engng.*, vol. 31, 1959, pp. 144–146.

2 Huff, V. N. and Fortini, A., "Theoretical Performance of JP-4 Fuel and Liquid Oxygen as a Rocket Propellant. I—Frozen Composition," NACA RM E56A27, 1956.

3 Huff, V. N. et al., "Theoretical Performance of JP-4 Fuel and Liquid Oxygen as a Rocket Propellant. II-Equilibrium Composition," NACA RM E56D24, 1956.

Some Weight Considerations for Manned Lunar Missions

HANS B. SCHECHTER[1]

The Rand Corp., Santa Monica, Calif.

The total weight requirements for three possible types of manned, round trip, soft landing lunar missions are investigated, all starting out from a space station circling Earth at an altitude of about 350 miles. The first and second missions follow direct hit flight trajectories and employ chemical and nuclear powerplants, respectively. Thrust magnitudes needed are determined by imposing an initial landing deceleration load factor of 3 Earth *g*. The third mission makes use of a nuclear powerplant as a sort of "ferry boat" to reach a circular orbit around the moon, whereas for the landing and ascent portions at the moon, the final payload is propelled by chemical rockets. After rendezvous with and attachment to the orbiting ferry boat, the payload is returned to the Earth space station.

ONE OF the first extraterrestrial targets for manned space flight will undoubtedly be the moon. The first scientific exploratory missions would conceivably be followed later on by full scale operations, involving large numbers of personnel and equipment. The tremendous mass ratios required for the soft landing of any payload on the moon by means of propulsion devices using rocket thrust put a premium on any scheme which can reduce these costs to a "tolerable" level.

The present paper is concerned with a comparison of the effect which the use of various powerplants has on starting weights required for three schemes of landing a manned payload on the moon.

In the first case, payloads are flown out directly along a lunar impact trajectory with the thrust supplied by a chemically powered rocket.

After making some optimistic assumptions concerning the thrust and power that could be expected from some future high thrust nuclear fueled rockets, the same trajectory is reflown under nuclear power.

In the third type of scheme it is assumed that only a low thrust (4000–5000 lb) nuclear fueled rocket is available to us, and is employed to ferry the payloads to a suitable satellite orbit around the moon. Once in this orbit, the payload could be detached from the nuclear "ferry boat" and, powered by chemical rockets, make its way down to the surface of the moon while the nuclear vehicle remained in orbit. After the completion of the mission, the payload ascends again to the orbit for a rendezvous with the orbiting tug boat and attaches itself to it. Departure from the lunar orbit, entry into the Earth centered orbit and rendezvous with the space station would then be accomplished on nuclear power. Fig. 1 shows the possible flight paths for the three schemes.

Although it is easy to see that the nuclear powerplant would be more economical than the chemical rocket for the case of direct lunar landing, the relative merits of the last two schemes are not immediately apparent. The direct nuclear landing uses an efficient propulsion device for the entire period of powered flight, but requires the soft landing and subsequent takeoff of the heavy nuclear reactor, shielding, as well as the propellant supplies for the return portion of the journey. The mixed powerplant scheme on the other hand permits the landing of only the payload plus a small quantity of propellant for ascent to the orbiting nuclear boat, and also allows the use of lighter shadow shielding in view of the smaller power output of the nuclear reactor. This beneficial

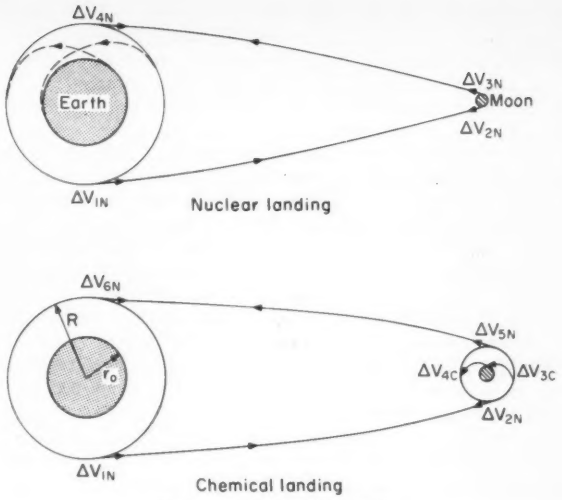

Fig. 1 Possible flight paths

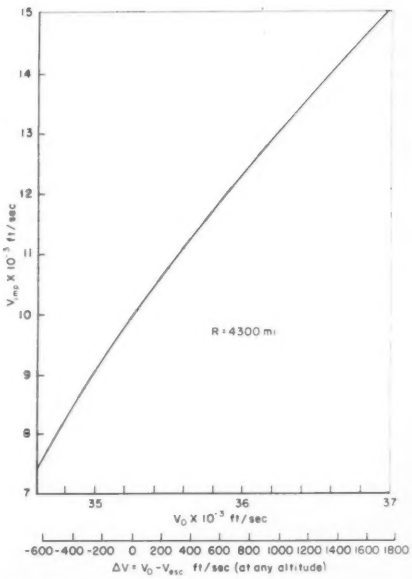

Fig. 2 Lunar impact velocities vs. hyperbolic excess velocities at departure

aspect is offset in part by the less efficient propulsion device used for landing, and the characteristic velocity penalties associated with the repeated entry into, and departure from, the circular lunar orbits.

Trajectory Requirements

In the present analysis it is assumed that the periods of powered flight are much shorter than the time required to traverse the distance between Earth and moon, thus enabling us to apply the concept of impulsive thrust maneuvers.

The velocity vector needed by a spaceship at any point in an orbit around Earth to impact on the moon has been determined in (1),[2] and the corresponding magnitudes of the im-

Received April 14 and revised Dec. 29, 1959.

[1] Research Engineer, Aero-Astronautics Department.

[2] Numbers in parentheses indicate References at end of paper.

pact (surface approach) velocities at the moon can be calculated by the application of the Jacobi energy integral. Fig. 2 shows the results of such a calculation. In order to eliminate the altitude of the starting orbit as a parameter, the lunar impact velocity has been plotted against the magnitude of the velocity increment over local orbital escape requirements needed to secure a lunar hit trajectory. The numerical portion of this paper assumes that a velocity increment of 10,000 ft per sec over local Earth orbital velocity would result in a lunar surface approach velocity of 9000 ft per sec. To this velocity there corresponds a velocity of 7200 ft per sec at the closest point of approach in a "near miss" flight path, which passes the moon's surface at an altitude of 1 lunar radius (h = 1080 miles), at which altitude the spaceship of Case 3 enters into a circular orbit around the moon. Descent from the orbit is accomplished along a Hohmann transfer ellipse, at a characteristic velocity outlay of about 1.82 V_{or}. The chemical rocket selected to propel a given payload was large enough to impart an acceleration of about 1.5–2.0 g_E to the payload at takeoff from the moon's surface. An initial deceleration of $3g_E$ is assumed for the direct approach landing. In all cases gravity losses are neglected.

Powerplants

The lack of information available in the unclassified literature on the behavior and performance characteristics of suitable nuclear powerplants makes an analysis of the present kind rather difficult. The magnitude of the various design parameters required for an estimation of the expected output from such a device will depend on the correctness of the guesses made by the author, and those in turn will depend on the degree of his optimism or pessimism.

For the purpose of the present investigation, the reactor used was assumed to be of the solid core type, having tungsten fuel elements and employing hydrogen as a propellant. An operating pressure P_1 of 25 atm and temperature of around 5800 R were selected for the numerical part. Specific impulses of 750 sec at sea level and 1110 sec at an ambient pressure of $p \cong 0$ were chosen. Powerplant weight and thrust were obtained from (2) by making suitable guesses for the various coefficients A_n. In particular, in the notation of (2), the optimistic values $A_7 \cong 25$, $A_8 \cong 1$, $A_{10} \cong 2000$ lb, $A_{11} \cong 0.1$, $A_{13} \cong 10^{-3}$, $\epsilon \cong 25$, $m_e \cong 2.5 \times \dot{w}_p$ were assumed. ($\dot{w}_p$ denotes the propellant weight flow rate.) No corrections were made for the additional exhaust skirts needed for proper expansion to the negligible outer pressures encountered throughout the region of operation.

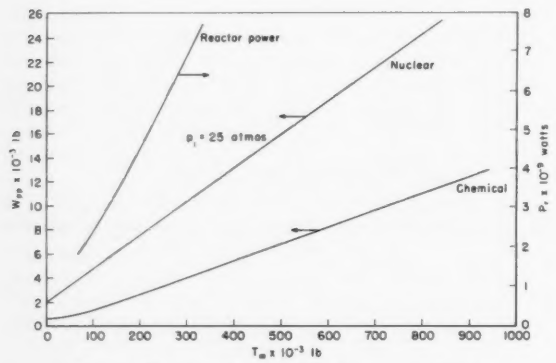

Fig. 3 Powerplant weight and power vs. thrust

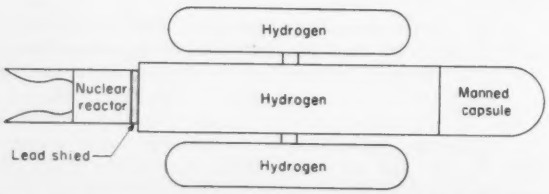

Fig. 4 Schematic model of spaceship considered (not to scale)

For the chemical powerplant an optimistic value of A_{17} = 0.016 and sea level and altitude specific impulses of 300 and 400 sec respectively were assumed. The estimate of the turbopump equipment required m_e is based on an assumed propellant tank pressurization of 30 psia, and a chamber pressure of about 500 psia. Fig. 3 shows the resultant weight-thrust characteristics of both powerplants at altitude, as well as the expected power output of the reactor as a function of powerplant thrust.

Shielding Considerations

Approximate theoretical considerations are employed to provide us with a rough idea of the order of magnitude of the shielding weights, since an exact analysis is beyond the scope of the present paper.

As is well known, the two components of reactor radiation which have to be attenuated through shielding are neutrons and gamma rays. The fact that the powered part of the flight will take place in a vacuum where scatter radiation is absent, enables one to limit the investigation to simple shadow shielding. A spaceship model, shown schematically in Fig. 4 is considered for the purpose of shielding requirement estimation. The two side propellant tanks are assumed to store the propellant for the outward leg of the journey, and could be dropped on the moon's surface prior to takeoff for the return trip. The major fuel tank, with its long column of hydrogen, serves as an excellent neutron attenuator, and a lead wall of appropriate thickness could take care of the gamma rays. The required amounts of the respective shieldings will of course depend on the power rating of the particular reactor employed, which in turn can be determined from the amount of thrust required for the lunar landing and takeoff portions of the powered flight. The required amount of attenuation depends also on the radiation dosages which one permits the crew to absorb. A maximum tolerated value of such a dose for the present mission could be about 25 rem per mission if one remembers that the AEC permissible continuous dose is 5 rem per yr, with occasional tolerated peak exposures up to 15 rem per yr. The calculations are simplified appreciably if one neglects the radiation buildup and decay during starting and shutdown of the reactor, and considers only the amount of radiation emitted during full power operation. Under this assumption, the permissible dose rate near the crew capsule is roughly

$$D_c/t_b \cong \dot{D}_c$$

where

D_c = radiation dose absorbed by crew capsule
$\dot{D}$ = time rate of change of dosage
t_b = time of full power operation of reactor

The powered flight portions are assumed to occur at both ends of the flight path, whereas at intermediate points the reactor is assumed shut down, and the vehicle subjected only to gravitational accelerations. The time t_b can be approximated roughly by

$$t_b = 2t_1 + 2t_2 \cong 4t_1 \qquad (t_2 \cong t_1)$$

where

t_1 = time needed for entry or departure from Earth's orbit
t_2 = time needed for landing or ascent at the moon

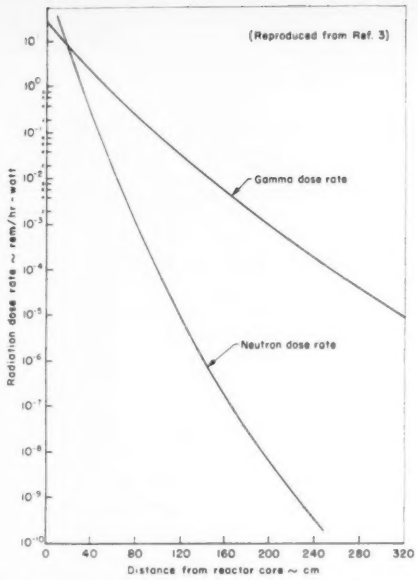

Fig. 5 Attenuation of neutrons and gamma rays in water

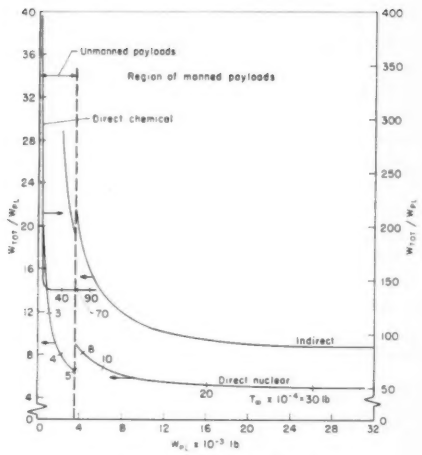

Fig. 6 Required weight ratios

A powerplant of, say, 150,000 lb thrust, can impart an initial deceleration of $a = 3g_E$ to a vehicle of mass (or weight) $W_i = 150{,}000/3.17 \cong 47{,}319$ lb. (The decimal portion 0.17 of the acceleration arises from the presence of the lunar gravitational field, which is taken to be of constant strength.) The total weight, W_{TOT}, needed at departure from Earth's orbit to bring 47,319 lb to the vicinity of the moon is found to be $W_{TOT} = W_i \cdot \exp\,[10{,}000/1110 \cdot 32.2] = 62{,}600$ lb so that $t_1 \cong 10{,}000 \cdot 62{,}600/150{,}000 \cdot 32.2 \cong 130$ sec. Similarly, to "kill" 9000 ft per sec at the moon with a deceleration of $3g_E$ takes about $t_2 \cong 9000/96.6 = 93$ sec, so that $t_b \cong 446$ sec.

As an extra measure of safety, a value of $t_b = 600$ sec is assumed. This value of reactor operation time limits the radiation dosage rate at the crew capsule to a maximum of approximately 150 rem per hr. The attenuation which can be achieved by means of a water shield is pointed out in (3), and the pertinent results are reproduced here for convenience in Fig. 5. If one assumes the radiation attenuation through liquid hydrogen to be similar to the one through water, it would seem that about 200 cm of H_2 would suffice for neutron attenuation. The lead shadow shield needed for gamma attenuation could be circular in shape and of radius equal to the lateral dimension of the reactor used. For the assumed thrust level, a cylindrical reactor might have an outside radius of about 28 to 30 in., which would lead to a lead shield weight of about 11,000 to 13,000 lb. Now for a payload of, say, 10,000 lb, the main propellant tank might have a length of about 20 to 25 m, which would drastically reduce the amount of radiation, both of gamma rays as well as of neutrons, that would reach the crew compartment. This favorable circumstance would permit us to reduce the amount of lead shadow shielding required. A maximum value of 2000 lb is assumed for this shield.

The main propellant tank is supposed to serve also as a structural member and carry all the inertial loads imposed on it during periods of acceleration. At an internal pressure of 30 psia one can approximate the tankage weight to be 8 per cent of the weight of the contained propellant.

Having calculated or assumed the magnitudes of most of the important factors, it is now possible to calculate the weights required for a complete round trip mission, and thus compare the relative merits of the various schemes.

Conclusions

The results of the calculations are presented in Fig. 6 which shows the ratio of required starting weight to payload weight for all the values of payload weights considered. It is hoped that in spite of the many assumptions made, the results might still be fairly representative for purposes of comparison. It is seen that weight savings of about 50 per cent could be achieved if the direct nuclear scheme is selected in preference to the mixed powerplant transfer. This is a sizable saving considering that anywhere from 40 to 1000 lb are needed on the ground to place 1 lb into an Earth orbit. The direct chemical missions are seen to require excessively high starting weights. We have picked a weight of 3500 lb as the smallest possible weight for a manned capsule. The absence of radiation shields for smaller payloads explains the break in the nuclear curves.

References

1 Lieske, H. A., "Lunar Trajectory Studies," The Rand Corp., Paper P-1293, Feb. 26, 1958.

2 Bussard, R. W. and R. D. DeLauer, "Nuclear Rocket Propulsion," McGraw-Hill Book Co., Inc., N. Y., 1958, Chap. 3.

3 Fraas, A. P., "Aircraft Design Considerations Associated with Shielding for Aircraft Nuclear Power Plants," IAS, Preprint No. 644, June 1956.

Some Exact Solutions of the Equations of Motion of a Solar Sail With Constant Sail Setting

HOWARD S. LONDON[1]

United Aircraft Corp., East Hartford, Conn.

THE EQUATIONS of motion of a solar sail admit to some simple solutions in the case of constant sail setting due to the fact that solar radiation pressure varies inversely as the square of the radial distance from the sun. Logarithmic spiral trajectories are one such class of solutions; the range of values of spiral angle ψ and sail setting θ for which these solutions exist depends upon the value of α, the acceleration due to radiation pressure for radial sail setting ($\theta = 0$) at Earth's orbit. Conic sections are another set of solutions, corresponding to the particular case of radial sail setting.

Logarithmic Spiral Solutions

In a recent article (1),[2] logarithmic spiral solutions were obtained from the approximate equations of motion which result when the radial acceleration $\ddot{r}$ is neglected. However, logarithmic spiral solutions can be deduced without making this approximation, and the results apply to a much larger range of values of ψ and α; these results reduce exactly to those of (1) for spiral angles ψ sufficiently small so that $\psi \approx \sin \psi \approx \tan \psi$.

The analysis used herein is analogous to that of (2) in which the author stipulated a logarithmic spiral trajectory for a vehicle in an inverse-square gravitational field and then showed in the case of tangential thrust that such a trajectory would be obtained if the thrust-to-mass ratio of the vehicle is varied as $1/r^2$. Since radiation pressure varies as $1/r^2$, it is not at all surprising that the exact equations of motion of the solar sail should have logarithmic spiral solutions.

The equations of motion of the solar sail as given in (1) are,

Received July 20, 1959.

[1] Research Engineer, Research Laboratories. Member ARS.

[2] Numbers in parentheses indicate References at end of paper.

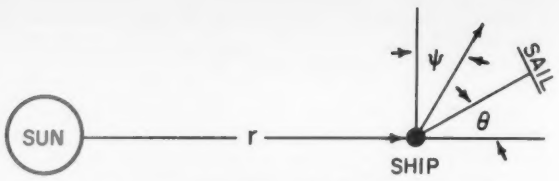

Fig. 1 Spiral angle and sail setting

in slightly different notation

$$(-a_0 + \alpha \cos^3 \theta)(r_0/r)^2 = \ddot{r} - r\dot{\phi}^2 \qquad [1]$$

$$\alpha \sin \theta \cos^2 \theta (r_0/r)^2 = r\ddot{\phi} + 2\dot{r}\dot{\phi} \qquad [2]$$

where

r, ϕ = polar coordinates, with the origin at the center of the sun
r_0 = mean distance of Earth from sun
a_0 = sun's gravitational acceleration at Earth's orbit = 0.592 cm/sec²

The equation of a logarithmic spiral is

$$r = r_0 e^{\phi \tan \psi} \qquad [3]$$

The sail setting and spiral angle are shown in Fig. 1.

Equation [3] is substituted into Equations [1 and 2] and $\ddot{\phi}$ is eliminated, giving

$$e^{3\phi \tan \psi}\, \dot{\phi}^2 = \frac{\cos^2 \psi}{r_0} [a_0 - \alpha \cos^2 \theta (\cos \theta - \tan \psi \sin \theta)] \qquad [4]$$

Differentiation of Equation [4] with respect to time yields

$$\ddot{\phi} = -(3/2)\dot{\phi}^2 \tan \psi \qquad [5]$$

Substitution of Equations [4 and 5] back into the equations of motion gives

$$\frac{\sin \psi \cos \psi}{2} \left[\frac{a_0}{\alpha} - \cos^2 \theta (\cos \theta - \tan \psi \sin \theta)\right] = \sin \theta \cos^2 \theta \qquad [6]$$

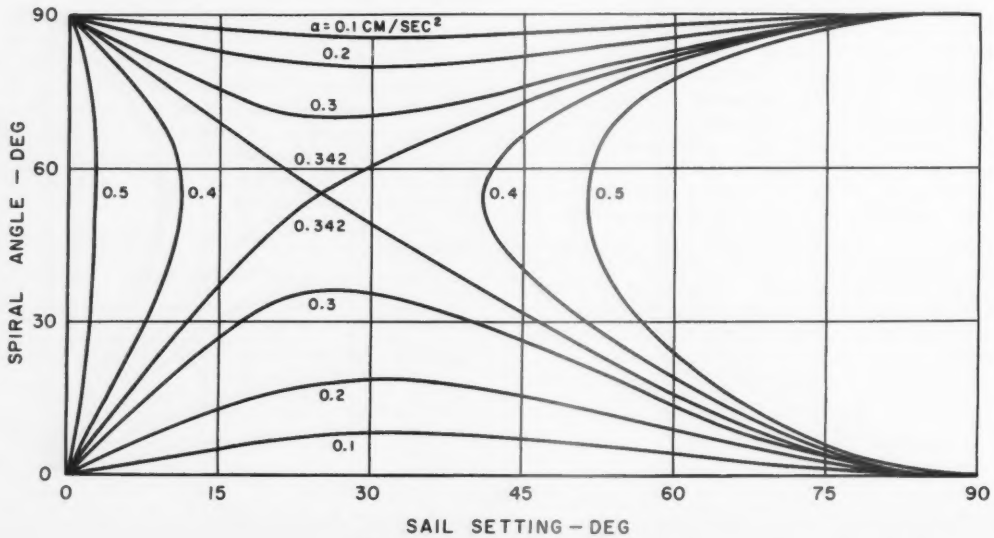

Fig. 2 Spiral angle vs. θ and α

or finally

$$\frac{\sin \psi \cos \psi}{2 - \sin^2 \psi} = \frac{\sin \theta \cos^2 \theta}{(a_0/\alpha) - \cos^3 \theta} \qquad [7]$$

Equation [7] was solved graphically for several values of α, and the results are shown in Fig. 2. For values of α less than 0.342 cm per sec^2, these solutions have upper and lower branches corresponding to large and small values of ψ, respectively; the approximate solution of (1) predicts only the lower branch curves. If α is greater than 0.342 cm per sec^2 there are also two branches, but now all values of ψ are admissible, whereas for each value of α there is an intermediate range of values of θ for which there are no solutions. The solution of (1), on the other hand, simply gives curves which are of the same form as the lower branch curves for smaller values of α. For values of ψ small enough so that $\psi \approx \sin \psi \approx \tan \psi$, Equation [7] reduces exactly to Equation [13] of (1), and the solutions are identical for all values of α.

The time of flight is obtained straightforwardly. Equation [4] is written in the form

$$\dot{\phi} = e^{-3/2\,\phi \tan \psi} \cos \psi \sqrt{\frac{a_0 - \alpha \cos^2 \theta\,(\cos \theta - \tan \psi \sin \theta)}{r_0}}$$

$$= r^{-3/2} r_0 \cos \psi \sqrt{a_0 - \alpha \cos^2 \theta\,(\cos \theta - \tan \psi \sin \theta)} \qquad [8]$$

Since, from Equation [3]

$$\dot{r} = r_0 \dot{\phi} \tan \psi\, e^{\phi \tan \psi} = r \dot{\phi} \tan \psi \qquad [9]$$

it follows that

$$\dot{r} = r^{-1/2} r_0 \sin \psi \sqrt{a_0 - \cos^2 \theta\,(\cos \theta - \tan \psi \sin \theta)} \qquad [10]$$

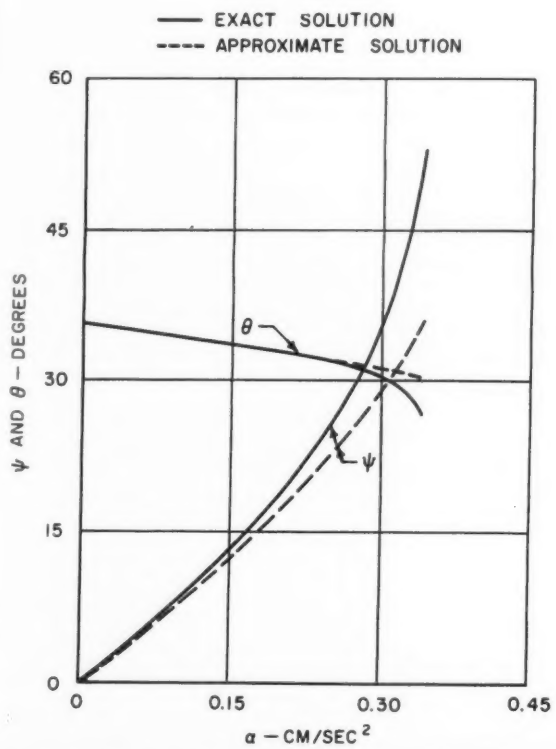

Fig. 3 Spiral angle and sail setting for lower branch minimum-time spirals

Substituting Equation [6] into Equation [10] and then integrating, the result is

$$t = \sqrt{\frac{2}{\alpha}} \frac{1}{3} \frac{(r^{3/2} - r_0^{3/2})}{r_0} \sqrt{\frac{\cot \psi}{\sin \theta \cos^2 \theta}} \qquad [11]$$

The minimum flight time is determined for each value of α by setting $dt/d\theta = 0$, and solving the resulting equation simultaneously with the graphical results of Equation [7]. For values of α greater than 0.342 cm per sec^2, the only solution is the "trivial" solution: $\psi = 90$ deg and $\theta = 0$, i.e., a radial flight path. For values of α less than 0.342 cm per sec^2, there is always a solution corresponding to a point on the lower branch curve of Fig. 2 as well as the radial flight path solution; the flight time on this lower branch spiral is, of course, greater than on the upper branch spiral for the same sail setting. Since, however, the initial velocity required increases rapidly with the spiral angle, the optimum solutions on the lower branch curves are of greatest interest. The optimum spiral angle and the required sail setting are plotted in Fig. 3 as a function of α; the approximate results of (1) are also shown for comparison.

The flight times calculated for a given spiral angle ψ from Equation [11] differ from those given in (1) only in the relationship between ψ and θ; the time differences for the lower branch curves are small, and the results of (1) are sufficient.

It is important to note that a logarithmic spiral of flight path angle ψ does not automatically result if the sail is set at an angle θ corresponding to a solution of Equation [7]; the magnitudes of the velocity components must initially be equal to those given by Equations [8 and 10].

Conic Sections

If the sail setting is radial, i.e., $\theta = 0$, the equations of motion reduce to

$$\ddot{r} - r\dot{\phi}^2 = (\alpha - a_0)(r_0/r)^2 \qquad [12]$$

$$(d/dt)(r^2\dot{\phi}) = 0 \qquad [13]$$

Equations [12 and 13] are exactly the same as the equations of ballistic motion of a vehicle in the gravitational field of a body whose gravitational constant is $(\alpha - a_0)r_0^2$. Therefore, with radial sail setting, the solar sail in effect simply reduces the value of the sun's gravitational constant $\mu = a_0 r_0^2$ to a value $\mu' = \mu(1 - \alpha/a_0)$. Since the solutions of the equations of ballistic motion in an inverse-square central force field are known to be conic sections, it follows that solar sail trajectories will also be conics if the sail setting is always radial. The eccentricity e and semimajor axis q of these conics are given by

$$e = \sqrt{1 + \frac{2[(V_0^2/2) - (\mu'/r_0)]L^2}{\mu'^2}} \qquad [14]$$

and

$$q = \frac{\mu'}{2\left|\frac{V_0^2}{2} - \frac{\mu'}{r_0}\right|} \qquad [15]$$

where

L = angular momentum
V_0 = initial helicentric velocity of the vehicle

For simplicity, consider the case where the initial velocity is normal to the radial direction, so that $L = r_0 V_0$. The resulting formulas are

$$e = \frac{\mu}{\mu'}\left(\frac{V_0^2}{V_e}\right) - 1 = \frac{1}{(1 - \alpha/a_0)}\left(\frac{V_0}{V_e}\right)^2 - 1 \qquad [16]$$

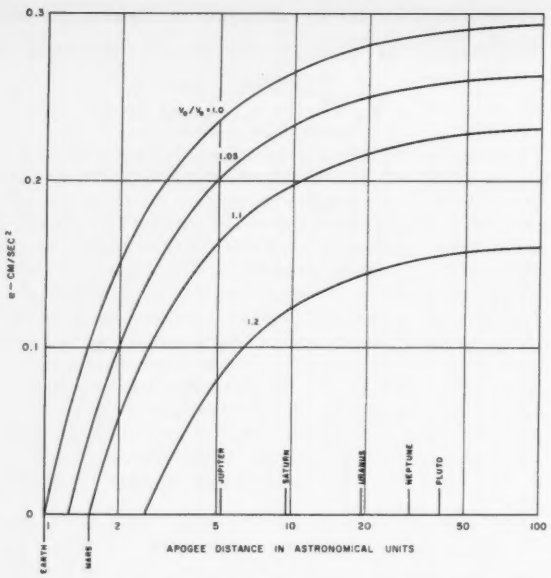

Fig. 4 Value of α required for cotangential transfer with radial sail setting

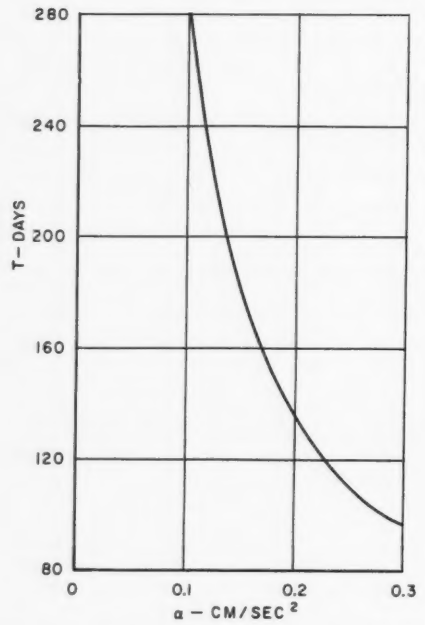

Fig. 5 Trip time to Mars with radial sail setting, $V_0/V_e = 1.0$

and

$$q = \frac{r_0}{\left|\left(\frac{V_0}{V_e}\right)^2 \frac{1}{(1 - \alpha/a_0)} - 2\right|} \qquad [17]$$

where V_e is the Earth's mean orbital velocity. Such trajectories are bounded (i.e., elliptical) if $e < 1$, and are not bounded (i.e., parabolic or hyperbolic) if $e \geq 1$; it follows therefore from Equation [16] that for $V_0/V_e = 1.0$ the vehicle will escape the solar system if $\alpha/a_0 \geq 1/2$.

As an example of the practical application of these conic trajectories, consider a transfer from Earth's orbit at r_0 to the circular orbit of another planet at r_1 (where $r_1 > r_0$) on an ellipse which is tangential to both orbits, i.e., the analogy of the ballistic Hohmann transfer. The requirement is that $2q = r_1 + r_0$; the required value of α can then be calculated from Equation [17]. Fig. 4 gives the value of α required as a function of r_1/r_0 and V_0/V_e. It is seen that an α of 0.1 cm per sec² is required for a cotangential transfer to Mars if $V_0/V_e = 1.0$; for sail mass per unit area of 2×10^{-4} gm per cm², this would correspond to total sail weight of about 22 per cent of the vehicle gross weight. Since the period of revolution on an elliptical orbit varies as $1/\sqrt{\mu'}$, the transfer time is $1/\sqrt{1 - \alpha/a_0}$ times as great as the transfer time on a ballistic Hohmann transfer. Therefore, the cotangential transfer to Mars would take 286 days, as compared to 259 days on the ballistic Hohmann transfer and about 247 days on the optimum logarithmic spiral ($\psi = 8.5$ deg) for $\alpha = 0.1$ cm per sec².

Faster trips can be made with radial sail setting if α is in excess of that required for cotangential transfer. The flight time to Mars is plotted vs. α in Fig. 5 for the case $V_0/V_e = 1.0$ and the initial velocity tangential to Earth's heliocentric orbit. The vehicle's velocity upon arrival at Mars is, of course, not tangential to the Mars orbit for $\alpha > 0.1$ cm per sec².

In comparing the spiral and conic section trajectories, it should be noted that a velocity increment at Earth's orbit is necessary in order to satisfy the initial conditions required to start the vehicle on a logarithmic spiral. For example, the optimum spiral of 8.5 deg for $\alpha = 0.1$ cm per sec² requires a velocity increment at Earth's orbit of about 15,000 fps, whereas no initial velocity increment is required for the cotangential transfer ellipse. On the other hand, since angular momentum is constant for radial sail setting, the apogee velocity on the cotangential ellipse is $(\sqrt{r_0/r_1})(V_0/V_e)$ times the local planet velocity, so that for V_0/V_e close to 1.0 a substantial increment in velocity would be required at the apogee to reduce the speed relative to the planet to zero. In general, then, neither the logarithmic spiral nor the conic section solution is optimum; other types of trajectories are undoubtedly necessary to utilize the sail most efficiently.

References

1 Tsu, T. C., "Interplanetary Travel by Solar Sail," ARS JOURNAL, vol. 29, no. 6, June 1959, pp. 422–427.

2 Bacon, R. H., "Logarithmic Spiral: An Ideal Trajectory for the Interplanetary Vehicle with Engines of Low Sustained Thrust," *Amer. J. Phys.*, vol. 27, no. 3, March 1959, pp. 164–165.

Hypervelocity Glider at Large Angles of Inclination

W. H. T. LOH[1]

National Science Foundation, Washington, D. C.

RESULTS on hypervelocity gliders, either from boost-glide or orbital re-entry, at small angles of inclination and constant lift/drag ratio were obtained recently in (1,2,3).[2] Results on hypervelocity gliders at large but constant angle of inclination and constant lift/drag ratio were treated approximately in (4). Because of the theoretical noncompatibility of assuming both constant angle of inclination and constant lift/drag ratio, the results obtained in (4), as pointed out there, are valid only in a region where the variation of lift/drag ratio is nearly a constant. This region usually exists in the middle portion of the re-entry trajectory. Since general results are sometimes desirable for constant lift/drag ratio at large but variable angles of inclination, the present note is written.

At large inclination angles, the differential equation(4)[3] is

$$\frac{dV^2}{ds} + \left[\frac{d\theta}{ds} - \frac{\cos\theta}{r}\right]\frac{2}{(L/D)}V^2 + \frac{2g}{(L/D)}\left[\cos\theta - \frac{L}{D}\sin\theta\right] = 0$$

which can be rewritten as

$$\frac{dV^2}{ds} + \frac{2}{(L/D)}V^2\left(\frac{d\theta}{ds}\right) + \frac{2g\cos\theta}{(L/D)}\left[1 - \frac{V^2}{gr}\right] - 2g\sin\theta = 0 \quad [1]$$

For high speed re-entry, the third term of Equation [1] is usually relatively small; consequently, it may be neglected. Based on this simplification alone, the solutions on instantaneous velocity, altitude, distance along flight path, range, deceleration, maximum deceleration, time rate and maximum time rate of average and local stagnation region heat transferred into vehicle, total heat transferred into vehicle and time of flight may easily be solved, in a similar manner as presented in (1), for re-entry at large angles of inclination, as follows:

1 Flight velocity

$$V^2 = V_f^2[C_{13}F_1(\theta) + C_{14}e^{C_1(\theta - \theta)}]$$

2 Flight altitude

$$y = -\frac{1}{\beta}\ln\left[e^{-\beta y_f} + C_4(\cos\theta_f - \cos\theta)\right]$$

3 Flight distance along flight path: When $C_3^2 > \beta^2$

$$s = \frac{2}{\sqrt{C_3^2 - \beta^2}}\left[\tan^{-1}\sqrt{\frac{C_3+\beta}{C_3-\beta}}\tan\left(\frac{\theta}{2}\right) - \tan^{-1}\sqrt{\frac{C_3+\beta}{C_3-\beta}}\tan\left(\frac{\theta_f}{2}\right)\right]$$

When $C_3^2 < \beta^2$

$$s = \frac{1}{\sqrt{\beta^2 - c_3^2}} \times \ln\left\{\left[\frac{C_3\cos\theta + \sqrt{\beta^2 - C_3^2}\sin\theta - \beta}{C_3\cos\theta_f + \sqrt{\beta^2 - C_3^2}\sin\theta_f - \beta}\right]\left[\frac{C_3 - \beta\cos\theta_f}{C_3 - \beta\cos\theta}\right]\right\}$$

4 Flight range

$$R = \frac{1}{\beta}(C_3 s - \theta)$$

5 Flight deceleration and maximum deceleration[4]

$$\left(\frac{dV}{dt}\right) = -\frac{V_f^2}{2}\left[C_2\left(\frac{\rho_f}{\rho_0}\right) + \beta C_1(\cos\theta_f - \cos\theta)\right][C_{13}F_1(\theta) + C_{14}e^{-C_1(\theta - \theta_f)}] + g\sin\theta$$

$$\left(\frac{dV}{dt}\right)_{\max} \cong -\frac{V_f^2}{2}\left[C_2\left(\frac{\rho_f}{\rho_0}\right) + \beta C_1(\cos\theta_f - \cos\theta_1)\right]e^{-C_1(\theta_1 - \theta_f)}$$

$$\theta_1 = \theta_{\left(\frac{dV}{dt}\right)_{\max}} \cong \cos^{-1}\left[\frac{C_1^2C_3 - \sqrt{C_1^2(\beta^2 - C_3^2) + \beta^2}}{\beta(C_1^2 + 1)}\right]$$

6 Time rate and maximum time rate of average heat input per unit area

$$\left(\frac{dH_{av}}{dt}\right) = (C_8 - C_9\cos\theta)[C_{13}F_1(\theta) + C_{14}e^{C_1(\theta_f - \theta)}]^{3/2}$$

$$\left(\frac{dH_{av}}{dt}\right)_{\max} \cong (C_8 - C_9\cos\theta_2)e^{-3/2C_1(\theta_2 - \theta_f)}$$

$$\theta_2 = \theta_{\left(\frac{dH_{av}}{dt}\right)_{\max}} \cong \cos^{-1}\left\{\frac{C_1^2C_3 - \frac{2}{3}\sqrt{C_1^2(\beta^2 - C_3^2) + \left(\frac{2}{3}\beta\right)^2}}{\beta\left[C_1^2 + \left(\frac{2}{3}\right)^2\right]}\right\}$$

7 Time rate and maximum time rate of local stagnation region heat input per unit area[4]

$$\left(\frac{dHs}{dt}\right) = C_{12}(C_{10} - C_{11}\cos\theta)^{1/2}[C_{13}F_1(\theta) + C_{14}e^{C_1(\theta_f - \theta)}]^{3/2}$$

$$\left(\frac{dHs}{dt}\right)_{\max} \cong C_{12}(C_{10} - C_{11}\cos\theta_3)^{1/2}e^{-3/2C_1(\theta_3 - \theta_f)}$$

$$\theta_3 = \theta_{\left(\frac{dHs}{dt}\right)_{\max}} \cong \cos^{-1}\left\{\frac{C_1^2C_3 - \frac{1}{3}\sqrt{C_1^2(\beta^2 - C_3^2) + \left(\frac{1}{3}\beta\right)^2}}{\beta\left[C_1^2 + \left(\frac{1}{3}\right)^2\right]}\right\}$$

8 Total aerodynamic heat input to the vehicle from the beginning to the point concerned

$$Q \cong \int_{\theta_f}^{\theta}\frac{C_5 - C_6\cos\theta}{C_3 - \beta\cos\theta}e^{-C_1(\theta - \theta_f)}\,d\theta$$

9 Flight time

$$t = C_7\int_{\theta_f}^{\theta}[C_{13}F_1(\theta) + C_{14}e^{C_1(\theta_f - \theta)}]^{-1/2}\frac{d\theta}{(C_3 - \beta\cos\theta)}$$

The last two expressions can easily be integrated by graphical means. For high speed re-entry, except in the terminal phase of flight, the gravity term may sometimes be neglected. In such cases, C_{13} and C_{14} become 0 and 1, respectively, and the

Received June 23, 1959.

[1] Senior Post Doctoral Fellow, Manchester University, England.

[2] Number in parentheses indicate References at end of paper.

[3] Other assumptions are the same as those given in (1).

[4] Minor terms are neglected in the derivation.

foregoing equations are all reduced to the simple results that are useful approximately.

Nomenclature

A = reference area for lift and drag expressions
C_D = drag coefficient
C'_F = equivalent skin friction coefficient,

$$C'_F = \frac{1}{S}\int_S C_{F_l}\left(\frac{\rho_l}{\rho}\right)\left(\frac{V_l}{V}\right)dS$$

C_F = skin friction coefficient
D = drag, lb
g = acceleration due to force of gravity, ft/sec^2
H = convective heat transferred per unit area
L = lift, lb
m = mass of the vehicle
r = distance of glider measured from center of earth, ft.; when altitude of the glider is small in comparison with Earth radius, r may be taken approximately as r_0
r_0 = radius of Eart , ft
Q = convective heat transferred
R = range, ft
s = distance along flight path, ft
S = surface area
t = time, sec
V = velocity, ft/sec
ρ = air density
θ = angle of inclination or angle of flight path to local Earth horizontal, degrees
σ = nose or leading edge radius of body or wing
β = constant in density–altitude relation $\rho = \rho_0 e^{-\beta y}$. Here ρ_0 = reference density = 0.0034 slug/ft,^{3} β = (1/22,000) ft^{-1} and y = altitude

C_1 = constant = $2(D/L)$
C_2 = constant = $(C_D\rho_0 A/m)$

$$C_3 = \text{constant} = \beta\cos\theta_f + \frac{C_D A\rho_f(L/D)}{2m} \cong \beta$$

C_4 = constant = $\beta\,(C_1/C_2)$
C_5 = constant = $(1/4)\,C'_F S V_f^2 e^{C_1\theta_f}\,[\rho_f + C_4\rho_0\cos\theta_f]$
C_6 = constant = $(1/4)\,C'_F S C_4\rho_0 V_f^2 e^{C_1\theta_f}$
C_7 = constant = $(1/V_f)$
C_8 = constant = $(1/4)C'_F(\rho_f + C_4\rho_0\cos\theta_f)V_f^3$
C_9 = constant = $(1/4)C'_F C_4\rho_0 V_f^3$
C_{10} = constant = $\rho_f + C_4\rho_0\cos\theta_f$
C_{11} = constant = $C_4\rho_0$
C_{12} = constant = $6.8\times 10^{-8}\,\sigma^{-1/2}V_f^3$
C_{13} = constant = $(4g/\beta V_f^2)$
C_{14} = constant = $1 - (4g/\beta V_f^2)F_1(\theta_f)$

$$C_{15} = \text{constant} = \frac{1}{2}\left\{\frac{[1+(\beta/C_3)^2][C_1^2+3^2]-6(\beta/C_3)^2}{(C_1^2+1)(C_1^2+3^2)}\right\} \cong \frac{1}{C_1^2+1} - \frac{3}{(C_1^2+1)(C_1^2+3^2)}$$

$$C_{16} = \text{constant} = \frac{\beta}{2C_3(C_1^2+2^2)} \cong \frac{1}{2(C_1^2+2^2)}$$

$$C_{17} = \text{constant} = \left(\frac{\beta}{2C_3}\right)^2\left(\frac{1}{C_1^2+3^2}\right) \cong \frac{1}{2}\left(\frac{1}{C_1^2+3^2}\right),$$

$$F_1(\theta) = \frac{\beta}{C_3}\left\{C_{15}[C_1\sin\theta - \cos\theta] + C_{16}\left[\frac{1}{2}C_1\sin 2\theta - \cos 2\theta\right] - C_{17}\sin^2\theta(C_1\sin\theta - 3\cos\theta)\right\},$$ preferable to use when θ is large

$$F_1(\theta) = \left[\ln\left(\frac{\theta}{2}\right) + (C_1\theta) + \left(\frac{C_1\theta}{2}\right)^2 + \frac{1}{18}(C_1\theta)^3\right]e^{-C_1\theta} - \left[\frac{\theta^3}{720C_1} - \frac{\theta^2}{240C_1^2} + \left(\frac{1}{120C_1^3} + \frac{1}{12C_1}\right)\theta - \left(\frac{1}{120C_1^4} + \frac{1}{12C_1^2}\right)\right],$$ preferable to use when θ is small

Subscripts

e = condition at end of unpowered glide
f = condition at end of powered boost or condition at beginning of unpowered glide.
l = local conditions
s = stagnation conditions
av = average values
max = maximum values

References

1 Eggers, A. J. and Allen, H. J., "A Comparative Analysis of the Performance of Long Range Hypervelocity Vehicles," NACA TN 4046, Oct. 1957.

2 Gazley, C., "Deceleration and Heating of a Body Entering a Planetary Atmosphere From Space," Rand Corp. Rep. P-955, Feb. 18, 1957.

3 Chapman, D. R., "An Approximate Analytical Method for Studying Entry Into Planetary Atmospheres," NACA TN 4276, May 1958.

4 Loh, W. H. T., "Hypervelocity Vehicles at Large Angles of Inclination," ARS JOURNAL, vol. 29, no. 7, July 1959, pp. 522–523.

Gravitational Torque on a Satellite of Arbitrary Shape

RUSSELL A. NIDEY[1]

Ball Brothers Research Corp., Boulder, Colo.

The gravitational torque on a rigid nonsymmetrical body in a divergent field is normal to local vertical. The component of the torque in a given horizontal direction is essentially proportional to the product of inertia relative to the vertical and horizontal planes intersecting in the direction of interest. In an inverse square field the torque is also proportional to the inverse cube of the geocentric distance of the center of mass of the body. The necessary (but in general, insufficient) condition for the torque to vanish is for the principal moments of inertia to be equal. The torque on a stabilized body in orbit in general has a secular component.

A FINITE nonsymmetrical rigid body is subject to a gravitational torque of appreciable magnitude in proximity to a major planet. Schindler (1)[2] has derived the torque on a dumbbell in the gravitational field of the Earth. Sohn (2) gives a so-called general expression which is obtained only if the longitudinal principal moment of inertia is negligible in comparison to equal transverse principal moments of inertia. Roberson (3) derives the torque assuming an oblate spheroid by differentiating the potential function. The following alternate and considerably simpler derivation making use of vector analysis neglects the nonspherical distribution of mass in the Earth but is formulated for an arbitrary mass distribution in the satellite.

Consider a rigid system of particles where m_i is the mass of the ith particle: $i = 1, \ldots, N$. Let vector quantities be denoted by boldface characters and scalar quantities by the usual lightface characters. Define

- $\boldsymbol{R}_i$ as the position vector of the ith particle relative to the center of mass of the system of particles
- $\boldsymbol{W}_i$ as the instantaneous gravitational force on the particle
- $\boldsymbol{\varrho}_i$ as the position vector of the particle relative to the geocenter
- ρ_0 as the separation of the center of mass of the system of particles from the geocenter

Let $\boldsymbol{i}, \boldsymbol{j}, \boldsymbol{k}$, be unit vectors describing the right-hand x, y, z coordinate system about the center of mass with $\boldsymbol{k}$ in the direction of local vertical.

The gravitational torque on the system of particles $\boldsymbol{M}$ is then

$$\boldsymbol{M} = \sum_i \boldsymbol{R}_i \times \boldsymbol{W}_i \qquad [1]$$

where x represents the cross vector product and $(\cdot)$ will be later used to represent the scalar vector product. But

$$\boldsymbol{W}_i = -\frac{g\rho_g^2 m_i}{\rho_i^3}\boldsymbol{\varrho}_i \qquad [2]$$

where g is the acceleration of gravity at the geocentric radius ρ_g and

$$\boldsymbol{\varrho}_i = \rho_0\boldsymbol{k} + \boldsymbol{R}_i \qquad [3]$$

Thus

$$\boldsymbol{R}_i \times \boldsymbol{\varrho}_i = \boldsymbol{\varrho}_0(\boldsymbol{R}_i \times \boldsymbol{k}) + (\boldsymbol{R}_i \times \boldsymbol{R}_i) = \rho_0(\boldsymbol{R}_i \times \boldsymbol{k}) \qquad [4]$$

Moreover

$$\begin{aligned}\rho_i^{-3} &= (\boldsymbol{\varrho}_i \cdot \boldsymbol{\varrho}_i)^{-3/2} \\ &= [(\rho_0\boldsymbol{k} + \boldsymbol{R}_i)\cdot(\rho_0\boldsymbol{k} + \boldsymbol{R}_i)]^{-3/2} \\ &= \rho_0^{-3}\left[1 + \left(\frac{\boldsymbol{R}_i}{\rho_0}\right)\cdot\left(\frac{\boldsymbol{R}_i}{\rho_0}\right) + 2\left(\frac{\boldsymbol{R}_i}{\rho_0}\right)\cdot\boldsymbol{k}\right]^{-3/2} \\ &\approx \rho_0^{-3}\left[1 - 3\left(\frac{\boldsymbol{R}_i}{\rho_0}\right)\cdot\boldsymbol{k}\right]\end{aligned} \qquad [5]$$

since $(R_i/\rho_0) \ll 1$ for any practical artificial satellite.

Hence

$$\begin{aligned}\boldsymbol{M} &= -g\rho_g^2 \sum_i \frac{m_i}{\rho_i^3}\boldsymbol{R}_i \times \boldsymbol{\varrho}_i \\ &\approx -\frac{g\rho_g^2}{\rho_0^2}\sum_i m_i\boldsymbol{R}_i\times\boldsymbol{k} + \frac{3g\rho_g^2}{\rho_0^3}\sum_i m_i(\boldsymbol{R}_i\times\boldsymbol{k})(\boldsymbol{R}_i\cdot\boldsymbol{k})\end{aligned} \qquad [6]$$

General Equation

But

$$\sum_i m_i\boldsymbol{R}_i = 0$$

defines the center of mass. Consequently

$$\boldsymbol{M} \approx 3\omega^2 \sum_i m_i(\boldsymbol{R}_i\times\boldsymbol{k})(\boldsymbol{R}_i\cdot\boldsymbol{k}) \qquad [7]$$

where $\omega^2 \equiv (g\rho_g^2/\rho_0^3)$. ω is numerically equal to the geocentric angular velocity of the satellite if the orbit is circular.

The magnitude of the x component of $\boldsymbol{M}$ is

$$\begin{aligned}\boldsymbol{M}\cdot\boldsymbol{i} &= 3\omega^2\sum_i m_i(\boldsymbol{R}_i\times\boldsymbol{k}\cdot\boldsymbol{i})(\boldsymbol{R}_i\cdot\boldsymbol{k}) \\ &= 3\omega^2\sum_i m_i(\boldsymbol{R}_i\cdot\boldsymbol{j})(\boldsymbol{R}_i\cdot\boldsymbol{k}) \\ &= -3\omega^2 I_{yz}\end{aligned} \qquad [8]$$

where $I_{yz} = -\sum_i m_i y_i z_i$, since

$$(\boldsymbol{R}_i\times\boldsymbol{k}\cdot\boldsymbol{i}) = (\boldsymbol{R}_i\cdot\boldsymbol{k}\times\boldsymbol{i}) = (\boldsymbol{R}_i\cdot\boldsymbol{j})$$

$$\boldsymbol{R}_i\cdot\boldsymbol{j} = y_i$$

$$\boldsymbol{R}_i\cdot\boldsymbol{k} = z_i$$

Similarly

$$\boldsymbol{M}\cdot\boldsymbol{j} = -3\omega^2\sum_i m_i(\boldsymbol{R}_i\cdot\boldsymbol{i})(\boldsymbol{R}_i\cdot\boldsymbol{k}) = +3\omega^2 I_{xz} \qquad [9]$$

and

$$\boldsymbol{M}\cdot\boldsymbol{k} = 0 \qquad [10]$$

Hence $\boldsymbol{M}$ is normal to local vertical.

The products of inertia can however be expressed in terms of the principal moments of inertia and direction cosines. Let $\boldsymbol{I}, \boldsymbol{J}, \boldsymbol{K}$ be a right-handed orthogonal set of unit position vectors with origin on the center of mass and co-linear with the three principal moment of inertia axes.

Then

$$\boldsymbol{j} = (\boldsymbol{j}\cdot\boldsymbol{I})\boldsymbol{I} + (\boldsymbol{j}\cdot\boldsymbol{J})\boldsymbol{J} + (\boldsymbol{j}\cdot\boldsymbol{K})\boldsymbol{K} \qquad [11]$$

$$\boldsymbol{k} = (\boldsymbol{k}\cdot\boldsymbol{I})\boldsymbol{I} + (\boldsymbol{k}\cdot\boldsymbol{J})\boldsymbol{J} + (\boldsymbol{k}\cdot\boldsymbol{K})\boldsymbol{K} \qquad [12]$$

$$\begin{aligned}(\boldsymbol{R}_i\cdot\boldsymbol{j})(\boldsymbol{R}_i\cdot\boldsymbol{k}) = {} & (\boldsymbol{j}\cdot\boldsymbol{I})(\boldsymbol{k}\cdot\boldsymbol{I})[(\boldsymbol{R}_i\cdot\boldsymbol{I})^2 - (\boldsymbol{R}_i\cdot\boldsymbol{K})^2] + \\ & (\boldsymbol{j}\cdot\boldsymbol{J})(\boldsymbol{k}\cdot\boldsymbol{J})[(\boldsymbol{R}_i\cdot\boldsymbol{J})^2 - (\boldsymbol{R}_i\cdot\boldsymbol{K})^2] + \\ & [(\boldsymbol{j}\cdot\boldsymbol{I})(\boldsymbol{k}\cdot\boldsymbol{J}) + (\boldsymbol{k}\cdot\boldsymbol{I})(\boldsymbol{j}\cdot\boldsymbol{J})](\boldsymbol{R}_i\cdot\boldsymbol{I})(\boldsymbol{R}_i\cdot\boldsymbol{J}) + \\ & [(\boldsymbol{j}\cdot\boldsymbol{I})(\boldsymbol{k}\cdot\boldsymbol{K}) + (\boldsymbol{k}\cdot\boldsymbol{I})(\boldsymbol{j}\cdot\boldsymbol{K})](\boldsymbol{R}_i\cdot\boldsymbol{I})(\boldsymbol{R}_i\cdot\boldsymbol{K}) + \\ & [(\boldsymbol{j}\cdot\boldsymbol{J})(\boldsymbol{k}\cdot\boldsymbol{K}) + (\boldsymbol{k}\cdot\boldsymbol{J})(\boldsymbol{j}\cdot\boldsymbol{K})](\boldsymbol{R}_i\cdot\boldsymbol{J})(\boldsymbol{R}_i\cdot\boldsymbol{K})\end{aligned} \qquad [13]$$

Received Aug. 17, 1959.

[1] Staff Scientist and member of the Senior Staff; present address AURA, Inc., Tucson, Ariz. Member ARS.

[2] Numbers in parentheses indicate References at end of paper.

since

$$(j\cdot k) = (j\cdot I)(k\cdot I) + (j\cdot J)(k\cdot J) + (j\cdot K)(k\cdot K) = 0 \quad [14]$$

Hence

$$\begin{aligned} I_{ys} &= -(j\cdot I)(k\cdot I)\sum_i m_i[(R_i\cdot I)^2 - (R_i\cdot K)^2] - \\ &\quad (j\cdot J)(k\cdot J)\sum_i m_i[(R_i\cdot J)^2 - (R_i\cdot K)^2] \\ &= -(j\cdot I)(k\cdot I)(I_3 - I_1) - (j\cdot J)(k\cdot J)(I_3 - I_2) \end{aligned} \quad [15]$$

where

$$\begin{aligned} I_3 &= \sum_i m_i[(R_i\cdot I)^2 + (R_i\cdot J)^2] \\ I_2 &= \sum_i m_i[(R_i\cdot I)^2 + (R_i\cdot K)^2] \\ I_1 &= \sum_i m_i[(R_i\cdot J)^2 + (R_i\cdot K)^2] \end{aligned}$$

are the principal moments of inertia since the product of inertias relative to the principal planes necessarily vanishes. Similarly

$$I_{zs} = -(i\cdot I)(k\cdot I)(I_3 - I_1) - (i\cdot J)(k\cdot J)(I_3 - I_2) \quad [16]$$

Hence Equations [8, 9 and 10] can be consolidated as

$$\begin{aligned} M = {} & 3\omega^2[(j\cdot I)(k\cdot I)(I_3 - I_1) + \\ & (j\cdot J)(k\cdot J)(I_3 - I_2)]i - 3\omega^2[(i\cdot I)(k\cdot I)(I_3 - I_1) + \\ & (i\cdot J)(k\cdot J)(I_3 - I_2)]j \end{aligned} \quad [17]$$

Note that if $I_3 = I_2 = I_1$ the torque vanishes subject to the approximation used in Equation [5]. The neglected terms constitute higher order products of inertia which must likewise vanish if the torque is to be truly zero. However, for all practical purposes (that is, to an accuracy of the order of one part in 10^6) equality of the principal moments of inertia is a sufficient as well as necessary condition for the torque to vanish.

Body of Revolution

If $I_2 = I_1$ as with a body of revolution such as a rocket airframe or a flywheel satellite the transverse principal axes are not unique. Hence i and I can arbitrarily be selected to be parallel so that $(i\cdot K) = 0$ and $(j\cdot K)i = -(k\times K)$. Hence

$$M = 3\omega^2\Delta I(k\cdot K)(k\times K) \quad [18]$$

where ΔI = longitudinal principal moment of inertia decreased by the transverse. Use has been made of Equation [14] and the corresponding relationship

$$(i\cdot k) = (i\cdot I)(k\cdot I) + (i\cdot J)(k\cdot J) + (i\cdot K)(k\cdot K) = 0 \quad [19]$$

Note that Equation [18] can be reconciled with the satellite expression given by Sohn (2) only if a circular orbit is assumed and if the longitudinal principal moment of inertia is neglected.

Average Torque

If a circular orbit is assumed, Equation [18] can be integrated over an entire orbit to obtain the time average. Define the right-handed orthogonal set of unit vectors $\mathbf{n}$, $\boldsymbol{\mu}$, ν where $\mathbf{n}$ is in the direction of ω and $\boldsymbol{\mu}$ is normal to K. Then

$$k = \sin\omega t\,\boldsymbol{\mu} - \cos\omega t\,\nu \quad [20]$$

$$\boldsymbol{\mu}\cdot K = 0 \quad [21]$$

Substituting in Equation [18], dividing by the orbit period and integrating over an orbit

$$\begin{aligned} (M)_{avg} &= (\omega/2\pi)\oint M\,dt \\ &= \frac{3\omega^2\Delta I}{2\pi}\oint \{[(\sin\omega t)\boldsymbol{\mu} - (\cos\omega t)\nu]\cdot K\} \times \\ &\quad \{[(\sin\omega t)\boldsymbol{\mu} - (\cos\omega t)\nu]\times K\}\,\omega dt \\ &= \frac{3\omega^2\Delta I}{2\pi}\Big[-(\nu\cdot K)(\boldsymbol{\mu}\times K)\oint(\cos\omega t)(\sin\omega t)\,\omega dt + \\ &\quad (\nu\cdot K)(\nu\times K)\oint(\cos^2\omega t)\,\omega dt\Big] \\ &= (3/2)\omega^2\Delta I(\nu\cdot K)(\nu\times K) \end{aligned} \quad [22]$$

or

$$(M)_{avg} = (3/4)\omega^2\,\Delta I\sin 2\beta|(M)_{avg}| \quad [23]$$

where β is the inclination of the longitudinal axis of the satellite to the orbital plane.

Conclusions

To prevent continual acquisition of angular momentum an inertially oriented satellite must either have equal principal moments of inertia or internal weights must be appropriately manipulated to null the gravitational torque. Conversely angular momentum can be ejected by interaction of the mass distribution within the satellite with the Earth's gravitational field as has been previously proposed by Princeton's Dr. Lyman Spitzer (4).

Though the torque given by Equations [17] or [18] is extremely small for a realistic satellite (of the order of 10^{-6} lb-ft) the cumulative effects of the secular term cannot be ignored.

References

1 Schindler, G. M., "On Satellite Librations," ARS JOURNAL, vol. 29, May 1959, pp. 368–370.

2 Sohn, R. L., "Attitude Stabilization by Means of Solar Radiation Pressure," ARS JOURNAL, vol. 29, May 1959, pp. 371–373.

3 Roberson, R. E., "Gravitational Torque on a Satellite Vehicle," J. Franklin Institute, vol. 265, Jan. 1958, pp. 13–22.

4 Spitzer, L., Verbal discourse during May 1959 Meeting of NASA Working Group on Orbiting Astronomical Observatories, Washington, D. C.

Perturbation Approach to the Effect of the Geomagnetic Field on a Charged Satellite

H. R. WESTERMAN[1]

Bell Telephone Laboratories, Inc., Whippany, N. J.

THE INVESTIGATION of the effect of the Earth's magnetic field on the orbit of a charged satellite, undertaken by Fain and Greer (1),[2] is interesting not only for the reason they suggest (dirigibility) but also because the charge may be acquired naturally (2).

It is possible to analyze part of the problem examined by Fain and Greer (circular orbit in the plane of the geomagnetic Equator) by a perturbation technique, and to obtain substantially the same results as they did on a computer. We write the Lagrangian of the system in MKS (meter-kilogram-second) units as

$$L = \frac{m}{2}[(\dot r)^2 + (r\dot f)^2] + \frac{mk}{r} + q\vec A\cdot\vec v \quad [1]$$

Received Aug. 17, 1959.

[1] Member of Technical Staff. Member ARS.

[2] Numbers in parentheses indicate References at end of paper.

where

m = mass of the satellite
$\dot{r}$ = radial velocity
$\dot{f}$ = "true anomaly"
k = product of the gravitational constant and the mass of the Earth
q = charge on the satellite
$\vec{v}$ = satellite's vector velocity
$\vec{A}$ = magnetic vector potential

$\vec{A}$ is given by

$$\vec{A} = \frac{\mu_0}{4\pi} \vec{M} \times \nabla \left(\frac{1}{r}\right) \qquad [2]$$

In Equation [2], $|\vec{M}|$ is the Earth's magnetic dipole moment whose value (3) is taken here to be 8.1×10^{22} amp-m^2.

If we let $r^2\dot{f} = p$, $r = 1/u$, and transform to f as the independent variable, we find the equations of motion derived from Equation [1] to be

$$\frac{d}{df}\left(p \frac{du}{df}\right) + pu - \frac{k}{p} + \alpha u^2 = 0 \qquad [3]$$

$$\frac{d}{df}(p - \alpha u) = 0 \qquad [4]$$

where $\alpha = q\mu_0 M/4\pi m$. We may write

$$p = p^0 + \alpha p' + \alpha^2 p'' + \ldots \qquad [5]$$

where p^0, p', . . . are functions (of f) yet to be determined. Similarly, let

$$u = u^0 + \alpha u' + \alpha^2 u'' + \ldots \qquad [6]$$

If the force exerted on the satellite by the magnetic field is small compared to the gravitational force, we need keep only the first few terms in the expansions of p and u. This is indeed true for the parameters used by Fain and Greer (1) in the case illustrated in their Fig. 1.

If we insert Equations [5 and 6] in Equations [3 and 4] and equate equal powers of α to zero, we get a series of equations which can be solved successively. For example

$$p^0 \frac{d^2u^0}{df^2} + \frac{dp^0}{df}\frac{du^0}{df} + p^0u^0 - \frac{k}{p^0} = 0$$

$$\frac{dp^0}{df} = 0$$

. . . . . [7]

and

$$p^0 \frac{d^2u'}{df^2} + p' \frac{d^2u^0}{df^2} + \frac{dp^0}{df}\frac{du'}{df} + \frac{dp'}{df}\frac{du^0}{df} + p^0u' +$$

$$p'u^0 + \frac{k}{(p^0)^2} p' + (u^0)^2 = 0$$

$$\frac{d}{df}(p' - u^0) = 0$$

. . . . . [8]

Equations [7] can be recognized as the equations of an ellipse. We treat here the special case of a circle, but obviously elliptic motion can also be treated. The solutions to [7] are then $p^0 = p_0$ and $u^0 = 1/r_0$, where p_0 is the angular momentum (a constant) and r_0 is the radius of the circle. With the conditions that, at $f = 0$, $p' = u' = du'/df = 0$, we find as solutions to [8]

$$p' = 0 \qquad u' = (\cos f - 1)/p_0 r_0^2 \qquad [9]$$

The second-order equations yield

$$p'' = u'$$

$$u'' = -2(f \sin f + 2 \cos f - 2)/p_0 r_0^3$$

. . . . . [10]

and the third-order equations give

$$p''' = u''$$

$$u''' = \left[\frac{23}{2} f \sin f + 19(\cos f - 1) - 2f^2 \cos f\right] \Big/ p_0^3 r_0^4$$

. . . . . [11]

We may note here that after one revolution ($f = 2\pi$) the sole contribution to u (hence to r) comes from terms of order greater than 2. We can, however, see this effect beginning to appear in the second-order terms, since, from $\dot{r} = -p(du/df)$, we have

$$\dot{r}^0 = 0$$

$$\dot{r}' = \sin f/r_0^2$$

$$\dot{r}'' = 2(f \cos f - \sin f)/p_0 r_0^3$$

. . . . . [12]

That is, there exists a secular term in $\dot{r}''$ which alerts us to changes in r to third order.

As regards periodic terms, we find

$$r - r_0 = \alpha(\cos f - 1)/p_0 \qquad [13]$$

ignoring higher orders. This is a function which has its maximum at $f = \pi$ and exhibits the same shape as that marked "1st revolution" on Fig. 1 of the Fain and Greer paper. Unfortunately, there seems to be the discrepancy of a factor of about 2.2 in comparing their results with that given by Equation [13]. That is, the peak value of $r - r_0$ obtained here, using the parameters of Fig. 1 (Fain and Greer) is about 8.9×10^3 m as opposed to the plotted value of about 20×10^3. However, close scrutiny of their Fig. 4 indicates that the value of m to be associated with this departure is less than 0.2 kg. It is suspected, therefore, that the mass indicated on Fig. 1 is in error by the factor for converting kilograms to pounds (2.20) and should be 0.165 kg (0.364 lb).

It is obvious that a great deal more can be done with this approach. The extension to elliptic orbits has already been mentioned; the only difficulty is the limit to one's patience. The method may also be used for a three-dimensional investigation if care is excercised in the choice of coordinate system. The advantage over numerical techniques is the usual one, that the effects of changes in parameters can be easily found. The disadvantage, of course, lies in the labor of obtaining results, especially when the disturbing force is not small compared to that of gravity.

References

1 Fain, W. W. and Greer, B. J., "Electrically Charged Bodies Moving in the Earth's Magnetic Field," ARS JOURNAL, vol. 29, no. 6, June 1959, pp. 451–453.

2 Jastrow, R. and Pearse, C. A., "Atmospheric Drag on the Satellite," *J. Geophys. Res.*, vol. 62, no. 3, Sept. 1957, p. 413.

3 Allen, C. W., "Astrophysical Quantities," U. London, Athlone Press, London, 1955, p. 128.

Approximate Method for Determining Laminar Heat Transfer Rates[1]

HAROLD S. PERGAMENT[2] and MELVIN EPSTEIN[3]

General Applied Science Laboratories, Inc., Westbury, N. Y.

Lees' result for the hypersonic laminar heat transfer around blunt nosed bodies of revolution has been applied to bodies of various shapes. It was found that if an appropriately defined heat transfer parameter is plotted against surface inclination angle, then, for a given free stream Mach number, the resulting curves are almost independent of body shape.

LEES has shown (1)[4] that the laminar heat transfer distribution about a blunt nosed body of revolution may be written as[5]

$$\frac{q}{q_0} = \frac{\frac{1}{2}\left(\frac{P}{P_0'}\right)\left(\frac{u_e}{u_\infty}\right) r_0}{\left[\int_0^s \left(\frac{P}{P_0'}\right)\left(\frac{u_e}{u_\infty}\right) r_0^2\, ds\right]^{1/2}} \frac{\sqrt{R_0}}{\sqrt{\frac{1}{u_\infty}\left(\frac{du_e}{d\theta}\right)_0}} \qquad [1]$$

In (1) this result is applied to the calculation of the laminar heat transfer rates about spherically blunted cones. Inspection of these results indicates that the local heat transfer rate depends largely on the local pressure level, with a smaller additional effect due to the distance from the stagnation point. A simple calculation shows, however, that the latter effect can be adequately accounted for by assuming that $q \sim s^{-1/2}$.

Ferri (2) shows that the pressure distribution is quite accurately determined by using the modified Newtonian approximation over the front part of the body followed by a Prandtl-Meyer expansion toward the rear. According to these approximations, the pressure depends only on the local surface inclination and the free stream Mach number. Thus, it is seen that the local heat transfer rate depends principally on the inclination angle and, to a lesser extent, on the distance from the stagnation point. It therefore appears plausible that a heat transfer parameter can be defined which eliminates the body shape as a parameter. That is, one can write

$$\frac{q}{q_0}\sqrt{\frac{s}{R_0}} = f(\theta, M_\infty) \qquad [2]$$

Equation [1] was used to calculate the variation of the quantity $(q/q_0)\left(\sqrt{s/R_0}\right)$ around ellipsoids and paraboloids for a range of fineness ratio from $\frac{1}{2}$ to 10. Fig. 1 was constructed by fitting curves through the average values of $(q/q_0) \times \left(\sqrt{s/R_0}\right)$ at each value of θ. The computations were restricted to Mach numbers no higher than 7 so that perfect gas relations could be used with reasonable accuracy. It was found that in the vicinity of the stagnation point the correlation is very accurate. This accuracy can be verified by expanding Equation [1] in a power series in s, about $s = 0$. The leading term of this series is then seen to be of the form given by Equation [2].

The validity of the correlation was found to decrease for decreasing values of the surface inclination. The scatter was found to be about ±5 per cent when $\theta = 50$ deg increasing to about ±20 per cent when $\theta = 0$ deg. A comparison of this method with the results of Equation [1] for a sphere is shown in Fig. 2 by the curve marked $s = s_j$.

Received Aug. 17, 1959.

[1] This research was supported in whole or in part by the U. S. Air Force under Contract no. AF 33 (616) 3956 monitored by the Electronic Technology Laboratory, WADC.

[2] Senior Scientist. Member ARS.

[3] Senior Scientist, present address: Engineering Center, University of Southern California, Los Angeles, Calif.

[4] Numbers in parentheses indicate References at end of paper.

[5] All symbols are as defined in (1).

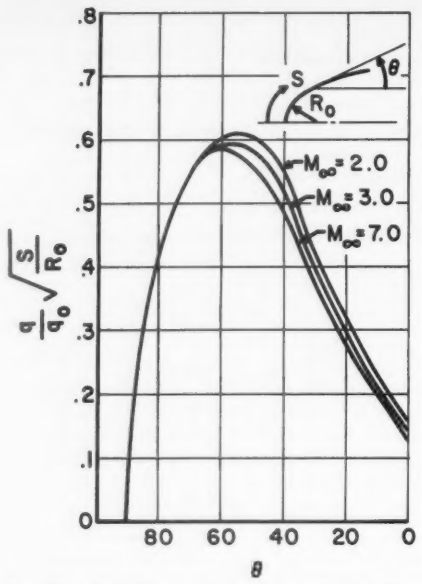

Fig. 1. Heat transfer parameter vs. surface inclination

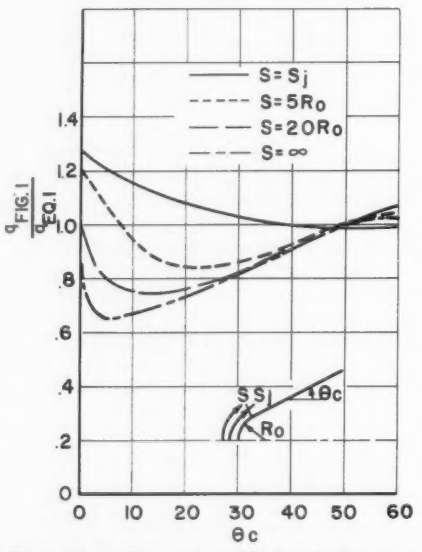

Fig. 2. Comparison of present method with Equation [1] for spherically blunted cones, $M_\infty = 7.0$

It is expected that the proposed approximation can be extended to bodies which are similar in shape to paraboloids or ellipsoids. An indication of the applicability of the present approximation to bodies of other shapes is shown in Fig. 2. Here, the ratio of heat transfer calculated by the present method to that given by Equation [1] is presented for spherically blunted cones (up to cone half-angles of 60 deg). On the spherical part, this ratio is shown by the curve $s = s_j$. It is seen that for short bodies ($s < 5s_j$), the approximation is within ±15 per cent for cone angles greater than 10 deg. In the limiting case of very long bodies, this method is still good for $\theta > 30$ deg.

References

1. Lees, L., "Laminar Heat Transfer Over Blunt-Nosed Bodies at Hypersonic Flight Speeds," JET PROPULSION, vol. 26, no. 4, 1956, pp. 259–269.

2. Ferri, A., "A Review of Some Recent Developments in Hypersonic Flow," WADC TN 58-230, Sept. 1958.

Maximum Turbulent Boundary Layer Heating Rates on a Hemispherical Nose[1]

PAUL D. ARTHUR[2] and JAMES C. WILLIAMS III[3]

Systems Corporation of America, Los Angeles, Calif.

THE PROBLEM of stagnation point heat transfer to blunt bodies in laminar flow has been the subject of a great deal of investigation, both theoretical and experimental, during the past few years. The stagnation point may not, however, be the most critical heating rate on a hemispherical nose moving at hypersonic speeds. Indeed, if boundary layer transition occurs near the stagnation point it is entirely possible that the maximum heat transfer rate will occur well beyond the stagnation point.

Van Driest noted the possibility of the maximum turbulent heat transfer rate exceeding the maximum laminar rate in an early survey of the aerodynamic heating problem (1).[4] Sibulkin, noticing the similarity between this problem and the problem of turbulent boundary layer heating in a wind tunnel throat, published a fairly comprehensive analysis of the problem in a recent paper (2). The present note points out a simple approximate expression for the maximum turbulent heat transfer rate based on the equations given by Van Driest.

The expression given by Van Driest for the turbulent boundary layer heat transfer rate in the immediate vicinity of the stagnation point is

$$\dot{q}_s = C_{H_s}\rho_\infty u_\infty (h_r - h_\omega) \qquad [1]$$

where the stagnation point Stanton number C_{H_s} is

$$C_{H_s} = 0.042\left(\frac{\beta_s D}{u_\infty}\right)^{4/5}\frac{Pr^{-2/3}}{Re_\infty^{1/5}}\left[\left(\frac{\rho_\delta}{\rho_\infty}\right)^{4/5}\left(\frac{\mu_\delta}{\mu_\infty}\right)^{1/5}\left(\frac{x}{D}\right)^{3/5}\right] \qquad [2a]$$

For later work it is convenient to rewrite this in the form

$$C_H = 0.042\left(\frac{\beta_s D}{u_\infty}\right)^{4/5}\frac{Pr^{-2/3}}{Re_\infty^{1/5}}\left(\frac{\rho_{0_2}}{\rho_\infty}\right)^{4/5}\left(\frac{\mu_{0_2}}{\mu_\infty}\right)^{1/5}\times \left[\left(\frac{\rho_\delta}{\rho_{0_2}}\right)^{4/5}\left(\frac{\mu_\delta}{\mu_{0_2}}\right)^{1/5}\left(\frac{x}{D}\right)^{3/5}\right] \qquad [2b]$$

In order to obtain the heat transfer rate away from the stagnation point, Van Driest suggests that Equations [1 and 2b] be used with the appropriate local values of β, ρ_δ and μ_δ used in Equation [2b] and that the numerical factor 0.042 be allowed to vary with β. However, in hypersonic flow, β remains constant over the major portion of the hemispherical nose, as has been pointed out by Li and Geiger (3). Thus if the suggestion of Van Driest is followed the only variation in heat transfer rate along the nose comes from the variations of the terms within the brackets.

If it is assumed that the flow just external to the boundary layer over the hemispherical nose is isentropic for the appropriate effective γ and that the viscosity is related to the temperature by

$$\frac{\mu}{\mu_{0_2}} = \left(\frac{T}{T_{0_2}}\right)^\alpha$$

The bracket in Equation [2b] becomes

$$\left[\left(\frac{\rho_\delta}{\rho_{0_2}}\right)^{4/5}\left(\frac{\mu_\delta}{\mu_{0_2}}\right)^{1/5}\left(\frac{x}{D}\right)^{3/5}\right] = \left(\frac{x}{D}\right)^{3/5}\left(\frac{p_\delta}{p_{0_2}}\right)^{\frac{4+\alpha(\gamma-1)}{5\gamma}}$$

In hypersonic flow the pressure distribution on a hemispherical nose is given by the approximate Newtonian relation

$$\frac{p_\delta}{p_{0_2}} = \cos^2\left(\frac{2x}{D}\right)$$

so that the bracket in Equation [2b] is finally written as

$$\left(\frac{x}{D}\right)^{3/5}\left(\cos^2\frac{2x}{D}\right)^{\frac{4+\alpha(\gamma-1)}{5\gamma}}$$

The maximum value of this function (and hence the maximum Stanton number and heat transfer rate) occurs at the value of x/D which satisfies the condition

$$\theta \tan\theta = \frac{3\gamma}{8 + 2\alpha(\gamma - 1)} \qquad \theta = \frac{2x}{D} \qquad [3]$$

For $\alpha = 0.76$ and $\gamma = 1.4$ the maximum occurs at $x/D = 0.322$ ($\theta = 37$ deg).[5] For a Prandtl number of 0.75 the maximum Stanton number becomes

$$C_{H_{max}} = \frac{0.0195}{Re_\infty^{1/5}}\left(\frac{\beta D}{u_\infty}\right)^{4/5}\left(\frac{\rho_{0_2}}{\rho_\infty}\right)^{4/5}\left(\frac{\mu_{0_2}}{\mu_\infty}\right)^{1/5} \qquad [4]$$

The maximum turbulent boundary layer heating rate is then

$$\dot{q}_{max\ TBL} = \frac{0.0195}{Re_\infty^{1/5}}\left(\frac{\beta D}{u_\infty}\right)^{4/5}\left(\frac{\rho_{0_2}}{\rho_\infty}\right)^{4/5}\left(\frac{\mu_{0_2}}{\mu_\infty}\right)^{1/5}\rho_\infty u_\infty (h_r - h_\omega)$$

The maximum laminar heat transfer rate occurs, of course, at the stagnation point, and the expression given by Van Driest for the stagnation point laminar heat transfer rate is

$$\dot{q}_{max\ LBL} = \frac{0.763}{Pr^{0.6}}\left(\frac{\beta D}{u_\infty}\right)^{1/2}\frac{1}{Re_\infty^{1/2}}\times \left(\frac{\rho_{0_2}}{\rho_\infty}\right)^{1/2}\left(\frac{\mu_{0_2}}{\mu_\infty}\right)^{1/2}\rho_\infty u_\infty (h_r - h_\omega)$$

The ratio of maximum turbulent heat transfer rate to maximum laminar heat transfer rate is

$$\frac{\dot{q}_{max\ TBL}}{\dot{q}_{max\ LBL}} = 0.0215\left(\frac{\beta D}{u_\infty}\right)^{0.3}\left(\frac{\rho_{0_2}u_\infty D}{\mu_{0_2}}\right)^{0.3}$$

Further, for hypersonic flight, $\beta D/u_\infty$ approximates 1.15 (1), so that Equation [5] becomes

$$\frac{\dot{q}_{max\ TBL}}{\dot{q}_{max\ LBL}} = 0.0226\ (Re_{0_2})^{0.3} \qquad [6]$$

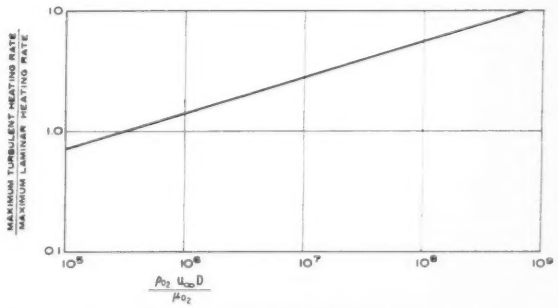

Fig. 1 Ratio of maximum turbulent heating rate to maximum laminar heating rate for blunt bodies

Received Aug. 17, 1959.

[1] Appreciation is expressed to Dr. A. Kartveli, Vice-President of Republic Aviation Corp., for permission to publish the present work.

[2] Consultant to Republic Aviation Corp. Member ARS.

[3] Research Associate, Engineering Center, University of Southern California.

[4] Numbers in parentheses indicate References at end of paper.

[5] The location of the maximum Stanton number and the numerical coefficient in [4] are fairly insensitive to variations in both γ and α; for $0.76 < \alpha < 1$ and $1.2 < \gamma < 1.6$, θ for $C_{H_{max}}$ varies from 35 to 38.5 deg and the numerical coefficient of [4] varies by only 3 per cent from the value given.

where

$$Re_{0_2} = \frac{\rho_{0_2} u_\infty D}{\mu_{0_2}}$$

Equation [6] is presented graphically in Fig. 1. A study of Fig. 1 shows that for Re_{0_2} less than approximately 3×10^5 the most critical point on a hemispherical nose, from the standpoint of aerodynamic heating, is the stagnation point; for Re_{0_2} greater than this value, the most critical heating *may* occur at about 37 deg off the stagnation point. Further, if transition occurs near the stagnation point and Re_{0_2} is much larger than 3×10^5, the turbulent heating rates on the body will be much greater than the values expected at the stagnation point.

Nomenclature

C_H = Stanton number
D = diameter of hemispherical nose
h = enthalpy
p = pressure
Pr = Prandtl number
q = heat transfer rate
Re_∞ = Reynolds number based on free stream conditions, $\rho_\infty u_\infty D/\mu_\infty$
Re_{0_2} = Reynolds number based on density and viscosity behind normal shock wave, $\rho_{0_2} u_\infty D/\mu_{0_2}$
T = temperature
u = velocity
x = distance along body surface from stagnation point
α = exponent in viscosity law
β = velocity gradient
δ = conditions at edge of the boundary layer
γ = ratio of specific heats
θ = angular distance from stagnation point
μ = viscosity
ρ = density

References

1 Van Driest, E. R., "The Problem of Aerodynamic Heating," *Aeron. Engng. Review*, vol. 15, no. 10, Oct. 1956.

2 Sibulkin, M., "Estimation of Turbulent Heat Transfer at the Sonic Point of a Blunt-Nosed Body," JET PROPULSION, vol. 28, no. 8, part 1, Aug. 1958, pp. 548–554.

3 Li, T.-Y. and Geiger, R. E., "Stagnation Point of a Blunt Body in Hypersonic Flow" *J. Aeron. Sci.*, vol. 24, no. 1, Jan. 1957.

Book Reviews

Ali Bulent Cambel, Northwestern University, *Associate Editor*

In past years, publications by multiple authors were relatively uncommon. Today it is probably correct to say that publications by single authors are uncommon. This should not be ascribed to "togetherness" or "belongingness" so eloquently described in the Organization Man. Rather the reason for multiple authorship is the need for diversified talents working together in developing or in understanding a complex system. This situation is most acute in the astronautical sciences, and your Book Review Editor finds it increasingly difficult to locate single reviewers willing to comment on volumes describing multifareous subjects.

ARS JOURNAL has attempted to publish reviews meaningful to its readers, and when the latest volume of the significant Princeton Series arrived the Editors were faced with a difficult task. Finally, it was decided that a book written by several authors might as well be reviewed by several reviewers. The review which follows is an example of this approach. The splendid cooperation of Donald R. Bartz and his colleagues who demonstrated their wisdom, knowledge and togetherness is greatly appreciated.

—**Ali Bulent Cambel**

Jet Propulsion Engines, edited by O. E. Lancaster, Vol. 11 of High Speed Aerodynamics and Jet Propulsion, Princeton University Press, Princeton, N. J., 1959.

Reviewed by D. R. BARTZ
AND COLLEAGUES
California Institute of Technology

As stated in the preface, this volume of the now renowned Princeton Series on High Speed Aerodynamics and Jet Propulsion "considers those principles and problems encountered in combining components to form a complete engine—relying heavily upon the other volumes which deal with basic principles and problems related to components of an engine." The types of engines to which separate sections of the volume are devoted include the turbojet, turboprop, ramjet, intermittent jet, liquid propellant rocket, solid propellant rocket, ram rocket and jet rotor. Because the scope of technology covered by this volume is so great, this reviewer sought the assistance of several of his colleagues having more intimate professional contact with the special field covered in several of the sections.

In treating "Historical Development of Jet Propulsion" F. J. Malina, R. C. Truax and A. D. Baxter have done a creditable job of showing where the original concepts of rocketry and jet propulsion appeared, and how they were alternately neglected and nourished in various countries until, in the period just preceding and during World War II, a surge of activity brought us to our present state of development. The fact that groups in many countries worked separately and in secrecy, and that even yet some work has not been reported, makes a balanced presentation difficult to compile. This the authors point out and then proceed to tie together the threads of history and weave the tapestry, showing the historical development of rockets and of jet propulsion devices up to the present time.

—WALTER B. POWELL

The short section covering "Basic Principles of Jet Propulsion," by Maurice Roy, begins by defining the differences between the several prominent types of jet propulsion engines but is devoted primarily to discussing the principles common to the various types of engines. Brief generalized treatments of the concepts of thrust, drag, powers and efficiencies of jet propulsion engines are presented, followed by the specialization of these relationships for several types of engines, including the rocket, turboprop, turbojet and ducted fan.

"The Turbojet Engine" section of the volume by C. A. Meyer is divided into six chapters: (1) basic types and simple cycle analysis, (2) analysis and matching of components, (3) engine performance, control and installation, (4) thrust augmentation, (5) coordination of design and (6) testing. The text is primarily descriptive, and it is assumed that the reader is familiar with the applied thermodynamics and fluid mechanics of gas turbine engines. A detailed development of the thrust and drag equations of an engine and vehicle are presented; however, in general there is little emphasis placed on the development of mathematical relationships. Various types of turbojet engines such as single-spool, two-spool, by-pass and ducted fan are discussed very briefly. Comparisons including the best ranges of flight speed are given for rockets, ramjets, pulse jets, turbojets, turboprops and reciprocating engines. Factors governing the design and matching of the various components of a turbojet engine are presented. The effects of starting, acceleration and operational requirements on design are discussed. Methods are given for controlling engine operation and correcting performance for altitude operation. Graphical trends are shown for progress that has been made in the development of the turbojet engine and its components.

—PAUL F. MASSIER

After defining the basic components that constitute "The Turboprop Engine," I. H. Driggs and O. E. Lancaster make a simple straightforward case for the turboprop engine. Brief descriptive treatments of the analyses of the performance

To assure a new order of reliability

MICRO-MODULE

EQUIPMENT

The micro-module is a new dimension in military electronics. It offers answers to the urgent and growing need for equipment which is smaller, lighter, more reliable and easier to maintain. Large scale automatic assembly will bring down the high cost of complex, military electronic equipment. Looking into the immediate future, we see a tactical digital computer occupying a space of less than two cubic feet. It will be capable of translating range, wind velocity, target position, barometric pressure, and other data into information for surface to surface missile firings. The soldier-technician monitoring the exchange of computer data will have modularized communications with the other elements of his tactical organization. RCA is the leader contractor of this important United States Army Signal Corps program and is working in close harmony with the electronic components industry.

RCA Tmk(s)®

RADIO CORPORATION of AMERICA

DEFENSE ELECTRONIC PRODUCTS

CAMDEN, NEW JERSEY

of the propeller, gas generator, turbine and complete engine are given with the aid of generalized plots of the principal parameters. A state of the art type of coverage is given to the practical problems as well as the current development practices of propeller turbine design, controls, gear box and accessories, propellers, engine testing and installation. The section concludes with an interesting discussion of the past, present and future roles of turboprop engines, concluding that they show great promise for long term application to certain commercial and transport operations and perhaps for helicopters.

The section on "The Ramjet Engine" contains a comprehensive treatment of the ramjet engine, emphasizing theoretical methods of performance calculations. Useful comparisons are made showing the loss in accuracy to be expected from performance calculations by approximate methods. Included is a chapter on ramjet control system methods and also a chapter on the difficult practical problem of ramjet test facilities. The authors D. D. Wyatt and B. T. Lundin show considerable restraint in their enthusiasm over the future of the ramjet engine.

—Fred C. Gunther

In his treatment of "Intermittent Jets" J. V. Foa begins with a historical account of the development of the intermittent jet engine idea, followed by the usual development of the relationships of thrust, impulse and cycle efficiency specialized to needs of the type of engine, making use of a mass flow rate-averaged velocity. The basic thermodynamics of the propulsive cycles and flow phenomena of intermittent jets is followed by separate chapters on the pulse jet engine and wave engine. The treatment is slanted much more toward the methods of analysis of the physical phenomena involved than toward the practical problems and practices of engine development. No serious effort is given to establishing the position of this type engine in the broad flight propulsion spectrum.

The section "The Liquid Propellant Rocket Engine," by M. Summerfield, begins with a very clear and straightforward presentation of a performance analysis of an ideal rocket motor, enumerating all of the approximations and assumptions. This is followed by equally clear discussions of all of the important departures from ideal performance, in which the reader is given a quantitative "feel" for the importance of each of these departures. These two subsections offer an excellent introduction into the theory of performance of any rocket, liquid or solid, for the engineer entering the propulsion field or for the engineer in another area of technology who needs to be acquainted with the principles of rocket propulsion. The section also contains discussions of the principles, problems and practices of some of the technical areas of liquid rocket engines, such as thermochemical performance calculations, combustor design, engine cooling and propellant transfer systems. Naturally, in a brief presentation such as this, the discussions can serve only as introductions, but this they do admirably. The principal criticism that the reviewer finds with these last subsections is the author's tendency to draw generalizations based on practices associated with types of engines which no longer dominate the development effort. The practices associated with very large thrust boosters and small-to-medium-size sustainers with very large expansion nozzles are such that some of the generalizations are inappropriate. It is difficult to see why the author has chosen to divide the discussion of the convective heat transfer from the combustion gases to the wall into three separate sections (chamber, throat and diverging section), applying separate correlations to each, since at least one of the papers listed in the bibliography handles all three regions with a single correlation based on turbulent boundary layer theory. Several other papers based on this approach have appeared in the open literature since 1955, and all agree with each other and with the three separate correlations discussed, well within the magnitudes of the uncertainties present because of nonuniform and unknown flow phenomena.

The section on "Solid Propellant Rockets," by C. E. Bartley and the late M. M. Mills, discusses in authoritative fashion the various types of solid propellants, interior ballistics theory and solid

The Navy's Polaris: *from nowhere to anywhere*

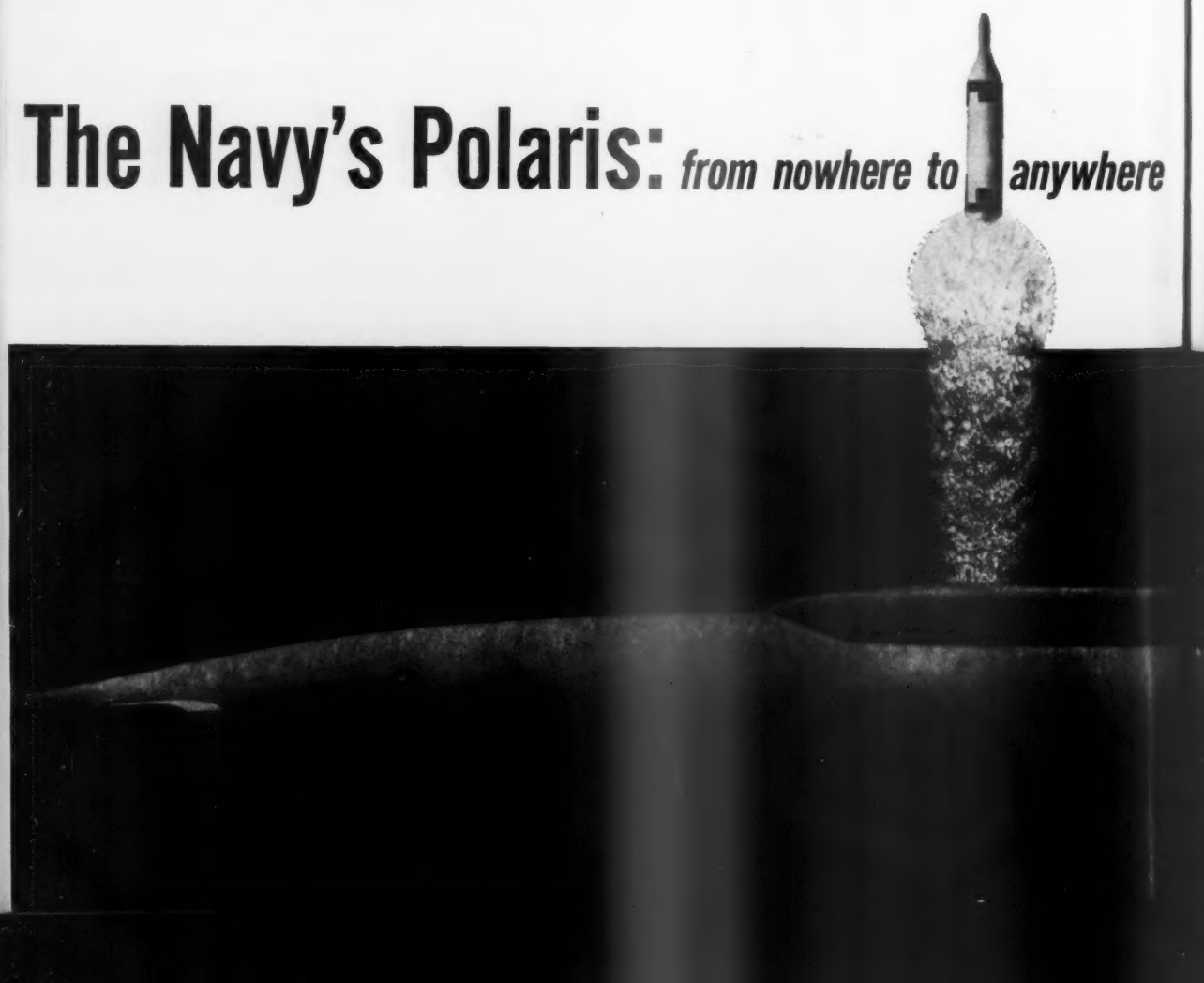

propellant rocket motor design. In a mere 140 pages the authors are hard put, however, to present more than a semi-quantitative coverage of this rather extensive field. As an introduction to the subject for technically trained people whose interests lie in other fields, the text is excellent, but the neophyte solid propellant engineer will need expert tutoring to supplement the printed material if he is to become qualified as a ballistician or designer. The problems of preparing an unclassified technical textbook in a highly classified and fast growing field are readily apparent.

—G. ROBILLARD

In the section on "The Ram Rocket' I. Glassman and J. V. Charyk compare this hybrid engine with the ramjet, indicating both the similarities and the differences. A brief thermodynamic analysis of the critical mixing problem of the ram rocket is given and is related to the overall engine performance. Although no real case is made for establishing the place of the ram rocket in the propulsion spectrum, certain areas of superiority over the ramjet are indicated in generalized curves. Evidently because of the very limited extent to which this type of engine has been developed there is little attention given to the practical problems of the engine.

In the section on "Jet Rotors" A. Gail begins with an informative discussion of the future potential role of the jet rotor, concluding that its most promising chance to advance beyond the prototype stage is in the large VTOL aircraft application. Philosophically, the author notes that "the failure to excel in competition with its rivals is as mercilessly damaging to an engineering design as the failure of crucial experiments is to a theory in the physical sciences." With somewhat more mathematical detail than is typical of other sections of the volume, the basic elements of the performance analysis of jet rotor engines for helicopter and VTOL applications are presented, including effects of stress limitations on blade design and weight.

The preface to this volume states that the section "Atomic Energy in Jet Propulsion," by R. Zirkind, "deals with the problems in making a nuclear jet powerplant suitable for aircraft. It gives the theory related to the shielding, heat transfer, and the production and control of a small lightweight reactor." The contents of the section consist of a 1-page introduction, 26 pages on reactor principles, 15 pages on shielding concepts, 3 pages on coolants, 2 pages on heat transfer, 3 pages on systems and 4 pages on preliminary design. The material titled "Reactor Principles" is a very brief exposition of the most elementary mathematical models available for describing the neutron population in a chain reacting system. It is certainly not related to the objectives set forth in the preface, nor is it of any use to the experienced analyst. If the intent was to provide the uninitiated with a glimpse of the methods of reactor analysis, then this treatment is far too detailed (and at times conceptually misleading). Inasmuch as several excellent texts are available on this very large subject, it is suggested that the author would have rendered a greater service by giving a general survey which included a discussion of the nature of the physical problems involved in reactor physics, the types of questions to be answered, and an extensive list of appropriate references and bibliography rather than a detailed mathematical development of such irrelevant topics as the solution of the Helmholtz equation by separation of variables. The treatment of shielding theory is somewhat more in the spirit of the suggested approach. Here some attention is given first to describing the essential physical concepts and phenomena involved. Next, a brief statement of the energy flux relation for gamma radiation is given with the aid of the Boltzmann equation. The solution to this equation is then given in terms of the dose buildup factor, and some useful results are summarized for several shielding materials. The discussions on coolants, heat transfer, systems and preliminary design are trivial. Perhaps this is due to the fact that very little unclassified information was available at the time this section was written. It is hard to believe, however, that this would explain the general lack of substance throughout. From the objectives stated in the preface, one would expect that these topics

Erupting from the ocean that blankets most of the earth, the Navy's Polaris missile will have the range to reach any strategic target. It will be launched from mobile bases that are safe from surprise attack—nuclear-powered submarines that cruise fast and deep for weeks on end, each carrying 16 Polaris missiles. This is the Navy's Fleet Ballistic Missile system. It becomes operational this year. Lockheed is prime contractor and system manager for the Polaris missile.

LOCKHEED MISSILES & SPACE DIVISION

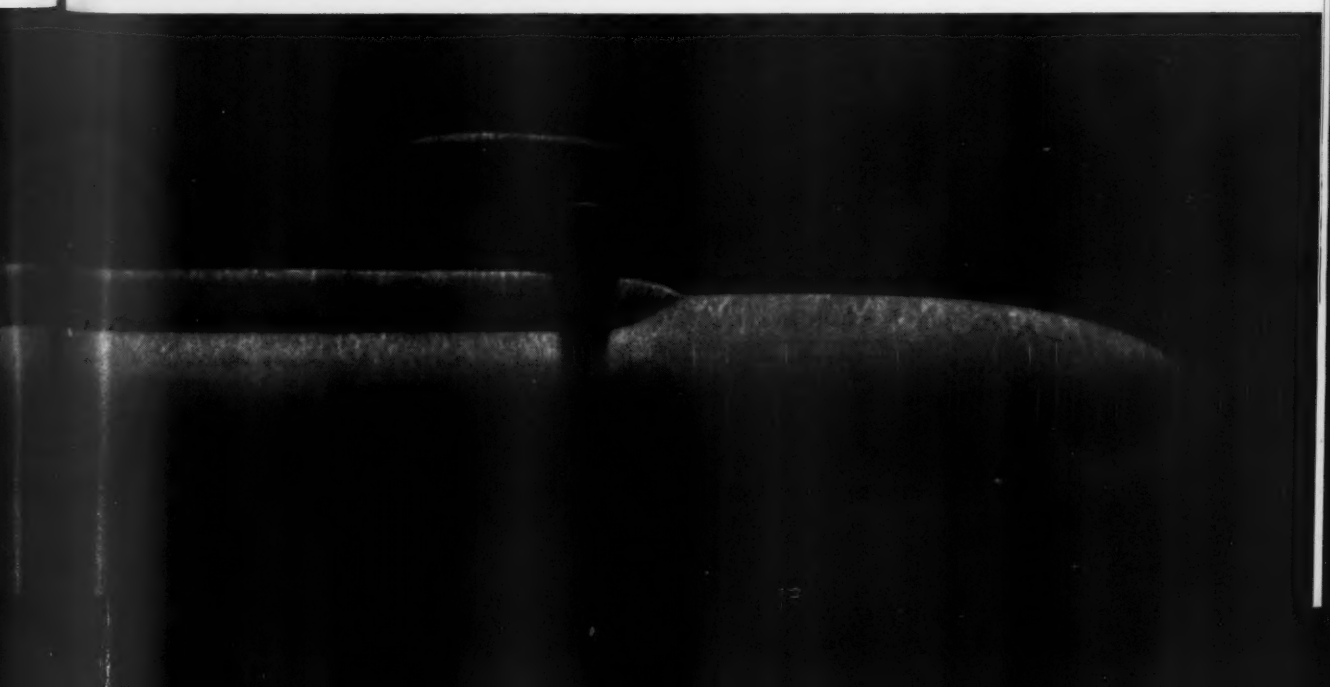

Academic Press
NEW YORK and LONDON

Hypersonic Flow Theory

WALLACE D. HAYES
RONALD F. PROBSTEIN

"The authors themselves have contributed significantly to the field. They write with a deep understanding of the present state of the art... the nature of the present volume makes it an important contribution to the contemporary scene as well as a book that will remain vital for many future years."—*ARS Journal*

1959, 464 pp., illus., $11.50

CONTENTS:
General Considerations—Small-Disturbance Theory—Newtonian Theory—Constant-Density Solutions—The Theory of Thin Shock Layers—Other Methods for... Blunt-Body Flows—Other Methods for Locally Supersonic Flows—Viscous Flows—Viscous Interactions—Free Molecule and Rarefied Gas Flows—CITED REFERENCES—SYMBOL INDEX—AUTHOR INDEX—SUBJECT INDEX.

Advances in Space Science

Edited by
FREDERICK I. ORDWAY, III
Editorial Advisory Board
WERNHER VON BRAUN
FREDERICK C. DURANT, III
EUGEN SÄNGER
LESLIE R. SHEPHERD
GEORGE P. SUTTON
ÉTIENNE VASSY

VOLUME 1

1959, 412 *pp., illus.*, $12.00

Interplanetary Rocket Trajectories, by DEREK LAWDEN
Interplanetary Communications, by J. R. PIERCE and C. C. CUTLER
Power Supplies for Orbital and Space Vehicles, by JOHN H. HUTH
Manned Space Cabin Systems, by EUGENE B. KONECCI
Radiation and Man in Space, by HERMANN J. SCHAEFER
Nutrition in Space Flight, by ROBERT G. TISCHER
Appendix: A Decimal Classification System for Astronautics, with an introduction by HEINZ HERMANN KOELLE
AUTHOR INDEX-SUBJECT INDEX.

VOLUME 2 *Ready May 1960*

List of forthcoming papers sent upon request

111 Fifth Avenue, New York 3, New York
17 Old Queen Street, London, S. W. 1

would receive the bulk of the author's attention. Instead, he has chosen to emphasize the reactor theory, which seems entirely irrelevant to the present purpose. The reviewer questions the usefulness of the present treatment in the light of these remarks and consequently does not believe that the overall tone and quality is in keeping with other sections of the series.

—ROBERT V. MEGHREBLIAN

In the last section "Future Prospects of Jet Propulsion" Dr. F. Zwicky describes and gives examples of the use of the "morphological method." This method, which strikes the reviewer as the familiar one of looking at the various possibilities, has been utilized for a very long time by people in and out of science. Dr. Zwicky has recognized the method as the important and useful tool that it is; he has named it, thus adding to its stature. In addition, he has clearly and explicitly demonstrated its power in such a complicated case as the enumeration of many possible kinds of jet engines. Although the manuscript for this section was submitted in 1951, it is unfortunate that the discussion was limited to chemical energy sources and did not include an application of the morphological method in the description of possible roles of nuclear and electromagnetic fields in jet propulsion. Such an exposition by Dr. Zwicky would have been most gratefully received, and, indeed, would have better fitted the title of the section.

—JOHN W. LUCAS

This particular volume of The Princeton Series is in marked contrast to most of the other volumes which deal with the basic scientific topics on which the technology of high speed flight is built. In writing about the various types of jet propulsion engines, the outstanding group of authors has devoted about equal space to the theoretical concepts and to the "current" development practices. In the latter effort, it is clear that the authors have been limited both by security restrictions and by the passage of time between the writing of the original manuscripts and the publication of the volume. Because of the number of engine types to which sections were devoted, each section is necessarily brief, making the treatment best suited as an introduction for engineers new to a particular engine field or for engineers who in their work must maintain a broad unbiased view of all types of jet propulsion engines. Of particular usefulness to the development of the new engineer will be the bibliographies of the classical references to each type of engine; hence, the volume itself should become a classical library reference volume.

—D. R. BARTZ

Servomechanisms and Regulating System Design, Vol. 1, by Harold Chestnut and Robert W. Mayer, John Wiley and Sons, Inc., New York, 1959, xvii + 680 pp. $12.50.

Reviewed by J. DENAVIT
Northwestern University

This second and appreciably augmented edition differs from the 1951 edition mainly in the addition of the root locus approach to servomechanism design, and a chapter on analog computers by William E. Sollecito.

The book covers linear servomechanism design; it starts with complex numbers, the solution of linear ordinary differential equations and Laplace transformation. These basic concepts are followed by the study of steady-state response to sinusoidal forcing, mostly applied to electrical networks, and a discussion of stability on the basis of Routh and Nyquist criteria. After a study of typical control elements and a classification of control systems according to the number of integrations involved in the system's loop, the authors present three methods for the design of linear control systems: The transfer locus, the attenuation and phase diagrams, and the root locus. Each of these methods is applied to stabilization by means of phase-lag, phase-lead and feedback networks. Five chapters are devoted to this extensive discussion, and many examples are given. Unfortunately, most of these examples are electrical. The remaining chapters are on multiple loop and multiple input systems, transient response as deduced from steady-state sinusoidal response and analog computers as mentioned previously. A good collection of problems is given.

The emphasis throughout is on design practice, rather than on the mathematical development of principles, most of which must be accepted "on faith" by the reader.

In the design of servomechanisms by the attenuation and phase approach (Chapters 11 and 12), the authors define minimum phase-shift networks—or systems—but the reviewer would have liked to see more examples of systems which are of the nonminimum phase-shift type, particularly mechanical systems. Bode's equations may be used for minimum phase-shift systems only; they do not apply to nonminimum phase-shift systems. This reviewer got the feeling that nonminimum phase-shift situations are discussed too lightly, suggesting that they are unimportant. However, they do occur, and the designer must be alert to their occurrence and have tests to identify them. Nonminimum phase-shift systems may often be detected without writing their complete transfer function by their characteristic response to a step input which may be described as "faulty at the outset." (See "Feedback Control Systems" by Gille, Pelegrin and Decaulne; McGraw-Hill Book Co., Inc., 1959, pp. 154–157.)

The solution of cubic, quartic and quintic algebraic equations as presented on pages 134–137 conceals the basic difficulty of the problem. In all the examples given, the authors are always lucky in guessing the exact value of a root at the first trial; they fail to indicate what might be done if the first trial does not happen to be a solution.

In the root locus method to determine stability (p. 164), the authors speak of the poles and the denominator of a polynomial. They evidently mean a rational fraction, since they refer to a transfer function.

EXCELCO

RV-A-10 • SERGEANT
AIR FORCE — RE-ENTRY X-17
POLARIS — RE-ENTRY X-36
JUPITER JR. • JUPITER SR.
POLARIS 0 • POLARIS A
POLARIS AIX • POLARIS A2-MOD 1-2-3
NIKE HERCULES • NIKE ZEUS
MINUTEMAN • PERSHING
N.A.S.A. PROGRAMS • SCOUT
LITTLE JOE

•

and many other classified projects

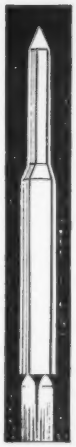

Builders of more large, thin wall, high strength solid propellant rocket engine cases and nozzles for development purposes than any other company in America.

A small experienced organization geared to handle your development and prototype requirements for static and flight tests in the shortest possible time.

Call or write:

EXCELCO DEVELOPMENTS

MILL STREET • SILVER CREEK, NEW YORK

New Patents

George F. McLaughlin, *Contributor*

Device for indicating the true vertical (2,893,248). C. A. Ecary, Paris, France, assignor to Societé Commerciale Eca.

Platform mounted about two axes at right angles to each other and parallel to the lines tangent to two orthogonal terrestrial characteristics circles. Means for angularly displacing the platform about the axes to maintain a fixed course, a third axis at right angles to the two axes detects accelerations imparted to the first two axes.

Afterburner fuel control (2,892,306). J. J. Intintolo, Philadelphia, Pa., assignor to the U. S. Navy.

Control for changing the size of the fuel pump inlet, the position of the balance and shutoff valve and the position of the rotor valve in a gas turbine engine.

Hot streak ignition for an afterburner fuel system (2,892,307). P. C. Mangan and W. E. Kohman, Kansas City, Mo., assignors to Westinghouse Electric Corp.

Arrangement for controlling an afterburner fuel control and an igniter fuel regulator by electrical and mechanical means external to a gas turbine powerplant.

Ramjet projectile (2,892,410). D. H. Sloan and W. H. Gross, Silver Spring, Md.

Body in the form of a duct and a fuel source having a tank defined by a diffuser contained within the duct. The tank has a compressible wall which forces fuel through a nozzle between the tank and the interior of the duct.

Turbojet convertible to a ramjet (2,896,408). W. J. O'Donnell (Member ARS), Freeport, N. Y., assignor to Republic Aviation Corp.

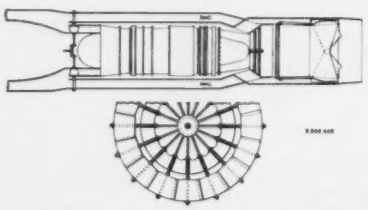

Combination power plant for individual and alternate operation. The combustion chamber for the ramjet engine is adapted as an afterburner during operation of the turbojet engine. Upon the attainment of predetermined flight conditions of the aircraft, one or the other of the engine types alternates.

Explosive bolt-type store suspension for aircraft (2,889,746). L. H. Glassman, R. E. Kemelhor and K. E. Schuessler, Philadelphia, Pa.

System for releasably fastening a store to a fixed member, consisting of a plurality of explosive bolts as the sole connection. The charge in each bolt gives the store the desired separation characteristic for overcoming adverse aerodynamic and inertia forces and moments.

Boundary layer control for a jet (2,892,582). N. W. O'Rourke (Member ARS), LaJolla, Calif., assignor to the U. S. Navy.

Jet pump effecting movement of a low pressure fluid by a high pressure fluid. Outer and inner shell members form a mixing chamber and passageway for the fluids. High pressure fluid is injected into a conical inlet upstream of the inlet. The boundary layer of fluid in a diffuser is discharged through ports into the inner shell.

Guided missile (2,892,600). W. K. Ergen, Oak Ridge, Tenn., assignor to the U. S. Army.

Self-propelled missile with control vanes operated by servomators. Universally mounted gyroscopes control movement of the servomotors in response to the relative angular movements of one gyroscope and casing about an axis parallel to the spin axis of the other gyroscope.

Ferromagnetic microwave device (2,894,224). A. H. Iversen, Santa Monica, Calif., assignor to Hughes Aircraft Co.

Device for rotating the plane of polarization of an electromagnetic wave. An elongated figure of revolution ferrite compact slug having a cylindrical midportion and tapered end portions. The slug, of ferromagnetic ferrite material having predetermined moisture sensitive and heat sensitive physical characteristics, has a coat of protective glass over its exposed surface.

Antenna array (2,894,261). N. Yaru, Santa Monica, Calif., assignor to Hughes Aircraft Co.

Reverse end fire waveguide array adapted to propagate orthogonal linearly polarized electromagnetic waves. One wall of the waveguide section includes radiation means excited by waves linearly polarized in a first plane. A source of waves for exciting linearly polarized waves in a second plane perpendicular to the first, is coupled to one end of the waveguide section.

Astrocompass (2,894,330). V. E. Carbonara, Manhasset, N. Y., assignor to Kollsman Instrument Co.

True heading indicator with a rotatable sighting member having an index alignable simultaneously with the object sighted and a portion of a circular scale. The scale has numerical indicia arranged clockwise when viewed from above the scale.

Method of burning ash-forming liquid fuel (2,895,293). R. I. Hodge, Church Crookham, England, assignor to Power Jets (Research and Development) Ltd.

Combustion apparatus for discharging fuel as a spray of droplets of various sizes into a region outside the combustion zone. Droplets of sizes less than a predetermined size are separated and completely burned under the conditions prevailing outside the zone. Remaining droplets are introduced into the combustion zone.

Variable speed gas turbine (2,895,295). P. G. Carlson, San Diego, Calif., assignor to Solar Aircraft Co.

Compact, light weight powerplant providing independently controllable main and auxiliary power outputs while maintaining efficient combustion and energy extraction. Two separate turbines may be coupled with two compressors to form high and low pressure compressor-turbine units.

Moving target radar system (2,896,203). P. M. Wright and N. M. Rust, Worthing, England, assignors to Marconi's Wireless Telegraph Co., Ltd.

Continuous wave radar for picking up moving targets and ascertaining and displaying their range and azimuth on a cathode ray tube. The ray is deflected in synchronism with the scanning means, and brightened by signals picked up by scanning.

Rocket propulsion methods. A. Zletz and D. R. Carmody, Crete, Ill., assignors to Standard Oil Co. of Indiana.

The following nine patents have been granted for the use of various combinations and proportions of chemicals for generating gases for propelling rockets: **(2,892,305; 2,896,400–2,896,407)** inclusive.

Simulated orbiting artificial satellite (2,897,607). A. C. Park, Sacramento, Calif.

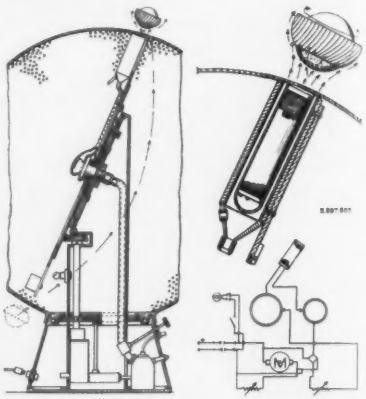

Educational device providing a satellite placed and maintained in an orbit about a simulated replica of Earth. The satellite is suspended by means of the attraction of an electromagnetic device, and the balanced current of air directed to the adjacent surface of the satellite.

High temperature protective coating for metals (2,898,253). E. B. Schneider and E. G. Stevens, El Segundo, Calif., assignors to North American Aviation, Inc.

Composition consisting of 100 parts (by weight) of a ceramic material, from 10 to 200 parts aluminum, from 1 to 100 parts of a bentonite clay, and an amount of diluent sufficient to permit spreadable consistency.

Proximity fuze (2,898,857). L. B. Hafstad and R. B. Roberts, Washington, D. C., assignors to the U. S. Navy.

An amplifier and thyratron coupled to a photoelectric cell unit. The thyratron is coupled to fire a detonator upon triggering of the thyratron by an amplified current pulse from the cell unit.

EDITOR'S NOTE: Patents listed above were selected from the Official Gazette of the U. S. Patent Office. Printed copies of patents may be obtained from the Commissioner of Patents, Washington 25, D. C., at a cost of 25 cents each; design patents, 10 cents.

Storable and Powerful Rocket Fuel Oxidizer

CTF

Chlorine Trifluoride (ClF_3)

Much is expected of Chlorine Trifluoride as a rocket fuel oxidizer. That's because it combines good handling and storage properties with very high performance. To be specific:

CTF is not difficult to handle! Boiling point of Chlorine Trifluoride is 53.15°F. Freezing point is −105.4°F. Vapor pressure at 140°F is 80 psia.

CTF may be stored conveniently! Chlorine Trifluoride is storable over a very wide range of temperatures. You can count on years of storage life!

CTF has excellent stability! Shock resistance of pure CTF is very high. And it is thermally stable to high temperatures.

CTF offers high performance! The high density of Chlorine Trifluoride (1.825 at 68°F) leads to outstanding density impulse values. An important plus—CTF is hypergolic with hydrogenic fuels over a wide range of pressures and temperatures.

Fluorine and other Fluorine-Based Oxidizers

CTF is one of several fluorine-based chemicals produced by General Chemical which are now considered as excellent rocket-fuel oxidizers for various missions. Another is Bromine Pentafluoride which shares many of CTF's desirable physical and chemical properties. General Chemical, the sole producer of elemental liquid fluorine, has extensive technical data available on Fluorine and Halogen Fluorides. Write today for further information on these high-energy oxidizers.

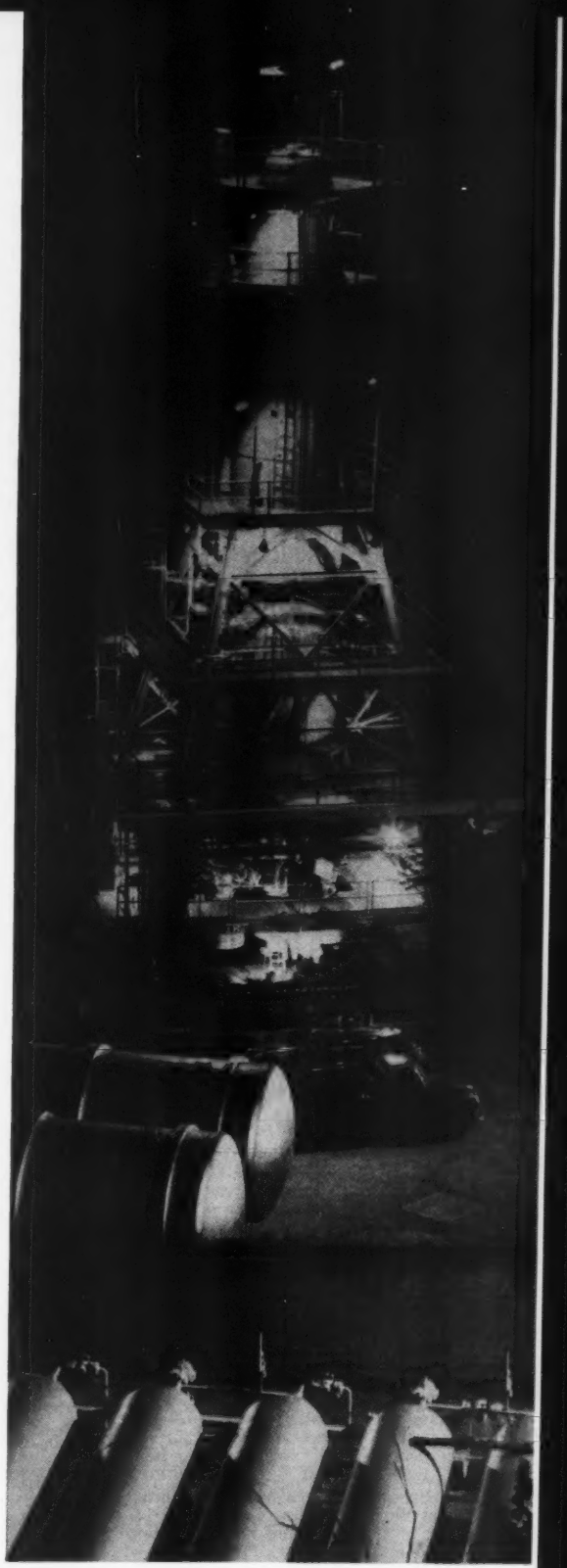

Typical test stand of Rocketdyne, a division of North American Aviation, Inc.

BAKER & ADAMSON® Products

Allied Chemical

GENERAL CHEMICAL DIVISION
40 Rector Street, New York 6, N. Y.

Technical Literature Digest

M. H. Smith, *Associate Editor*
The James Forrestal Research Center, Princeton University

Propulsion and Power (Combustion Systems)

Changes in the Density and Temperature of Liquid Propellants in Rocket Engine Supply Systems, by S. L. Bragg, ARS JOURNAL, vol. 29, Sept. 1959, pp. 672–674.

Rocket Propulsion Systems for Interplanetary Flight, by George Paul Sutton, *J. Aero/Space Sci.*, vol. 26, Oct. 1959, pp 609–625.

Analysis of Injection-velocity Effects on Rocket Motor Dynamics and Stability, by Herbert C. Hurrell, *NASA Tech. Rep.* 43, Sept. 1959, 40 pp.

The Effect of Combustor Outlet Temperature Profiles on Ramjet Thrust, by M. R. Williams and S. W. Greenwood, *Cranfield, The College of Aeron., CoA Note* 59, July 1959, 14 pp.

Design of Axisymmetric Exhaust Nozzles by Method of Characteristics Incorporating a Variable Isentropic Exponent, by Eleanor Costilow Guentert and Harvey E. Neumann, *NASA Tech. Rep.* R-33, Sept. 1959, 31 pp.

Canned Liquid-rocket Engines, by F. M. Fulton, ASTRONAUTICS, vol. 4, Oct. 1959, pp. 37–39, 105.

Variable-thrust Rocket Engines, by Eugene V. Rutkowski, ASTRONAUTICS, vol. 4, Oct. 1959, pp. 40–41, 80.

Analysis of Injection-velocity Effects on Rocket Motor Dynamics and Stability, by Herbert G. Hurrell, *NASA Tech. Rep.* R-43, Sept. 1959, 40 pp.

Near-field and Far-field Noise Surveys of Solid-fuel Rocket Engines for a Range of Nozzle Exit Pressures, by William H. Mayes, Wade E. Lanford and Harvey H. Hubbard, *NASA TN* D-21, Aug. 1959, 32 pp.

Propellant Vaporization as a Criterion for Rocket-engine Design; Experimental Effect of Chamber Diameter on Liquid Oxygen—Heptane Performance, by Marcus F. Heidmann, *NASA TN* D-65, Sept. 1959, 22 pp.

Analysis of Effects of Rocket-engine Design Parameters on Regenerative-cooling Capabilities of Several Propellants, by Arthur N. Curren, Harold G. Price Jr. and Howard W. Douglass, *NASA TN* D-66, Sept. 1959, 47 pp.

Comparison of Energy Requirements of Rockets with Constant or Variable Jet Speeds, by G. Zebel, *Raketentechnik und Raumfahrtforschung*, vol. 3, no. 3, July-Sept. 1959, pp. 81–82. (In German.)

A High-performance 250 Pound-thrust Rocket Engine Utilizing Coaxial-flow Injection of JP-4 Fuel and Liquid Oxygen, by Samuel Stein, *NASA TN* D-126, Oct. 1959, 14 pp.

The Historical Development of Turbojet and Ram-jet Engines in the Soviet Union, by Donald J. Ritchie, *Aero/Space Engng.*, Oct. 1959, pp. 45–51.

Design Progress: Thor Ramjet Develops 100,000 HP, by Randolph Hawthorne, *Space/Aeron.*, vol. 32, Nov. 1959, pp. 114–116.

Propulsion and Power (Non-Combustion)

Powerplant Heat Cycles for Space Vehicles, by D. B. Mackay, *Inst. Aeron. Sci., Paper* 59–104, June 1959, 45 pp.

The Central Problem of Large Scale Power Generation in Space-Waste Heat Disposal, by P. M. Diamond, *Inst. Aeron. Sci., Paper* 59–96, June 1959, 36 pp.

Design of Ion Rockets and Test Facilities, by. J. H. Childs, *Inst. Aeron. Sci., Paper* 59–103, June 1959, 35 pp., illus.

Performance of Nuclear Rocket for Large-payload, Earth-satellite Booster, by Eldon W. Sams, *Inst. Aeron. Sci., Paper* 59–94, June 1959, 31 pp.

An Airborne Cryogenic System for Pneumatic Power Generation, Cooling, and Other Uses, by R. H. Ball, *Proc., Cryogenic Engng. Conf., Cambridge, Mass., Sept. 1958,* Univ. of Colo., Boulder, Jan. 1959 (498 pp.), pp. 174–183.

Cryogenic Systems as Auxiliary Power Sources for Aircraft and Missile Applications, by C. Hohmann and W. Patterson, *Proc., Cryogenic Engng. Conf., Cambridge, Mass., Sept. 1958,* Univ. of Colo., Boulder, Jan. 1959 (498 pp.), pp. 184–195.

A Description of a Propulsive Device Which Employs a Magnetic Field as the Driving Force, by Richard M. Patrick, *Vistas in Astronautics,* vol. 2 (2d Annual Astronautics Symposium), Pergamon Press, N. Y., 1959 (318 pp.), pp. 119–126.

Problems of Thrust Production by Electrostatic Fields, by David B. Langmuir, *Vistas in Astronautics,* vol. 2 (2d Annual Astronautics Symposium), Pergamon Press, N. Y., 1959 (318 pp.), pp. 127–136.

Preliminary Evaluation of Helium as an Electric Arc Heated Propellant, by Thomas R. Brogan, ARS JOURNAL, vol. 29, Sept. 1959, pp. 662–663.

A Compilation of Some Rates and Cross Sections of Interest in Controlled Thermonuclear Research, by C. F. Wandel, T. Hesselberg Jensen and O. Kofoed-Hansen, *Nuclear Instr. and Methods,* vol. 4, no. 5, June 1959, pp. 249–260.

The Quest for Thermonuclear Power, by Robert G. Mills, *Princeton Univ., Proj. Matterhorn, Matt-15,* Aug. 1959, 11 pp.

Plasma Motors, by Winston H. Bostick, *Advances in Astronautical Sciences,* vol. 2 (Proc., 4th Annual Meeting, Amer. Astron. Soc., Dec. 1957), Plenum Press, N. Y., 1958. *Paper* 1, 11 pp.

Hydrogen Peroxide as a Source of Oxygen, Water, Heat and Power for Space Travel, by Noah S. Davis, *Advances in Astronautical Sciences,* vol. 2 (Proc., 4th Ann. Meeting, Amer. Astron. Soc., Dec. 1957), Plenum Press, N. Y., 1958, *Paper* 31, 14 pp.

On Magnetohydrodynamic Propulsion, by Yusuf A. Yoler, *Advances in Astronautical Sciences,* vol. 2 (Proc., 4th Ann. Meeting, Amer. Astron. Soc., Dec. 1957), Plenum Press, N. Y., 1958, *Paper* 45, 13 pp.

The Use of Planetary Atmospheres for Propulsion, by Sterge T. Demetriades and Carl Kretschmer, *Advances in Astronautical Sciences,* vol. 2 (Proc., 4th Ann. Meeting, Amer. Astron. Soc., Dec. 1957), Plenum Press, N. Y., 1958, *Paper* 46, 14 pp.

Satellite Propulsion Systems, by W. R. Corliss and M. A. Zipkin, *Advances in Astronautical Sciences,* vol. 3 (Proc., Western Regional Meeting, Amer. Astron. Soc., Aug. 1958), Plenum Press, N. Y. 1958, *Paper* 5, 23 pp.

Laboratory Experiments in Hydromagnetic Propulsion, by Joseroy Gauger, Victor Vali and T. E. Turner, *Advances in Astronautical Sciences,* vol. 3 (Proc., Western Regional Meeting, Amer. Astron. Soc., Aug. 1958), Plenum Press, N. Y., 1958, *Paper* 7, 11 pp.

Solar Turbo-Powerplant Design, by D. B. Mackay and E. L. Leventhal, *Advances in Astronautical Sciences,* vol. 4 (Proc. 5th Ann. Meeting, Amer. Astron. Soc., Nov. 1958), Plenum Press, N. Y., 1959, pp. 129–141.

Advanced Reactor Concepts for Nuclear Propulsion, by Frank E. Rom, ASTRONAUTICS, vol. 4, Oct. 1959, pp. 20–22, 46, 48, 50.

Gaseous-Core Nuclear Rockets, by Jerry Grey, ASTRONAUTICS, vol. 4, Oct. 1959, pp. 23–25, 110, 112.

Solid-core Nuclear-Rocket Design, by Franklin P. Durham, ASTRONAUTICS, vol. 4, Oct. 1959, pp. 26–27, 102,–104.

Applications of Magnetofluidmechanics, by Theodore von Kármán, ASTRONAUTICS, vol. 4, Oct. 1959, pp. 30.

Boundary Conditions for Nuclear Propulsion, by Robert W. Bussard, ASTRONAUTICS, vol. 4, Oct. 1959, pp. 28–29, 119–122.

Plasma Propulsion of Spacecraft, by Morton Camac, ASTRONAUTICS, vol. 4, Oct. 1959, pp. 31–33, 113–115.

Cesium-Ion Propulsion, by A. T. Forrester and R. C. Speiser, ASTRONAUTICS, vol. 4, Oct. 1959, pp. 34–35, 92, 94–97.

Photon Rocket Propulsion, by Ernest Stuhlinger, ASTRONAUTICS, vol. 4, Oct. 1959, pp. 36, 69, 72.

Hybrid Propulsion Systems, by Douglas D. Ordahl, ASTRONAUTICS, vol. 4, Oct. 1959, pp. 42–43, 84.

The Payload Capabilities of Ion Propulsion Rocket Systems, by Robert H. Fox, *J. Astron. Sci.*, vol. 6, Autumn 1959, pp. 33–39.

Radiator Areas of Thermopile Generators in Space, by Douglas L. Kerr, *Aero/Space Engng., Rev.*, vol. 18, Sept. 1959, pp. 57–62.

Irreversible Thermodynamics and Kinetic Theory in the Derivations of Thermoelectric Relations, by. J. W. Leech, *Canadian J. Phys.*, vol. 37, Sept. 1959, pp. 1044–1054.

EDITOR'S NOTE: Contributions from Professors E. R. G. Eckert, J. P. Hartnett, T. F. Irvine Jr. and P. J. Schneider of the Heat Transfer Laboratory, University of Minnesota, are gratefully acknowledged.

A Multi-channel, Time-of-flight Fast-neutron Spectrometer, by A. A. Kurashov, A. F. Linev, B. V. Rynakov and V. A. Sidorov, *J. Nuclear Energy*, Pt. A, *Reactor Science*, vol. 10, no. 1/2, July 1959, pp. 85–88.

Theory of Thermoelectric Power of Ionic Crystals, II, by Eijiro Haga, *J. Phys. Soc. Japan*, vol. 14, Aug. 1959, pp. 992–996.

Experimental Studies on Plasma Jet Propulsion, by D. F. Howard, *Vistas in Astronautics*, vol. 2 (2d Annual Astron. Symposium), Pergamon Press, N. Y., 1959 (318 pp.), pp. 95–103.

A Magnetohydrodynamic Model for a Two-dimensional Magnetic Piston, by Rudolf X. Meyer, *Space Tech. Labs., TR* 59-0000-00617, March 4, 1959, 12 pp.

Radiation Pressure Confinement the Shock Pinch and Feasibility of Fusion Propulsion, by M. V. Clauser and E. S. Weibel, *Space Tech. Labs.*, 1958, 12 pp.

Recent Advances in Space Propulsion, by George S. Sutherland, ARS JOURNAL, vol. 29, Oct. 1959, pp. 698–705.

Propellants and Combustion

The Strain Analysis of Solid Propellant Rocket Grains, by M. L. Williams, *Inst. Aeron. Sci., Paper* 59-110, June 1959, 40 pp.

The Recombination Problem in a Jet Exhaust Nozzle, by William G. Browne, *Inst. Aeron. Sci., Paper* 59-105, June 1959, 16 pp.

Flight Investigation of Pentaborane Fuel in Rocket Boosted 9.75 inch-diameter Ramjet Engine With Convergent-divergent Exhaust Nozzle, by John H. Disher, *NACA Res. Mem.* E57F27, Sept. 1957, 24 pp. (Declassified from Confidential by authority *NASA TPA* 9, 9/29/59.)

Proc., Cryogenic Engng. Conf., Cambridge, Mass., Sept. 1958. Univ. of Colo., Boulder, Jan. 1959, 498 pp.

High Energy Liquid Propellants for Rockets, by G. R. Kinney, pp. 1–10.

High Performance Cryogenic Containers, by J. M. Canty and R. Gabarro, pp. 154–159.

Analytical Methods for Liquid Oxygen, by C. P. Smith, pp. 436–442.

Methods of Gaging Liquid Oxygen, by C. C. Bowersock, P. G. Campbell and R. C. Reid, pp. 443-453.

Far Infrared Spectrum of Hydrazine, by Akiko Yamaguchi, Isao Ichishima, Takehiko Shimanouchi and San-ichiro Mizushima, *J. Chem. Phys.*, vol. 31, Sept. 1959, pp. 843.

Vibrational Relaxation of CN in the Shock Tube, by W. Roth, *J. Chem. Phys.*, vol. 31, Sept. 1959, pp. 720–721.

Interactions Between Oxygen and Nitrogen: O-N, O-N_2, and O_2-N_2, by Joseph T. Vanderslice, Edward A. Mason and William G. Maisch, *J. Chem. Phys.*, vol. 31, Sept. 1959, pp. 738–746.

On the Velocity Distribution in a Chemically Reacting Gas, by R. D. Present, *J. Chem. Phys.*, vol. 31, Sept. 1959, pp. 747–750.

Simultaneous Detonation Along a Line, by J. O. Erkman, *Rev. Sci. Instr.*, vol. 30, Sept. 1959, pp. 818–820.

Analytical Comparison of Hydrazine With Primary Propellants as the Turbine Drive Fluid for Hydrogen-Fluorine and Hydrogen-Oxygen Altitude Stage Rockets, by William T. Wintucky, *NASA TN* D-78, Oct. 1959, 26 pp.

A General Method for Automatic Com-

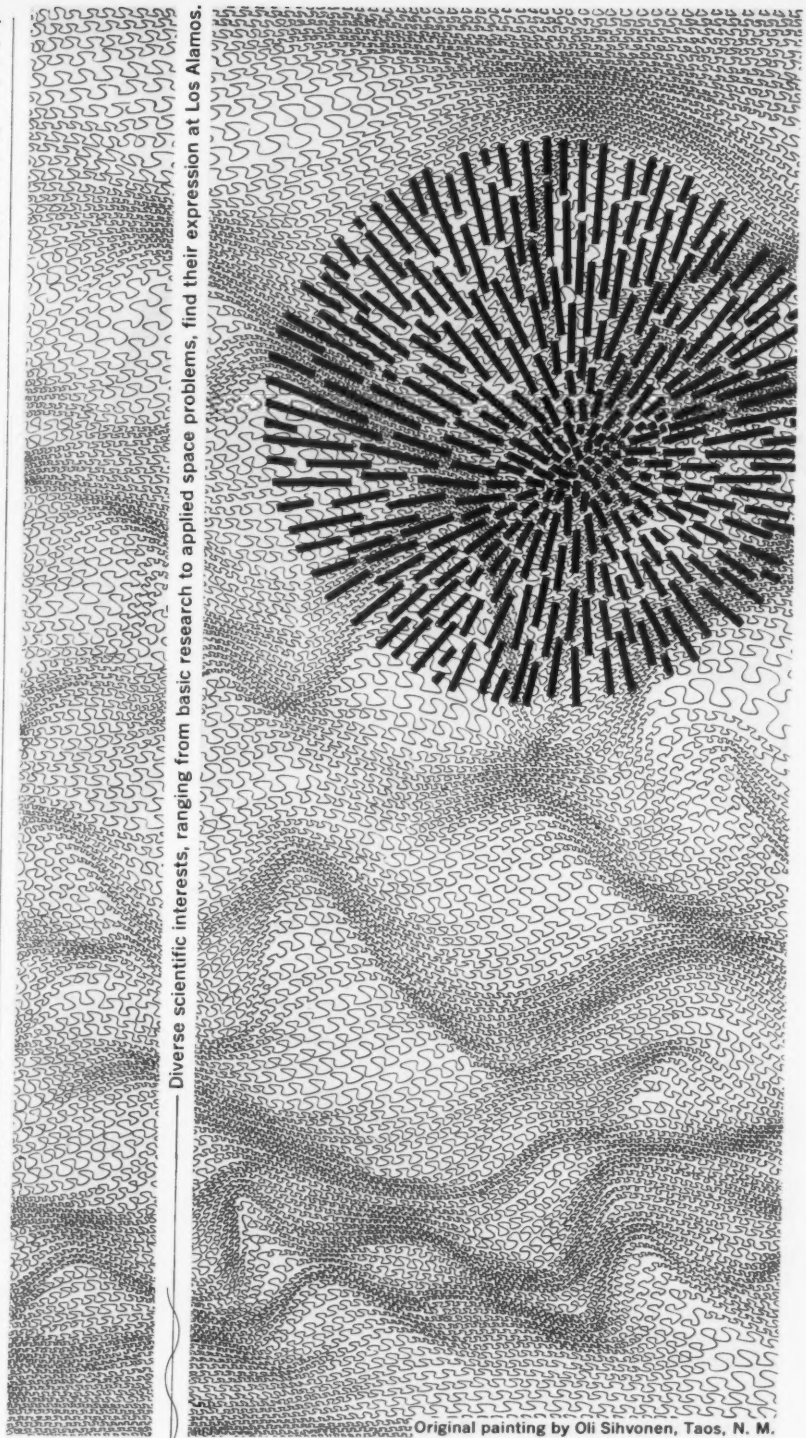
Diverse scientific interests, ranging from basic research to applied space problems, find their expression at Los Alamos.
Original painting by Oli Sihvonen, Taos, N. M.

For employment information write: Personnel Director, Department 60-11

los alamos
scientific laboratory
OF THE UNIVERSITY OF CALIFORNIA
LOS ALAMOS, NEW MEXICO

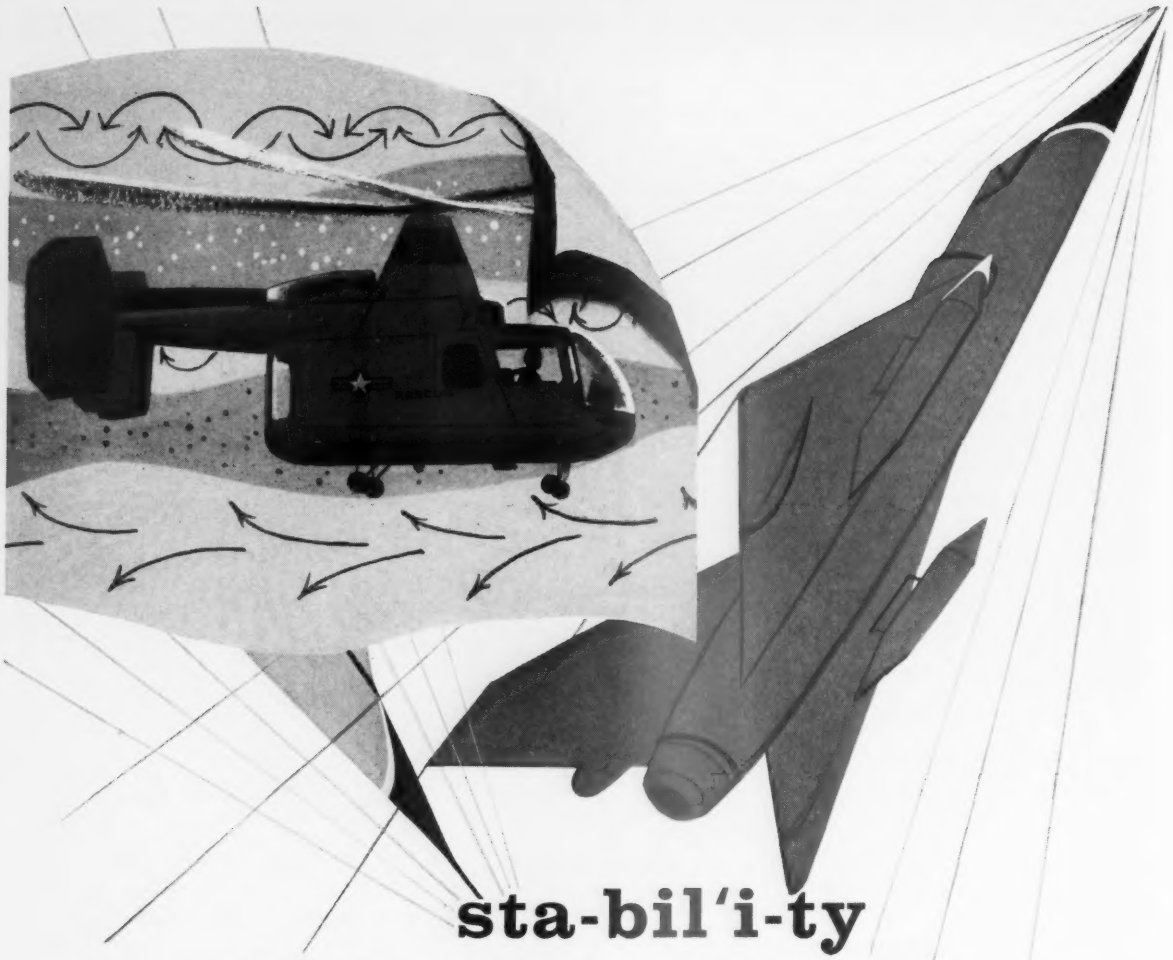

sta-bil'i-ty

World's Record #1

Bloomfield, Conn. — Air Force established new world record by flying Kaman H43-B turbine helicopter to 30,100 ft.

World's Record #2

Edwards AFB, Calif. — Air Force established new world record by flying Convair F-106 over an 18 km course twice, averaging 1,525.9 mph.

Stability augmentation from American-Standard steadies both of these record-setting vehicles. And in missiles — the Navy Terrier and Tartar; and submarines — the Polaris class, American-Standard, Military Products Division supplies gyros fundamental to accurate positioning and control.*

Company sponsored development in the Military Products Division has produced a family of gyroscopes, accelerometers and miniature components whose quality, performance and reliability make them unique in the field of navigation and stabilization systems.

Opportunities for Engineers

Winning this degree of acceptance has created new career opportunities in advanced design, production and applications engineering. American-Standard, Military Products Division, Norwood, Massachusetts.

*American-Standard and Standard® are trademarks of American Radiator & Standard Sanitary Corporation.

American-Standard
MILITARY PRODUCTS DIVISION

putation of Equilibrium Compositions and Theoretical Rocket Performance of Propellants, by Sanford Gordon, Frank J. Zeleznik and Vearl N. Huff, *NASA TN* D-132, Oct. 1959, 161 pp.

Studies on Deflagration to Detonation in Propellants and Explosives, by C. M. Mason, F. C. Gibson, C. R. Summers and F. H. Scott, *Bur. Mines, Div. Explosives, Tech. Quart. Rep.*, April 1, 1959–June 30, 1959, 6 pp., 4 figs.

Annual Review of Physical Chemistry, vol. 10, ed. by H. Eyring, C. J. Christiansen and H. S. Johnston, Annual Reviews Inc., Palo Alto, Calif., 1959, 537 pp.

Thermochemistry and Thermodynamic Properties of Substances, by J. M. Sturtevant, pp. 1–30.

The Kinetics of Reaction in Gases, by A. F. Trotman-Dickenson, pp. 53–76, 163 refs.

Trapped Energetic Radicals, by J. L. Franklin and H. P. Broida, pp. 145–168, 198 refs.

High Temperature Chemistry, by J. L. Margrave, pp. 457–586, 533 refs.

Free-radical Fuels—A Tough Problem, by John M. Flournoy, ASTRONAUTICS, vol. 4, Oct. 1959, pp. 44, 106.

Water May Have Rocket Power Use, *Aviation Week*, vol. 71, Oct. 12, 1959, pp. 59, 61.

Recombination of Atoms at Surfaces, *Trans., Faraday Soc.*, vol. 55, Aug. 1959.

Part 4. Theory of Method and Measurement of Atom Concentrations, by J. C. Greaves and J. W. Linnett, pp. 1338–1345.

Part 5. Oxygen Atoms at Oxide Surfaces, by J. C. Greaves and J. W. Linnett, pp. 1346–1354.

Part 6. Recombination of Oxygen Atoms on Silica from 20°C to 600°C, by J. C. Greaves and J. W. Linnett, pp. 1355–1361.

Steady State Flow of Detonating Gas Around a Cone, by S. S. Kvashnina and G. G. Chernyi, *PMM: J. Appl. Math. and Mech.* (trans. of *Prikladnaya Mathematika i Mekhanika*), vol. 23, no. 1, 1959, pp. 252–259.

An Investigation of the Ignition Temperatures of Solid Metals, by W. C. Reynolds, *Stanford Univ., Mech. Engng. Dept., Summary Report*, June 15, 1957, 76 pp.

An Investigation of the Ignition Temperatures of Solid Metals, by W. C. Reynolds and J. J. Williams, *Stanford Univ., Dept. Mech. Engng., Tech. Rep.* 1, Aug. 15, 1956, 130 pp.

Production and Measurement of Single Drops, Sprays, and Solid Suspensions, by James A. Browning, reprinted from *Advances in Chemistry Series* 20 (*Amer. Chem. Soc.*), Washington, D. C. 1958, pp. 136–154.

Field Experiments on Treatment of Fluorine Spills with Water or Soda Ash, by R. James Rollbuhler, George R. Kinney and Lorenz C. Leopold, *NASA TN* D-63, Sept. 1959, 14 pp.

Two Cases of Unstable Combustion, by K. I. Shchelkin, *Soviet Phys.–JETP*, vol. 63(9), no. 2, Aug. 1959, pp. 416–420.

Plasma—A Substitute for the Oxy-fuel Flame, by James A. Browning, *Welding J.*, vol. 38, Sept. 1959, pp. 870–875.

Study of Additive Effects of Solid Propellant Burning, by Herman Burwasser, *AeroChem Res. Labs., Inc., TM*-14, July 1959, 7 pp.

Combustion of Elemental Boron, by *Experiment Inc.*, Quarter. Summary Rep. for Feb. through April 1959, *TM*-1105, May 1959, 11 pp.

Thermal Functions and Heats of Formation of Some of the Major Vapor Species in the Boron-Oxygen-hydrogen System at Elevated Temperatures, by D. White, P. N. Walsh, D. E. Mann and A. Somer, *Ohio State Univ., Res. Found. RF Proj.* 691, *Tech. Rep.* 4, July 1959, 21 pp.

Mechanisms of the Autodecomposition of Liquid Acetylenic Monopropellants, *Experiment Inc.*, Quart. Progr. Rep. for April through June 1959, *TM*-1102, July 1959, 9 pp.

Comparison of Hydrazine-Nitrogen Tetroxide and Hydrazine-Chlorine Trifluoride in Small-scale Rocket Chambers, by R. James Rollbuhler and William A. Tomazic, *NASA TN* D-131, Oct. 1959, 16 pp.

Infrared Emission Spectra of Gaseous B_2O_3, Frequency Assignment and Thermal Function, by D. White, D. E. Mann, P. N. Walsh and A. Sommer, *Ohio State Univ., Res. Found, RF Proj.* 691, *Tech. Rep.* 2, June 1959, 27 pp.

Structure of Hydrocarbon (C_2) - Oxygen Flames, by R. M. Fristrom, W. H. Avery, and C. Grunfelder, *Johns Hopkins Univ., Appl. Phys. Lab., Bumblebee Rep.* 283, 1959 (65 pp.), pp. 29–34.

Study of Oscillatory Flame Velocity in Combustion, by Carl A. Zierman, *Inst. Aeron. Sci., 1959 First Award Papers, IAS Student Branch Papers Competition*, Inst. Aeron. Sci., N. Y., 1959 (227 pp.), pp. 216–227

Control of Solid Propellant Burning Rates by Acoustic Energy, by Martin Summerfield, ARS JOURNAL, vol. 29, Oct. 1959, pp. 791–792.

Abnormal Excitation of OH in $H_2/O_2/N_2$ Flames, by Walter E. Kaskan, *J. Chem. Phys.*, vol. 31, Oct. 1959, pp. 944–956.

Method for the Study of Deflagration to Detonation Transition, by Frank C. Gibson, Merle L. Bowser and Charles M. Mason, *Rec. Sci. Instr.*, vol. 39, Oct. 1959, pp. 916–919.

Theory of Flames Produced by Unimolecular Reactions, I: Accurate Numerical Solutions, by Joseph O. Hirschfelder and Alan McCone Jr., *Phys. Fluids*, vol. 2, no. 5, Sept.-Oct. 1959, pp. 551–564.

Theory of Flames Produced by Unimolecular Reactions, II: Ignition Temperature and Other Types of Approximations, by Joseph O. Hirschfelder, *Phys. Fluids*, vol. 2, no. 5, Sept.-Oct. 1959, pp. 565–574.

Choosing Filter Media for Liquid Propellants, by Gerald J. Harman, *Space/Aeron.*, vol. 32, Nov. 1959, pp. 135–136, 138.

Converging Cylindrical Detonation Wave, by Ya. B. Zel'dovich., *Soviet Phys.–JETP*, vol. 36 (9), no. 3, Sept. 1959, pp. 550–554.

Investigation of Ignition Temperatures of Solid Metals, by W. C. Reynolds. *NASA TN* D-182, Oct. 1959, 71 pp.

Proc. Cryogenic Engng. Conf., Cambridge, Mass., Sept. 1958, Univ. of Colo., Boulder, Jan. 1959, 498 pp.

Design Study of Liquid Oxygen Pumping Systems for Missile Fueling Incorporating Vented Storage Tanks, by T. A. Carter Jr. and C. R. Crusan, pp. 218–230.

High Pressure Pumping Equipment for Cryogenic Liquids, by C. F. Gottzmann and A. H. Halcombe, pp. 231–240.

Pumping of Liquid Hydrogen, by G. Caine, L. Schafer and D. Burgeson, pp. 241–254.

sta-bil'i-ty

A note for talented engineers:

Stability at American-Standard is the result of dynamic action and can mean a lot in terms of professional growth at the expanding Military Products Division.*

The logical growth from the projects already in the house extends a tremendous challenge. And, the "off-site" advantages are as stimulating as the in-plant creative environment.

To repeat them just for the record; Residential Boston suburb, excellent benefits, relocation assistance, company-sponsored education, and the wide cultural and recreational attractions of the area.

Footnote: Excellent salaries for qualified engineers in both our Systems and Components Departments.

Please submit resume to

Mr. J. A. Reardon,
Employment Manager,
American-Standard
Military Products Division,
Norwood, Massachusetts

*American-Standard and Standard ® are trademarks of American Radiator & Standard Sanitary Corporation.

AMERICAN-Standard
MILITARY PRODUCTS DIVISION

Comparison and Correlation of Centrifugal Pump Cavitation Test Results Handling Liquid Oxygen and Water, by T. A. Carter Jr., C. R. Crusan and F. Thodal, pp. 255–263.

An Analysis of Dual-phase Flow at the Inlet to a Centrifugal Cryogenic Pump, by S. Prelowski and G. H. Caine, pp. 264–271.

Measurement of the Flow of Liquefied Gases with Sharp-edge Orifices, by R. J. Richards, R. B. Jacobs and W. J. Pestalozzi, pp. 272–285.

Atmospheric Heat Transfer to Vertical Tanks Filled with Liquid Oxygen, by F. E. Ruccia and C. M. Mohr, pp. 307–318.

A Vacuum-insulated Transfer Line for Liquified Gases, by D. H. Tantum and F. Farrar, pp. 326–334.

Economic and Design Considerations for a 650-foot High Vacuum Insulated Transfer Line, by P. D. Fuller and W. R. Peary, pp. 335–341.

Pressurized Transfer of Cryogenic Liquids, by D. C. Bowersock, R. W. Gardner and R. C. Reid, pp. 342–356.

Pressurized Cooldown of Cryogenic Transfer Lines, by J. C. Burke, W. R. Byrnes, A. H. Post and F. E. Ruccia, pp. 378–395.

Pressurized Discharge of Liquid Nitrogen from an Uninsulated Tank, by G. J. VanWylen, S. K. Fenester, H. Merte Jr. and W. A. Warren, pp. 395–402.

Ultrasonic Gaging of Cryogenic Liquids, by P. Turkheimer, pp. 403–409.

Some Methods for Reducing Heat Leak through Support Members in Liquified Gas Storage Vessels, by R. W. Arnett, L. O. Mullen and K. A. Warren, pp. 410–417.

Wide-range Cryostat Temperature Control, by R. D. Goodwin, pp. 487–495.

Materials and Structures

Feasibility of Titanium for Welded Missiles, by Carl E. Hartbower, George M. Orner and Daniel M. Daley, *Welding J.*, vol. 38, Sept. 1959, pp. 345-s–352-s.

The Structural Design of Maximum-area Astronautical Vehicles, by George A. Hoffman, *Inst. Aeron. Sci., Paper* 59-89, June 1959, 17 pp.

Selection of Materials for Hypersonic Leading Edge Applications, by Frank M. Anthony and Harry A. Pearl, *Inst. Aeron. Sci., Paper* 59-111, June 1959, 44 pp., diagrs.

Exploratory Materials and Missile-nose-shape Tests in a 4,000°F Supersonic Air Jet, by Paul E. Purser and Russell N. Hopko, *NACA Res. Mem.* L56J09, Dec. 1956, 11 pp., diagrs., photos. (Declassified from Confidential by authority *NASA TPA* 9, 9/29/59.)

Exploratory Tests of the Behavior of Several Materials in a Supersonic Air Jet at 4,000°F, by Russell N. Hopko and Otto F. Trout Jr., *NACA Res. Mem.* L57E24, July 1957, 13 pp., diagrs., photos. (Declassified from Confidential by authority *NASA TPA* 9, 9/29/59.)

Proc., Cryogenic Engng. Conf., Cambridge, Mass., Sept. 1958, Univ. of Colo., Boulder, Jan. 1959, 498 pp.

Compatibility of Materials with Liquid Oxygen, by H. M. Peckham and R. L. Hauser, pp. 26–46.

Wear and Friction in Liquid Nitrogen with Austenitic Stainless Steel Having Various Surface Coatings, by D. W. Wisander and R. L. Johnson, pp. 71–83.

The Stability of Austenitic Stainless Steels at Low Temperatures as Determined by Magnetic Measurements, by R. P. Reed and R. P. Mikesell, pp. 84–100.

The Tensile and Impact Strength of Annealed and Welded 5086 Aluminum down to 20°K, by R. P. Mikesell and R. P. Reed, pp. 101–113.

Mechanical Testing of Aluminum Weldments, by S. A. Nuccitelli and M. W. Motes Jr., pp. 114–122.

Ductile Ceramics, I: Factors Affecting the Plasticity of Sodium Chloride, Lithium Fluoride, and Magnesium Oxide Single Crystals, by Carl A. Sterns, Ann E. Pack and Robert A. Lad, *NASA TN* D-75, Oct. 1959, 43 pp.

Ductile Ceramics, II: Introductory Study of Ductility in Polycrystalline Sodium Chloride and Magnesium Oxide, by Charles E. May, *NASA TN* D-76, Oct. 1959, 22 pp.

Beryllium: Promising Metal of the Space Age, by Reginald E. Foster and Louis A. Riedinger, *Advances in Astronautical Sciences*, vol. 2 (Proc., 4th Ann. Meeting, Amer. Astron. Soc., Dec. 1957), Plenum Press, N. Y., 1958, *Paper* 3, 12 pp.

Structural Aspects of Earth Glide Reentry Vehicles, by Max T. Braun and Edwin G. Czarnecki, *Advances in Astronautical Sciences*, vol. 3, (Proc., Western Regional Meeting, Amer. Astron. Soc., Aug. 1958), Plenum Press, N. Y., 1958, *Paper* 9, 9 pp.

Lubrication Problems in Space Vehicles, by Martin M. Freundlich and Arthur D. Robertson, *Advances in Astronautical Sciences*, vol. 4 (Proc., 5th Ann. Meeting, Amer. Astron. Soc., Nov. 1958), Plenum Press, N. Y., 1959, pp. 142–153.

Radiation Effects on Materials and Systems, by Richard E. Bowman and Carl J. Lyons, *Battelle Tech. Rev.*, vol. 8, Oct. 1959, pp. 8–12.

The Heat Protection Potential of Several Ablation Material for Satellite and Ballistic Re-entry into Earth's Atmosphere, by N. S. Diaconis, J. B. Fanucci and G. W. Sutton, *General Electric, Missile and Space Vehicle Dept., Aerosci. Lab., R59 SD 423* (TIS) Sept. 1959, 28 pp.

Selected Abstracts on the Mechanical Behavior of Ceramics, by Hayne Palmour, III, W. W. Kriegel, J. J. DuPlessis and G. O. Harrell, *North Carolina State College, Engng. School Bull.* 73, July 1959, 151 pp.

Research Program on High Vacuum Friction, *Litton Industries, Space Res. Labs. Final Rep. Pub.* 1023 March 30-1959, 122 pp., diagrs. (*AFOSR Rep.* TR-59-97).

Evaluation of Protective Coatings for Molybdenum Nozzle Guide Vanes, by John R. Ciancola, *Wright Air Dev. Center, TN* 58-241, June 1959, 39 pp. (*ASTIA AD* 215 442).

Thin-walled Compression Members, by A. Pflüger, *Hannover Tech. Hochschule, Inst. für Statik, Report* No. 2, July 1959, 14 pp. (AFOSR TR 59–138).

The Applicability of Sandwich Construction to Missile Shapes, by Joseph S. Pratt, *Inst. Aeron. Sci., 1959 First Award Papers*, 1959 (227 pp.), pp. 109–119.

High-temperature Tensile Properties of Wrought Sintered Tungsten, by Paul F. Sikora and Robert W. Hall, *NASA TN* D-79, Sept. 1959, 16 pp.

Fluid Dynamics, Heat Transfer and MHD

Atomization in High Velocity Airstreams, by Malcolm A. Weiss and Charles H. Worsham, ARS JOURNAL, vol. 29, April 1959, pp. 252–259.

Reflection of Weak Shock Waves from Nozzles With No Flow and Critical Flow, by Charles E. Feiler, ARS JOURNAL, vol. 29, April 1959, pp. 272–274.

Particle Impaction on Spheres at High Mach Numbers, by S. K. Friedlander, ARS JOURNAL, vol. 29, April 1959, pp. 296–297.

Simple Analytical Approximation to the Equation of State of Dissociated Air, by W. L. Bade, ARS JOURNAL, vol. 29, April 1959, pp. 298–299.

Microwave Measurement of Dielectric Properties under Extreme Thermal Environments, by D. M. Bowie and J. J. Huminik Jr., *Industrial Labs.*, vol. 10, May 1959, pp. 42–47.

Impulse from an Exploding Wire Plasma Accelerator, by W. L. Starr, *J. Appl. Phys.*, vol. 30, April 1959, p. 594.

The Propagation of Small Disturbances in Hydromagnetics, by G. S. S. Ludford, *J. Fluid Mech.*, vol. 5, April 1959, pp. 387–400.

Chemically Frozen Boundary Layers with Catalytic Surface Reaction, by Daniel E. Rosner, *J. Aero/Space Sci.*, vol. 26, May 1959, pp. 281–286.

The Matching of the Viscid and Inviscid Regions for the Stagnation Magnetic Flow, by Paul S. Lykoudis, *J. Aero/Space Sci.*, vol. 26, May 1959, pp. 315–316.

Oscillations of a Finite Cold Plasma in a Strong Magnetic Field, by John Dawson and Carl Oberman, *Phys. Fluids*, vol. 2, March–April 1959, pp. 103–111.

Theory of Electrostatic Probes in a Low-density Plasma, by Ira B. Bernstein and Irving N. Rabinowitz, *Phys. Fluids*, vol. 2, March–April 1959, pp. 112–120.

Some Exact Solutions of the Navier-Stokes and the Hydromagnetic Equations, by William C. Meecham, *Phys. Fluids*, vol. 2, March–April 1959, pp. 121–124.

Inhibition of Hydrodynamic Instability by an Electric Current, by Chia-Shun Yih, *Phys. Fluids*, vol. 2, March–April 1959, pp. 125–130.

Equilibrium Statistical Mechanics of Dissociating Diatomic Gases, by Leon Heller, *Phys. Fluids*, vol. 2, March–April 1959, pp. 147–152.

Optical Refractivity of High-temperature Gases, I: Effects Resulting from Dissociation of Diatomic Gases, by Ralph A. Alpher and Donald R. White, *Phys. Fluids*, vol. 2, March–April 1959, pp. 153–161.

Optical Refractivity of High-temperature Gases, II: Effects Resulting from Ionization of Monatomic Gases, by Ralph A. Alpher and Donald R. White, *Phys. Fluids*, vol. 2, March–April 1959, pp. 162–169.

Interferometric Measurement in the Shock Tube of the Dissociation Rate of Oxygen, by D. L. Matthews, *Phys. Fluids*, vol. 2, March–April 1959, pp. 170–178.

Evaporation into a Boundary Layer, II: Dissociation in Evaporation, by Ernest Bauer and Martin Zlotnick, *Phys. Fluids*, vol. 2, March–April 1959, p. 236.

Second Approximations for the Stress Tensor and the Heat Flux in a Gas, by Hsun-Tiao Yang, *Phys. Fluids*, vol. 2, March–April 1959, p. 237.

Thermal Instability of Viscous Fluids, by Chia-Shun Yih, *Quart. Appl. Math.* vol. 17, no. 1, April 1959, pp. 25–42.

NORTHWESTERN UNIVERSITY PRESS

Announces the Publication of

The Dynamics of Conducting Gases

PROCEEDINGS OF THE THIRD BIENNIAL GAS DYNAMICS SYMPOSIUM

Edited by Ali Bulent Cambel, Northwestern University, and John B. Fenn, ONR Project Squid and Co-sponsored by Northwestern University and the American Rocket Society

IN THE FIELD of power production, propulsion and flight, the use of conducting gases, namely plasmas, has become an important central problem. Among the various aspects of interest to engineers and scientists are the properties and the dynamics of plasmas as well as the interaction between the fluid dynamic and the electromagnetic fields.

In the Proceedings of the Third Biennial Gas Dynamics Symposium, 19 papers on the physics of plasmas, magneto gas dynamics, plasma phenomenology and the various engineering applications associated with conducting gases are presented.

THE DYNAMICS OF CONDUCTING GASES will be significant to scientists and engineers in universities, government establishments and industrial laboratories. The theories proposed, the experimental techniques outlined and the applications which are proposed should be of interest to persons in the flight sciences and the power production fields.

7" x 9¾", 224 pages, 190 illust., $12.50

Contents

PART ONE: FUNDAMENTAL PROCESS AND IONIZED GAS PROPERTIES

W. P. ALLIS and S. J. BUCHSBAUM: *The Conductivity of an Ionized Gas in a Magnetic Field*

R. A. GROSS and C. L. EISEN: *Some Properties of a Hydrogen Plasma*

I. PRIGOGINE: *The Statistical Mechanics of the Approach to Equilibrium in Gases*

RADU BALESCU: *Irreversible Processes in a Plasma: Effect of Long Range Forces*

H. F. CALCOTE: *Relaxation Processes in Plasma*

PART TWO: THEORETICAL CONSIDERATIONS ON THE INTERACTION OF MAGNETIC FIELDS AND FLOWS OF IONIZED GASES

W. R. SEARS: *Some Solutions of the Macroscopic Equations of Magnetohydrodynamics*

RUDOLPH X. MEYER: *Magnetohydrodynamics in the Limit of Small Inertial Forces*

F. D. HAINS, YUSUF A. YOLER and EDWARD EHLERS: *Axially Symmetric Hydromagnetic Channel Flow*

PART THREE: LABORATORY EXPERIENCE WITH THE FLOW OF IONIZED GASES

WINSTON H. BOSTICK, JOHN NANKIVELL, SAMUEL KOSLOV and GEORGE SCHMIDT: *Experimental Studies on Plasma Dynamics*

JAMES A. BROWNING: *Techniques for Producing Plasma Jets*

RICHARD W. ZIEMER: *Electromagnetic Shock Tubes*

M. CAMAC and G. S. JANES: *Applied Magnetohydrodynamics at Avco-Everett Research Laboratory*

PART FOUR: APPLICATIONS OF MAGNETO GAS DYNAMICS EFFECTS

JOSEPH L. NEURINGER: *Optimum Power Generation Using a Plasma as the Working Fluid*

MARK L. GHAI: *Space Propulsion Engines—A Problem in Production of High Velocity Gases*

ALFRED E. KUNEN and WILLIAM MCILROY: *The Electromagnetic Pinch Effect for Space Propulsion*

ROBERT V. HESS and KARLHEINZ THOM: *Plasma Acceleration by Guided Microwaves*

GEORGE P. WOOD and ARLEN F. CARTER: *Considerations in the Design of a Steady DC Plasma Accelerator*

AEROTHERMOCHEMISTRY, edited by Donald K. Fleming. Proceedings of the First Biennial Gas Dynamics Symposium. $5.00

TRANSPORT PROPERTIES IN GASES, edited by Ali Bulent Cambel and John B. Fenn. Proceedings of the Second Biennial Gas Dynamics Symposium. $7.50

ORDER FORM

Please send me —— copy (copies) of THE DYNAMICS OF CONDUCTING GASES (*$12.50 list price*)

NAME ——————————

ADDRESS ——————————

CITY —————— ZONE —— STATE ——————

Payment encl. ☐ Please bill ☐

NORTHWESTERN UNIVERSITY PRESS
1840 Sheridan Road, Evanston, Ill.

Recording Optical Pyrometer, by Norman A. Blum, *Rev. Sci. Instr.*, vol. 30, April 1959, pp. 251–253.

Vacuum-type Gas Flow Calibrator, by William A. Strauss and Rudolph Edse, *Rev. Sci. Instr.*, vol. 30, April 1959, pp. 258–261.

Shock Wave Propagation in an Infinitely Electrically Conductive Gas with Transverse Magnetic Field and Gravitation, by S. I. Pai, *Zeitschrift fur Angewandte Mathematik und Mechanik*, vol. 39, Jan.-Feb. 1959, pp. 40–49.

Asymptotic Laws of Turbulent Spreading of Hot Air Streams into Moving and Quiet Surrounding Air, by W. Szablewski, *Zeitschrift fur Angewandte Mathematik und Mechanik*, vol. 39, Jan.-Feb. 1959, pp. 50–67. (In German.)

Unsteady Boundary Layer Behind Condensation Shocks and Expansion Waves, by E. Becker, *Zeitschrift fur Flugwissenschaften*, vol. 7, March 1959, pp. 61–72. (In German.)

Performance Characteristics of Several Types of Axially Symmetric Nose Inlets at Mach Number 3.85, by James F. Connors and Richard R. Woolett, *NACA RM* E52I15, Nov. 1952, 42 pp. (Declassified from Confidential by authority of *NASA Pub. Ann.* 4, p. 18, 3/16/59).

Experimental Investigation of Methods of Improving Diffuser-exit Total-pressure Profiles for a Side-inlet Model at Mach Number 3.05, by Thomas G. Piercy and John L. Klann, *NACA RM* E55F24, Aug. 1955, 42 pp. (Declassified from Confidential by authority of *NASA Pub. Ann.* 4, p. 21, 3/16/59.)

Performance Comparison at Supersonic Speeds of Inlets Spilling Excess Flow by Means of Bow Shock, Conical Shock or Bypass, by J. L. Allen and Andrew Beke, *NACA RM* E53H11, Oct. 1953, 20 pp. (Declassified from Confidential by authority of *NASA Pub. Ann.* 4, p. 18, 3/16/59.)

Problems of Performance and Heating of Hypersonic Vehicles, by H. Julian Allen and Stanford E. Neice, *NACA RM* A55L15, March 1956, 20 pp. (Declassified from Confidential by authority of *NASA Pub. Ann.* 4, p. 17, 3/16/59.)

Application of the Hypersonic Similarity Rule to Conical Flow of Dissociated Air, by Mary F. Romig, *Aero/Space Engng.*, vol. 18, March 1959, pp. 56–59, 75.

Gas Flow Tables, by C. J. Wang, J. B. Peterson and R. Anderson, *Ramo-Wooldridge Corp., Guided Missile Res. Div.*, GM-TR-154, March 1958.

Viscous Hypersonic Similitude, by Wallace D. Hayes and Ronald F. Probstein, *Inst. Aeron. Sci., Rep.* 59–63, Jan. 1959, 44 pp.

Viscous Aerodynamic Characteristics in Hypersonic Rarefied Gas Flow, by Ronald F. Probstein and Nelson H. Kemp, *Inst. Aeron. Sci., Rep.* 59–62, Jan. 1959, 48 pp.

Aerodynamic Ablation of Melting Bodies, by Theodore R. Goodman, *3rd Nat. Congr. Appl. Mech., Proc., New York, ASME*, 1958, pp. 735–746.

Hypersonic Stagnation Point Heat Transfer to Surfaces Having Finite Catalytic Efficiency, by Sinclaire M. Scala, *3rd Nat. Congr. Appl. Mech., Proc., New York, ASME*, 1958, pp. 799–806.

Performance Analysis of Plug Nozzles for Turbojet and Rocket Exhausts, by W. H. Krase, *Rand Corp.*, P-1506, Sept. 1958, 27 pp.

Behavior of a Plasma under Rapidly Changing Conditions, by R. Rompe and H. Rother, *Annalen der Physik*, vol. 3, nos. 1–2, 1959, pp. 28–36. (In German.)

Recent Advances in Cryogenic Engineering, by Robert B. Jacobs, ARS JOURNAL, vol. 29, April 1959, pp. 245–251.

Methods of Calculating Fundamental Solutions of the Wave Equation, with Tables, by William A. Mersman, *NASA TN* D-86, Oct. 1959, 129 pp.

A Numerical Comparison between Exact and Approximate Theories of Hypersonic Inviscid Flow Past Slender Blunt-nosed Bodies, by Saul Feldman, *Avco-Everett Res. Lab. Rep. 71*, June 1959, 19 pp.

Blunt Nose and Real Fluid Effects in Hypersonic Aerodynamics, by Andrew F. Burke, *Inst. Aeron. Sci., Paper* 59-114, June 1959, 37 pp.

Nonequilibrium Flow in Gas Dynamics, by T. Y. Li, *Rensselaer Polytech. Inst., TR AE* 5901, May 1959, 54 pp., 35 refs. (*AFOSR TN* 59-389; *ASTIA AD* 213 893).

Study of Supersonic Flows with Chemical Reactions, III: Experiments on the Departure from Chemical Equilibrium in a Supersonic Flow, by Peter P. Wegener, *Calif. Inst. Tech., Jet Prop. Lab., Progr. Rep.* 20-388, June 1959, 15 pp.

An Interferometric Study of Shock Tube Boundary Layers, by John R. Ashbridge, *Lehigh Univ., Inst. Res., Tech. Rep.* 14, April 1959, 97 pp.

Theory of Flow in the Magnetic Annular Shock Tube, by Nelson H. Kemp and Harry E. Petschek, *Avco-Everett Res. Lab. Rep.* 60, July 1959, 35 pp.

The Wave Motions of Small Amplitude in Radiation-electro-magneto-gas Dynamics, by S. I. Pai and A. I. Speth, *Maryland Univ., Inst. Fluid Dynam. and Appl. Math., TN* BN-180, 19 pp.

The Effect of Velocity of Motion of a Fluid on Heat Transfer During Boiling, by N. G. Styushchin and L. S. Sterman (trans. from *Zhyrnal Tekhnicheskoi Fiziki*, vol. 21, 1951, pp. 448–452), *Atomic Energy Comm., Trans.* AEC TR-1781, Dec. 1951, 11 pp.

A Continuous High Temperature Gas Flow Facility for Magnetohydrodynamic Studies, by Vernon H. Blackman, *Plasmadyne Corp.*, Santa Ana, Calif., T-ITNO69-334, June 1959, 46 pp. (*AFOSR-TN*-59-681).

An Experimental Investigation of Hypersonic Stagnation Temperature Probes, by Richard D. Wood, *Calif. Inst. Tech., Guggenheim Aeron. Lab., Hypersonic Res. Proj., Memo* 50, July 1959, 90 pp.

Aerothermodynamic and Electrical Properties of Some Gas Mixtures to Mach 20, by W. Chinitz, C. L. Eisen and R. A. Gross, *Fairchild Engine Div.*, Deer Park, N. Y., Oct. 1958, 15 pp.

Thermal Diffusivity of Nitrogen as Determined by the Cyclic Heat Transfer Method, by W. B. Harrison, Final Report, Project B-109, ASME, Oct. 1959–June 1958, *Georgia Inst. Tech., Engng. Expt. Sta.*, 1959, 26 pp., 14 figs.

Equilibrium in a Toroidal System, by Harold R. Koenig, *AEC, Princeton Univ., Proj. Matterhorn*, NYO-8054, Jan. 1959, 70 pp.

Some Hydromagnetic Equilibria, by John L. Johnson and John M. Green, *Princeton Univ., Proj. Matterhorn*, Matt-5, April 23, 1959, 5 pp.

Advances in Astronautical Sciences, vol. 2, (Proc., 4th Ann. Meeting, Amer. Astron. Soc., Dec. 1957), Plenum Press, N. Y., 1958.

On the Generation of Temperatures to 30,000°K, by Peter E. Glaser, *Paper* 35, 11 pp., 31 refs.

Prediction of Cratering Caused by Meteoroid Impacts, by Maury Kornhauser, *Paper* 33, 12 pp.

Advances in Astronautical Sciences, vol. 3 (Proc., Western Regional Meeting, Amer. Astron. Soc., Aug. 1958), Plenum Press, N. Y., 1958.

Manned Cabin Surface Temperatures and Heat-Transfer Rates for a Re-entry Hypersonic Glide Vehicle, by T. E. Mouritsen, *Paper* 3, pp. 1–13.

Problems of Re-entry into the Earth's Atmosphere, by Alfred C. Robinson, *Paper* 33, 23 pp.

Advances in Astronautical Sciences, vol. 4 (Proc., 5th Annual Meeting, Amer. Astron. Soc., Nov. 1958), Plenum Press, N. Y., c. 1959.

Heat Transfer in High-speed Slip Flow, by Richard A. Oman and Richard A. Scheuing, pp. 19–36.

Discontinuity Surfaces in Magneto-fluid-dynamics, by Luigi G. Napolitano, pp. 51–73.

A Study of Entry into the Earth's Atmosphere, by Douglas Cross, pp. 74–85.

On Circulation in Relativistic Hydrodynamics, by A. H. Taub, *Archive for Rational Mech. and Analysis*, vol. 3, no. 4, April 8, 1959, pp. 312–324.

The Thermal Conductivities of Mixtures of Rare Gases at 29°C and 520°C, by H. von Ubisch, *Arkiv. für Fysik*, vol. 16, no. 1, 1959, pp. 93–100.

Hydromagnetic Equilibrium, III: Axisymmetric Incompressible Media, by L. Woltjer, *Astrophys. J.*, vol. 13, Sept. 1959, pp. 400–406.

Hydromagnetic Equilibrium, IV: Axisymmetric Compressible Media, by L. Woltjer, *Astrophys. J.* vol. 13, Sept. 1959, pp. 405–413.

Method of Determining Coefficients in Flows, II, by F. Grün and B. Marzetta, *Helvetica Physica Acta*, vol. 32, no. 4, Aug. 1959, pp. 339–348. (In German.)

The Theory of Electromagnetically Driven Shock Waves, by J. K. Wright and M. C. Black, *J. Fluid Mech.*, vol. 6, Aug. 1959, pp. 289–301.

Compressible Turbulent Boundary Layers with Heat Transfer and Pressure Gradient in Flow Direction, by Alfred Walz, *J. Res. Nat. Bur. Standards*, vol. 63B, July-Sept. 1959, pp. 53–70.

Magnetodynamics of Plane and Axisymmetric Flows of a Gas with Infinite Electric Conductivity, by M. N. Kogan, *PMM: J. Appl. Math & Mech.* (trans. of *Prikladnaya Matematika i Mekhanika*), vol. 23, no. 1, 1959, pp. 92–106.

Analysis of Weak Discontinuities in Magnetohydrodynamics, by V. N. Zhigulev, *PMM: J. Appl. Math. & Mech.* (trans. of *Prikladnaya Matematika i Mekhanika*), vol. 23, no. 1, 1959, pp. 107–113.

On the Reflection of Weak Discontinuities from the Throat of a Laval Nozzle, by O. S. Ryzhov and S. Iu. Cherniavskii, *PMM: J. Appl. Math. & Mech.* (trans. of *Prikladnaya Matematika i Mekhanika*), vol. 23, no. 1, 1959, pp. 114–122.

The Solution of the Equation of Magnetohydrodynamics Describing the One-dimensional Axisymmetrical Motion of a Gas in a Gravitational Field, by E. V. Riazanov, *PMM: J. Appl. Math. & Mech.* (trans. of *Prikladnaya Matematika i Mekhanika*), vol. 23, no. 1, 1959, pp. 260–265.

On the Similarity of Hypersonic Viscous Gas Flows Around Slender Bodies,

by V. V. Luniev, *PMM: J. Appl. Math & Mech.*, (trans. of *Prikladnaya Matematika i Mekhanika*), vol. 23, no. 1, 1959, pp. 273–280.

Selfsimilar Motions of Gas with Shock Waves, Spreading with Constant Speed into a Gas at Rest, by G. L. Grodzovskii, A. N. Diukalov, V. V. Tokarev and A. I. Tolstykh, *PMM: J. Appl. Math. & Mech.*, (trans. of *Prikladnaya Matematika i Mekhanika*), vol. 23, no. 1, 1959, pp. 281–286.

Growth of Electron Space-charge and Radio Waves in Moving Ion Streams, by R. Q. Twiss, *Phil. Mag.*, vol. 4, July 1959, pp. 868–874.

Superconductivity of a Charged Ideal 2-Dimensional Bose Gas, by R. M. May, *Phys. Rev.*, vol. 115, July 15, 1959, pp. 254–261.

Correlation Function Method for Transport Phenomena, by Hazime Mori, *Phys. Rev.*, vol. 115, July 15, 1959, pp. 298–300.

On Exact Solutions of the Equations of One-dimensional Gas Dynamics with Shock and Detonation Waves, by I. S. Shikin, *Soviet Phys.-Doklady*, vol. 3, no. 5, Sept.-Oct. 1958, pp. 915–917.

Heat Conduction from a Cylindrical Source with Increasing Radius, by H. R. Bailey, *Quart. Appl. Math.*, vol. 17, Oct. 1959, pp. 255–262.

Effects of Chemical Dissociation and Molecular Vibrations on Steady One-dimensional Flow, by Steve P. Heims, *NASA TN* D-87, Aug. 1959, 66 pp.

Laminar Skin-friction and Heat-transfer Parameters for a Flat Plate at Hypersonic Speeds in Terms of Free-stream Flow Properties, by James F. Schmidt, *NASA TN* D-8, Sept. 1959, 57 pp.

On the Theory of Heat Transfer from a Boiling Fluid, by L. S. Sterman (trans. from *Zhurnal Tekhnicheskoi Fiziki*, vol. 23(2), 1953, p. 341–351), *John Crerar Library, SLA Trans. Pool, RT*-3455, 1954, 10 pp.

Shock-tube Heat-transfer Measurements on Inner Surface of a Cylinder (Simulating a Flat Plate) for Stagnation-temperature Range 4,100° to 8,300°R, by Jim J. Jones, *NASA TN* D-54, Sept. 1959, 18 pp.

An Approximate Analysis of Unsteady Vaporization Near the Stagnation Point of Blunt Bodies, by Leonard Roberts, *NASA TN* D-41, Sept. 1959, 31 pp.

Investigation of Heat Exchange in the Boiling of a Liquid in Pipes, by L. S. Sterman (trans. from *Zhurnal Tekhnicheskoi Fiziki*, vol. 24, no. 11, 1954, pp. 2046–2053), *Gt. Brit., Atomic Energy Res. Estab., AERE Library Trans.* 565, 1955, 8 pp.

An Investigation into the Influence of Speed of Circulation on the Values of Critical Heat Flows for Liquid Boiling in Tubes, by L. S. Sterman and N. G. Styushin (trans. from *Zhurnal Tekhnicheskoi Fiziki*, vol. 22, no. 3, 1952, pp. 446–454), *Gt. Brit., U.K. Atomic Energy Author., Industrial Group*, IGRL-T/W-40, 1957, 11 pp.

First Ionization Coefficients in Hydrogen, Neon, and Argon, by D. E. Davies and J. G. C. Milne, *Brit. J. Appl. Phys.*, vol. 10, July 1959, pp. 301–305.

Variational Principle for Transport Phenomena, by G. E. Tauber, *J. Franklin Inst.*, vol. 268, Sept. 1959, pp. 175–221.

Thermal Conductivity of Nitrogen-Carbon Dioxide Mixtures, by Richard S.. Brokaw, *J. Chem. Phys.*, vol. 31, Aug. 1959, pp. 571–574.

Heat Transfer to a Vaporizing, Ablating Surface, by Richard G. Fleddermann,

rockets perform reliably with BERMITE PRECISION IGNITION SYSTEMS

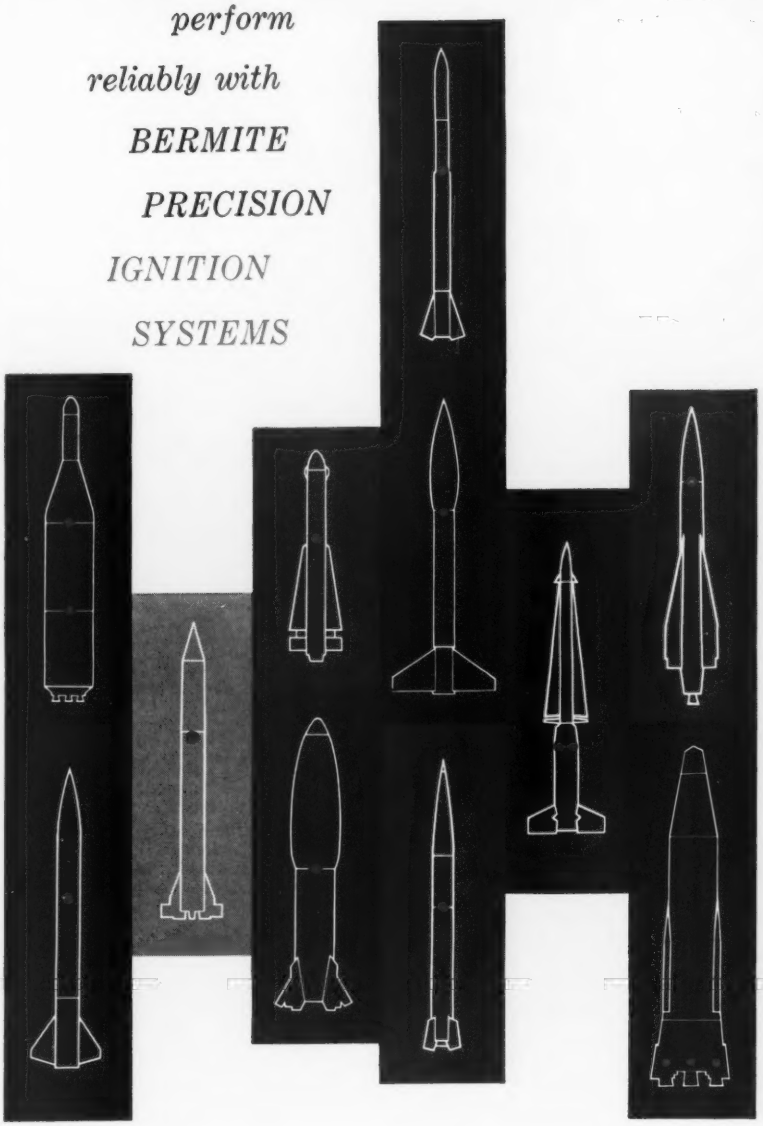

Bermite's leadership in ignition systems has been brought about by basic and applied research programs, development of specific systems to meet special customer needs, and production of the largest volume of reliable and qualified igniters for the missile industry.

In addition, Bermite produces safety and arming devices, squibs, ignition materials and unique inert components found in reliable missile systems and JATO units.

Explosive engineers interested in sophisticated projects may submit resumes to the Research and Development director, or at the Washington area office, 914 North Chambliss Street, Alexandria, Virginia.

BERMITE —built ordnance is better built through research, development and production.

Bermite Powder Company

22116 West Soledad Canyon Road, Saugus, California

J. Aero/Space Sci., vol. 26, Sept. 1959, pp. 604–605.

Excitation of Oscillations in a Plasma Layer, by Masao Sumi, *J. Phys. Soc. Japan*, vol. 14, Aug. 1959, pp. 1093–1097.

Experimental Hypersonic Research, by H. Oertel, *Raketentechnik und Raumfahrtforschung*, vol. 3, no. 3, July-Sept. 1959, pp. 65–75. (In German.)

Stability of a Hot Laminar Boundary Layer Having a Refrigerant Added, by J. F. Gross, *Raketectechnik und Raumfahrtforschung*, vol. 3, no. 3, July-Sept. 1959, pp. 76–80. (In German.)

On Solutions to the Equation of Magnetogasdynamics with Zero Temperature Gradient, by V. P. Korobeinikov and E. V. Ryazanov, *Soviet. Phys.-Doklady*, vol. 4, no. 1, Aug. 1959, pp. 41–42.

Theory of the Magnetic Boundary Layer, by V. N. Zhigulev, *Soviet Phys.-Doklady*, vol. 4, no. 1, Aug. 1959, pp. 57–60.

Increase of the Stability of an Arc in a Magnetic Field and the Maximum Field Principle, by I. G. Kesaev, *Soviet Phys.-Doklady*, vol. 4, no. 1, Aug. 1959, pp. 125–128.

Plasma Acceleration, by I. S. Shpigel, *Soviet Phys.-JETP*, vol. 36(9), no. 2, Aug. 1959, pp. 285–289.

Thermodynamic Properties of a Degenerate Plasma, by A. A. Bedenov, *Soviet Phys.-JETP*, vol. 36(9), no. 2, Aug. 1959, pp. 446–447.

Aerodynamic Heating of a Wing as Determined from a Free-flight Rocket-model Test to Mach Number 3.64, by Andrew G. Swanson and Charles B. Rumsey, *NACA Res. Mem.* L56F11a, Sept. 1956, 33 pp. (Declassified from Confidential by authority *NASA TPA* 9, 9/29/59.)

Aerodynamic Heating of Rocket-powered Research Vehicles at Hypersonic Speeds, by Robert O. Piland and Katherine A. Collie, *NACA Res. Mem.* L55E10c, July 1955, 8 pp. (Declassified from Confidential by authority *NASA TPA* 9, 9/29/59.)

A Discussion of Methods for Reducing Aerodynamic Heating in Supersonic Flight, by A. J. Eggers Jr., *NACA Res. Mem.* A55F21a, Sept. 1955, 16 pp. (Declassified from Confidential by authority *NASA TPA* 9, 9/29/59.)

Theoretical and Experimental Investigation of the Effect of Yaw on Heat Transfer to Circular Cylinders in Hypersonic Flow, by A. J. Eggers Jr., C. Frederick Hanson and Bernard E. Cunningham, *NACA Res. Mem.* A55E02, July 1955, 79 pp. (Declassified from Confidential by authority *NASA TPA* 9, 9/29/59.)

Performance of Separation Nose Inlets at Mach Number 5.5, by Rudolph C. Haefeli and Harry Bernstein, *NACA Res. Mem.* E53I23, Dec. 1953, 28 pp. (Declassified from Confidential by authority *NASA TPA* 9, 9/29/59.)

Effectiveness of Radiation as a Structural Cooling Technique for Hypersonic Vehicles, by Roger A. Anderson and William A. Brooks Jr., *Inst. Aeron. Sci., Rep.* 59-65, Jan. 1959, 27 pp.

Theory of the Flow in the Magnetic Annular Shock Tube, by Nelson H. Kemp and Harry E. Petschek, *Avco-Everett Res. Lab., Rep.* 60, July 1959, 35 pp.

Compressible Flow Tables, k=1.40; Adiabatic Flow with Friction, by C. Hoebich, *Army Rocket & Guided Missile Agency, Ordn. Missile Labs. Divs., Design and Devel. Lab., Redstone Arsenal, Alabama, TN* 1H1N-3, April 1959, rev. Aug. 1959, 89 pp.

On the Theory of Heat Exchange in Boiling in Pipes, by L. S. Sterman, *Gt. Brit., Atomic Energy Res. Estab., Library Trans.* 597, Aug. 2, 1955, 9 pp. (trans. from *Zhurnal Teckhnicheskoi Fiziki*, vol.. 24, no. 2, 1954, pp. 250–257).

Electro-gasdynamic Motion of a Charged Body in a Plasma, by L. Kraus and H. Yoshihara, *Inst. Aeron. Sci., Rep.* 59-75, Jan. 1959, 16 pp.

Heat Conduction in a Melting Slab by Stephen J. Citron, *Inst. Aeron. Sci., Rep.* 59-68, Jan. 1959, 36 pp.

Propagation of Weak Disturbances in a Gas Subject to Relaxation Effects, by F. K. Moore and W. E. Gibson, *Inst. Aeron. Sci., Rep.* 59-64, Jan. 1959, 36 pp.

Correlation Between the Sound Power Spectrum of a Free Jet and Its Aerodynamic Characteristics, by R. Lee and J. Wenzelberger, *Inst. Aeron. Sci., Paper* 59-106, June 1959, 17 pp.

A New Method for Detecting Cavitation and Turbulence in Cryogenic Fluids, by J. Clark, *Proc., Cryogenic Engng. Conf., Cambridge, Mass., Sept. 1958*, Univ. of Colo., Boulder, Jan. 1959 (498 pp.), pp. 203–217.

Prediction of Pressure Drop in Two Phase Single-component Fluid Flow, by M. R. Hatch, R. B. Jacobs, R. J. Richards, R. N. Boggs and G. R. Phelps, *Proc., Cryogenic Engng. Conf., Cambridge, Mass., Sept. 1958*, Univ. of Colo., Boulder, Jan. 1959 (498 pp.), pp. 357–377.

Liquid Flow in Tubes, II: The Transition Process Under Less Disturbed Inlet Flow Conditions, by E. R. Lindgren, *Arkiv för Fysik*, vol. 15, no. 6, 1959, pp. 503–520.

A Note on the Confinement of Charged Particles by a Magnetic Field, by B. Lehnert, *Arkiv för Fysik*, vol. 15, no. 6, 1959, pp. 579–582.

Rayleigh's Problem in Hydromagnetics: The Impulsive Motion of a Pole-piece, by G. S. S. Ludford, *Archive for Rational Mech. and Anal.*, vol. 3, no. 1, 1959, pp. 14–27.

Experimental Investigation in Magnetoaerodynamics, by Richard W. Ziemer, ARS JOURNAL, vol. 29, Sept. 1959, pp. 642–647.

The Electric Arc Wind Tunnel—A Tool for Atmospheric Re-entry Research, by Thomas R. Brogan, ARS JOURNAL, vol. 29, Sept. 1959, pp. 648–653.

Heat Conduction in a Circular Cylinder Rotating With Its Axis Normal to the Direction of Flight, by Anthony Demetriades, ARS JOURNAL, vol. 29, Sept. 1959, pp. 653–655.

Ablation Characteristics of a Subliming Material Using Arch Heated Air, by R. R. John and J. Recesso, ARS JOURNAL, vol. 29, Sept. 1959, pp. 663–665.

Adiabatic Wall Temperature Due to Mass Transfer Cooling with a Combustible Gas, by D. B. Spalding, ARS JOURNAL, vol. 29, Sept. 1959, pp. 666–668.

Thermal Protection of a Re-entry Satellite, by Sinclaire M. Scala, ARS JOURNAL, vol. 29, Sept. 1959, pp. 670–672.

Electric Stress and Heat Transfer, by P. H. G. Allen, *Brit. J. Appl. Phys.*, vol. 10, Aug. 1959, pp. 347–351.

High Magnetic Fields for Advanced Research, by H. Kolm, *Electronics*, vol. 32, Oct. 2, 1959, pp. 43–47.

Atomic Recombination in a Hypersonic Wind Tunnel Nozzle, by K. N. C. Bray, *J. Fluid Mech.*, vol. 6, July 1959, pp. 1–32.

Notes on Some Theoretical Investigations of the Physics of High Temperature Plasmas, by R. Lüst, *Nuclear Instruments & Methods*, vol. 4, no. 5, June 1959, pp. 247–248.

Plasma Diagnostics by Spectroscopical Means, by H. Wulff, *Nuclear Instruments & Methods*, vol. 4, no. 5, June 1959, pp. 352–362.

On Heating and Melting of a Solid Body Owing to Friction, by S. S. Grigorian, *PMM(J. Appl. Math. and Mech.)*, vol. 22, no. 5, 1958, pp. 815–825.

Measurement of Ionization and Attachment Coefficients in Dry Air in Uniform Fields and the Mechanism of Breakdown, by A. N. Prasad, *Proc., Physical Soc. London*, vol. 74, Pt. 1, July 1, 1959, pp. 33–41.

Construction of Exact Solutions of Equations of Gas Dynamics with Discontinuities, by E. V. Riazanov, *PMM: J. Appl. Math. & Mech.*, vol. 22, no. 5, 1958, pp. 1020–1029.

A Fluid-dynamic Mechanism of Meteorite Pitting, by David T. Williams, *Smithsonian Contrib. to Astrophys.*, vol. 3, no. 6, 1959, pp. 47–67.

Radiation from a Current-carrying Ring Moving Uniformly in a Plasma Situated in a Magnetic Field, by L. S. Bogdankevich, *Soviet Phys.-JETP*, vol. 36(9), no. 3, Sept. 1959, pp. 589–591.

Oscillations of a Completely Ionized Plasma in a Cylindrical Cavity, by L. M. Kovrizhnykh, *Soviet Phys.-JETP*, vol. 36(9), no. 3, Sept. 1959, pp. 592–593.

Zemplen's Theorem in Relativistic Hydrodynamics, by R. V. Polovin, *Soviet Phys.-JETP*, vol. 36(9), no. 3, Sept. 1959, pp. 675.

Rate of Heat-transfer Near the Stagnation Point of a Blunt Body of Revolution in the Presence of a Magnetic Field, by Rudolf X. Meyer, *Space Tech. Labs.*, CM-TR-0127-00016, March 14, 1958, 59 pp.

Chemical Non-equilibrium Effects in the Laminar Hypersonic Boundary Layer, by George R. Inger, *Bell Aircr. Corp., Rep.* 7010-6, March 1959, 132 pp. (*AFOSR TN* 59-237; *ASTIA AD* 212-007).

A Study of Hypersonic Ablation, by Sinclaire M. Scala, *General Electric, Missile and Space Vehicle Dept., T.I.S.* R59SD438, Sept. 1959, 62 pp.

The Wave Motion of Small Amplitude in Radiation-electro-magneto-gas Dynamics, by S. I. Pai and A. I. Speth, *Maryland Univ., Inst. for Fluid Dynam. & Appl. Math., TN* BN-180, July 1959, 21 pp.

On One-dimensional Channel Flow in the Presence of a Magnetic Field, by William B. Bush, *Space Tech. Labs., TR*-59-0000-00660, May 4, 1959, 17 pp.

Axi-symmetric Hydromagnetic Channel Flow, by F. D. Hains, Y. A. Yoler and E. E. Ehlers, *Boeing Airplane Co., Doc.* D1-82-0008. Aug. 1959, 57 pp., 15 refs.

Unsteady Stagnation-point Heat Transfer, by Ephraim M. Sparrow, *NASA TN* D-77, Oct. 1959, 26 pp.

Some Aspects of Air-Helium Simulation and Hypersonic Approximations by Eugene S. Love, Arthur Henderson Jr. and Mitchel H. Bertram, *NASA TN* D-49, Oct. 1959, 84 pp.

Theoretical and Experimental Investigation of Heat Conduction in Air, Including Effects of Oxygen Dissociation, by Frederick Hansen, Richard A. Early, Frederick E. Alzofon and Fred C. Witteborn, *NASA Tech. Rep.* R-27, 1959, 43 pp.

The Magnetohydrodynamic Flow Past a Flat Plate, by H. P. Greenspan and G. F. Carrier, *J. Fluid Mech.*, vol. 6, July 1959. pp. 77–96.

On the Instability Theory of the Melted Surface of an Ablating Body when Entering the Atmosphere, by Saul Feldman, *J. Fluid Mech.*, vol. 6, July 1959, pp. 131–145.

On the Flow Past a Sphere at Hypersonic Speed with a Magnetic Field, by N. C. Freeman, *J. Aero/Space Sci.*, vol. 26, Oct. 1959, pp. 670–673.

On the Concepts of Moving Electric and Magnetic Fields in Magnetohydrodynamics, by J. E. McCune and W. R. Sears, *J. Aero/Space Sci.*, vol. 26, Oct. 1959, pp. 674–675.

High Temperature Heat Transfer from Gases to Cylinders and Nozzles, by I. E. Kanter, F. Martinek and M. L. Ghai, *General Electric Co., Flight Prop. Lab., Dept., TN*, Feb. 1958–59, 128 pp.

Measurements of Heat Transfer and Friction Coefficients for Helium Flowing in a Tube at Surface Temperature up to 5900°R, by Maynard F. Taylor and Thomas A. Kirchgessner, *NASA TN* D-113, Oct. 1959, 29 pp.

Nonequilibrium Flow in Gas Dynamics, by T. Y. Li, *Rensselaer Polytech. Inst., Tech. Rep.* AE-5901, May 1959, 67 pp. (*AFOSR TN* 590389; *ASTIA AD* 213,893).

Application to Fluid Dynamics of the Theory of Reversible Heat Addition, by Barrett S. Baldwin Jr., *NASA TN* D-93, Oct. 1959, 16 pp.

On Mass Transfer and Shock-generated Vorticity, Part I: Axisymmetric Flow, by H. Hoshizaki, *Lockheed Aircr. Corp., Missiles and Space Div., LMSD-49721*, May 1959, 35 pp.

Recent Advances in Chemical Kinetics of Homogeneous Reaction in Dissociated Air, by W. G. Zinman, *General Electric Missile and Space Vehicle Dept., TIS*, R59SD426, Sept. 1959, 19 pp.

Use of Multiple Polarizations for Electron Density Profile Measurements in High Temperature Plasma, by Robert Motley and Mark A. Heald, *Princeton Univ., Proj. Matterhorn*, Matt-2, April 23, 1959, 12 pp., 11 figs.

Investigations of the Properties of the Pinch Effect in an Ionized Gas Carrying a High Current, by Winston H. Bostick, Lewis S. Combes and Morton A. Levine, *Tufts Univ., Physics Dept., Res. Lab. Final Rep.*, Jan. 1956, 96 pp.

Stabilization of a Pinch by an Alternating Magnetic Field, by Erich S. Weible, *Space Tech. Labs.*, GM-TR-0127-00399, June 4, 1958, 20 pp.

Plasma Oscillations, by J. D. Jackson, *Space Tech. Labs.*, GM-TR-0165-00535, Dec. 3, 1958, 55 pp.

Non-linear Alfven Waves in a Cold Ionized Gas, by David Montgomery, *Princeton Univ., Proj. Matterhorn*, Matt-7, June 20, 1959, 12 pp.

On the Minimum Number of Dimensionless Ratios Required to Express the Similarity Parameters of Magneto-Fluid-dynamics, by David. L. Clingman, *Inst. Aeron. Sci., 1959 First Award Papers*, 1959 (227 pp.), pp. 7–20.

Laminar Boundary Layer Control by Magnetogasdynamic Techniques, by Charlie M. Jackson Jr., *Inst. Aeron. Sci., 1959 First Award Papers*, 1959 (227 pp.), pp. 45–66.

Molecular Diffusion Studies in Gases at High Temperatures, by R. E. Waker and A. A. Westenberg, *Johns Hopkins Univ.*,

SOUTHWEST

"Monoball"®

SELF-ALIGNING BEARINGS

CHARACTERISTICS

	ANALYSIS	RECOMMENDED USE
1	Stainless Steel Ball and Race	For types operating under high temperature (800-1200 degrees F.).
2	Chrome Alloy Steel Ball and Race	For types operating under high radial ultimate loads (3000-893,000 lbs.).
3	Bronze Race and Chrome Steel Ball	For types operating under normal loads with minimum friction requirements.

Thousands in use. Backed by years of service life. Wide variety of Plain Types in bore sizes 3/16" to 6" Dia. Rod end types in similar size range with externally or internally threaded shanks. Our Engineers welcome an opportunity of studying individual requirements and prescribing a type or types which will serve under your demanding conditions. Southwest can design special types to fit individual specifications. As a result of thorough study of different operating conditions, various steel alloys have been used to meet specific needs. Write for Engineering Manual No. 551. Address Dept. ARS-60.

SOUTHWEST PRODUCTS CO.

1705 SO. MOUNTAIN AVE., MONROVIA, CALIFORNIA

New Gateway to Achievement in Astronautics and Aeronautics

Republic Aviation's

New Research & Development Center

Engineers and scientists whose minds are challenged by unsolved problems across the entire spectrum of technologies concerned with space exploration and upper atmosphere flight, are invited to inquire about the exceptional facilities for both theoretical and experimental investigations provided by Republic's new Research and Development Center (scheduled to open Spring 1960).

Senior level openings exist in the following areas:

Space Electronics *(Guidance, Navigation, Communications)* / Hydromagnetics / Advanced Computer Technology / Applied Mathematics / Nuclear Power Packages / Space Environmental Studies *(Life Science)* / Celestial Mechanics / Hypersonics / Electronic Theory / Plasma Physics / Radiation Studies / Re-entry Techniques / Materials Research & Development / Fluid Mechanics

Please forward resumes to: Mr. George R. Hickman
Technical Employment Manager, Dept. 10B

REPUBLIC AVIATION

Farmingdale, Long Island, New York

Appl. Phys. Lab., Bumblebee Rep. 283, 1959 (65 pp.), pp. 35–39.

Proc., 3d U. S. National Congress, Appl. Mech., 1958, New York, *ASME,* 1959, 864 pp.

Aerodynamic Ablation of Melting Bodies, by Theodore R. Goodman, pp. 535–546.

Determination of Nitrogen Temperature by Velocity of Sound Measurements, by Vito D. Agosta and H. Dean Baker, pp. 709–716.

Hypersonic Stagnation Point Heat Transfer to Surfaces Having Final Catalytic Efficiency, by Sinclaire M. Scala, pp. 799–806.

Thermal Entrance Region of a Circular Tube under Transient Heating Conditions, by E. M. Sparrow and R. Siegel, pp. 817–826.

Some Experimental Techniques in Mass Transfer Cooling, by Bernard M. Leadon, *Aero/Space Engng.*, vol. 18, Oct. 1959, pp. 28–32.

Transport Coefficients of Air to 8000 K, by Ernest Bauer and Martin Zlotnick, ARS JOURNAL, vol. 29, Oct. 1959, pp. 721–728.

Prediction of Inviscid Induced Pressures from Round Leading Edge Blunting at Hypersonic Speeds, by E. S. Love, ARS JOURNAL, vol. 29, Oct. 1959, pp. 792–794.

Investigation of Fast Ionization Processes in the Gas Flow Behind a Shock Wave, by A. A. Brandt and R. Kh. Kurtmulaev, *Instruments and Exptl. Tech.* (trans. of *Pribory i Tekhnika Eksperimenta*), no. 6, Nov.-Dec. 1958, pp. 808–810.

Measurement of Rapidly Varying Pressures in a Gas, by S. G. Zaitsev, *Instruments and Exptl. Tech.* (trans. of *Pribory i Tekhnika Eksperimenta*), no. 6, Nov.-Dec. 1958, pp. 811–813.

Model for Vibrational Relaxation of Diatomic Gases Behind Shock Waves, by Robert Herman and Robert J. Rubin, *Phys. Fluids,* vol. 2, no. 5, Sept.-Oct. 1959, pp. 547–550.

Magnetohydrodynamic Wave of Finite Amplitude at Magnetic Prandtl Number 1, by Hidenori Hasimoto, *Phys. Fluids,* vol. 2, no. 5, Sept.-Oct. 1959, pp. 575.

Oscillations of a Plasma in a Magnetic Field at Frequencies Close to the Cyclotron Frequency, by V. N. Lazukin, *Soviet Phys.-JETP,* vol. 36(9), no. 4, Oct. 1959, pp. 685–690.

Anomalous Electron Scattering; the Excitation of Plasma Oscillations, by M. D. Gabovich and L. L. Pasechnik, *Soviet Phys.-JETP,* vol. 36(9), no. 4, Oct. 1959, pp. 757–733.

The Disintegration of Unstable Shock Waves in Magnetohydrodynamics, by G. Ya. Lyubarskii and R. V. Polovin, *Soviet Phys.-JETP,* vol. 36(9), no. 4, Oct. 1959, pp. 902–906.

Hypersonic Flow about Ogives for Gases in Chemical and Thermodynamic Equilibrium, by Richard L. Riebe, *Trend in Engng.* (Univ. of Washington), vol. 11, Oct. 1959, pp. 5–12.

X-ray Analysis Technique for Very High Temperatures, by E. Aruja, J. H. Welch and W. Gutt, *J. Sci. Instr.*, vol. 26, Jan. 1959, pp. 16–19.

Equation of State and Thermodynamic Properties of Gases at High Temperatures, I: Diatomic Molecules, by O. Sinanoglu and K. S. Pitzer, *J. Chem. Phys.*, vol. 31, Oct. 1959, pp. 960–967.

Calculation of Reaction Profiles Behind Steady State Shock Waves, II: The Dissociation of Air, by Russell E. Duff and Norman Davidson, *J. Chem. Phys.*, vol. 31, Oct. 1959, pp. 1018–1026.

Collision Theory of the Kinetics of Dissociation of Diatomic Molecules, by B. Widom, *J. Chem. Phys.*, vol. 31, Oct. 1959, pp. 1027–1029.

Interactions of Detonation Waves, by E. Larisch, *J. Fluid Mech.*, vol. 6, Oct. 1959, pp. 392–400.

Electron Density and Ionization Rate in Thermally Ionized Gases Produced by Medium Strength Shock Waves, by Y. Manheimer-Timnat and W. Low, *J. Fluid Mech.*, vol. 6, Oct. 1959, pp. 449–461.

Thermodynamics of Electrically Conducting Fluids, by Boa-Teh Chu, *Phys. Fluids,* vol. 2, no. 5, Sept.-Oct. 1959, pp. 473–484.

Collisionless Plasma Shock, by Stirling A. Colgate, *Phys. Fluids,* vol. 2, no. 5, Sept.-Oct. 1959, pp. 485–493.

Confinement of Plasma by Standing Electromagnetic Wave, by Vincent Cushing and Mahendra S. Sodha, *Phys. Fluids* vol. 2, no. 5, Sept.-Oct. 1959, pp. 494–498.

Laminar Flow in the Entrance Region of a Porous Pipe, by Harold L. Weissberg, *Phys. Fluids,* vol. 2, no. 5, Sept.-Oct. 1959, pp. 510–516.

Instability in Hypersonic Flow about Blunt Bodies, by Robert H. Johnson, *Phys. Fluids,* vol. 2, no. 5, Sept.-Oct. 1959, pp. 526–532.

Investigation of Fast Ionization Processes in the Gas Flow Behind a Shock Wave, by A. A. Brandt and R. Kh. Kurtmulaev, *Instruments and Exptl. Tech.* (trans. of *Pribory i Tekhnika Eksperimenta*), no. 6, Nov.-Dec. 1958, pp. 808–810.

Plasma Oscillations of a Large Number of Electron Beams, by John M. Dawson, *Princeton Univ., Proj. Matterhorn,* Matt-19, Aug. 1959, 31 pp.

Measurement of Plasma Temperature and Electron Density, by Koyoshi Murakawa and Shizuyo Mizuno-Hashimoto, *J. Phys. Soc., Japan,* vol. 14, Sept. 1959, pp. 1235–1242.

Mixing of Wakes in a Turbulent Shear Flow, by Salamon Eskinazi, *NASA TN* D-83, Sept. 1959, 53 pp.

Vehicle Design, Testing and Performance

Some Aspects of Missile Launch Dispersion, by John W. Whitehurst, *Inst. Aeron. Sci., 1959 First Award Papers,* 227 pp., pp. 205–215.

Advances in Astronautical Sciences, vol. 3 (Proc., Western Regional Meeting, 1958), Plenum Press, N. Y., 1958.

Some Design Aspects of an Interplanetary Exploratory Vehicle, by Henry K. Hebeler and Richard D. White, *Paper* 8, pp. 1–15.

Techniques in the Prediction of Space Vehicle Reliability, by John S. Youtcheff and Edwin I. Karmiel, *Paper* 10, pp. 10–11.

Temperature Equilibria in Space Vehicles, by Robert A. Cornog, *Paper* 22, 11 pp.

Advances in Astronautical Sciences, vol. 4 (Proc., 5th Annual Meeting, Amer. Astron. Soc., Nov. 1958), Plenum Press, N. Y., Inc., c.1959.

The High-temperature Research Challenge in Space Vehicle Design, by Peter E. Glaser, pp. 117–128.

Assembly of a Multi-manned Satellite by Richard A. Byers and Saunders B, Kramer, pp. 154–172.

The Strato-laboratory as a Systems Testing Platform, by James R. Smith, *Inst. Aeron. Sci., Rep.* 59-48, Jan. 1959, 10 pp.

Proc., Cryogenic Engng. Conf., Cambridge, Mass., Sept. 1958, Univ. of Colo., Boulder, Jan. 1959, 498 pp.

Ultra Low Temperature Production and Control in Environmental Testing and Application Facilities, by J. Meisler, pp. 160–173.

Sealed Cabin Reliability as Related to Structure and Internal Atmosphere, by F. L. Dickey and G. H. Knipp, ARS JOURNAL, vol. 29, Sept. 1959, pp. 656–661.

Pre-cooling to Eliminate Countdowns?, by James A. Snyder, *Missiles and Rockets,* Sept. 21, 1959, pp. 35–37.

British Missiles, *Flight,* vol. 75, Sept. 4, 1959, pp. 146–150.

Black Knight Re-entry Vehicle Engineering Details Revealed, *Aviation Week,* vol. 71, Sept. 21, 1959, pp. 116.

Space Applications for Rocket Vehicles by Everett T. Welmers, *Aero/Space Engng.*, vol. 18, Sept. 1959, pp. 38–42.

Guidance and Control

On the Motion of a Gyroscope with Universal (Cardan's) Suspension and a Nonaxially Placed Rotor, by D. M. Klimov, *Soviet Phys.-Doklady,* vol. 4, no. 1, Aug. 1959, pp. 80–82.

Simplified Dynamics for Easier Inertial Design, by Bernard Lee, *Space/Aeron.*, vol. 32, Oct. 1959, pp. 191–195.

A Perturbation Solution of the Equations of Motion of a Gyroscope, by Robert Goodstein, *J. Appl. Mech.* (ASME Trans.), vol. 26, Series E., Sept. 1959, pp. 349–352.

Some Considerations Pertaining to Space Navigation, by Y. C. Lee and K. P. Conrad, *Vistas in Astronautics,* vol. 2, 2d Annual Astron. Symposium, Pergamon Press, N. Y., 1959, 318 pp., pp. 104–118.

Terminal Guidance System for Satellite Rendezvous, by W. H. Clohessy and R. S. Wiltshire, *Inst. Aeron. Sci., Paper* 59-93, June 1959, 24 pp.

Electrical Primary Flight Control Systems, by F. Gene Keyt, *Inst. Aeron. Sci., Paper* 59-99, June 1959, 18 pp.

An Adaptive System for Control of the Dynamic Performance of Aircraft and Spacecraft, by H. Philip Whitaker, *Inst. Aeron. Sci., Paper* 59-100, June 1959, 12 pp.

Bibliography of NACA Reports Related to Aircraft Control and Guidance Systems, January 1949-April 1954, by Roy J. Niewald and Jack D. Brewer, *NACA Res. Mem.* 54FO1, July 1954, iii, 55 pp. (Declassified from Confidential by authority *NASA TPA* 9, 9/29/59.)

Effects of Body and Fin Deflections on the Aerodynamic Characteristics in Pitch of a 0.065-scale Model of a Four-stage Rocket Configuration at Mach Numbers of 1.41 and 1.82, by Ross B. Robinson, *NASA TN* D-37, Sept. 1959, 33 pp., diagrs.

Advances in Astronautical Sciences, vol. 2, (Proc. 4th Ann. Meeting Amer. Astron. Soc., Dec. 1957), Plenum Press, N. Y., 1958.

Fundamentals of Inertial Guidance and Navigation, by William E. Frye, *Paper* 9, 12 pp.

Steering of an Ascent Rocket for Maxi-

mum Cutoff Velocity, by W. H. Foy Jr., *Paper* 14, 18 pp.

Synthesis of Human-automatic Control Systems for High-performance Vehicles, by William L. Morris and Richard C. Kaehler, *Paper* 20, 11 pp.

Interplanetary Applications of Automatic Navigation, by Edward V. Stearns, *Paper* 40, 12 pp.

Advances in Astronautical Sciences, vol. 3 (Proc. Western Regional Meeting, Amer. Astron. Soc., Aug. 1958), Plenum Press, N. Y., 1958.

Next: Maneuverable Satellites, by C. C. Kelber, *Paper* 17, pp. 1–18.

Microthrust Maneuver Capabilities, by A. Dobrowalski, *Paper* 18, pp. 1–14.

Practical Considerations for Astronautical Guidance and Control, by K. P. Gow and R. E. Roberson, *Paper* 30, 16 pp.

Advances in Astronautical Sciences, vol. 4 (Proc., 5th Ann. Meet., Amer. Astron. Soc., Nov. 1958), Plenum Press, N. Y., c.1959.

Space Vehicle Attitude Problems, by Harold Perkel, pp. 173–192.

Simplified Space Guidance System Analysis, by C. A. Brown and R. Fleisig, pp. 195–219.

Proposed Method of Navigation on the Earth by Means of an Earth Satellite, by Robert Etcheverry, Richard Brooks and Jack Russel, pp. 220–225.

On the Autonomous Determination of the Position of a Moving Object by Means of a Space Gyrocompass, a Directional Gyroscope and Integrating Device, by A. Iu. Ishlinskii, *PMM: J. Appl. Math. & Mech.* (trans. of *Prikladnaya Matematika i Mekhanika*), vol. 23, no. 1, 1959, pp. 75–82.

Synthesis and Flight Test of a Ballistic Missiles-Adaptive Flight Control System, by Ordway B. Gates Jr. and Orrin C. Kaste, *Inst. Aeron. Sci. Paper* 59-124, June 1959, 24 pp.

Johns Hopkins Univ., Appl. Phys. Lab., Technical Papers from the Quarterly Review of Bumblebee Activities, Jan.-Dec. 1958; Bumblebee Rep. 282, 1959, 65 pp.

Analysis of a Transistor Operational Amplified, by R. E. Gorozdos and S. A. Kramer, pp. 17–21.

Design and Performance Criteria of the Accelerating Switching Hydraulic Servo, by W. Seamons, pp. 22–28

Frequency Analysis of a Control Loop Containing a Bistable Element by R. E. Gorozdos, pp. 40–44.

A Transistorized Voltage—Controlled FM Subcarrier Oscillator, by A. M. Chwastyk, pp. 45–50.

Evaluation Study of a Transistor Operational Amplifier, by R. L. Konigsberg, pp. 51–56.

Method for Determining Steering Programs for Low Thrust Interplanetary Vehicles, by Edward Rodriguez, ARS JOURNAL, vol. 29, Oct. 1959, pp. 783–788.

Instrumentation and Communications

Development of Switching Components for Controlled Fusion Research, by David B. Cummings, *Atomic Energy Comm., UCRL-5284,* June 1958, 19 pp.

Infrared Communications Receiver for Space Vehicles, by W. E. Osborne, *Electronics,* vol. 32, Sept. 18, 1959, pp. 38–39.

Specifications and Fabrication Instructions for Pressure and Force Gages at

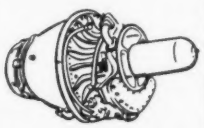
TURBINE PROPULSION

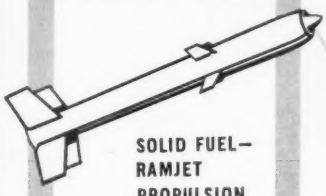
SOLID FUEL–
RAMJET
PROPULSION

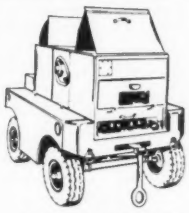
GROUND SUPPORT

CAE POWER

- Research
- Development
- Production

● Continental Aviation & Engineering Corp. is exceptionally well qualified, both by experience and by facilities, for work on the weapons systems of tomorrow. Our background embraces not only a half-century of internal combustion engine experience, but also years of pioneering in gas turbine engine development, and more than a decade in the field of solid fuels for ramjet propulsion of missiles and target drones . . . Continental is staffed and equipped for a wide range of assignments, military and commercial. The Detroit Division Research and Development Department is supported by our modern-to-the-minute Component Testing Laboratory complete with environmental facilities located at Toledo. The Toledo Production Division now producing various turbine engines in volume is capable of supporting diversified programs . . . The CAE record of achievement is one of which many a larger company might be proud. Inquiries are invited from those having propulsion problems, on the ground, on the water, in the air.

CONTINENTAL AVIATION

CONTINENTAL AVIATION & ENGINEERING CORPORATION

GENERAL OFFICES AND RESEARCH AND DEVELOPMENT DEPARTMENTS AT 12700 KERCHEVAL AVENUE, DETROIT 15, MICHIGAN . . . PRODUCTION DIVISION AND FIELD SUPPORT, 1330 LASKEY ROAD, TOLEDO, OHIO.

SUBSIDIARY OF CONTINENTAL MOTORS CORPORATION

Index to Advertisers

ACADEMIC PRESS, INC. 212

AEROJET GENERAL CORP. ..... Back cover
D'Arcy Advertising Co., Los Angeles, Calif.

ALLIED CHEMICAL CORP., GENERAL CHEMICAL DIV. 215
Kastor, Hilton, Chesley, Clifford & Atherton, Inc., New York, N. Y.

AMCEL PROPULSION, INC. 149
Deutsch & Shea, Inc., New York, N. Y.

AMERICAN-STANDARD, MILITARY PRODUCTS DIV. 218, 219
S. Gunnar Myrbeck & Co., Inc., Quincy, Mass.

BERMITE POWDER CO. 223
John R. MacFaden, Los Angeles, Calif.

BULOVA WATCH CO. 145
Duncan-Brooks, Inc., Garden City, N. Y.

CONTINENTAL AVIATION & ENGINEERING CORP. 227
The Hopkins Agency, Detroit, Mich.

CONVAIR, A DIV. OF GENERAL DYNAMICS CORP. ..... Third cover
Lennen & Newell, Inc., Beverly Hills, Calif.

EXCELCO DEVELOPMENTS 213
Melvin F. Hall Advertising Agency, Inc., Buffalo, N. Y.

GENERAL MOTORS CORP., OLDSMOBILE DIV. 150
D. P. Brother & Co., Detroit, Mich.

LOCKHEED AIRCRAFT CORP. 210, 211
Foote, Cone & Belding, Los Angeles, Calif.

LOS ALAMOS SCIENTIFIC LABORATORY 217
Ward Hicks Advertising, Albuquerque, N. Mex.

THE MARTIN CO., ACTIVATION DIV. ..... Second cover
E. M. Halvorson Co., Denver, Colo.

RADIO CORP. OF AMERICA, DEFENSE ELECTRONIC PRODUCTS 209
Al Paul Lefton Co., Inc., Philadelphia, Pa.

REPUBLIC AVIATION CORP. 225
Deutsch & Shea, Inc., New York, N. Y.

SOUTHWEST PRODUCTS CO. 225
O. K. Fagan Advertising Agency, Los Angeles, Calif.

THIOKOL CHEMICAL CORP. 146, 147
Brown & Butcher, Inc., New York, N. Y.

Allegany Ballistics Laboratory, *Hercules Powder Co., Allegany Ball. Lab.*, ABL/B-21, Aug. 1959.

Advances in Astronautical Sciences, vol. 3 (Proc., Western Regional Meet., Amer. Astron. Soc., Aug. 1958), Plenum Press, N. Y., 1958.

Space-to-Space Propagation Phenomena, by C. N. Lee, *Paper* 11, pp. 1–21.

Flame Attenuation of R. F. Signals, by R. J. Schmelzer, *Paper* 15, pp. 1–5.

A New Instrument for Measuring Density and Temperature at Satellite Altitude, by H. A. Dessler, W. B. Hanson, M. Hertzberg, D. D. McKibbin and R. C. Wrigley, *Paper* 24, 3 pp.

Advances in Astronautical Sciences, vol. 4 (Proc., 5th Ann. Meet. Amer. Astron. Soc., Nov. 1958), Plenum Press, N. Y., c.1959.

Long-range Detection by Star Occultation, by Harvey Dubner, pp. 226–242.

A Television Camera for Space Application, by M. H. Mesner, J. R. Staniszewski and P. H. Werenfels, pp. 243–349.

The Analysis of Temperature Fluctuations by Pulse-counting Techniques, by A. A. Townsend, *J. Fluid Mech.*, vol. 6, Aug. 1959, pp. 261–271.

First Order Error Propagation in a Stagewise Smoothing Procedure for Satellite Observations, by Peter Swerling, *J. Astron. Sci.*, vol. 6, Autumn 1959, pp. 46–52.

Requirements of High-resolution Photography of the Planets, by Gerald De Vaucouleurs, *Inst. Aeron. Sci., Rep.* 59-73, Jan 1959, 10 pp.

Preliminary Considerations on the Instrumentation of a Photographic Reconnaissance of Mars, by G. Halcombe Laning Jr., Elmer J. Frey and Milton B. Trageser, *Vistas in Astron.*, vol. 2, 2d Ann. Astron. Symposium, Pergamon Press, N. Y., 1959 (318 pp.), pp. 63–94.

Pulse Technique for Probe Measurements in Gas Discharges, by John F. Waymouth, *J. Appl. Phys.*, vol. 30, Sept. 1959, pp. 1404–1411.

Electromechanical Switches for Telemetering Systems, by A. S. Kramer, *Electronics*, vol. 32, Oct. 2, 1959, pp. 54–55.

Millimicrosecond Pulse Generator Capable of 10 Million Pulse Per Second, by Michiyuki Nakamura, *Rev. Sci. Instr.*, vol. 30, Sept. 1959, pp. 778–782.

Temperature Measurements of Shock Waves by Spectrum-line Reversal, II: A Double-beam Method, by J. G. Clouston, A. G. Gaydon and I. R. Hurle, *Proc., Roy. Soc., London*, vol. A252, Sept. 8, 1959, pp. 143–155.

An Electronic Framing Camera for Millimicrosecond Photography, by George L. Clark, *Space Tech. Labs.* (presented at Westcon-Conference, Aug. 19–22, 1958), 14 pp.

Johns Hopkins Univ., Appl. Phys. Lab., Bumblebee Rep. 283, 1959, 65 pp.

Skin Friction Measurements During Ascending Viking Flight, by F. W. Fenter and W. C. Lyons Jr., pp. 5–13.

Ceramic Rod Antennas, by D. T. Collins and E. A. Beck, pp. 14–16.

Accuracy of Zero-counters and Their Use in High-precision Doppler Measuring Devices, by Edwin Shotland, pp. 57–61.

Pressure Sensing Probes for Detecting Shock Waves, by Adolph B. Amster, and Raymond L. Beauregard, *Rev. Sci. Instr.*, vol. 39, Oct. 1959, pp. 942.